CONTROLLED DRAFT 0
DECEMBER 22, 1986

SITE CHARACTERIZATION PLAN

Chapter 4.0

GEOCHEMISTRY

G. S. Barney
Lead Author

TABLE OF CONTENTS

TABLE OF CONTENTS (Continued)

Chapter 4

GEOCHEMISTRY

4.0 INTRODUCTION

The long-term safety of a nuclear waste repository in basalt depends on geochemical parameters that control the release and transport of waste radionuclides from the engineered barrier system. Safety assessment of the waste disposal system requires an understanding of probable radionuclide release and transport scenarios and the chemical and physical processes associated with these scenarios. The most credible scenario appears to be a gradual degradation of engineered barriers and subsequent transport of radionuclides by groundwater through fissures in the basalt into porous flow tops and interbed layers. Because geochemical processes along flow paths will influence radionuclide movement, relevant geochemical processes must be identified and characterized. Chemical and physical processes involved in this scenario include saturation of packing material by groundwater; corrosion of the metallic container; dissolution and leaching of radionuclides from the

waste form; radionuclide precipitation; radionuclide sorption on engineered barrier materials and geologic solids; radionuclide diffusion; hydrothermal reactions with engineered barriers and geologic solids; and radiolysis of groundwater. These processes (and others) must be synthesized into models that describe the overall performance of the repository.

PURPOSE OF THE GEOCHEMICAL PROGRAM

The overall purpose of geochemical studies of the Hanford Site is to characterize geochemical parameters and processes that will affect long-term containment of waste radionuclides within engineered barriers and isolation of waste radionuclides from the accessible environment. Since transport via groundwater is the most credible means of radionuclide movement from the repository, geochemical processes that are expected to occur along potential groundwater flow paths from the repository to the accessible environment must be identified and characterized. This chapter emphasizes geochemical processes that occur in the natural system, such as radionuclide sorption and desorption, diffusion into the rock matrix, redox reactions, complexation reactions, and reactions of minerals with groundwater. Chemical reactions that occur within the engineered barriers system are discussed in Chapter 7 (Sections 7.4.6, 7.4.7.4, and 7.4.3.4.3). A detailed description of geochemical processes and parameters important in different regions of the repository is given in this section.

In the natural system, groundwater is expected to move laterally in basalt flow tops and interbeds (potential aquifers) and vertically across flow interiors (aquitards) (see Chapter 3). The existing geohydrology data base is not yet complete enough to support a detailed model of the groundwater flow path. However, it is likely that the top of the Cohassett flow is an early segment of the flow path because of a slightly upward hydraulic head gradient across the flow. The remainder of the flow path consists of basalt flow interiors, relatively porous flow tops, and sedimentary interbeds above the repository horizon. Geochemical parameters for each of these flow path segments must be characterized to accurately predict the long-term isolation performance of the repository.

Federal regulatory performance criteria for geologic repositories have been specified by the U.S. Nuclear Regulatory Commission (NRC) (NRC, 1985, pp. 563-593) and the U.S. Environmental Protection Agency (EPA) (EPA, 1985, pp. 38066-38089). These regulations require essentially complete containment of the waste within the waste packages for a minimum period of 300 to 1,000 yr and a subsequent maximum release rate from the engineered barrier system of 1 part in 100,000/yr of the radionuclide inventory at 1,000 yr following repository closure (radionuclides released at a rate less than 0.1% of the total release rate limit are exempt from this requirement). In addition, the disposal system must be designed so that the cumulative releases of radionuclides to the accessible environment over 10,000 yr have a low, specified probability of exceeding the quantities given in Table 1 (Appendix A) of 40 CFR 191 (EPA, 1985, pp. 38087-38088). The geochemical parameters that

control radionuclide containment and release are groundwater composition, pH, redox potential, colloid concentration, composition of engineered barriers, and mineralogy of geologic solids. The regulatory performance criteria and the geochemical information required to provide assurance that the criteria will be met are given in Table 4.0-1. These geochemical data must be incorporated into performance assessment models (along with physical parameters and processes) that will predict long-term containment and release of radionuclides.

In addition to the performance criteria, siting criteria in 10 CFR 60 (NRC, 1985, pp. 563-592) and 10 CFR 960 (DOE, 1984, pp. 47714-47770) give specific geochemical conditions that are favorable and unfavorable for providing reasonable assurance that the performance objectives of waste isolation will be met. These regulations imply that certain geochemical parameters and processes must be evaluated in order to select a site for a repository. The required geochemical information is summarized in Table 4.0-2. The location of this information in Chapter 4 and the corresponding studies (from Chapter 8) needed to obtain the remainder of the required geochemical data are also presented in Table 4.0-2.

SOURCES OF GEOCHEMICAL DATA

The methods used to gather the data presented in this chapter are described briefly below. Refer to Section 4.1 for details.

Both laboratory and field techniques have been developed and applied in gathering geochemical data. Mineralogical and petrological data were obtained by analyzing drill core samples and samples of outcrops. Major and selected trace element concentrations in the rock samples were determined by x-ray fluorescence. Neutron activation analysis was also used for measurement of some trace elements. Individual phases were identified using electron microprobe, x-ray diffraction, scanning electron microscope, and optical microscope techniques.

Groundwater samples from various stratigraphic zones were obtained by pumping from a number of boreholes drilled in the Hanford Site. Some springs have also been sampled. Concentrations of inorganic components in these groundwaters were measured using inductively coupled plasma spectroscopy techniques for cations and ion chromatography for anions. Total organic carbon was determined using a total organic carbon analyzer and dissolved gases were determined with a gas chromatograph. Inorganic carbon was determined by titrimetry.

The distribution of radionuclides between groundwater and mineral phases was measured in the laboratory under conditions that simulate those expected in groundwater flow paths from the repository. Batch equilibrations of radionuclide-groundwater-rock systems were used to obtain radionuclide

sorption and desorption information. Future studies will also include flow-through or column measurements. Additional details of these methods are given in Section 4.1.3.2.

The redox environment of the natural system was estimated using three different methods: (1) identification of redox-sensitive secondary minerals in basalt flows, (2) measurement of concentrations of both reducing and oxidizing species of several redox couples dissolved in groundwater, and (3) electrode potential measurements using platinum electrodes. These three methods yield independent estimates of the redox state of the natural system.

Temperature increases in the natural system due to emplacement of the waste were estimated using heat flow models. These models are based on repository design, the age and quantity of waste in the repository, thermal conductivity of repository components and host rock, and the time at which resaturation of the waste package occurs.

Natural analog studies of geochemical processes that are relevant to repository performance require methods for characterization of minerals and groundwaters in the natural system. These methods are essentially the same as those described above.

The methodology to be used for field tracer tests that determine radionuclide chemistry and transport is still under development. Plans for these tests are presented in Section 8.3.1.4.2.3.

The geochemical data presented in this chapter were obtained before January 31, 1986. Geochemical information obtained after this date will be presented in 6-month progress reports of the Site Characterization Plan.

PLANS FOR OBTAINING ADDITIONAL GEOCHEMICAL DATA

Plans for obtaining additional geochemical data on the natural system are presented in Sections 8.3.1.2.2.5 and 8.3.1.4, and a short summary of site geochemistry plans is given in Section 4.5.3. These plans include additional mineralogical and petrological characterization of primary and secondary minerals in basalt flows and sedimentary interbeds; characterization of groundwaters (e.g., inorganic and organic composition, dissolved gases, stable and radioactive isotopes, redox status); laboratory and field studies of radionuclide retardation (e.g., batch and column sorption-desorption measurements, reactive field tracer tests, measurements of natural radioactive disequilibrium); and characterization of natural analogs.

USES OF GEOCHEMICAL DATA

The use of natural system geochemical data in site characterization is described in more detail in Chapter 8 (see Table 4.0-2 for appropriate sections). A brief summary of how the geochemical data presented in this chapter will be used by various components of the Basalt Waste Isolation Project (BWIP) is given below.

- Host Rock Geochemistry. The geochemistry of basalt and interbed materials will be a major input to the development of a mineralogy-petrology model. This model will be used to assess current and future geochemical changes in the natural system and to present a complete picture of the distribution of minerals that influence radionuclide transport. Mineralogy will influence groundwater chemistry and, thus, will input to geochemical and hydrochemical models. Primary mineralogy and bulk chemical composition of the basalt flows are also useful tools for determining intraflow structure and stratigraphic correlations that are needed for estimating the areal extent and thickness of basalt flows to be used for repository construction.

- Groundwater Geochemistry. Groundwater geochemical data provide independent evidence for hydrologic flow models of aquifers underlying the Hanford Site that may affect waste isolation. These flow models predict the direction and rate of groundwater flow along credible flow paths from the repository. In addition, the geochemical properties of the groundwater will influence radionuclide retardation mechanisms such as ion exchange, chemisorption, and precipitation. Finally, groundwater chemistry must be defined for laboratory and field test programs that determine corrosion rates of container materials, waste-barrier-rock hydrothermal reactions, and radiolysis effects on groundwater chemistry and radionuclide behavior.

- Geochemical Retardation. Natural system radionuclide sorption data (i.e., sorption and desorption isotherms, and distribution coefficients) will be input to radionuclide transport models that predict the performance of the repository. Sorption of radionuclides on minerals in the natural system is an important mechanism for retardation of radionuclide transport in groundwater. The effects of groundwater parameters (e.g., pH, Eh, groundwater composition, temperature) on sorption must also be incorporated into these computer codes.

  Chemical and physical environmental factors that affect radionuclide retardation processes include groundwater composition, pH, and redox potential; rock mineral composition and microstructure; and temperature and pressure. These parameters must be known in order to perform valid experimental measurements of radionuclide sorption and solubility in the natural system.

- Geochemical Effects of Waste Emplacement. The primary effect of waste emplacement will be to increase the temperature on the host rock. Radiation effects are not expected to be important for the natural system, but are evaluated in Chapter 7 for effects on the waste package. Data describing temperature effects on hydrothermal alteration of minerals, changes in water chemistry, and the resultant effects on radionuclide transport will be input to geochemical models and radionuclide transport models. Estimates of the thermal pulse and its geochemical effects will allow realistic limits for temperature, groundwater composition, and mineral composition to be set for experimental measurements of radionuclide behavior.

- Natural Analogs and Field Tests. Natural analog studies will yield only qualitative information on geochemical processes that might affect waste isolation. These results will be used in concert with laboratory tests and performance models to help evaluate the long-term geochemical stability of the natural and engineered barriers systems. Data from field testing will be compared to laboratory results so that scaling factors can be calculated and used in radionuclide transport models.

QUALITY OF GEOCHEMICAL DATA AND MODELS

Conceptual models as defined here are hypothetical representations of geochemical processes expected to occur in the repository system. Only qualitative descriptions are presented in this section. Quantitative models of geochemical processes considered in performance assessment are described in Chapter 8 (Section 8.3.5).

The chemical processes significant in determining the ability of a mined geological repository in basalt to isolate radionuclides differ according to the location in which these processes occur. These processes depend on the types of solid materials present, groundwater composition, groundwater flow rate, temperature, pressure, identity and quantity of radionuclides present, and the radiation field. These factors are different in the three regions of the repository system defined by NRC (1985, pp. 563-593) and the Mission Plan (DOE, 1985, p. 429). These regions are shown in Figure 4.0-1 and are described as follows.

- The engineered barriers system includes all the manmade barriers (i.e., waste form, canister, container, packing material, and repository backfill material).

- The disturbed zone consists of the region of the host rock that is immediately surrounding the excavations and is affected by emplacing the waste (e.g., fractures caused by mining, increased temperature, radiation field) to the extent that performance of the repository could be significantly changed.

- The natural system constitutes the remainder of the repository system (i.e., basalt flows, interbeds, and groundwaters) and terminates at the boundary to the accessible environment. The accessible environment is defined as the atmosphere, the land surface, surface water, oceans, and the portion of the lithosphere that is 5 km (3 mi) from the underground facility.

In an analogous manner to this spatial division of a nuclear waste repository in basalt, a division can also be made on the basis of time with respect to the NRC criteria regarding the emplacement of waste and isolation of the waste thereafter. Four distinct time intervals are described in the following.

- The pre-emplacement period is when ambient conditions will persist. Geochemical parameters that are important to site characterization during this period are host rock composition (mineral composition, chemical composition, grain size) and ambient groundwater composition (pH, Eh, dissolved minerals, gases, organics, colloids).

- The preclosure operational/retrieval period begins during excavation and construction of the repository. It continues through waste emplacement and ends with closure of the repository. During this period the host rock is exposed to air, radiation, and elevated temperatures. These conditions lead to chemical alteration of the host rock and groundwater. Excavation-induced damage of the host rock will also occur during this period.

- The containment period begins after the closure of the repository: The radionuclides must be substantially contained within the waste package during the required containment period of 300 to 1,000 yr (NRC, 1985, pp. 563-593). Gamma radiation, elevated temperatures, ambient oxygen from the operating period, and corrosion of the waste container will alter the groundwater composition within the engineered barriers and disturbed zone. The initially dry environment of the waste package will be saturated with groundwater. The reactions taking place in the engineered barriers and the disturbed zone are discussed in Section 7.1.

- The isolation period begins when the physical containment of the waste form has been breached and groundwater comes into contact with the waste form. This time period is normally defined as 1,000 yr for BWIP although the majority of waste packages may keep their integrity for longer time periods. The rate of release of radionuclides to the host rock will be controlled by dissolution of the waste form and transport through the packing material. Sorption reactions of radionuclides in each of the three regions of the repository will retard radionuclide transport. Precipitation will likely occur mainly in the engineered barrier system and the disturbed zone.

As shown in Table 4.0-3, a combined matrix of spatial regions and time periods for a nuclear waste repository in basalt can be used to define what geochemical processes and associated physicochemical parameters are relevant for demonstrating performance compliance with Federal regulatory criteria (NRC, 1985, pp. 563-593; EPA, 1985, pp. 58196-58206).

Geochemical processes and parameters will affect containment of waste radionuclides within engineered barriers and also isolation of radionuclides from the accessible environment. Prior to repository closure, air will be present in underground excavations and will lead to oxidation of some iron(II)-containing minerals in the host rock, backfill, and packing materials. Air exposure will also cause corrosion of the waste package container. Reducing conditions will be slowly restored after closure by the large reducing capacity of the host rock and engineered components. The underground excavations will be gradually saturated with groundwater and the containers will continue to slowly corrode until they are breached, allowing groundwater to contact the waste form. The waste form, including radionuclides, will slowly dissolve in groundwater. Dissolved radionuclides will then diffuse through container corrosion products, packing material, and backfill material into fissures in the host rock basalt flow. Dissolution of most radionuclides in groundwater will generally be limited by low solubilities in this slightly basic groundwater (pH 9 to 10). Sorption reactions of dissolved radionuclides with surfaces of corrosion products, packing material, backfill material, and minerals contained in basalt fissures and flow tops (probable groundwater flow paths) will delay radionuclide transport to the accessible environment. The formation of inorganic or organic complexes with dissolved radionuclides may increase their solubility and (or) decrease their sorption. Redox reactions of radionuclides with the reducing environment of the host rock and engineered barriers will tend to keep some radionuclides in reduced oxidation states in which their solubilities are lowered and sorption is increased. Colloids suspended in groundwater may carry sorbed or precipitated radionuclides along flow paths if they are chemically stable and mobile. Because of the small pore sizes expected in porous media in flow paths and the slow velocity of groundwater flow, physical filtration and gravitational settling of colloids is expected to immobilize them.

Acceptable levels of uncertainty in the geochemical parameters described above can be estimated using two different approaches. In the first approach (a deterministic approach), a worst case is determined and the most pessimistic values of parameters are used in radionuclide containment and release models. If the models yield containment and release limits that are allowable by Federal regulations, then the data uncertainties are acceptable. The difficulty in this approach lies in drawing the line between credible and unrealistic data sets. The second approach (a probabilistic approach) is to use sensitivity/uncertainty analysis to quantify uncertainties in the results that are created by uncertainties in input parameters. This approach will allow the identification of parameters that exert the greatest influence on radionuclide containment and release and will allow estimation of uncertainties in model outputs. This approach will be used when uncertainties in input parameters can be estimated. Plans for performing

sensitivity/uncertainty analyses of geochemical parameters using models of radionuclide containment and release are described in Chapter 8 (Sections 8.3.4.5 and 8.3.5.2.3).

Not all models that use geochemical data (e.g., radionuclide release, transport, corrosion, geochemical models, etc.) are refined enough to allow sensitivity/uncertainty analysis of geochemical parameters. Therefore, it is not possible to accurately judge the quality of all available geochemical data at present. In some cases, the processes that influence repository performance are not yet well understood and, thus, the models have a high degree of uncertainty.

Additional uncertainties in the geochemical data are a result of difficulties in sampling and analysis of geologic materials. Problems involved in sampling deep groundwaters (contamination by drilling mud, by air, and by the sampling apparatus; loss of dissolved gases; etc.) are discussed in Chapter 3. A significant effort is planned (Chapter 8, Section 8.3.1.3) to obtain uncontaminated, representative groundwater samples by improving drilling methods and sampling equipment. Similar problems are involved in sampling the rock. Analytical methods for determination of most major components of geologic samples are well-developed. However, analyses of some trace components (e.g., organic chemicals in groundwater) are difficult.

Most of the available data on geochemical behavior of radionuclides reported in this chapter were obtained in laboratory experiments. Since geochemical conditions in the natural system are complex, it is difficult to reproduce field conditions precisely in the laboratory. Examples of parameters difficult to duplicate are redox conditions and the composition of geologic materials in the natural system. The amount of uncertainty introduced because of these problems is difficult to estimate, since it depends on the chemistry of the radionuclide involved and the variability of geologic materials in groundwater flow paths. To help overcome these difficulties, field tracer tests using reactive and nonreactive tracers in postulated groundwater flow paths are planned (see Chapter 8). The laboratory and field test data complement one another and provide a more complete description of radionuclide behavior.

The slow rates of some geochemical reactions result in uncertainties in the geochemical data. Observations of chemical reactions in the laboratory are practically limited to a few years, whereas reactions in groundwater flow paths can occur over hundreds or thousands of years. Therefore, data obtained from slow reactions in the laboratory must be extrapolated to very long times. This can lead to uncertainties in the extrapolated data. The possibility also exists that some slow reactions could be overlooked. These reactions can be accelerated (within limitations) by changing experimental parameters (e.g., increasing the temperature, surface area of solid reactants, flow rates, etc.). The measurement of reaction kinetics is an important aspect of planned geochemical studies outlined in Chapter 8.

ORGANIZATION OF CHAPTER 4

The objective of Chapter 4 is to present natural system geochemical data as it is now understood. Geochemical processes and parameters important to radionuclide isolation are presented along with current best values for parameters. Areas where the geochemical data are incomplete are noted, and references for plans for getting more data are given.

The geochemistry of the host basalt and surrounding basalt flows, flow tops, and interbeds is presented in Section 4.1. Chemical, mineralogic, and petrographic data that may influence radionuclide isolation are given in Section 4.1.1. Groundwater geochemistry that can influence radionuclide movement along flowpaths is discussed in Section 4.1.2. Specific geochemical retardation processes, especially sorption and desorption, are discussed in Section 4.1.3.

Waste emplacement will cause an increase in temperature. The effects of increased temperature on the geochemical properties that influence radionuclide isolation are discussed in Section 4.2.

More information about the expected geochemical environment and geochemical stability of a mined geologic repository in basalt come from natural analog studies and field tests. Current data on such studies and tests are presented in Section 4.3.

Human activity and natural changes could both affect the stability of the proposed repository. Section 4.4 explores these possibilities.

Significant results are summarized in Section 4.5 and plans to collect more data are referenced.

4.1 GEOCHEMISTRY OF THE HOST ROCK AND SURROUNDING UNITS

The geochemistry of the host rock and surrounding basalt flows, flow tops, and interbeds is important to radionuclide isolation because the geochemistry will determine radionuclide behavior along pathways to the accessible environment. The purpose of the geochemical investigations reported in this section is to help define the geochemistry of the host rock and surrounding units well enough to determine whether the proposed repository can meet the applicable regulations for waste isolation. The plans for investigations to finish this effort are given in Sections 8.3.1.4 and 8.3.4.

This section describes potential pathways for radionuclide transport in the natural system. Sections 4.1.1 and 4.1.2 describe the geochemistry of rocks and groundwaters, respectively, in the preferred emplacement horizon (the Cohassett flow) and surrounding basalt flows, flow tops, and interbeds. Section 4.1.3 describes chemical processes influencing radionuclide transport along expected pathways to the accessible environment. Geochemical interactions in the engineered system are discussed in Chapter 7.

The mineralogic and petrologic data collected so far show that the major element and trace element compositions and primary mineralogy are laterally uniform throughout the controlled area study zone. There is some stratigraphic variation in chemical and elemental compositions, but differences are small and are not expected to result in radically different basalt-water-waste reactions. The stratigraphic and lateral distribution of secondary phases appears to be more variable than those of primary phases. Cristobalite is more abundant than quartz above about 1,000 m (3,280 ft) and quartz is more abundant below about 1,000 m (3,280 ft). Mordenite has been identified only below about 1,000 m (3,280 ft).

Current data allow some general conclusions about groundwater geochemistry. The geochemical data collected so far show that the groundwaters are alkaline and the major ions are Na^+, K^+, Ca^{2+}, Mg^{2+}, Cl^-, F^-, and SO_4^{2-}. Not enough information is available to reach a conclusion about the organic content of the groundwater or about background radioactivity. Dissolved methane is the major gas in groundwater samples, but not enough information is available to accurately determine the concentration. The U.S. Department of Energy (DOE) is evaluating the usefulness of computer models of mineralogic control on water composition.

Sorption and desorption are the most important geochemical retardation processes in the natural system. Experiments show that radionuclides that exist in groundwater solution as hydrated metal ions are strongly sorbed by geologic solids in potential flow paths. Nonmetallic radionuclides such as ^{129}I and ^{14}C are not measurably sorbed. Sorption reactions for most radionuclides are partially irreversible. Studies so far also show that the preemplacement natural system is reducing (see Section 4.1.3.4), and a reducing environment will retard radionuclide migration by decreasing solubility and increasing sorption. Diffusion and precipitation processes are expected to be less important in the natural system than in the engineered system.

4.1.1 MINERALOGY AND PETROLOGY

The mineralogy and petrology of the site will influence radionuclide isolation. Certain minerals can react with each other, with groundwater, and with radionuclides, changing some aspects of the geochemical environment and, depending on the specific nature of the change, either inhibit or enhance radionuclide sorption and transport. Certain minerals may precipitate in, or dissolve from, fractures and interconnected pores in the rock. These reactions might physically alter groundwater flow paths and the paths of radionuclide transport to the accessible environment.

The data presented in this section are discussed with respect to the repository isolation system, the reference repository location, and the controlled area study zone. The repository isolation system is defined by stratigraphy and is subdivided into a primary isolation zone, an upper buffer zone, and a lower buffer zone (Fig. 4.1-1). The reference repository location

is the lateral area in which the repository will be located. The controlled area study zone is the focus of site characterization activities and represents the sum of all likely controlled areas for a repository at the reference repository location plus a border of 5 km (3.1 mi). The lateral boundaries of the repository will lie within the reference repository location.

This section discusses the geochemical, mineralogic, and petrologic characteristics of the repository isolation system with emphasis on the primary isolation zone. The repository isolation system is briefly described in Section 4.1.1.1; the analytical techniques used to obtain the data are briefly described in Section 4.1.1.2; the data are presented in Section 4.1.1.3; and, mineral stability is discussed in Section 4.1.1.4.

4.1.1.1 General description of the host rock and surrounding units

The potential repository site at Hanford is located in the Columbia River basalts. The Columbia River basalts are tholeiitic continental flood basalts that erupted 6 to 17 m.y. ago from linear vent systems up to 150 km (93 mi) in length (McKee et al., 1977, p. 463; McKee et al., 1981, pp. 31-33). These vent systems, which erupted sheetlike floods of relatively low-viscosity magma, were predominantly east of the Pasco Basin in eastern Washington, western Idaho, and northeastern Oregon. Several eruptions commonly congealed into single lava flows covering as much as 75,000 km^2 (29,000 mi^2). Volumes of individual flows are typically 10 to 30 km^3 (2.4 to 7.2 mi^3) but some are known to be about 700 km^3 (168 mi^3) (Swanson and Wright, 1981, p. 1). Large volume flows are generally thick (greater than 40 m (130 ft)), widespread, and appear laterally continuous (see Section 1.2).

The Columbia River Basalt Group is divided into five formations that are, from oldest to youngest, Imnaha Basalt, Picture Gorge Basalt, Grande Ronde Basalt, Wanapum Basalt, and Saddle Mountains Basalt. Each formation is divided in several members or sequences and each of these consist of more than one flow. Of these five formations, only the Grande Ronde, Wanapum, and Saddle Mountains Basalts are present in the Pasco Basin and the controlled area study zone, and only the Grande Ronde and Wanapum Basalts are included in the repository isolation system. In addition, not all members and not all flows in a given member are present in the controlled area study zone. The portion of the stratigraphic column pertinent to the repository isolation system within the controlled area study zone is shown in Figure 4.1-1.

The primary isolation zone consists of several flows of the Grande Ronde Basalt and the overlying Vantage interbed, which is part of the Ellensburg Formation (Fig. 4.1-1). The Grande Ronde Basalt flows are about 280 m (920 ft) thick and have a volume of about 61 km^3 (15 mi^3) in the primary isolation zone (based on flow thicknesses in drill hole RRL-2). These basalts consist principally of 0% to 35% pyroxene, 25% to 48% plagioclase, 0% to 6% iron-titanium oxides, 0% to 3% olivine, and 20% to 65% mesostasis of variable

composition (Noonan et al., 1980, pp. 1-7; Table 4.1-1). Textures vary considerably but are dominated by lath-shaped plagioclase and pyroxene in a glassy matrix. Grain size is also variable but averages about 0.1 to 0.2 mm (0.004 to 0.008 in.).

Although all Grande Ronde Basalt flows are similar in chemical composition, slight differences in some elemental abundances, particularly magnesium and titanium, allow each flow to be placed in one of three groups called Grande Ronde Basalt chemical types; very high magnesium, high magnesium, and low magnesium (Wright et al., 1979, pp. 1-13; Swanson et al., 1979, pp. G1-G59). (See Section 1.2 for a detailed description of chemical types.) Chemical analyses of any given flow are very similar throughout much of the Columbia Plateau so that chemical composition, or chemical types, can be used as a stratigraphic correlation tool. Only two of the three chemical types, the low-magnesium chemical type and the high-magnesium chemical type, are represented in the primary isolation zone. A more detailed discussion of the chemical composition and mineralogy of Grande Ronde Basalt within the controlled area study zone is given in Section 4.1.1.3.

Subsequent burial of the flows in the primary isolation zone by younger flows and interaction with groundwater resulted in partial alteration of basalt along fractures and partial filling of most vesicles and cooling joints with secondary minerals. Alternatively, some secondary minerals could have formed by deuteric processes. The dominant secondary minerals are clays, zeolites, and silica with lesser amounts of calcite and pyrite. In addition to filling fractures and vesicles, secondary alteration products are associated with breccias, both primary and tectonic, and with fault gouges. Secondary minerals in faults and breccias have not been studied, but investigations are planned as described in Section 8.3.

The secondary minerals in Grande Ronde Basalt formed as a result of basalt-water reactions. The specific, physicochemical conditions under which the secondary minerals formed are currently not well documented or well understood. Benson and Teague (1982, pp. 595-613) indicate that the secondary minerals in vesicles and fractures formed at temperatures slightly above surface temperature. However, secondary minerals similar to those found in the Grande Ronde Basalt are presently forming at temperatures up to 200 °C in Icelandic basalts (Kristmannsdottir, 1976, pp. 30-39; 1979, pp. 359-367). Future studies designed to elucidate the formation conditions and subsequent history of secondary minerals are described in Section 8.3.

The Vantage interbed overlies the Grande Ronde Basalt. The Vantage interbed varies in nature throughout the central Columbia Plateau from a clay-rich saprolite, to an erosion surface, to fluvial sands, muds, and gravels. Schmincke (1964) has made the most comprehensive study of the mineralogy and petrology of the Vantage interbed that exists to date. Schmincke's work, however, was primarily west and northwest of the Pasco Basin where the Vantage interbed is dominated by fluvial sediments. Within the controlled area study zone, the Vantage interbed varies from about 9 m (30 ft) of fluvial sediment in the western portion (McGee well) to less than about 0.5 m (1.6 ft) of

weathered basalt in the central and eastern portions (borehole RRL-2). Studies to describe the mineralogy and petrology of the Vantage interbed in the controlled area study zone are described in Section 8.3.

The lower buffer zone consists of Grande Ronde Basalt flows between the Umtanum flow, or base of the primary isolation zone, and the N^2/R^2 contact. These flows are similar mineralogically, petrographically, and geochemically to the Grande Ronde Basalt flows constituting the primary isolation zone, which is described above. All three Grande Ronde Basalt chemical types are represented in the lower buffer zone. A more detailed description of the Grande Ronde Basalt in the lower buffer zone is given in Sections 4.1.1.3.3 and 4.1.1.3.4.

The upper buffer zone consists of the Wanapum Basalt and the interbedded Squaw Creek and Quincy interbeds. The Wanapum Basalt is about 330 m (1,083 ft) thick and has a volume of about 70 km^3 (17 mi^3) in the controlled area study zone (based on thickness in drill hole RRL-2). It consists of four members, three of which are present in the controlled area study zone. The Wanapum Basalt flows consist principally of about 15% to 30% pyroxene, 20% to 50% plagioclase, up to 15% opaques, 0% to 7% olivine, and 15% to 60% mesostasis glass (Taylor, 1976, pp. 109-110; Myers, 1973, pp. 37-90). In general, Wanapum Basalt flows are mostly intergranular, intersertal, and hyalophitic. Some flows are coarsely plagioclase-phyric, but most are fine to medium grained.

Chemical analyses of Wanapum Basalt flows can be grouped, like the Grande Ronde Basalt flows, into chemical types. There are 14 Wanapum Basalt chemical types, 10 of which are present in the controlled area study zone. As with the Grande Ronde Basalt flows, Wanapum Basalt flows have fairly constant chemical compositions across the controlled area study zone and across much of the Columbia Plateau and have been used as a tool for geologic mapping and stratigraphic correlation (Wright et al., 1979; Swanson et al., 1979; Reidel, 1983; Holden and Hooper, 1976; Beeson et al., 1985).

The Squaw Creek and Quincy interbeds occur in the Wanapum Basalt. The Quincy interbed occurs between the Roza and Priest Rapids Members and the Squaw Creek occurs between the Frenchman Springs and Roza Members (see Figure 4.1-1). Very little work has been done on these interbeds in the controlled area study zone and central Pasco Basin. Schmincke (1964, p. 190) studied the Squaw Creek interbed outside the Pasco Basin and found it to consist of diatomite and arkosic sandstone between the Yakima and Columbia Rivers outside the Pasco Basin. Schmincke's work is mentioned here for completeness but, because the fluvial nature of the interbeds makes their distribution and lithology quite variable, it is likely that Schmincke's work may not be applicable to the controlled area study zone. The studies described in Section 8.3.1 are to be done in order to characterize the interbeds within the controlled area study zone.

4.1.1.2 Analytical techniques

Major element concentrations were obtained from samples of whole-rock Grande Ronde Basalt by x-ray fluorescence methods at Washington State University. Sample preparation and analytical techniques are described by Hooper et al. (1976, pp. 1-6). Trace element concentrations were determined by instrumental neutron activation analysis at the Oregon State University Center for Volcanology. Details of analytical techniques and data reduction techniques are given in Goles (1977, pp. 343-369). Selected trace element concentrations (zirconium, strontium, barium, rubidium, cerium, and yttrium) were also determined by x-ray fluorescence.

The FeO was determined by the method described in Wilson (1955, pp. 56-58). Briefly, the method involves dissolution of the sample and oxidation of iron with ammonium metavanadate. The solution is then colorimetrically titrated for the amount of vanadium reduced during the oxidation of iron. The method assumes that the ferrous/ferric ratio of the sample is not altered during sample preparation and that the sample contains no element, other than iron, that will be oxidized by the metavanadate. The Fe_2O_3 was calculated by the difference between total iron (determined by instrumental neutron activation analysis) and FeO concentrations.

Absorbed water was determined by the difference in weight before and after drying at 150 °C. Structural water was determined by the microcoulometric method described in Cremer et al. (1972, pp. 183-192).

Petrographic data (modes, textural description, and grain size) were obtained from polished thin-sections using a standard petrographic microscope and standard petrographic techniques. Modal analyses were done in reflected light and 4,000 points were included in each analysis.

The chemical compositions of individual, primary phases were obtained by electron microprobe methods. Mineral compositions reported in Section 4.1.1.3 are summarized from the work of Schiffman and Lofgren (1982, pp. 49-78), Long and Strope (1983, pp. 57-60), Reidel et al. (1978, pp. 2-10), and Noonan et al. (1980). These references can be consulted for beam currents, beam sizes, matrix corrections, and other specific analytical details.

Most of the information concerning secondary minerals presented in Section 4.1.1 is summarized from Benson and Teague (1979, pp. 1.146), Ames (1980, pp. 152-214), Rawson (1986a, 1986b), and Horton (1985). These workers used x-ray diffraction, optical microscopy, and scanning electron microscopy for mineral identification and electron microprobe methods for chemical compositions. Abundances of secondary minerals were obtained by visual estimation from scanning electron microscopy photomicrographs of 25 samples and by point count results of 9 thin sections (Benson and Teague, 1979, pp. 31-33 and p. 71).

4.1.1.3 Mineralogic, petrologic, and chemical composition of the repository isolation system

The geochemical, mineralogic, and petrologic characteristics of the repository isolation system are discussed in this section. These chracteristics will affect radionuclide isolation. The primary isolation zone is discussed in Sections 4.1.1.3.1 and 4.1.1.3.2, the lower buffer zone is discussed in Sections 4.1.1.3.3 and 4.1.1.3.4, and the upper buffer zone is discussed in Sections 4.1.1.3.5 and 4.1.1.3.6. The stratigraphic and lateral distribution of secondary phases can be used to predict potential changes in groundwater composition and radionuclide sorption along flowpaths to the accessible environment. Information on stratigraphic and lateral distributions of secondary phases is given in Section 4.1.1.3.7.

4.1.1.3.1 Chemical composition of the primary isolation zone

The whole-rock chemical composition of the Grande Ronde Basalt in the controlled area study zone and the central Pasco Basin are discussed in this section. The chemical composition of rock within the primary isolation zone is important to waste isolation because interactions between basalt and groundwater produce the secondary phases that will probably be responsible for most radionuclide retardation. Also, the fairly constant chemical composition within a given flow provides an important tool for stratigraphic correlation.

Major element composition of the primary isolation zone

Landon (1984) presented major element concentrations obtained from samples from boreholes throughout the Pasco Basin. Of the analyses presented by Landon, 342 are from Grande Ronde Basalt flows within the primary isolation zone. The results of these major element analyses are summarized in Table 4.1-2. The analyses used to construct the table are from boreholes not only within the controlled area study zone but scattered throughout the central Pasco Basin. A map of sample locations (boreholes) is shown in Figure 4.1-2. Detailed sample locations and depths are found in Landon (1984). Because chemical analyses for a given flow are fairly constant across much of the Columbia Plateau, the results shown in Table 4.1-2 that summarize the results obtained from throughout the central Pasco Basin differ little from results obtained only from the controlled area study zone. Analyses from the entire central Pasco Basin were used in Table 4.1-2 because data are available from 13 drill holes in the central Pasco Basin, but only 5 of these are within the controlled area study zone. (Drill holes DH-4 and DH-5, included in Landon (1984), were not used because they are in the northern Pasco Basin).

Several flows have been singled out in Table 4.1-2. Data for the Cohassett flow are shown separately because the Cohassett flow is the candidate horizon. The Levering and Birkett flows, respectively, overlie and underlie the Cohassett flow. The Rocky Coulee, McCoy Canyon, and Umtanum flows are represented separately because they were at one time considered

candidate repository horizons and much more is known about these flows and the Cohassett flow than is known about most other flows. Chemical analyses of all other Grande Ronde Basalt flows in the primary isolation zone are grouped together as high-magnesium chemical types. The Umtanum flow is the only flow in the primary isolation zone belonging to the low-magnesium chemical type.

As shown in the data in Table 4.1-2, there are no major differences in major element oxide concentrations among the Grande Ronde Basalt flows in the primary isolation zone. Slight differences do exist (e.g., the ranges of FeO, MgO, TiO, and P_2O_5 do not overlap for all flows), but the general similarity in the chemical composition of all flows in the primary isolation zone indicates that the types and rates of basalt-water reactions which are responsible for secondary mineral precipitation or dissolution and radionuclide retardation should be similar throughout the primary isolation zone in the controlled area study zone.

The data used to construct Table 4.1-2 are mostly from samples from flow interiors. Approximately 5% of the analyses (14 analyses), however, represent portions of drill core that were logged as brecciated, vesicular, or vuggy (Cross, 1983, pp. 1-142), and all but two of these samples yield one or more oxide values lying outside the two standard deviation range of the reported means. These differences may be due to secondary mineralization. This suggests that it may be useful during future work to look specifically at the major element composition of flow tops and vesicular zones to determine whether or not they are significantly different than flow interiors. Such work is described in Section 8.3.1. This also suggests that it may be important to group samples collected from brecciated, vesicular, and vuggy zones separately from flow interior samples during future manipulations of geochemical data.

Trace element composition of the primary isolation zone

Analyses of 23 trace elements were obtained from about 52 samples of Grande Ronde Basalt flows in the primary isolation zone (BRMC Index Record Nos. B062365-68, B062301-03, B062287-91, B062293). The results of these analyses are summarized in Table 4.1-3. Most trace element concentrations do not differ substantially between the two chemical types; only the means for chromium and thorium differ by one standard deviation or more. The differences, however, are in parts per million and are not expected to affect changes in any basalt-water-waste reactions that may occur in the primary isolation zone. All trace elements are present in such small quantities that they are not expected to influence basalt-water-waste reactions in the repository isolation system.

Water content of the primary isolation zone

Most basaltic magmas contain less than about 2 wt% H_2O, particularly at low pressure (see data for Columbia River basalt in Burnham, 1979, p. 448). Therefore, water content reflects, in part, the extent of alteration, especially hydration, that has affected the rock subsequent to formation.

Structural water (H_2O+), absorbed water (H_2O-), and total water were measured on several samples from the flow interiors of specific flows within the primary isolation zone. A summary of the data is given in Table 4.1-4. Sample locations and individual results are tabulated in Long et al. (1984, p. I-E-1). Because no analyses are available from samples collected within the controlled area study zone, the data used to construct the table are from drill holes throughout the central Pasco Basin. Also, data are only available from the basalt flows that were considered candidate repository horizons. Plans to obtain measurements of structural, absorbed, and total water from samples from other flows within the primary isolation zone within the controlled area study zone are discussed in Section 8.3.

Differences between the data given in Table 4.1-4, which is for the central Pasco Basin, and other data given in Long et al. (1984, p. I-97), from samples in the northern Pasco Basin and from the area near Vantage, Washington, are generally less than 10% and always less than 14%. This suggests that differences between the data in Table 4.1-4 and that expected from the controlled area study zone should not be great for the flows represented. Also, the similarity of results from the four represented flows suggests that water data from other flows in the primary isolation zone should be similar.

The values for H_2O- given in Table 4.1-4 represent the amount of water driven off the samples at temperatures below 150 °C. Most of this water is generally considered to be absorbed onto the sample and is not chemically bound or structural water. Water driven off the samples at temperatures above 150 °C (H_2O+) is mostly structural water and exists primarily as hydroxyls in the crystal structure of hydrous minerals and as hydroxyls and molecular water in mesostasis glass. Thus, the amount of this water is, in part, a function of the amounts of certain secondary minerals and mesostasis glass. The total water contents of flow interiors are, in general, well within the range of values reported for basaltic rocks (Carmichael et al., 1974, p. 9; Clark, 1966, p. 4). Based on the data from which Table 4.1-4 was constructed, Long et al. (1984, p. I-97) concluded that there were no statistically significant differences in water content among the flow interiors of the studied flows; i.e., all flows have the same water content within two standard deviations.

Flow tops and fault infillings generally contain larger quantities of hydrous secondary minerals, such as clays and zeolites, than do flow interiors. Thus, flow tops and fault infillings are expected to have slightly higher H_2O+ and H_2O- values than those shown in Table 4.1-4. Future chemical analysis of secondary minerals and secondary mineral-bearing samples of flow top will include H_2O where possible.

Oxidation state of iron in the primary isolation zone

The Eh of the basalt-water-waste system can exert a strong influence on the mobility of Eh-sensitive radionuclides. Thus, the potential for basalt to influence the Eh of the repository environment must be assessed (see

Section 4.1.3.4). Chemical analyses (see Table 4.1-2) indicate that iron is the most abundant Eh-sensitive element in the primary isolation zone.

A summary of the available data concerning the oxidation state of iron in Grande Ronde Basalt flows in the primary isolation zone is given in Table 4.1-5. Because analyses from only three samples from the Cohassett flow and three samples from the Umtanum flows are available from samples taken in the controlled area study zone, the table was constructed using data from drill holes throughout the central Pasco Basin. The sample locations and individual datum used for the table are tabulated in Long et al. (1984, p. I-F-1). Also, data are only available from the flow interiors of basalt flows that were considered candidate repository horizons. Plans to obtain measurements of FeO and Fe_2O_3 from samples of other flows within the primary isolation zone within the controlled area study zone are discussed in Section 8.3.

Differences in the data for samples from the Vantage, Washington, area (given in Long et al., 1984, p. I-F-1) and those given in Table 4.1-5 are not statistically significant; all Vantage, Washington, area samples are within two standard deviations of the mean values in Table 4.1-5. Based on the data in Table 4.1-5, there do not appear to be any significant differences in the oxidation state of iron among the four represented flows. This similarity of results from the four flows suggests that the oxidation state of iron in other flows in the primary isolation zone may be similar. Studies are described in Section 8.3 to determine what differences, if any, exist in the oxidation state of iron in flow tops and flow interiors. Also, work is outlined in Section 8.3.1 to investigate the Fe^{2+}/Fe^{3+} ratio of individual iron-bearing phases, particularly primary glass and secondary minerals, and to relate the results to the Fe^{2+}/Fe^{3+} ratio of the bulk rock.

4.1.1.3.2 General mineralogy and petrography in the primary isolation zone

The mineralogy and chemical composition of primary and secondary phases determine, in part, the chemical composition of species in groundwater, the kinds of basalt-water-waste reactions that may occur, and the magnitudes of possible interactions. For these reasons, the mineralogy and petrography of the primary isolation zone are important parameters when considering the performance of a mined geologic disposal system.

The mineralogy and petrography of Grande Ronde Basalt in the controlled area study zone have been described by Long et al. (1984, pp. I-99 to I-133). The following discussion of primary phases in the primary isolation zone is based on their descriptions, which are based on samples from the interiors of the four flows that were once considered candidate horizons. Preliminary examination shows that the same primary phases present in flow interiors are present in flow tops (Horton, 1985), but the petrography and mineralogy of primary phases described in this section strictly apply only to flow interiors. Petrographic and mineralogic investigations of flow top are under

way (as described in Section 8.3.1). Also, petrographic and mineralogic studies for flows other than the Rocky Coulee, Cohassett, McCoy Canyon, and Umtanum flows are planned and described in Section 8.3.1.

Grande Ronde Basalt flows are aphyric to microphyric to very sparsely phyric basalt with hyalophitic, intersertal to intergranular, or slightly ophitic textures. The dominant primary phases include plagioclase, clinopyroxene (augite), iron-titanium oxides, and glassy mesostasis. Less abundant phases include orthopyroxene, pigeonite, olivine, sulfide blebs, and apatite. The chemical and textural characteristics of primary phases in the primary isolation zone were listed in Table 4.1-1.

The mineralogy and petrology of secondary phases in Grande Ronde Basalt have been described by Benson and Teague (1979; 1982, pp. 595-613), Horton (1985), McKinley (1986), and Rawson (1986a). None of the samples studied by Benson and Teague were from drill holes within the controlled area study zone, and only four of nine drill holes studied by Horton, Rawson, and McKinley are in the controlled area study zone. Thus, because of the lack of information, the descriptions of secondary minerals given in this section are based on all available data from the central Pasco Basin. With the possible exception of celadonite, there do not appear to be any differences in the kinds or abundances of secondary phases between the central Pasco Basin as a whole and the controlled area study zone.

Reported secondary phases in Grande Ronde Basalt include clay minerals, principally smectites; zeolites, mainly clinoptilolite and mordenite; and calcite, pyrite, and silica in the forms of opal, quartz, chalcedony, cristobalite, and tridymite (Benson and Teague, 1979, pp. 25-41; 1982, pp. 595-613; Horton, 1985; McKinley, 1986; Rawson, 1986a). Also reported are minor amounts of erionite, chabazite, vermiculite, phillipsite, gypsum (one occurrence in borehole DH-5), celadonite, and illite (Benson and Teague, 1979, pp. 25-41; 1982, pp. 595-613). Each primary and secondary phase is discussed in more detail in the following sections. Phases that buffer pH and Eh of the groundwater are discussed in detail in Section 4.1.3.4.

Composition of primary phases in the primary isolation zone

Plagioclase. Plagioclase is the most abundant mineral in all Grande Ronde Basalt flows. It most commonly occurs as euhedral to subhedral laths ranging in length from about 0.02 to 6 mm (0.8×10^{-3} to 0.24 in.) and in width from about 0.01 to 1 mm (0.4×10^{-3} to 0.04 in.). Although plagioclase is almost invariably tabular or lath shaped, the details of crystal outline, size distribution, and general arrangement create notable differences in rock texture that have been used to differentiate intraflow structures (see Section 1.4). Samples from the interior of Grande Ronde Basalt flows exhibit no obvious preferred orientation of plagioclase laths, whereas samples from the glassy basal zones and vesicular flow tops may exhibit a strong preferred orientation (Long and Davidson, 1981, pp. 5-36).

Microphenocrysts of plagioclase are common, but typically not abundant; they, and the minute crystal inclusions in the mesostasis, impart a slight bimodal size distribution to the plagioclase grains (Long et al., 1984, p. I-109). Microphenocrysts contain glass or devitrified glass inclusions that presumably represent melt trapped in the crystals as they grew. These inclusions commonly occur along twin planes or are associated with embayed and corroded crystal interiors. Other inclusions are principally minute pyroxene grains arranged linearly along major changes in anorthite content (Long and Davidson, 1981, pp. 5-36).

Augite. Augite is the dominant clinopyroxene and the second most abundant mineral in the primary isolation zone. Early-formed augite grains exhibit prismatic forms that are best developed at the base of flows. In flow interiors, the prismatic morphology is obscured by late growth on early-formed crystals and by the formation of separate, smaller pyroxene grains. This yields an overall subhedral, slightly ragged shape to most pyroxene grains and imparts an apparent seriate to bimodal size distribution. Seriate distributions are most common in colonnades, whereas entablatures appear to have bimodal distributions. Augite grains range from about 0.01 to 5.0 mm (0.4×10^{-3} to 0.2 in.) in length, with an average of about 0.08 mm (3.2×10^{-3} in.). Prismatic grains are about four times as long as they are wide. Slight normal chemical zoning is nearly ubiquitous in the augite. The molar ratio of magnesium to magnesium plus iron spans the range of 55 to 70, and calcium contents range from about 30 to 40 mol% wollastonite (see Table 4.1-1). Inclusions are less common in clinopyroxene than in plagioclase, but both glass and unidentified crystalline inclusions do occur in the larger grains.

Pigeonite. Pigeonite, a second clinopyroxene phase, occurs in moderate to low abundance in many Grande Ronde Basalt flows. It occurs as both early-formed grains and as groundmass grains (Schiffman and Lofgren, 1982, pp. 49-78; Long and Strope, 1983). Long and Strope (1983) reported a range in pigeonite compositions of Wo_{13} En_{50} Fs_{27} to Wo_{9} En_{64} Fs_{29}. The distribution of pigeonite varies within single flows probably because of variations in the composition of residual liquid during the late stages of crystallization and variations in the degree of preservation of early-formed pigeonite microphenocrysts; both may reflect the cooling history.

Orthopyroxene. Orthopyroxene rarely occurs in Grande Ronde Basalt flows but has been reported from widely scattered localities across the Columbia Plateau (Reidel, 1978, pp. 148-163). Orthopyroxene grains are prismatic to rounded and about 1 to 2 mm (0.04 to 0.08 in.) in length. Reaction rims and resorption features are ubiquitous, and intimate intergrowth with large plagioclase grains is very common. Zoning is slight to absent, with most grains exhibiting a uniform, inclusion-free interior.

Iron-titanium oxides. Iron-titanium oxide constitutes 0 to 6 modal percent of Grande Ronde Basalt in the controlled area study zone. Some samples from very hackly entablature, flow bases, and flow tops exhibit a low abundance of iron-titanium oxides or lack iron-titanium oxides entirely. The dominant iron-titanium oxide is titaniferous magnetite. It occurs as

octahedral, cruciform, or dendritic grains ranging in size from 0.02 to 0.4 mm (0.8×10^{-3} to 0.02 in.). Octahedral or cruciform grains are typically subhedral. Blade-shaped laths of ilmenite also occur, although it is far less common than magnetite and is apparently absent from most samples (Long et al., 1984, p. I-101). The texture of iron-titanium oxides can be correlated with intraflow structures. Typically, colonnades have relatively coarse cruciform or octahedral crystals, whereas entablatures have dendritic crystals (Long and Wood, 1986, in press; McKinley and Rawson, 1985).

The complete composition range for titaniferous magnetite is not known, but samples from the Umtanum flow show a nearly constant TiO_2 content ranging from 28 to 32 wt% (Noonan et al., 1980, pp. 1-7). Further work is planned to determine the composition of magnetite in other flows within the primary isolation zone (see Section 8.3).

Preliminary investigations have noted hematite in 11 of 29 flow top samples from the Rocky Coulee and Cohassett flows in the central Pasco Basin (Horton, 1985). The hematite occurs as minute blebs, generally less than 0.02 mm (0.8×10^{-3} in.) in size, disseminated throughout the groundmass and as inclusions in plagioclase phenocrysts. Commonly, hematite is concentrated near the rims of vesicles and near the margin of flow-brecciated fragments. The hematite is interpreted to be a primary phase, based on its presence in basalt fragments and its absence from secondary infillings. The hematite may have formed when the flow tops were exposed to oxidizing, atmospheric conditions at high temperature (greater than several hundred degrees Celsius). Planned investigations to quantify the abundance of hematite in the primary isolation zone are described in Section 8.3.

Olivine. Olivine is relatively rare in Grande Ronde Basalt. Olivine compositions typically range from Fo_{67} to Fo_{47}, with moderate, normal zoning. Olivine phenocrysts are anhedral, equant, and about 0.05 mm (2×10^{-3} in.) in diameter.

Apatite. Apatite ranges from 0 to 2 modal percent. It generally occurs as 0.01- to 0.06-mm (0.4×10^{-3}- to 0.04-in.) acicular crystals in the mesostasis (Allen and Strope, 1983, pp. 1-7). Analyses indicate that these are fluorapatites. It has not been demonstrated whether sufficient fluoride can be leached from apatites to provide the observed fluoride concentrations in groundwater in the primary isolation zone. Further work is planned to investigate more adequately this and other possible chloride and fluoride sources (see Section 8.3).

Glassy mesostasis. Mesostasis is the last-formed interstitial material in Grande Ronde Basalt. It is most abundant in entablature and glassy flow bases and least abundant in colonnades. Texture within the mesostasis varies considerably with position in the flow. Glass in the colonnade, for example, contains abundant rod-shaped fluorapatite crystals, 10 to 60 μm in length, but is otherwise relatively inclusion free (Allen and Strope, 1983, p. 2). Glass or mesostasis in the entablature is invariably charged with 0.01 to 1.0 μm inclusions that are dominantly pyroxene but also include fluorapatite and magnetite. Some of the crystalline inclusions occur as rounded blebs,

suggesting that they represent a crystallized immiscible liquid (Philpotts, 1982, pp. 201-218). Similar evidence for liquid immiscibility is also present in colonnade samples but is absent from flow tops. The mesostasis in flow tops is characterized by felted masses of extremely fine-grained crystalline material within a selvage of glass; presumably, the crystallites are pyroxene (Long and Davidson, 1981, pp. 5-33 to 5-40).

Studies by Noonan et al. (1980, pp. 1-7) and Allen and Strope (1983) indicate that the mesostasis in the Umtanum flow is highly fractionated with a bulk composition that is essentially "granitic" (60 to 74 wt% SiO_2). Similar results have been obtained on mesostasis from colonnade samples of the Cohassett flow (Long et al., 1984, p. I-119). Variations in cation abundances exist between the mesostasis of entablature and colonnade. The Umtanum flow colonnade mesostasis contains relatively more K_2O and SiO_2, and less CaO, Na_2O, FeO, and P_2O_5 than the Umtanum flow entablature mesostasis (Noonan et al., 1980, pp. 1-7). Similar data will be collected for the Cohassett flow (see Section 8.3.1).

Apted and Myers (1982, pp. 1-78) demonstrated that mesostasis glass is the most reactive basaltic phase in groundwater at low to moderate temperatures (less than 300 °C). Laboratory tests and preliminary analysis of in situ groundwater chemical composition confirm that hydrolysis and dissolution of silicate glass (and possibly associated minerals) buffer, in part, the pH of groundwaters in contact with Grande Ronde Basalt (see Sections 3.9.1 and 3.7.3). Confirmation of pH controlling mechanisms is being investigated by hydrothermal tests (see Section 8.3.4). The testing and available results are discussed in Section 7.4.

Relative abundances of primary phases in the primary isolation zone

Long et al. (1984, pp. I-111 to I-116) reported results of point counts (modes) on 21 samples from the interiors of the Rocky Coulee, Cohassett, McCoy Canyon, and Umtanum flows. The modes indicate that plagioclase is more abundant than pyroxene in all studied flows. The modal abundance of glass in the Cohassett and McCoy Canyon flows is less than that of pyroxene (excluding pyroxene crystallites in glass), whereas pyroxene in the Rocky Coulee flow is approximately equal in abundance to glass. The Umtanum flow has a higher percentage of mesostasis and glass and slightly less plagioclase and pyroxene relative to that in other flows. Iron-titanium oxide abundance is approximately equal to all four flows (2 to 3 modal percent). Olivine abundance ranges from 0 to 3 modal percent, with the majority of samples containing less than 0.25 modal percent. Interstitial alteration products are fewer in the Umtanum flow (about 2 modal percent) than in other flows (about 5 to 6 modal percent).

Mesostasis makes up 20 to 65 modal percent of flow interiors. It contains primary glass (16 to 38 modal percent), minute primary crystals of plagioclase (2 to 20 modal percent), pyroxene (3 to 14 modal percent), iron-

titanium oxides (0 to 1 modal percent), and up to 8 modal percent polycrystalline inclusions (Long et al., 1984, p. I-113). Mesostasis also contains 0 to 0.5 modal percent sulfide blebs.

Composition of secondary phases in the primary isolation zone

The mineralogy of secondary phases may affect nuclear waste isolation in several ways. (1) Certain minerals can adsorb or otherwise fix radionuclides in their structure. Other minerals may avoid incorporation of radionuclides. (2) Certain minerals react with each other, with groundwater and, with radionuclides, thus changing some aspects of the geochemical environment. The new environment may inhibit or enhance radionuclide fixation and transport. (3) Certain minerals may precipitate in, or dissolve from, fractures and interconnected pore spaces. These reactions may physically alter groundwater flow paths.

Secondary minerals are potentially involved in all the above reactions for two reasons. First, secondary minerals are commonly concentrated in flow tops that are generally more porous and permeable than flow interiors. Flow tops are, therefore, probable aquifers in which chemical reactions can take place. Second, secondary minerals commonly line fractures and vesicles, which places them in intimate contact with the groundwater.

The principal secondary minerals in Grande Ronde Basalt are smectitic clays, zeolites (clinoptilolite and mordenite), and silica (Table 4.1-6). Celadonite, calcite, and pyrite are less common. Numerous other secondary minerals have been identified but are present in much lower abundances. The secondary minerals occur along fractures, in vugs, and in relatively porous, vesicular, and brecciated flow tops and flow bottoms. The basaltic glass (mesostasis) and groundmass adjacent to vesicles and fractures containing secondary minerals commonly are altered.

The data on secondary minerals reported herein are primarily from the work of Benson and Teague (1979; 1982, pp. 595-613), Ames (1980, pp. 152-215), Teague (1980, pp. 1-11), Horton (1985), and Rawson (1986a; 1986b). The work of Benson and Teague (1979; 1982), Teague (1980), and Ames (1980) is based on samples from drill cores in the central Pasco Basin but not within the controlled area study zone. The works of Horton (1985) and Rawson (1986a) are also based on samples from drill cores in the central Pasco Basin, but four of the nine drill cores studied by them are within the controlled area study zone. In addition, the works of Horton and Rawson are from the flow top zones for the four flows that were once considered candidate horizons. Benson and Teague, Teague, and Ames worked with samples from throughout the primary isolation zone.

Data obtained thus far on secondary minerals are incomplete and, in part, inconsistent. For example, the only x-ray diffraction pattern given by Benson and Teague (1979, p. 97) shows characteristics that suggest that the material they call smectite may be mixed-layer clay. In addition, most chemical analyses, as determined by electron microprobe, are incompatible with reported

mineralogic data in that they do not yield reasonable structural formulas. Finally, the dominant smectite is referred to as montmorillonite and nontronite by Ames (1980), as nontronite by Benson and Teague (1979), and as iron-saponite by Horton (1985). Each of these minerals has a different chemical composition and probably different stability fields. Therefore, the following descriptions of secondary minerals are tentative. Extensive work is in progress to resolve the inconsistencies (see Section 8.3.1). This work includes detailed mineralogic and chemical analyses (both major and trace elements) aimed at better defining the phases present and their relative abundances.

Smectite. Smectite is one of the most abundant and widespread secondary minerals in the primary isolation zone (Benson and Teague, 1979; Rawson, 1986a). Benson and Teague (1979) state that the smectite is probably nontronite (a dioctahedral iron-rich smectite), Ames (1980) identified the smectite as montmorillonite and nontronite, and Horton (1985) identified the smectite as iron-saponite. Rawson (1986a) presents x-ray diffraction data indicating that the smectite is trioctahedral, and the electron microprobe data (BRMC Index Record No. B088328) indicate that it is iron-rich. Thus, the smectite is an iron-saponite. (See Section 4.1.1.4 for discussion of the stabilities of the various smectite minerals.)

Horton (1985) distinguished three different, but mineralogically similar, trioctahedral smectites based on thin section petrography and microprobe analyses in the Rocky Coulee and Cohassett flow tops. These are called early, intermediate, and late smectite based on paragenetic position. The early smectite is an alteration product of mesostasis glass and, to a lesser extent, pyroxene. The other two are precipitates: the intermediate smectite is generally fibrous, banded, and predates zeolite; the late smectite is generally massive and postdates zeolite. The average compositions, as determined by electron microprobe, for the three smectites are shown in Table 4.1-7 (BRMC Index Record No. B088328). Because the compositions are averages, they do not represent any specific mineral. All iron is assumed to be divalent rather than trivalent because this is more consistent with a trioctahedral smectite, although the assumption is probably not strictly true. Experiments are under way to partition iron in secondary minerals into FeO and Fe_2O_3. These experiments are described in Section 8.3.1.

Benson and Teague (1979, pp. 136-138) also give average analyses, but their data include some analyses from the lower buffer zone and a few analyses from the upper buffer zone. Also, they do not distinguish the same three specific smectites. Their average for all clays, however, is similar to the averages shown in Table 4.1-7.

The early smectites, which are an alteration product of mesostasis glass, are characterized by relatively high FeO and Al_2O_3 and relatively low MgO. The intermediate smectites, which precipitated in voids prior to zeolite deposition, are characterized by relatively low FeO and relatively high Al_2O_3 and MgO. Finally, late smectites, which precipitated after zeolite deposition, are characterized by relatively high FeO and relatively low Al_2O_3 and MgO. Although the mean of certain oxides, and especially oxide ratios,

are fairly distinct among the three smectites, the ranges for some oxide values are fairly broad, particularly for the intermediate smectites. It is possible that the broad ranges are real and reflect the greater number of analyses for the intermediate than for other two smectites. However, the decision to classify a specific analysis as early or intermediate smectite is sometimes difficult, especially where definitive textures are not present. Therefore, it is possible that some analyses are placed in the wrong category and, thus, are partly responsible for the broad ranges. Also, some of the analyses may represent non-monomineralic areas under the electron beam. For example, the 9.65 wt% TiO_2 indicated as the maximum value for intermediate smectite is unreasonably high for this clay. In addition, many individual analyses do not give reasonable structural formulas, which again suggests a non-monomineralic sample. Work is under way to determine what phases, if any, are mixed with the smectite on the scale of the electron beam (see Section 8.3.1).

Smectites, similar to those reported in the Grande Ronde Basalt flows in the primary isolation zone, reversibly lose interlayer water when heated to the relatively low temperatures of 100 °C to about 370 °C at atmospheric pressure (MacEwan, 1972, pp. 188 and 201; Palmer et al., 1983, p. 1-27). Above this temperature range, loss of water and collapse of the structure is irreversible, and low-temperature minerals are converted to higher temperature phases. The exact temperature, at fixed pressure, at which irreversible loss of water occurs depends on the particular mineral and the exchangeable cations (MacEwan, 1972, p. 188). Recently, a thermal analysis of the current Basalt Waste Isolation Project (BWIP) waste package design in the postemplacement environment was completed (Yung et al., 1986). The analysis indicated that the container for consolidated spent fuel may reach a maximum temperature of about 250 °C and that the adjacent basalt may reach 186 °C. The latter temperature is well within the range for which some natural trioctahedral smectites reversibly dehydrate at one atmosphere pressure.

The effect of pressure on smectite dehydration has been investigated by Koster van Groos and Guggenheim (1984, pp. 872-879) who found a large increase in the stability of a hydrated smectite with only a small increase in pressure. Loss of interlayer water leads to a reduction in volume and an increase in porosity.

Estimates of the amount of water available for release from smectite and the amount of associated volume reduction can be obtained from data available in the literature (Brigatti, 1982, p. 98). Nine chemical analyses of nontronite (a smectite similar to the iron-saponite reported in the primary isolation zone) that include values for H_2O- have been compiled by Brigatti (1982, p. 98; analyses N.1, N.6, N.7, N.8, N.10, N.11, N.14, N.19, and N.21). If these clays were heated to completely dehydrate the interlayers, 34 to 66 g H_2O/mol clay or 1.9 to 3.6 mol H_2O/mol clay could be evolved. It must be remembered that these are estimates based on the water content, at one atmosphere, of clays reported in the literature. The analyses given by Brigatti (1982, p. 98) contain calcium as the dominant interlayer cation. The average chemical analysis given in Table 4.1-7 suggests that sodium and potassium are also important interlayer cations in the smectites. Since

interlayers containing monovalent cations often contain less water than interlayers with divalent cations, the clays in the primary isolation zone might be expected to evolve less water than that given by the above estimates. However, further work is needed to confirm this. Investigations discussed in Section 8.3.1 will allow more precise estimates of water loss for clays and zeolites specific to the primary isolation zone.

The volume change associated with dehydration of a smectite can be estimated using $\underline{a}$ = 5.12 Å, $\underline{b}$ = 9.02 Å (Brindley, 1980, p. 172), and $\underline{c}$ = 12.5 Å for a Na^+ or K^+ saturated clay and $\underline{c}$ = 15.2 Å for a Ca^{2+} or a Mg^{2+} saturated clay ($\underline{a}$, $\underline{b}$, and $\underline{c}$ are crystallographic axes). These values are for hydrated smectites. Thus, the unit cell volume of hydrated smectite is about 577 $Å^3$ with monovalent interlayer cations and about 702 $Å^3$ with divalent interlayer cations. Dehydration does not greatly affect the $\underline{a}$ or $\underline{b}$ dimensions of a smectite but does cause the $\underline{c}$ dimension to collapse to about 10 Å. Therefore, unit cell volumes for dehydrated smectite will be about 470 $Å^3$ regardless of interlayer cation species. This represents a volume reduction of 18% or 33%. This does not, however, mean an increase of 18% or 33% in overall porosity because, in the primary isolation zone, smectite makes up about 75% of the minerals in fractures (see Table 4.1-6) and fractures make up less than about 0.27% to 0.32% by volume (determined visually in drill core) of the total rock (Long et al., 1984, p. I-126; Long and Davidson, 1981, p. 5-27). Using the above values for volume reduction, percent smectite, and percent fractures, an increase in porosity of 0.036% to 0.079% is estimated. The estimated increases in porosity are preliminary estimates because only fractures and not vugs and vesicles have been considered and because the estimated clay content is from samples throughout the Pasco Basin and not solely within the controlled area study zone. Further work is planned to refine these estimates (see Section 8.3.1).

Zeolites. Clinoptilolite is the most abundant zeolite in the basalt flows making up the primary isolation zone (Benson and Teague, 1979; Horton, 1985; Rawson, 1986a). Clinoptilolite generally occurs as intergrown, blocky or tabular crystals that are generally 0.01 to 0.09 mm (0.4×10^{-3} to 3.5×10^{-3} in.) and uncommonly up to about 0.8 mm (3×10^{-3}) long (Horton, 1985). Benson and Teague (1979) interpreted mineral textures seen with the scanning electron microscope to indicate minor clinoptilolite dissolution. Horton (1985) found no petrographic evidence for clinoptilolite dissolution in samples of Rocky Coulee and Cohassett flow tops. The average composition of clinoptilolite from the Rocky Coulee and Cohassett flow tops (BRMC Index Record No. B088328) and from the work of Benson and Teague (1979) is shown in Table 4.1-8. The average oxide values given in Benson and Teague are mostly for analyses of clinoptilolite in the primary isolation zone but do contain some analyses from the lower buffer zone and a few from the upper buffer zone. Nevertheless, their averages are similar to those from the Cohassett and Rocky Coulee flows.

Most electron microprobe analyses of clinoptilolite used to construct Table 4.1-8 yield structural formulas that are not electrically neutral. This probably results from migration and volatization of sodium and potassium due to too high a beam current and too small a spot size. Work is under way to

determine whether or not this is the cause for the charge imbalances and, if so, what the optimum electron beam conditions are to produce electrically neutral analyses of clinoptilolite (Chapter 8.3.1).

Zeolites other than clinoptilolite have been reported from samples in the primary isolation zone. Benson and Teague (1979) report one sample each containing analcime, erionite, mordenite, chabazite, and phillipsite. Ames (1980) reports heulandite and gmelinite. Neither Benson and Teague nor Ames published diffraction patterns or chemical analyses of these zeolites. Ames distinguished heulandite from clinoptilolite by x-ray diffraction methods that are much less reliable than chemical analyses or reaction to heat treatment prior to x-ray diffraction analysis. Rawson (1986a) found no zeolites other than clinoptilolite in the primary isolation zone.

Zeolites, like clays, undergo dehydration-hydration and volume changes with changes in temperature. The specific temperature at which these changes take place depends on the specific zeolite species and its composition (Boles, 1972, pp. 1463-1493; Bish, 1984, pp. 444-452). For example, Bish (1984) found that sodium-saturated clinoptilolite underwent a volume decrease of 8.4% between 50 and 300 °C, whereas potassium-saturated clinoptilolite decreased only 1.6% over the same temperature range. Investigations are planned that will allow estimation of the physical changes that the zeolites in the primary isolation zone may undergo in response to temperature perturbations in order to estimate volume changes that might affect porosity (see Section 8.3.1).

Silica. Silica occurs as amorphous silica, cristobalite, tridymite, and quartz in the primary isolation zone (Benson and Teague, 1979, 1982; Rawson, 1986a; Horton, 1985). X-ray diffraction patterns of cristobalitic and tridymitic samples resemble diffraction patterns of opal-C and opal-CT. In thin section, amorphous silica (opal-A) is colorless to brown and isotropic. Opal-C and opal-CT are generally colorless and commonly have chalcedonic, acicular, and bladed textures. Where quartz is present with chalcedonic silica, it generally overlies the opaline varieties (Horton, 1985).

Electron microprobe analyses of silica precipitated in the Rocky Coulee and Cohassett flow tops is presented in Table 4.1-9 (BRMC Index Record No. B088328). The analyses have been separated into two groups depending on whether the silica is colored (usually brown) or colorless to slightly gray. The colored varieties, which are generally isotropic, contain significantly more of the oxides other than SiO_2, whereas the colorless varieties are essentially all silica and commonly have chalcedonic textures. The colored siliceous material may represent the precursor to some clay or zeolitic mineral.

Analyses of the colorless varieties generally total greater than 90 wt%, whereas the colored varieties generally total about 50 to 60 wt% (Horton, 1985). The reasons for the low totals for the colored varieties are not known at this time but are probably due to a combination of void space under the electron beam and water included in the siliceous material. Work is planned and discussed in Section 8.3.1 to obtain x-ray diffraction and electron

microprobe analyses of siliceous materials from flow tops other than the Rocky Coulee and Cohassett flow tops and to understand the low totals for the colored varieties of silica.

Celadonite is not as abundant or widespread as smectite, zeolite, or silica. Rawson (1986a) and Horton (1985) found celadonite in only four of nine drill holes and only one sample from within the controlled area study zone. Benson and Teague (1979) identified a mineral as illite that they consider may be celadonite in drill holes outside the controlled area study zone but within the central Pasco Basin. No chemical analyses are available for the celadonite found by Rawson (1986a) within the controlled area study zone, but the chemical composition for some analyses of celadonite outside the controlled area study zone and within the central Pasco Basin is given in Table 4.1-10 (BRMC Index Record No. B088328).

Calcite and pyrite are less abundant and less widespread than clay, zeolite, and silica (Benson and Teague, 1979; Rawson, 1986a; Horton, 1985). Calcite generally occurs as sparry crystals although fine-grained, granular, calcite has been noted. Two electron microprobe analyses of calcite indicate that the mineral is low-magnesium, low-iron, and low-manganese calcite (Horton, 1985). Pyrite generally occurs as fined-grained, disseminated cubes on fracture surfaces and surfaces of breccia fragments. Extremely small pyrite framboids were found in one sample (Horton, 1985). Electron microprobe analyses of pyrite indicates that the mineral is more than 99 normalized wt% FeS_2 (McKinley, 1986).

Relative abundance of secondary phases in the primary isolation zone

Benson and Teague (1979) estimated relative abundances using drill holes throughout the Pasco Basin. However, no work has been done specifically within the controlled area study zone. Benson and Teague's estimates of the relative abundances of the principal secondary minerals in the Grande Ronde Basalt in the central Pasco Basin were given in Table 4.1-6. These estimates include a few samples from the lower buffer zone and are visual estimates based on scanning electron microscopy observations. Long et al. (1984, p. I-124) and Lindberg (1986, p. 48) made similar estimates for specific flow interiors within the controlled area study zone. Their data are shown in Table 4.1-11. Plans to estimate relative abundances by more precise methods such as x-ray diffraction and point count techniques are described in Section 8.3.1.

Comparison of the results shown in Tables 4.1-6 and 4.1-11 indicates that the relative abundances of secondary minerals in the controlled area study zone is similar to that throughout the central Pasco Basin. Specifically, clay is the dominant secondary mineral in fractures, followed by zeolite and then silica. As shown by the Long et al. (1984) and Lindberg (1986) data in Table 4.1-11, the relative abundances of secondary minerals in the interiors of all proposed candidate flows are similar except for the Umtanum flow. The Umtanum flow has a significantly lower average proportion of clay and higher proportion of zeolite than do the other proposed candidate flows. In

addition, Lindberg (1986, p. 49) found that the Umtanum flow is the only studied flow that has significant differences in the percentage of predominant fracture filling minerals between the entablature and colonnade; clay is more abundant and zeolite less abundant in the colonnade than in the entablature. It is not yet understood why the relative abundances of secondary minerals in the Umtanum flow differ from those in other flows within the primary isolation zone. Studies are planned and described in Section 8.3.1, which should lead to an understanding of secondary mineral distributions.

Differences in the relative abundances of secondary minerals between flows may result in differences in their sorptive capacities for certain radionuclides. The data in Table 4.1-11, however, indicate that most of the flows in the primary isolation zone are similar; therefore, reactions involving secondary minerals should be similar and proceed to the same extent throughout the primary isolation zone. However, more work should be done with relative abundances in other flows within the primary isolation zone to support this conclusion; such work is described in Section 8.3.1.

Origin and paragenesis of secondary phases in the primary isolation zone

The origin and paragenesis of secondary minerals present within the host rock and along potential flow paths need to be understood. The origin and paragenesis could be used to interpret past geochemical conditions and the rates of change of past conditions. The rates of change may be extrapolated so that future geochemical conditions may be predicted.

The secondary minerals in Grande Ronde Basalt formed as a result of interaction between rock, primarily mesostasis (Lane et al., 1984, p. 95-103; Allen et al., 1985) and water. Benson and Teague (1982, pp. 595-613) believe that the secondary minerals formed from alteration of basalt by groundwaters at temperatures slightly above surface temperature. Almost all the identified secondary minerals are known to form from alteration of basalt, but they are also known to form and exist over a wide range of temperatures from ambient, or slightly above ambient, to about 200 °C (e.g., see Kristmannsdottir, 1975, pp. 441-445). A study of fluid inclusions in secondary minerals was attempted to ascertain the temperature and salinity of depositional fluids, but the appropriate inclusions with vapor bubbles large enough to see did not exist (BRMC Index Record No. B057636). Petrographic, stable isotopic, and radiometric age dating studies are planned to help determine the formation conditions of existing secondary phases. These studies are described in Section 8.3.1.

Horton (1985), based on petrographic observations, found the paragenetic sequence of secondary minerals in two flow tops to be early smectite (oldest), intermediate smectite, clinoptilolite, late smectite, and calcite (youngest). Silica is older than zeolite in some samples but younger than zeolite in other samples. Celadonite predates intermediate smectite.

Paragenetic studies by Benson and Teague (1979) on secondary mineral assemblages yielded the following observations.

- o In vesicles and fractures having multiple generations of clay or clinoptilolite, chemical composition often changes significantly from generation to generation.
- o Single generations of clay in vesicles and fractures appear homogeneous.
- o All generations from the same depth appear to exhibit similar compositional variations.
- o No overall systematic trend in composition as a function of distance from vesicle or fracture walls has been found. This last statement is in contrast to the early, intermediate, and late smectites described by Horton (1985).

Benson and Teague (1979, pp. 14-15) state that clay is the first mineral to form in 96% of the fractures and in 94% of the vesicles. Clinoptilolite is the first formed mineral in the remaining fractures and vesicles and is the second formed phase in 81% of the fractures and in 97% of the vesicles. For fractures and vesicles with additional layers, silica followed by clinoptilolite is the sequence in 100% of the fractures and 67% of the vesicles. Clay precipitated after zeolite in the remaining 33% of the vesicles. None of these observations are in conflict with the paragenetic sequence of Horton (1985). The fact that clinoptilolite and not clay was the first mineral to precipitate in some vesicles probably simply reflects a changing hydrologic system such that older clay-precipitating fluids did not enter all vesicles.

Interbed in the primary isolation zone

The Vantage interbed, the only interbed in the primary isolation zone, overlies the Grande Ronde Basalt and is the uppermost rock unit in the primary isolation zone. It occurs in all cored drill holes in the controlled area study zone but in only 11 of 14 cored drill holes in the central Pasco Basin. To date, little is known about the petrology of the Vantage interbed. What information is known comes mostly from stratigraphic studies (see Section 1.2) and from petrographic, stratigraphic, and sedimentologic descriptions given in Schmincke (1964, pp. 1-425). Unfortunately, Schmincke's description of the Vantage interbed is from areas northwest of the central Pasco Basin where the Vantage is represented by up to 10 m (33 ft) of mostly fluvial sandstone and siltstone. Within the controlled area study zone and central Pasco Basin, the Vantage interbed is much thinner, on the order of 2 m (7 ft) or less (Landon, 1985), and consists mostly of siltstone, mudstone, and saprolite, which are indurated or baked at the contacts with overlying basalt (Wintczak, 1983; Diediker, 1983). Thus Schmincke's description is probably not applicable to the controlled area study zone. Studies are planned (see Section 8.3.1) to characterize the mineralogy and petrology of the Vantage interbed in the controlled area study zone.

4.1.1.3.3 Chemical composition of the lower buffer zone

This section discusses the whole-rock, chemical composition and mineralogy of the lower buffer zone in the controlled area study zone and central Pasco Basin. The lower buffer zone consists of the Grande Ronde Basalt flow below the Umtanum flow and above the N_2/R_2 paleomagnetic horizon. The chemical composition of rock within the lower buffer zone is important to waste isolation because basalt-water interactions in this zone will produce secondary phases that will be partly responsible for retardation of any downward transported radionuclides not sorbed in the primary isolation zone. Also, as with the primary isolation zone, the fairly constant chemical composition within a given flow provides an important tool for stratigraphic correlation. Less is known about the lower buffer zone than is known about the primary isolation zone primarily because the primary isolation zone is where the majority of radionuclide sorption is expected to take place and, therefore, has been the focus of BWIP studies.

Major element composition of the lower buffer zone

Major element concentrations of rocks from the lower buffer zone have been obtained from drill holes throughout the controlled area study zone and the central Pasco Basin (Landon, 1984). The means of those analyses are presented in Table 4.1-12. A borehole location map was given in Figure 4.1-2, and detailed sample locations and depths are given in Landon (1984).

There is only one flow in the lower buffer zone that belongs to the very high-magnesium chemical type. Thus, all the analyses for this chemical type in Table 4.1-12 are from a single flow. Also, analyses of the high-magnesium chemical type are from three flows near the top of the lower buffer zone. Most flows in the lower buffer zone are of the low-magnesium chemical type. Although there are differences in the three types of flows in the lower buffer zone, all analyses are more similar than they are different. Also, comparison of the analyses of the lower buffer zone (see Table 4.1-12) with those of the primary isolation zone (see Table 4.1-2) shows that there are no major differences between the basalts in the primary isolation zone and lower buffer zone. The general similarities suggest that the types and rates of basalt-water reactions expected to occur in the lower buffer zone should be similar to those that will occur in the primary isolation zone, and because the chemical composition for a given flow is fairly constant throughout the Pasco Basin and Columbia Plateau, the types and rates of reactions are not expected to vary due to changing whole-rock chemical composition across the controlled area study zone.

Trace element composition of the lower buffer zone

Analyses of 21 trace elements were obtained from samples of Grande Ronde Basalt flows in the lower buffer zone (BRMC Index Record No. B062365-68, B062301-03, B062297-99, B062294-95, B062287-91, B062293). The results of these analyses are summarized in Table 4.1-13. Most trace element concentrations do not differ substantially among the three chemical types; only the means for chromium, rubidium, lanthanum, and thorium differ by one

standard deviation or more. With the exception of lanthanum, these are the same elements that showed some variation in the primary isolation zone. Just as for the primary isolation zone, all trace elements are present in small quantities, and differences among trace element concentrations for the three chemical types are in parts per million. Therefore, trace elements are not expected to influence basalt-water-waste reactions in the repository isolation system. More trace element analyses will be obtained, however, for use in stratigrahic correlation and as possible analog elements (see Section 8.3.1).

Water content and oxidation state of iron in the lower buffer zone

No analyses for structural, adsorbed, and total water and for the ferrous/ferric partition of iron have been done on Grande Ronde Basalt in the lower buffer zone. Because the chemical composition of the basalts in the lower buffer zone is similar to the composition of basalts in the primary isolation zone, it might be expected that water content and iron speciation are similar. This, however, remains to be shown, and studies are planned and described in Section 8.3.1 to make some iron and water determinations for rocks from the lower buffer zone.

4.1.1.3.4 General mineralogy and petrography of the lower buffer zone

There are no published petrographic descriptions specific to basalt flows in the lower buffer zone. Petrographic work done on Grande Ronde Basalt flows throughout the Columbia Plateau do not indicate, however, that there are any major differences in the mineralogy or petrographic textures between flows occurring above and below the Umtanum flow (Taylor, 1976; Ross, 1978). Thus, the textures and mineralogy of the lower buffer zone are, in general, similar to those in the primary isolation zone. Work is planned in Section 8.3.1 to support this conclusion for the lower buffer zone within the controlled area study zone.

Petrographic modal analysis for six samples from one flow in the lower buffer zone within the controlled area study zone are available (BRMC Index Record No. B052882 through B052887). The results of the analyses are shown in Table 4.1-14. The values for plagioclase, pyroxene, and olivine include both microphenocrysts and microlites; microphenocrysts alone total 8 modal percent to 11 modal percent for plagioclase, 3 modal percent to 10 modal percent for pyroxene, and less than 1 modal percent for olivine. Values for mesostasis include both glass and smectite crystallites; glass alone totals between less than 1 modal percent to about 6 modal percent for the samples listed. Alteration products for all samples are dominated by clay, and the sample entitled "Other" includes apatite, sulfide blebs, and void space. Comparison of the modes for the lower buffer zone with those for the primary isolation zone (see Table 4.1-6) shows that the two are mineralogically similar just as they are chemically similar. Studies to obtain petrographic modes for other flows in the lower buffer zone are described in Section 8.3.1.

Not as much is known about the secondary phases in the lower buffer zone as is known about these phases in the primary isolation zone. Benson and Teague (1979) studied secondary minerals in 15 samples from the lower buffer zone obtained from two drill holes one of which is within the controlled area study zone and the other in the central Pasco Basin. They found that the types of secondary minerals present are similar to those present in the primary isolation zone; that is, smectite, clinoptilolite, and silica are the dominant phases and mordenite and calcite are less abundant. Rawson (1986b) presented x-ray diffraction data from eight samples of secondary minerals in Grande Ronde Basalt flows below the lower buffer zone, and the results indicated that smectite, clinoptilolite, and silica are the dominant phases and celadonite and calcite are less abundant. Thus, it appears that the types of secondary phases present in the lower buffer zone are similar to those in the primary isolation zone and to those in flows below the lower buffer zone. Based on the limited data, there may be differences, however, in the relative abundances of secondary phases between the primary isolation zone and lower buffer zone. Quartz appears to be more abundant relative to opal-C and opal-CT, and mordenite seems to be more common in the lower buffer zone than in the primary isolation zone (Benson and Teague, 1979; Rawson, 1986b). Further work needs to be done to better document the apparent changes in relative abundances of secondary minerals with depth. This work is described in Section 8.3.1.

4.1.1.3.5 Chemical composition of the upper buffer zone

The upper buffer zone consists of basalt flows of the Wanapum Basalt and minor discontinuous sedimentary interbeds (see Fig. 4.1-1). Not as much information is available for rock within the upper buffer zone as is available for the primary isolation zone because past work has concentrated on flows within the primary isolation zone that were considered candidate horizons. Additional work is planned for the upper buffer zone (see Section 8.3.1) because the mineralogy and petrology of this zone is important in interpreting and predicting potential basalt-water-waste reactions involving any upward transported radionuclides not sorbed in the primary isolation zone.

Major element composition of the upper buffer zone

Major element concentrations for rock within the upper buffer zone have been obtained from drill holes throughout the controlled area study zone and the central Pasco Basin (Landon, 1984). The means of those analyses are presented in Table 4.1-15. A borehole location map was given in Figure 4.1-2, and detailed sample locations and depths are given in Landon (1984). Each of the formations listed in Table 4.1.15 is composed of several flows. Thus, the data are averages for the entire formations.

Comparison of the chemical composition of the upper buffer zone with that of the primary isolation zone (see Table 4.1-2) indicates that the two are, in general, the same. There are, however, slight differences such as slightly

lower SiO_2 and greater FeO in the upper buffer zone compared with the primary isolation zone, but these differences are small and are not expected to result in radically different basalt-water reactions.

Trace element composition of the upper buffer zone

Analyses of 23 trace elements were obtained from four samples of the Frenchman Springs Member of the Wanapum Basalt in the upper buffer zone (BRMC Index Records No. B062297-99). The results of these analyses are summarized in Table 4.1-16. Plans are described in Section 8.3.1 to obtain trace element compositions for the Roza and Priest Rapids Members of the Wanapum Basalt in the upper buffer zone. As shown in the data in Table 4.1-16, all trace elements are present in small quantities and so, as for the primary isolation zone and lower buffer zone, trace element concentrations are not expected to influence basalt-water-waste reactions in the repository isolation system.

Water content and oxidation state of iron in the upper buffer zone

No data concerning the distribution of iron between the ferrous and ferric state or for structural, adsorbed, and total water are available for rock from the upper buffer zone. Planned studies to obtain this information are described in Section 8.3.1.

4.1.1.3.6 General mineralogy and petrography of the upper buffer zone

Little mineralogic and petrographic work has been done on the upper buffer zone in the controlled area study zone. Several studies, however, have been done on equivalent rocks outside the controlled area study zone and Pasco Basin (Ross, 1978; Beeson et al., 1985; Gardner et al., 1981; Myers, 1973; Taylor, 1976).

These studies have found that, in general, basalt flows in rocks equivalent to the upper buffer zone in the controlled area study zone are composed dominantly of plagioclase, clinopyroxene, and glass with lesser amounts of olivine and opaques. Rock textures are typically sparsely phyric to abundantly phyric and intergranular or intersertial (Beeson et al., 1985; Ross, 1978). Plagioclase glomerocrysts are common in some flows. The groundmass is fine to coarse grained and generally contains equant or acicular, plagioclase microphenocrysts (Beeson et al., 1985). Taylor (1976) indicated that in the Saddle Mountains north of the Pasco Basin, the basalts in the Wanapum Basalt are generally coarser grained than those in the Grande Ronde Basalt.

Modal analyses for four samples from the Frenchman Springs Member of the Wanapum Basalt obtained from drill hole RRL-6 in the controlled area study zone are presented in Table 4.1-17 (BRMC Index Record No. B052844 through B052847; see Figure 4.1-2 for location of drill hole). The values for

plagioclase, pyroxene and olivine include both microphenocrysts and microlites; microphenocrysts alone total about 1.8% to 4% for plagioclase, about 0.5% to 10% for pyroxene, and no olivine microphenocrysts were noted. Values for mesostasis include both glass and minute crystallites; glass alone totals about 15% to 19% for the samples listed. Alteration products for all samples are exclusively clay, and the sample entitled "Other" includes apatite, sulfides, and void space, which apatite dominates. Average modal analyses of each of the basalt members of the Wanapum Basalt are also presented in Table 4.1-17. The averages and standard deviations were calculated from data in Taylor (1976) who studied the Wanapum Basalt in the Saddle Mountains north of the Pasco Basin.

Comparison of the modes from rock within the controlled area study zone with those from the Saddle Mountains indicates that, although there are minor differences the mineralogic makeup of the Frenchman Springs Member, it is fairly constant between the controlled area study zone and the Saddle Mountains. The major differences appear to be in the amounts of mesostasis and opaques (iron-titanium oxides). In addition, there appears to be little difference in the average mode among the three members in the Saddle Mountains area. This suggests that no major differences are to be expected among modal analyses from the three members in the controlled area study zone. Plans to gather modal analyses from the Priest Rapids and Roza Members within the controlled area study zone to support this supposition are described in Section 8.3.1.

Finally, comparison of the modes for rocks within the upper buffer zone (see Table 4.1-17) with those from rocks in the primary isolation zone (see Table 4.1-1) indicates that there is more olivine in the upper buffer zone than there is in the primary isolation zone; otherwise, basalts in the two zones within the controlled area study zone are mineralogically similar. This suggests that mineralogical effects on basalt-water-waste reactions in the primary isolation zone should be similar to those in the upper buffer zone.

Not as much is known about the secondary phases in the upper buffer zone as is known about these phases in the primary isolation zone. Rawson (1986b) presented x-ray diffraction data for 5 samples from the Frenchman Springs Member, 12 samples from the Roza Member, and 1 sample from the Priest Rapids Member of the Wanapum Basalt. All of the samples are from drill holes in the central Pasco Basin, but only eight samples are from drill holes in the controlled area study zone. Rawson (1986b) found trioctahedral smectite, clinoptilolite, calcite, and pyrite in the Priest Rapids Member sample. Smectite and clinoptilolite were found in all the Frenchman Springs Member samples, but the smectite in two of the samples is dioctahedral. Minor quartz, opal-C, opal-CT, celadonite, and calcite were found in some of the Frenchman Springs Member samples. All samples from the Roza Member contained trioctahedral smectite, and all but one contained clinoptilolite. Minor silica (quartz, opal-C, and opal-CT), pyrite (three samples), calcite (one sample), and phillipsite (one sample) were identified in the Roza Member. Benson and Teague (1979) studied the secondary minerals in two samples from the Frenchman Springs Member in the central Pasco Basin and found smectite,

quartz, and minor opal. Comparison of the x-ray diffraction patterns from samples of the upper buffer zone (Rawson, 1986b) with those from the primary isolation zone (Rawson, 1986a) indicates that the x-ray characteristics (mineralogic and crystallographic characteristics) are similar, in general, between the two zones. However, the dioctahedral smectite found in two samples from the upper buffer zone has not been found in the primary isolation zone.

Section 8.3.1.4 contains plans to study the petrography and chemical composition of secondary minerals in the upper buffer zone.

The Quincy and Squaw Creek interbeds occur in the upper buffer zone (see Fig. 4.1-1). The Quincy interbed occurs between the Priest Rapids and Roza Members of the Wanapum Basalt and exists in two of seven cored drill holes in the controlled area study zone. The Squaw Creek interbed occurs between the Roza and Frenchman Springs Members and exists in two of seven cored drill holes in the controlled area study zone. Both the Quincy and Squaw Creek interbeds are 1 m (3.3 ft) or less in thickness everywhere they are encountered in the controlled area study zone. In addition, an unnamed interbed occurs in three of seven cored drill holes in the controlled area study zone. This interbed occurs within the Frenchman Springs Member and is 2 m (6.6 ft) or less in thickness. No work has been done to characterize the mineralogy and petrology of these interbeds within the controlled area study zone. Some work has been done outside the Pasco Basin, but the fluvial nature of the deposits results in rapid changes in lithology and thickness over relatively short distances so that extrapolation of this work to the controlled area study zone may not be warranted. Studies are planned and described in Section 8.3.1 to characterize the interbeds in the upper buffer zone.

4.1.1.3.7 Stratigraphic and lateral distribution of secondary phases

The stratigraphic and lateral distribution of secondary minerals along potential flow paths can be used as a means of predicting potential changes in the composition of groundwater and potential sites of radionuclide sorption. An understanding of the three-dimensional distribution of secondary minerals could aid in the evaluation of the origin and stability of these phases. Overall, information on the distribution of these phases will provide a basis for predicting the reactions of basalt, water, and waste along potential flow paths from the repository to the accessible environment.

The distribution of secondary minerals as a function of depth has been studied by Benson and Teague (1979, pp. 1-20) and Ames (1980, pp. 152-215). Their results indicate that smectite occurs at all depths in all examined cores, although it might be less abundant below 600 m (1,970 ft). Illite occurs sporadically throughout the section, and quartz is ubiquitous. Cristobalite has a distribution similar to that of quartz and is the dominant silica phase between 600 and 1,000 m (1,970 and 3,280 ft) in the central Pasco Basin.

Clinoptilolite exists in all examined samples in the primary isolation zone. Scanning electron microscopy observations show textures that can be interpreted as evidence of clinoptilolite dissolution near the base of the primary isolation zone and in the lower buffer zone (below about 950 m (3,120 ft)), which is the approximate depth at which mordenite first appears (Benson and Teague, 1982, pp. 595-613). The apparent clinoptilolite to mordenite transition noted by Benson and Teague (1982, pp. 595-613) has been observed elsewhere and has been produced by laboratory hydrothermal experiments (Boles, 1981, pp. 103-135; Hawkins et al., 1978, pp. 337-343). However, both clinoptilolite and mordenite are in some samples below 950 m (3,120 ft).

The depth to mordenite, apparently, is not perturbed by folds in the basalt (Smith et al., 1980, pp. 2-67 to 2-69), suggesting that mordenite formed after folding or that the formation of mordenite kept pace with folding. There is no textural evidence, such as partly dissolved mordenite, to support the latter possibility. This suggests that the mordenite distribution was largely established postfolding. Further work is required to better define the vertical zonations of secondary minerals (see Section 8.3.1).

The only apparent geographic variation in secondary mineralization noted thus far is the distribution of celadonite. Rawson (1986a) and Horton (1985) noted celadonite in most samples of Rocky Coulee and Cohassett flow tops from drill holes outside the controlled area study zone in the southwest portion of the central Pasco Basin. They noted celadonite in only one sample obtained from drill holes within the controlled area study zone. More samples need to be studied in order to better understand and define this and other possible geographic distributions of secondary minerals (see Section 8.3.1).

4.1.1.4 Mineral stability

Basalt-water-waste reactions may change groundwater composition with time and, therefore, may affect radionuclide transport and release. For this reason, it is important to understand the stability of primary and secondary phases in the present and future geochemical environments.

4.1.1.4.1 Primary phases

All of the primary phases discussed in Section 4.1.1.3 formed at magmatic temperatures (800 to 1,000 °C) and are not in equilibrium with the present in situ physicochemical conditions. They persist as metastable phases, however, because the kinetics of alteration processes are slow at the present, relatively low temperatures. For this reason, most primary crystals, even those adjacent to fractures and vesicles, remain unaltered or are only slightly altered.

Glass is the most reactive of the primary phases. Generally, primary glass in dense interiors, particularly glass near fractures, is incipiently altered, whereas glass in flow-top breccias is, in places, more intensely altered (McKinley et al., 1986; Horton, 1985). Hydrothermal experiments in which crushed Grande Ronde Basalt was reacted with synthetic groundwater between 100 and 300 °C have produced a variety of secondary phases including iron smectite, mixed-layer chlorite/smectite, cristobalite, quartz, mordenite, clinoptilolite, wairakite, illite, and potassium feldspar (Lane et al., 1984, p. 99; Moore et al., 1984, p. 23). Some of these phases have been found as natural alteration products of Grande Ronde Basalt. The specific alteration processes and the time of alteration are not known. Planned investigations are described in Section 8.3.1 that will help determine the products of glass alteration and the time of alteration (i.e., early deuteric versus late-stage diagenetic). These aspects of alteration are important in attempts to predict the stability or reactivity of glass in future geochemical environments.

4.1.1.4.2 Secondary phases

Little is known about the stability of the secondary phases in Grande Ronde Basalt. There are virtually no available, reliable, measured thermochemical data for the dominant zeolites (clinoptilolite and mordenite) or the iron-rich smectites found at the Hanford Site. Thus, a rigorous treatment of secondary mineral stability is not feasible at this time. Instead, mineral stability (or mineral persistence in the case of metastable phases) is evaluated here by comparing the occurrence of each secondary phase in Grande Ronde Basalt with its occurrence in other geologic environments. It is not the intent here to compare environments but only to get a general impression of the stability or persistence of the secondary minerals. As more thermodynamic data become available in the technical literature and as more field occurrences are documented, better estimates of secondary mineral stability can be made. This is an ongoing process and part of the petrologic model development described in Section 8.3.1.2.4.6.

Those secondary minerals found by Benson and Teague (1979, pp. 35-40) to exist in Grande Ronde Basalt are listed in column one of Table 4.1-18. Almost all the reported secondary minerals have been identified throughout the world in weathering diagenetic, burial metamorphic, and geothermal environments. The temperature ranges, listed in Table 4.1-18, are those over which these minerals are interpreted to be forming today. The distinction between common and less common minerals is based on Table 3 of Benson and Teague (1979, pp. 35-40); minerals listed in their "Other" column are considered less common. Table 4.1-18 is not intended to be an exhaustive compilation of mineral-temperature relationships but is intended only to aid discussions of mineral stability with respect to temperature. Sea floor temperature, which is the lower temperature limit for the range in which many of the minerals are known to form, is represented in the table by 4 °C.

Smectites are known to form on the sea floor (Perry, 1975, pp. 287-295), in weathering environments (Borchardt, 1977, pp. 293-330), and in geothermal environments (Kristmannsdottir, 1976, pp. 30-39). The formation and persistence of smectite with respect to other clays, zeolites, and feldspars are functions of the geochemical environment, kinetics, and temperature. Once formed, however, smectites often persist (smectites as old as the Cretaceous Period, 65 to 141 m.y. ago, are known--see Anderson and Reynolds, 1966, pp. 1443-1456 for example) until leaching in acidic environments converts them to kaolins and associated oxide phases, weathering processes converts them to pedogenic chloritic phases (Borchardt, 1977, p. 312), or diagenetic processes transform them to smectite-bearing mixed-layer phases.

The smectites at the Hanford Site are iron-rich and, except for three known occurrences, are trioctahedral. Generally, iron- and magnesium-rich trioctahedral smectites persist to higher temperatures than do aluminous dioctahedral smectites (Eberl et al., 1978, pp. 400-409). Dioctahedral smectites begin transformation to mixed-layer clays at about 60 °C and the transformation is complete at temperatures greater than about 200 °C (Hoffman and Hower, 1979, pp. 55-79). Trioctahedral smectites, on the other hand, persist to much higher temperatures. In Icelandic basalts, for example, trioctahedral smectite does not begin transformation to mixed-layer chlorite/smectite until temperatures of about 200 °C (Kristmannsdottir, 1976, pp. 30-39). Therefore, most smectite in the repository isolation system may be stable (but not necessarily in the thermodynamic sense) at the in situ physicochemical conditions at depth.

The effect of pressure on smectite stability has been investigated by laboratory experiments. Koster van Groos and Guggenheim (1984, pp. 872-879) found that an increase in pressure increased the stability of hydrated smectite; that is, an increase in pressure increased the temperature of dehydration. Eberl et al. (1978, pp. 401-409) found that an increase in pressure increased the stability of smectite with respect to that of illite.

Benson and Teague (1979, pp. 35-40) report the existence of an "illite-like clay, probably celadonite." Illite and celadonite are two different minerals with different physical properties, chemical characteristics, and geologic occurrences. Although there are reports of illite being formed in low-temperature environments by repeated wetting and drying of smectite (Mamy and Gaultier, 1975, pp. 149-155), most discrete illite forms at temperatures above about 200 °C (Hoffman and Hower, 1979, pp. 55-79). If the mineral reported by Benson and Teague is illite, it probably did not form under the present physicochemical regime. It may persist metastability, however, at low temperatures for geologically long periods of time as indicated by the many published potassium-argon ages for early to middle Paleozoic illites (about 300 to 600 m.y. ago) (Weaver, 1984, pp. 153-183). Celadonite, on the other hand, is a commonly reported low- to medium-temperature, alteration product of basaltic rocks (Andrews, 1980, pp. 323-340; Seyfried et al., 1976, pp. 385-392). If the mineral reported by Benson and Teague is celadonite, it may be stable.

Although zeolites are fairly common minerals in the repository isolation system and in other natural environments, Hawkins et al. (1978) and Dibble and Tiller (1981, pp. 323-330) believe that they may be unstable with respect to quartz and feldspars and that their metastable persistence is due to slow rates of transformation at low temperatures. Thus, all zeolites reported from the repository isolation system may be metastable phases. Nevertheless, comparing the occurrences at the Hanford Site with those elsewhere may yield information as to their possible persistence.

Clinoptilolite has been found to occur on the sea floor (Nathan and Flexer, 1977, pp. 845-855) and in diagenetic sequences and geothermal environments up to about 120 °C (Sheppard and Gude, 1973, pp. 1-36; Aoyagi and Kazama, 1980, pp. 179-188). Thus, the existence of clinoptilolite in the repository isolation system is within the temperature range of clinoptilolite reported from other environments (see Section 4.2 for discussion of repository temperatures). In geothermal and low-grade metamorphic terrains with temperatures above 120 °C, clinoptilolite commonly disappears and is replaced by mordenite (Aoyagi and Kazama, 1980, pp. 179-188; Boles, 1981, p. 103). However, the temperature ranges over which clinoptilolite and mordenite exist greatly overlap as shown in Table 4.1-18. The coexistence of clinoptilolite and mordenite in Grande Ronde Basalt and in other geologic environments, such as the Nevada Test Site (Bish et al., 1982) suggests that some factor in addition to temperature must also be important in controlling the reaction of clinoptilolite to mordenite or the coprecipitation of both.

Both clinoptilolite and mordenite may be metastably persistent. Although it has not been radiometrically dated, clinoptilolite may have existed at sea floor temperature since Cretaceous time (141 to 65 m.y. ago) (Nathan and Flexer, 1977, p. 851). Mordenite is known in rocks as old as Eocene (57 to 36 m.y. ago) (Sheppard, 1971, pp. 288-291). The persistence of clinoptilolite and mordenite may be due to metastable precipitation and slow reaction kinetics.

Opal, cristobalite, and quartz in the repository isolation system exist at temperatures within the ranges that these minerals are commonly found (see Table 4.1-18). The coexistence of cristobalite and quartz reported by Benson and Teague (1979, pp. 35-40) may reflect the instability of cristobalite with respect to quartz at present conditions. Alternatively, both could have precipitated from different solutions at different times. At any rate, cristobalite is unstable with respect to quartz at all temperatures less than 1,470 °C. Likewise, tridymite is unstable with respect to quartz at temperatures less than 870 °C (Deer et al., 1966, p. 341).

The less common phases identified in Grande Ronde Basalt by Benson and Teague (1979, pp. 35-40) are listed in Table 4.1-18 and grouped by them in the heading "Other" in their Table 3. The zeolites phillipsite, chabazite, and erionite are low temperature phases found in alkaline, saline lakes (Surdam, 1981, pp. 65-91), and as authigenic phases in mafic volcanics (Hay and Sheppard, 1981, pp. 93-102). Geologic evidence suggests that, with time, these zeolites may alter to other zeolites and feldspars (Boles, 1981, pp. 103-135; Hay and Sheppard, 1981, pp. 93-102). However, phillipsite,

chabazite, and erionite are known in rocks as old as Eocene (Sheppard, 1971, pp. 279-310), and in trachytic tuff in Italy, phillipsite and chabazite are thought to be 5,000 to 8,000 yr old (Hay and Sheppard, 1981, pp. 93-102). Thus, these zeolites are metastably persistent.

Analcime is known to form and exist at temperatures ranging from that of the near surface to greater than 600 °C (Helgeson et al., 1978, pp. 149-156). Wairakite, reported in Grande Ronde Basalt, is most commonly found in geothermal systems and low-grade metamorphic environments at temperatures greater than about 200 °C (Elders et al., 1981; Kristmannsdottir, 1975; Boles, 1981, pp. 103-135). Thus, wairakite within the Grande Ronde Basalt is probably unstable but may be metastably persistent.

Pyrite and calcite are very common mineral phases in many geologic environments. Calcite is found in soil environments (Donner and Lynn, 1977, pp. 75-98), in diagenetic environments (Yeh and Savin, 1977, pp. 1321-1330), and in geothermal environments (Kristmannsdottir, 1975, pp. 441-445). The existence of calcite in Grande Ronde Basalt is in agreement with its usual geological occurrence. In addition, the calcite in Grande Ronde Basalt may be thermodynamically stable under present conditions (see discussion in Section 4.1.2). Pyrite is a very common mineral forming in environments ranging from sea floor sediments (Berner, 1971, p. 202) to geothermal systems (Kristmannsdottir, 1975, pp. 441-445). Evidence is presented in Section 4.1.3 suggesting that the pyrite in Grande Ronde Basalt may be thermodynamically stable under existing conditions.

4.1.2 GROUNDWATER GEOCHEMISTRY

The objective of Section 4.1.2 is to summarize known preemplacement hydrochemistry compositional properties of the preferred candidate horizon (Cohassett flow) and other proximal stratigraphic units that, potentially, represent pathways to the accessible environment (see Fig. 4.1-1). This compositional information is necessary for the design of experimental studies to investigate the stability of engineered barriers components and to provide experimental evaluation of radionuclide transport from the waste package and through the natural system. Such studies require sufficient groundwater chemistry data so that reference compositions for major aquifers along potential flow paths can be defined.

These information needs are met by summarizing the observed compositional data for appropriate groundwaters in terms of major and trace inorganic species, organic components, dissolved gases, and background radioactivity. Four candidate repository horizons in the Grande Ronde Basalt have been proposed (Rocky Coulee, Cohassett, McCoy Canyon, and Umtanum flows). For this section, all discussions of the Grande Ronde Basalt focus on the Cohassett flow as the preferred candidate horizon. However, from a hydrochemical perspective, differences among the candidate flows are insignificant (Early et al., 1986).

Potential flowpaths and the general hydrochemistry along them are discussed in Section 4.1.2.1. Subsequent sections contain details about major inorganic content (Section 4.1.2.2), trace elements (Section 4.1.2.3), organic content (Section 4.1.2.4), dissolved gases (Section 4.1.2.5), background radioactivity (Section 4.1.2.6), particulates and colloids (Section 4.1.2.7), and temperature and pressure (Section 4.1.2.8). Methods of assessing mineralogical controls on water composition and current ideas about mineralogical controls are discussed in Section 4.1.2.9. The synthetic groundwater compositions used in previous and current experimental studies, including sorption, basalt-water reactions, and engineered barriers stability investigations, are summarized in Section 4.1.2.10.

The characterization and variation of hydrochemical parameters along potential flow paths from the repository are summarized in Section 4.1.2, while Chapter 3 contains detailed discussions of all components of hydrochemical studies under investigation at the Hanford Site. Included in Chapter 3 is a treatment of sample quality and analysis procedures (Section 3.9.1.3), evidence for basalt-water reactions (Section 3.9.3.7.2.2), and a thorough review of the implications for conceptual groundwater flow models of the Hanford Site (Section 3.9.3.7.3.2). Evaluation of the control and interpretation of redox and pH conditions in the basalt geochemical system is found in Sections 4.1.3.4.1, 7.1, and 7.4.4.1. Plans for additional hydrochemical sample collection and analyses are presented in Section 8.3.1.4.

4.1.2.1 General description of the hydrochemistry

Based on preliminary performance assessment modeling as reported in Clifton (1986), the principal anticipated flow path for groundwater from a repository in the Cohassett flow to the accessible environment is assumed to be laterally along the Cohassett flow top. While these modeling results tend to emphasize lateral migration of groundwater, measured values of vertical hydraulic conductivity for the basalt flows at the Hanford Site have not been made.

Conceptually, the potential exists for vertical flow along primary fractures or faults within the dense interiors of flows. If this occurs, it is possible that the groundwater flow pathway could cross the contact between the Wanapum and Grande Ronde Basalts and that some component of flow could take place in the Vantage interbed and (or) in flow tops of the lower Frenchman Springs Member. In order to provide a basis for evaluating the effects of this flow pathway, this section examines the hydrochemical properties of groundwaters in the Frenchman Springs Member in addition to those from neighboring flows of the Cohassett flow (above and below) within the Grande Ronde Basalt. This approach should permit a hydrochemical assessment of a wide stratigraphic window along potential flow paths from a mined geologic disposal system in the Cohassett flow at the reference repository location.

In the following sections (4.1.2.2 through 4.1.2.6) , hydrochemical data are presented as compositional histograms for the Frenchman Springs Member, Cohassett flow, and other flows (both above and below the Cohassett flow) within the Grande Ronde Basalt. Samples taken from the reference repository location within these units are highlighted for emphasis. A complete tabulation of all hydrochemical data used in this chapter is available in Early et al. (1986). No attempt is made to duplicate the more extensive hydrochemical discussions found in Chapter 3.

Groundwater data are available from flow tops and(or) bottoms within basaltic units. These groundwaters are assumed to be representative of those from the entire flow. Groundwater samples have not been collected from flow interiors for any basaltic units because of their generally low permeability. In addition to data for flow tops, hydrochemical data from a sedimentary interbed at the base of the Wanapum Basalt (Vantage interbed; see Fig. 4.1-1) are included in the following discussions.

In general, groundwaters associated with basalts from the Frenchman Springs Member and Grande Ronde Basalt at the Hanford Site are either Na-Cl or Na-Cl-SO_4 types. Groundwaters from the Frenchman Springs Member typically are of a Na-Cl type. However, within the Grande Ronde Basalts, the Na-Cl type waters tend to be characteristic of the vicinity of the reference repository location while Na-Cl-SO_4 groundwaters are found further to the east. In addition, dissolved gases in the Na-Cl type groundwaters in the reference repository location are dominated by methane, whereas Na-Cl-SO_4 waters are nitrogen dominated. Groundwaters from both the Frenchman Springs Member and Grande Ronde Basalt tend to have relatively high fluoride concentrations reaching levels of about 50 mg/L in some Grande Ronde Basalt samples from the eastern part of the Hanford Site.

Only preliminary information exists for trace elements, organic components, background radioactivity, and particulates and colloids. Although a variety of trace elements have been evaluated, they are generally below detection limits for the techniques used. Total organic carbon is routinely measured in groundwater samples, but little information is available about specific organic constituents. Indirect information is available on background radioactivity, but that information is subject to errors caused by potential contamination of groundwater samples by drilling activities. Limited information is also available on naturally occurring particulates and colloids in Hanford groundwaters. Planned studies will provide more information on background radioactivity and on particulates and colloids. These studies must resolve the problem of contamination due to borehole construction techniques. The impact of man-induced particulates and colloids on radionuclide transport in the post-emplacement environment will also be studied.

4.1.2.2 Major inorganic content

Compositional data for the major inorganic components (including pH and alkalinity) measured in groundwaters from the Frenchman Springs Member (and Vantage interbed), Cohassett flow, and other flows of the Grande Ronde Basalt are presented in Figures 4.1-3 and 4.1-4. The locations of the boreholes from which samples were taken for analysis are shown in Figure 4.1-5. In general, most groundwaters from the lower Wanapum and upper Grande Ronde Basalts at the Hanford Site are dominated by sodium and chloride (sulfate is an important constituent in some samples).

A more detailed examination of Figures 4.1-3 and 4.1-4 reveals both vertical and lateral compositional differences in groundwaters between and within the Frenchman Springs Member and Grande Ronde Basalt. These observations are summarized as follows:

- o Vertical compositional variations.
  - Concentrations of sodium, chloride, and fluoride tend to increase with increasing depth.
  - Concentrations of potassium and calcium tend to decrease with increasing depth.
- o Lateral compositional variations.
  - Groundwaters from the reference repository location tend to have higher sodium and chloride concentrations than those from outside the reference repository location.
  - In general, groundwaters from the Cohassett flow across the Hanford Site exhibit a total range of composition similar to all other Grande Ronde Basalt groundwaters sampled.

The existence of vertical and lateral variations of groundwater sulfate concentrations was discussed in Chapter 3 (see Section 3.9.1.3.6, Fig. 3.9.2-16, and related discussion in Section 3.9.3.7.3.2) and also was shown in Figure 4.1-4. However, study of available data reveals that sulfate concentrations are relatively low (less than 35 mg/L) for all horizons across the Hanford Site except the Grande Ronde Basalt in boreholes DC-6, -7, -14, and -15 (see Fig. 4.1-5). The apparently restricted stratigraphic and geographic extent of this sulfate anomaly does not have a satisfactory explanation at present. Potential sources of recharge to the Grande Ronde Basalt that have been characterized in this region (e.g., water from overlying aquifers and(or) the Columbia River) exhibit low concentrations of sulfate and cannot explain the high-sulfate groundwater. Possibly, there is a deeper source of groundwater migrating upward into this region; or, alternatively, sulfate-bearing phases locally associated with the Grande Ronde Basalt control its concentration to the high levels observed. This is an unresolved question that is actively under study (see Chapter 8, Section 8.3.1.4).

Systematic increase of compositional parameters, such as sodium, chloride, and fluoride, with increasing depth in the reference repository location is discussed in Section 3.9.1.3. In general, there appears to be a chemical transition zone that separates shallow and deep groundwaters (each with unique chemical signatures). Similar changes in relation to depth are observed for other parts of the Hanford Site, but the stratigraphic level where the transition zone occurs varies from borehole to borehole (see Fig. 3.9-64). For example, within the reference repository location, the geochemical gradient occurs in groundwaters from across the entire Wanapum Basalt, while further to the east in the Cold Creek syncline the transition zone appears at deeper stratigraphic levels. In addition, near anticlinal structures bounding to Cold Creek syncline, a sharp transition occurs in groundwaters from the uppermost part of the Wanapum Basalt. Consequently, the vertical chemical variations observed in groundwater do not appear to be directly associated with concomitant changes in host rock chemistry.

Evidence pointing to systematic lateral variation in ambient groundwater chemistry within the Frenchman Springs Member and Grande Ronde Basalt is discussed in Section 3.9.1.3. This discussion tentatively concludes that observed lateral chemical gradients result from localized upward movement of more mineralized Grande Ronde Basalt groundwaters in the vicinity of the reference repository location and from mixing with groundwaters chemically similar to those found in aquifers of the Saddle Mountains Basalt. Within the limitations of available data, it appears that these lateral chemical variations include decreases in sodium and chloride concentrations radiating outward from the reference repository location. As the gradients appear to emanate from the vicinity of the reference repository location (see Fig. 3.9.3-23 and 3.9.3-24), it is reasonable to conclude that groundwater traveling laterally along a flow top within the lower Wanapum and upper Grande Ronde Basalts in any direction away from the reference repository location will systematically change in chemical composition as described above.

The value of these observations becomes clear when an attempt is made to estimate specific differences in the preemplacement hydrochemistry along likely flow paths from a mined geologic disposal system in basalt. For example, if groundwater flow from the repository follows a path within the Cohassett flow top, it is anticipated that decreases in sodium and chloride will be encountered as the water leaves the reference repository location. Alternatively, if the flow path from the repository involves vertical flow to the Frenchman Springs Member followed by lateral movement outside of the reference repository location, decreases in the sodium, chloride, and fluoride and increases in calcium concentrations are expected. The potential effect of these chemical changes on the mobility of radionuclides, should they be released from the repository, is important to evaluate and currently is being addressed from both theoretical and experimental perspectives by radionuclide retardation studies (see Section 8.3.1.4.1.3).

The elevated fluoride concentrations of groundwaters in the Grande Ronde Basalt (about 10 to 50 mg/L) are of interest in that they may provide insight into the specific basalt-water reactions occurring in these deep basalts. The source of fluoride in the groundwater is currently uncertain, although (as

noted in Section 4.1.1.3) fluoride is present as a minor constituent in basalt, primarily occurring in basaltic glass and fluorapatite (Allen and Strope, 1983, p. 7). One occurrence of fluorine-bearing apophyllite in the Saddle Mountains Basalt also has been reported (Rawson, 1986b). It is possible that fluoride is selectively leached from these phases during basalt-water reactions (hydrolysis) along interflow contacts. Noble et al. (1967) confirm that leaching of fluoride from silicic volcanic glass by groundwater is a common occurrence. Alternatively, fluoride may have a source outside the basalts and become part of the basalt hydrochemical system via natural groundwater flow paths. One such source could be the sedimentary rocks that have been observed in the cuttings of deep gas exploration wells north and west of the Pasco Basin and whose existence are predicted by magnetotelluric methods to lie beneath the basalts at the Hanford Site (see discussion on sub-basalt sedimentary rocks in Sections 1.2.2.1 and 1.7.2.2). Current investigations in solids characterization and geochemical modeling attempt to identify possible solubility controlling phases for fluoride (e.g., see Section 4.1.2.9). Furthermore, results from laboratory basalt-water reaction studies are being examined for evidence of controls on fluoride concentrations in experimental solutions (see Section 8.3.1.4).

The concentration of dissolved oxygen, hydrogen, and other redox couples such as HS^-/SO_4^{2-} and iron(II)/iron(III) in Hanford Site groundwaters are of value in reconstructing the redox conditions of the Hanford Site. Tabulations of appropriate data and relevant discussions are incorporated into Section 4.1.3.4.

4.1.2.3 Trace elements

In addition to major inorganic species, groundwaters (filtered through an 0.45-μm (18×10^{-6}-in.) filter) from boreholes on the Hanford Site have been analyzed for a variety of elements occurring in trace amounts (generally less than 1 mg/L) including lithium, aluminum, boron, phosphorous, several alkaline earths (strontium and barium), transition metals (chromium, manganese, iron, cobalt, nickel, copper, and zinc), molybdenum, lead, and uranium. Concentrations of these constituents in groundwater sampled from Frenchman Springs Member and Grande Ronde Basalt horizons are presented in Early et al. (1986).

The principal value of trace element analyses is for examining alternative models of basalt-water reaction. For example, in comparison to calcium, other alkaline earths present in trace amounts, such as strontium and barium, partition differently between groundwater and certain solid phases (e.g., calcite, feldspars). Therefore, their relative abundances in groundwater can help identify possible reactions. In addition, aluminum and iron are particularly important elements in many primary and secondary phases (e.g., glass, feldspar, clays, zeolites) in basalt; and accurate analyses of them in groundwater are necessary to support geochemical and reaction path modeling studies.

Because of the low concentration levels of trace elements observed in these groundwaters, they are particularly sensitive to contamination during sampling. For example, drilling fluids containing various additives have been used during construction of many boreholes at the Hanford Site and are possible sources of contamination for trace constituents in groundwater (e.g., Halko, 1984). In addition, groundwater samples have been collected at the surface by pumping water through steel pipe from a zone isolated by packers. In view of the contact of groundwater with the pipe and pipe-joint lubricant, the potential exists for contamination. Currently (1986), a stainless steel, downhole sampling device (see Section _____) that will obviate contamination problems associated with sampling collection is being tested. To date, only limited use of trace element data has been made in view of possible contamination problems.

Lithium, the transition metals (except iron), and lead are normally at or below the detection limit of the analytical technique used in these samples (inductively coupled plasma atomic emission spectrometry). Of the remaining trace components, aluminum is not generally detected with sufficient sensitivity by inductively coupled plasma atomic emission spectroscopy to be well defined. However, aluminum concentrations normally are less than 0.5 mg/L. Groundwater analysis for magnesium, aluminum, and manganese by atomic absorption spectroscopy was initiated in 1983, but more sensitive and reliable analytical techniques are required to support geochemical modeling studies (see the Groundwater Flow System Hydrochemistry study plan as referenced in Section 8.3.1.4.2.3.1).

Boron, strontium, and barium are most likely accessory components of basalt glass and typically are found at concentrations of 0 to 2, less than 0.1, and less than 0.1 mg/L, respectively. These trace elements are believed to enter the groundwater through basalt-water reactions that occur primarily within fractures and along flow contacts. Phosphorous may result from dissolution of minor phosphate phases such as fluorapatite and is found normally at concentration levels of less than 1 mg/L. Iron exists as a major component of Columbia River Basalt Group flows (see Table 4.1-2) and may enter the water through basalt-water reactions. A second source for iron may be contamination from borehole casing and other drilling/sample collection equipment, especially when the swab technique is used for collection. While iron concentrations exceeding 50 mg/L have been determined for groundwater samples suspected of being contaminated, values normally lie below 0.2 mg/L.

Uranium concentrations (determined mass spectrometrically) in groundwaters from Frenchman Springs Member and Grande Ronde Basalt horizons are low (generally less than about 0.1 µg/L) compared to concentrations usually observed in natural waters at the Earth's surface (0.1 to 10.0 µg/L) (Osmond, 1980, p. 259). The low value may be due to low uranium solubility under reducing conditions (see Section 7.4.3.5) that exist in basalt groundwaters or low uranium concentrations in the host basalts.

4.1.2.4 Organic content

Knowledge of the type and concentrations of natural organic constituents in Hanford groundwaters is important primarily for evaluating the potential for formation of organic complexes with radionuclides released from the proposed repository. Only limited data exist regarding the identity and concentration of organic constituents in groundwater from the flow tops and interbeds of the Columbia River Basalt Group at the Hanford Site. For example, the BWIP has been determining the total organic carbon content of groundwater samples since 1982. In addition, Means (1982, pp. 1-22) has characterized the organic compounds found in one sample of Grande Ronde Basalt groundwater from the Hanford Site. The gaseous organic component (i.e., methane) is discussed in Section 4.1.2.5.

The purpose of total organic carbon analyses is to monitor borehole cleanup procedures prior to sample collection for hydrochemical analyses. Organic carbon in several forms may be introduced into the borehole during the drilling process. Total organic carbon analysis provides a means of determining the progress of aquifer cleanup. Only preliminary evaluation of results of total organic carbon analyses is available, but it appears that groundwaters from Wanapum and Grande Ronde Basalts may have a natural background level of total organic carbon of less than 1 mg/L. This lower limit is observed in samples from those aquifers that have been pumped extensively or flow freely under artesian conditions. A frequency distribution of observed total organic carbon concentrations for all groundwaters collected through April 15, 1986, in the Frenchman Springs Member and Grande Ronde Basalt is shown in Figure 4.1-6. With few exceptions the samples come from individual aquifers isolated from other water-producing zones in the boreholes by inflatable packers. Maps identifying the sampled boreholes from which these data come are found in Figure 4.1-7. The results suggest that relatively few of these samples may be free of organic carbon contamination from drilling fluid, a factor that must be considered before detailed organic characterization takes place. A more complete discussion of the effects of drilling fluid on groundwater chemistry can be found in Graham et al. (1985).

The identification of the specific organic constituents in these groundwaters has been attempted in only one sample as reported in Means (1982, pp. 1-22). In this study, a sample was taken from a horizon about 200 m (656 ft) below the Umtanum flow top in borehole DC-6 (see Fig. 4.1-67. The sample was collected after the test horizon had been flowing under artesian conditions at about 20 L/min (5.3 gal/min) for over 1 yr. The sample contained 0.34 mg/L of dissolved organic carbon. While the extensive period of flow for the sampled horizon and the low level of observed organic carbon jointly suggest a "pristine" groundwater sample, the possibility cannot be ignored that organics added during the drilling process still may be present. Consequently, the analysis of the organic content of this sample should be interpreted with caution.

The results of this study (Means, 1982, pp. 1-22) indicate that about 2.5 µg/L of the organic matter in this sample is in the form of fatty acids and phenols. The remainder of the organic carbon is present as fulvic acids in which about 90% have apparent molecular weights falling in the range of 300 to 1,000, as determined by gel filtration chromatography. No humic acids were detected. All of the organic compounds identified have the capacity for complexing some radionuclides and may facilitate their migration should they be released from the repository.

From the above discussion, it is apparent that insufficient data are available relative to the identity, concentration, and potential complexing ability of natural organic constituents in groundwaters of the Hanford Site. For example, no organic characterization of Grande Ronde Basalt groundwaters from the reference repository location region in the vicinity of the proposed repository has been performed. Furthermore, identification of the presence of organic components representing drilling fluid contaminants has not been attempted yet. Plans to address these questions are discussed in Section 8.3.1.4.2.

4.1.2.5 Dissolved gas

Dissolved gases in Hanford groundwaters have at least three major uses: (1) methane has potential as a groundwater flow tracer, similar to chloride; (2) the noble gases (He, Ne, Ar, Kr, Xe) can be used to estimate groundwater recharge temperatures; and, (3) accumulation of He and ^{40}Ar may provide some constraints on groundwater flow rates. In addition, methane in groundwaters around the proposed repository, coupled with estimates of inflow to the mined drifts, are important for evaluating ventilation requirements.

Information available on dissolved methane in groundwater from the Frenchman Springs Member and Grande Ronde Basalt is summarized in Figure 4.1-8. Besides methane, nitrogen is the other major dissolved gas constituent found in Hanford groundwaters. The location of all boreholes from which dissolved gas data have been obtained is given in Figure 4.1-9. In groundwater samples taken from both of these stratigraphic units within the reference repository location, methane is the major gas component with minor amounts of nitrogen, argon, and carbon dioxide. Hydrocarbons, other than methane, and noble gases, other than helium and argon, have been detected only in very small quantities. Analysis of gases for hydrogen sulfide has not been attempted, but owing to the high pH of most lower Wanapum and Grande Ronde Basalt groundwaters (greater than 8.5) little hydrogen sulfide gas is anticipated. However, the decision not to analyze for hydrogen sulfide is being reconsidered.

Estimates of dissolved methane concentrations within reference repository location boreholes (DC-16A, RRL-2, RRL-6B, and RRL-14) have been made based on the amount of methane evolving from groundwater discharging through a gas separator (Table 4.1-19; Early, 1986). These estimates fall in the range of approximately 100 to 1,200 mg of methane per liter of water or about 10% to

100% saturated at formation temperature and pressure for groundwaters in the Grande Ronde Basalt. Similar measurements for Wanapum Basalt groundwaters in reference repository location boreholes have been successful in only two instances. Attempts to make analogous measurements in shallower sections of these boreholes have been unsuccessful due to the low total gas concentrations encountered.

Beyond the reference repository location, dissolved gas concentrations are inadequately known at present (Early, 1986). In Section 8.3.1.4, plans are described for modification of the gas sampling and analysis procedures, which will permit a quantitative determination of gas concentrations elsewhere in the Hanford Site. Future resampling programs in existing boreholes will supplement the data presented in Table 4.1-19.

The origin of methane associated with these groundwaters is not well understood. Carbon isotope data for methane samples are limited but suggest that for samples from the Grande Ronde Basalt within the reference repository location $\delta^{13}C^*$ values of greater than -50 per mil are observed. Most methane samples from shallower horizons across the site have $\delta^{13}C$ values of less than -50 per mil. These results indicate that the methane from the sampled Grande Ronde Basalt horizons may be of thermocatalytic origin, while that from shallower zones is more compatible with a biogenic origin (Barker and Fritz, 1981). The thermogenic methane possibly was generated from lignite or coal which is occasionally found interbedded with the basalts and in the sub-basalt sediments. However, uncertainties exist as to whether specific ranges of $\delta^{13}C$ (and δD) values for methane can reliably distinguish between biogenic and abiogenic reaction mechanisms. Work in progress may provide a more definitive answer to this question (see Section 8.3.1.4).

For boreholes outside of the reference repository location, dissolved gases in nearly all Grande Ronde Basalt groundwater sampled to date are strongly dominated by nitrogen. The only exceptions that have been observed are in boreholes in close proximity to the reference repository location (McGee and DC-19C) where nearly equal amounts of nitrogen and methane are found. In contrast, methane domination of dissolved gases outside of the reference repository location is a more common occurrence in Frenchman Springs Basalt groundwaters than in Grande Ronde Basalt groundwaters across the Hanford Site. The exceptions are for distant boreholes DC-14 and DC-15 (nitrogen dominated) and the McGee well (approximately equal amounts of nitrogen and methane). Currently it is assumed, but not proven, that the methane-rich dissolved gases in the vicinity of the reference repository location are from a deep (possibly sub-basalt) source and have migrated upward in association with groundwater. Within the Wanapum Basalts in this region,

$$*\delta^{13}C = \left[\frac{(^{13}C/^{12}C)_{sample} - (^{13}C/^{12}C)_{standard}}{(^{13}C\ ^{12}C)_{standard}}\right] \times 1{,}000 \text{ per mil}$$

where the standard is the Pee Dee Belemnite.

mixing of deep and shallow groundwaters occurs as hypothesized in Section 3.9.1.3 and summarized in Section 4.1.2.2. Future activities designed to address this question include more detailed gas analyses in proposed and existing boreholes on the Hanford Site (see Section 8.3.1.4).

4.1.2.6 Background radioactivity

At present, there are limited documented measurements of background radioactivity in the basalts at the Hanford Site or associated groundwaters. Information is available in terms of the observed concentrations of selected radionuclides and radioactive elements. These constituents include the following:

- o Tritium.
- o Carbon-14.
- o Chlorine-36.
- o Total uranium.
- o Selected decay chain daughters of uranium and thorium.

Tritium is measured in groundwaters at the Hanford Site and used as an indicator of drilling fluid contamination (Graham et al., 1985). Most boreholes have been drilled with a fluid made up with Columbia River water. Because of natural fallout, Columbia River water contains tritium at concentration levels considerably higher than those found in groundwaters from confined aquifers at the Hanford Site.* Therefore, tritium is a useful geochemical tracer with which to monitor borehole development. A frequency distribution of all measured tritium values in Frenchman Springs Member and Grande Ronde Basalt groundwaters is included in Figure 4.1-10. Because of the likelihood of groundwater contamination with river water prior to sampling, it is anticipated that the observed tritium concentrations are upper bounding values for the sampled zones rather than reflecting true baseline concentrations.

Carbon-14 and chlorine-36 analyses are performed on groundwater samples with the intent of obtaining information about groundwater ages. Because of its relatively short half-life (5,730 yr), ^{14}C is subject to the contaminating effects of modern carbon present in drilling fluid. Many of the analyses presented in Figure 4.1-10 probably show the effect of contamination with modern carbon and, as such, represent upper bounding estimates of the baseline ^{14}C concentrations present. On the other hand, ^{36}Cl has a long half-life (3×10^5 yr); and contamination effects, while present, may be of lesser importance

*Sula et al. (1983, pp. 14-15) report tritium concentrations (measured in tritium units (Tu)) for the Columbia River ranging from 71 pCi/L (22 Tu) to 607 pCi/L (207 Tu). Average Values for 1982 were 160 pCi/L (50 Tu) and 220 pCi/L (68 Tu) upstream and downstream of the Hanford Site, respectively. Additional tritium analyses for Columbia River water in the vicinity of the Hanford Site range from 25 to 78 Tu between 1978 and 1985, as reported by Early et al. (1986).

than for ^{14}C because less decay has occurred for ^{36}Cl. Consequently, to a first approximation, concentrations presented in Figure 4.1-10 may be reasonable baseline estimates of ^{36}Cl values for the zones sampled. Inferences as to groundwater ages from ^{14}C and ^{36}Cl data are discussed in Section 3.9.3.7.3.2.

Uranium, as a trace constituent of groundwater, also is subject to contamination by drilling and sampling activities. While observed values in Figure 4.1-9 range over more than three orders of magnitude, there is a suggestion that most samples lie in the range of 0.001 to 0.1 µg/L in Frenchman Springs Member and Grande Ronde Basalt groundwaters.

Work is in progress to obtain quantitative measurements of the concentrations of decay chain daughters of uranium and thorium in groundwater on the Hanford Site (e.g., see Laul et al., 1985). These data will be reported in a future update of the Site Characterization Plan when they have been determined.

In summary, it appears that the available baseline radioactivity data for Frenchman Springs Member and Grande Ronde Basalt groundwaters as presented in Figure 4.1-9 are subject to the potential effects of contamination by drilling fluids. Consequently, this figure probably provides upper bounding estimates for most constituents. Further observation of available data suggests that there are no significant differences in the amounts of these constituents in groundwaters from the reference repository location as compared to those from outside of this region.

Information for other radioactive constituents (e.g., ^{129}I) in lower Wanapum and Grande Ronde Basalt are not currently available, but plans for more extensive data acquisition are included in the study plan associated with Section 8.3.1.4.2.3.1.

4.1.2.7 Particulates and colloids

The existence of naturally occurring particulate matter in groundwaters on the Hanford Site has not been fully studied. Unfortunately, both the use of bentonite-based drilling fluids in most boreholes and the generation of fine rock fragments as the drill bit cuts through the rock interfere with this evaluation. Laul et al. (1985) attempted to determine if naturally occurring radionuclides in Grande Ronde Basalt groundwater at borehole DC-14 are associated with suspended particulates. Filtration of water through a 0.1 µm filter revealed that ^{210}Pb and ^{210}Po concentrations were 3 to 5 times lower in the filtrate than in unfiltered water suggesting that these radionuclides might be associated with colloids. Section 8.3.1.4.3.3.1 references the Radionuclide Reactivity study plan in which plans for characterizing the abundance and composition of natural particulates and colloids in these groundwaters are discussed.

In addition to naturally occurring colloids, the potential formation of particulates from human activities cannot be ignored. For example, the bentonite clay currently being considered as a waste package backfill component may be the source of particulates in the post-emplacement period. In Section 7.4.5.3 the results of a literature survey on the possibility of colloid formation from packing materials is discussed, but no definitive conclusions are reached. Section 8.3.4.3.4 presents plans that address these data deficiencies and will investigate the importance of man-induced colloids in radionuclide transport.

4.1.2.8 Temperature and pressure

4.1.2.8.1 Temperature

The increase of fluid temperature with depth beneath the Hanford Site is illustrated in Figure 4.1-11. Borehole locations are presented in Figure 4.1-12. This plot uses data from the downhole geophysical logs from 32 boreholes including 11 boreholes in the reference repository location. Linear regression analysis of all of the data yields a mean geothermal gradient of 0.0388 °C/m (0.0118 °C/ft). It is possible to estimate the average fluid temperature at depth underlying the Hanford Site using the equation given in Figure 4.1-11. Included in Figure 4.1-11 is the linear regression line and a 95% confidence band for the data. Based on the regression equation, temperature estimates for expected depth to repository midline of the Cohassett flow are given in Table 4.1-20. The depth is taken from the observed stratigraphic section for borehole RRL-2 and represents the depth of the repository midline near the center of the proposed layout. In addition, Table 4.1-20 contains the range of temperatures expected for the Frenchman Springs Member of the Wanapum Basalt at borehole RRL-2. In combination, these temperature estimates include the approximate total range of ambient temperatures likely to be encountered along possible groundwater flow paths from a mined geologic disposal system in basalt.

Temperature data for several boreholes tend to diverge from the main trend illustrated in Figure 4.1-11 and fall outside of the 95% confidence band. The specific causes for these divergences are not known. Additionally, close examination of Figure 4.1-11 suggests that the borehole thermal gradients may be nonlinear with steeper gradients at increasing depth. This observation may not be significant due to the scatter of the data and the restricted depth range included. However, it may be a consequence of upward migration of deeper and warmer groundwater beneath the Hanford Site, as hypothesized in Section 3.9.3.7.3.

4.1.2.8.2 Pressure

The variation of hydrostatic pressure with depth beneath the Hanford Site based on measurements made at the piezometer clusters at boreholes DC-19, DC-20, and DC-22 is given in Figure 4.1-13. Observed head measurements have been corrected for density variations in the water standing in the piezometers (Spane, 1986). Hydrostatic pressure at depth can be estimated using the equation given in Figure 4.1-13. Based on this equation, hydrostatic pressure estimates for the Frenchman Springs Member and Cohassett flow horizons are given in Table 4.1-20.

4.1.2.9 Mineralogical controls on water composition

Geochemical modeling codes such as WATEQ (Truesdell and Jones, 1974), EQ3 (Wolery, 1979; 1983), PHREEQE (Parkhurst et al., 1980), and MINTEQ (Felmy et al., 1984a; 1984b) provide a means by which one can attempt to identify those solid phases that are in permissible (thermodynamic) equilibrium with a specific groundwater composition. Geochemical modeling of this type, when coupled with an understanding of the hydrologic system, can help focus future solids characterization activities on the identification of solid phases that may be important in controlling groundwater composition. Furthermore, linking the results of speciation calculations with reaction path models such as EQ6 or that associated with PHREEQE can result in reasonable assumptions as to the identity of solid/water reactions from which the progressive evolution of groundwater compositions can be predicted (e.g., see Plummer et al., 1983).

Available geochemical speciation and reaction path codes are based on the principles of equilibrium thermodynamics. However, in natural water-rock systems metastability and precipitation/dissolution reaction kinetics may be important considerations. The observed presence of metastable phases such as glass, cristobalite, and tridymite in units of the Columbia River Basalt Group is an example of this problem. Therefore, as a predictive tool, equilibrium models of this type have limitations; and results from their use must be interpreted with caution. However, the model user can choose to suppress the formation of more stable phases when metastability is believed to be a problem. Furthermore, some reaction path models have the ability to consider user-supplied reaction rate information (e.g., EQ6).

The thermodynamic data base associated with each geochemical code represents another significant limitation. Adequate thermodynamic data for the important phases in the Columbia River basalts are lacking. For example, the observed clays and zeolites within Grande Ronde Basalt have complex chemistries reflecting solid solution not closely matched by any phases currently in the thermodynamic data bases for geochemical models. While techniques for estimating thermodynamic parameters for selected minerals exist (e.g., Tardy and Garrels, 1974; Chen, 1975; Nriagu, 1975; Mattigod and Sposito, 1978), their applicability to modeling is uncertain. At present it

is only possible to examine the saturation state of groundwaters with respect to selected ideal end-member compositions for clays and zeolites. Therefore, only general inferences as to the stability of these phases are possible.

During 1983, the DOE initiated a geochemical modeling program using the MINTEQ code developed by Pacific Northwest Laboratory to evaluate water samples representing all components of the hydrologic system at the Hanford Site. This program was aimed at establishing the thermodynamic activities of chemical species in solution and determining the saturation state of solid phases appropriate to the basalt system under ambient conditions.

While this investigation is the most recent and ambitious modeling project undertaken as of 1986, results from several other studies have been reported. For example, Deutsch et al. (1980; 1982a; 1982b) modeled a limited number of groundwaters from all stratigraphic levels within the mid-Columbia Plateau region. Few of these samples were obtained on the Hanford Site, and many come from boreholes open to more than one water-producing zone. Therefore, incomplete knowledge of the depth of the samples exists. In addition, the DOE reported modeling results for a small number of groundwaters from basalts at the Hanford Site (DOE, 1982, pp. 5.1-98, 5.1-116, 5.1-127). Significant limitations exist for both of these studies. First, groundwater samples were modeled at collection rather than in situ temperatures. Secondly, corrections to saturation indexes due to hydrostatic pressure were not included for sensitive phases. As discussed in Early et al. (1984a), calcite and fluorite are the principal examples where the effect of pressure on equilibrium should not be ignored.

In the study conducted for the DOE by the Pacific Northwest Laboratory (see Early et al., 1984a for a summary), several dozen spring samples and more than 100 groundwater analyses from all major water-bearing units on the Hanford Site were chosen for modeling. These data were drawn from a preliminary BWIP hydrochemical data base that had not undergone systematic evaluation as to data quality and traceability to original records. Consequently, the results should be considered as tentative and subject to revision.

Speciation for the samples was first computed at the temperature and pH values measured at the time of sampling and at atmospheric pressure. The total mass of hydrogen was determined and used as a mass balance constraint, and the pH value of the sample was calculated at the correct in situ pressure and temperature. Pressure corrections to the thermodynamic data for aqueous species were included. Finally, the corrected pH value was used to determine the speciation and solubility equilibriums for the sample using pressure corrections to the thermodynamic data.

In general, these studies (as reported by Early et al., 1984a) suggest that most groundwaters from the Wanapum and Grande Ronde Basalts tend to be undersaturated with respect to amorphous silica and allophane. Conversely, calcite and fluorite generally tend to reach saturation with increasing depth. Nearly all of the clays and zeolites in the MINTEQ data base are oversaturated in groundwaters from these stratigraphic zones. However, these phases are

ideal end-member compositions and do not closely match the more complex chemistry of clays and zeolites associated with the Columbia River Basalts. It is acknowledged that the saturation state of these end-members may not accurately reflect that for observed clays and zeolites. Therefore, the apparent oversaturation of these phases may be misleading relative to the clays and zeolites commonly observed as secondary phases in the basalts.

Of the principal phases that compute to be in permissible equilibrium with groundwaters at the Hanford Site, only amorphous silica and calcite have been positively identified. The fact that allophane and fluorite have not been observed does not mean that previous solids characterization work has been inadequate. Rather, speciation models such as MINTEQ only determine permissible equilibrium. However, the results of these modeling studies should not be ignored as future characterization work of secondary phases is performed. As noted above, the documented occurrence of a variety of secondary clays (smectite) and zeolites (e.g., clinoptilolite, mordenite) in basalts at the Hanford Site (Ames, 1980; Benson and Teague, 1982) and their apparent oversaturation in the associated groundwaters suggest that incorporation of a reaction kinetic capability into geochemical models might be useful in obtaining a closer match between the observed chemical evolution of groundwaters and model predictions. Plans to address these present limitations are discussed in Section 8.3.1.4.

Currently, the DOE has adopted the EQ3/EQ6 modeling package and will use it for future geochemical and reaction path modeling (see Section 8.3.1.4). Validation, benchmarking, and verification of these codes is in progress.

The results of preliminary modeling studies on regional groundwaters from the Columbia River Basalt aquifers obtained from the U.S. Geological Survey WATSTORE data base have been reported by Warner et al. (1986). They conclude that these shallow, regional groundwaters probably evolved by reactions including glass dissolution and precipitation of calcite, zeolites, and smectites (see also Hearn and Steinkampf, 1984). In contrast, mass balance calculations indicate that the high-chloride (>50 mg/L) groundwaters frequently observed in the Frenchman Springs Member and Grande Ronde Basalt aquifers at the Hanford Site cannot have attained their elevated chloride concentrations by simple basalt-water reactions. Future modeling activities will need to incorporate elements of the conceptual groundwater flow models developed in Section 3.9.5.2 in an attempt to understand the geochemical evolution of these deep groundwaters.

4.1.2.10 Reference groundwater compositions

The experimental geochemistry program, which is discussed summarily in the following sections of this chapter and in more detail in Chapter 7, includes extensive hydrothermal testing of basalt, bentonite, and candidate container materials and waste forms, both alone and in various combinations. In addition, experimental characterization of radionuclide solubility and

sorption behavior, as discussed in Sections 7._____ and 4.1.3, is in progress. These studies require the use of an aqueous phase that simulates observed groundwater compositions.

To simulate the geochemical environment of the basalt system as closely as possible for these experiments, reference groundwaters have been defined that are representative of flow tops and interbeds along credible flow paths underlying the Hanford Site. The compositions of the synthetic groundwaters used in experimental studies are given in Table 4.1-21. Groundwater GR-1 simulates the dominant groundwaters in the Saddle Mountains and upper Wanapum Basalts. Groundwater GR-1A simulates the groundwater composition of the Mabton interbed in the Saddle Mountains Basalt. Groundwaters GR-2, GR-2A, GR-3, and GR-4 simulate the dominant groundwaters in the Grande Ronde Basalt. The adopted compositions for reference Grande Ronde Basalt groundwater have evolved as additional hydrochemical data from new boreholes were collected. The composition of GR-4 is based on a groundwater sample from the Cohassett flow from borehole RRL-2 in the reference repository location and currently is used as a starting material for all experimental studies related to waste form and barrier material stability. Most previous experimental studies used reference groundwater GR-2 and GR-3.

Because one or more flow tops of the Frenchman Springs Member of the Wanapum Basalt may be a pathway for groundwater flow from a repository to the accessible environment, future experimental sorption studies will require a reference Frenchman Springs Member groundwater. Currently, these tests have been incorporated into hydrochemistry plans (see Section 8.3.1.4), and a reference groundwater will be chosen before the investigations begin.

4.1.3 GEOCHEMICAL RETARDATION PROCESSES

Geochemical retardation processes are important because parameters describing retardation will be input to models predicting radionuclide transport to the accessible environment. The processes and parameters that control transport of radionuclides via groundwater in the natural system are discussed in this section. A general discussion of processes that retard radionuclide movement is given in Section 4.1.3.1. The experimental techniques used to obtain sorption and desorption data on important radionuclides are briefly described in Section 4.1.3.2 along with the description of how information on chemical speciation was obtained. A summary of sorption and desorption data is presented in Section 4.1.3.3. Effects of the redox environment, pH, ionizing radiation, and complex formation on the chemical speciation and transport of radionuclides are discussed in Section 4.1.3.4. Brief discussions of matrix diffusion and conceptual aspects of radionuclide transport are presented in Sections 4.1.3.5 and 4.1.3.6, respectively. Finally, the expected transport behavior for individual key radionuclides is presented in Section 4.1.3.7.

4.1.3.1 General description of geochemical retardation processes

Physical and chemical processes within the engineered and natural systems combine to control radionuclide release to the accessible environment. These processes involve interactions of radionuclides with the groundwater-solid phases of both the engineered and the natural systems. Controlling processes include (1) sorption and desorption, (2) dissolution and precipitation, (3) diffusion, and (4) hydrodynamic dispersion of radionuclides.

Sorption involves the physical or chemical adsorption of radionuclides from groundwater by solid phases in the engineered and natural systems. Radionuclide sorption behavior is highly dependent on the environmental conditions of the groundwater flow path. Temperature, pH, Eh, and groundwater composition, in particular, are important factors that can control radionuclide sorption behavior. The physical and chemical characteristics of the geologic substrate (e.g., surface area and mineral composition) along postulated flow paths also control radionuclide sorption behavior. Sorption data relevant to the natural system are presented in Section 4.1.3.3. Sorption reactions with waste package components are discussed in Section 7.4.4.2.

Radionuclide dissolution and precipitation processes are expected to be less important in the natural system than in the engineered system. Precipitation in the natural system can only result from substantial chemical or temperature changes as the groundwater flows out from the engineered system. Evidence suggests such changes will be small; for example, the expected pH will range from 8.5 to 9.5 (Section 4.1.3.4.2), and redox conditions are expected to be reducing in both the engineered (Section 7.1) and natural systems (Section 4.1.3.4.1). Also, radionuclide dissolution and precipitation will be less in the natural system because diffusion, hydrodynamic dispersion, and sorption hysteresis will decrease radionuclide concentration along the flow path from the engineered system. Radionuclide dissolution and precipitation in the engineered system are discussed in Section 7.4.4.

Diffusion of radionuclides into pores and matrices of solid phases also retards radionuclide transport. Diffusional control of radionuclide transport in waste package packing material will be discussed in Section 7.4.3.

Hydrodynamic dispersion is a spreading or dissipation process that results in a dilution of radionuclide concentrations along the flow path. It is caused by mechanical mixing during groundwater advection and by molecular diffusion. Hydrodynamic dispersion depends on the physical structure of groundwater flow paths and, therefore, must be measured in field experiments. These field experiments are described in Section 8.3.1.4.2.3.6.

Although high-level radioactive wastes will contain many radionuclides, only a relatively small number will be present in quantities that are significant to long-term repository performance. These key radionuclides are

those that have long half-lives and large initial inventories (or large maximum inventories for daughter radionuclides). Key radionuclides were selected for sorption studies using two screening criteria that follow:

- Those with half-lives greater than 20 yr.
- Those with an inventory in the waste (after 1,000 yr decay) greater than or equal to 6.0% of the proposed EPA cumulative release limit (EPA, 1985, p. 38087).

The 20-yr half-life criterion eliminates those radionuclides that will decay to insignificant levels during the required containment period of 300 to 1,000 yr (15 to 50 half-lives or more). The second criterion eliminates radionuclides that cannot make a significant contribution to radionuclide release at the accessible environment regardless of their migration rates. A significant release is conservatively defined as greater than or equal to 6.0% of the EPA cumulative release limit.

The radionuclides remaining after applying these screening criteria are presented in Table 4.1-22. Sorption studies have emphasized the use of these radionuclides, along with several others (isotopes of strontium, radium, and lead) that were previously thought to be important. Sorption information already gathered on these nonkey radionuclides provides a better understanding of sorption processes in general and, therefore, is included in Section 4.1.3.3.

4.1.3.2 Analytical techniques

The analytical and experimental techniques described in this section apply only to radionuclide sorption and desorption measurements. As discussed previously, radionuclide dissolution and precipitation processes are not expected to be important in controlling retardation of radionuclides in the natural system. The techniques used for obtaining dissolution and precipitation information are presented in Sections 8.3.4.2.3 and 8.3.4.3.4. A description of techniques for measuring diffusion processes (Relyea et al., 1986) is given in Section 8.3.4.3.3.

4.1.3.2.1 Sorption and desorption models

Models of sorption and desorption are being developed from sorption studies and incorporated into transport models that predict radionuclide migration. A frequently used, simple sorption (or desorption) model is the empirical distribution coefficient, Kd. This quantity is simply the concentration of radionuclide sorbed on a solid divided by the concentration of radionuclide in a solution that is in equilibrium with the solid. Although the representation of distribution coefficients by Kd values implies equilibrium constants, equilibrium is rarely achieved in laboratory sorption

measurements because most rock-groundwater systems are not in equilibrium. The Kd values given in Section 4.1.3.3 are steady-state values obtained over weeks or months of equilibration time. Those values are considered to be conservative since longer equilibration times increase sorption.

Values of Kd can be used to calculate a retardation factor, R_f, that is used in solute transport models to predict radionuclide migration in groundwater. The use of K_d values in transport models requires the assumption of single-valued, linear sorption and desorption isotherms. Although this assumption yields "conservative" (high) transport rates for radionuclides, it has been shown to be erroneous for solute sorption in several groundwater-soil systems (Di Toro and Horzempa, 1982, pp. 594-602; Van Genuchten et al., 1974, pp. 29-35). A more accurate description of radionuclide sorption in many systems can be obtained by employing an empirical isotherm equation such as the Freundlich equation:

$$S = KC^N \qquad (4.1\text{-}1)$$

where

S = equilibrium concentration of sorbed radionuclide (moles per gram)

C = equilibrium concentration of radionuclide in solution (moles per liter)

K and N = empirical constants.

The Freundlich equation accurately describes many sorption and desorption reactions of dissolved metals and organic compounds. In the case of irreversible sorption (hysteresis), the sorption and desorption isotherms are not identical. When these conditions occur, both sorption and desorption Freundlich isotherm equations can be substituted into transport equations (Van Genuchten et al., 1974, pp. 29-35).

4.1.3.2.2 Experimental sorption techniques

Batch steady-state techniques were used to measure the distribution of radionuclides between the solid and liquid phases for construction of sorption and desorption isotherms. Essentially, the batch sorption method consists of contacting a known volume and composition of solution containing a radionuclide with a characterized solid of known weight for a specific length of time. The solid and liquid phases are then separated, and the steady-state concentration (concentration does not change with time) of the radionuclide in the liquid phase is determined. The amount of radionuclide sorbed on the solid phase is the difference between the radionuclide steady-state solution concentration and the initial radionuclide concentration, minus a correction

for radionuclide sorption onto the container walls. The desorption method is similar except that the solid with sorbed radionuclide is contacted with radionuclide-free groundwater for a specific length of time. The distribution of radionuclide between solid and liquid phases is then measured. The liquid phase is separated and discarded, and fresh radionuclide-free groundwater is equilibrated with the solid again. This process is repeated until a desorption isotherm is generated. Details of the sorption and desorption procedures used by the DOE are given in Salter et al. (1982, pp. 4-6) and Barney (1983, pp. 3-5).

Flowthrough (column) measurements of sorption processes are considered essential to complement and to verify data obtained from the batch experiments described above under static conditions. These experiments also will allow the identification of multiple species of radionuclides in groundwater solution. Flowthrough studies are planned (see Section 8.3.1.4.2.2), but no reliable results are available at this time.

4.1.3.2.3 Control of Eh and pH in experimental systems

The Eh and pH of the basalt geochemical system are critical variables in radionuclide sorption experiments with basalt materials. The Eh will control oxidation states of many key radioelements (e.g., technetium, neptunium, selenium, iodine, uranium, and plutonium) and, therefore, will partially determine their sorption and solubility characteristics. Similarly, groundwater pH will influence the radionuclide species that exist in solution and will also affect the sorption and solubility of radionuclides.

Because oxidation states of some radionuclides during transport along the groundwater flow path may be difficult to assess, the DOE has attempted to bound the possible oxidation states of key radionuclides by using conditions that are more oxidizing (air-saturated solutions) and more reducing (solutions containing hydrazine) than will exist in the natural system. Uncertainties exist in identifying redox reactions that control radionuclide oxidation states and in predicting the kinetics of these reactions. The concept of a single master Eh value that controls all oxidation states is probably not applicable to these systems because (1) some redox reactions probably occur on solid surfaces rather than in solution (Meyer et al., 1984, pp. 27-37); (2) some redox couples in the same groundwater solution may not be at equilibrium with each other (Lindberg and Runnells, 1984); and (3) reactions of radionuclides with redox couples in the system may be kinetically hindered (see also Section 4.1.3.4.1). The actual sorption behavior of radionuclides likely will be intermediate between the extremes of air-saturated solutions and solutions containing hydrazine (all other factors being the same).

Hydrazine was chosen as a reducing agent for radionuclides in some sorption experiments with reduced radionuclide species because of the following reasons.

- It is soluble and chemically stable at the pH and temperatures of the experiments.

- It reacts rapidly with most radionuclides of interest to produce low-oxidation states in solution.

- It does not form complexes with radionuclides at the pH and temperatures of the sorption measurements. (Complexation would likely decrease sorption. Experimental evidence indicates that for radionuclides that can be reduced in solution, the addition of hydrazine increases sorption.)

- It produces innocuous oxidation reaction products (N_2 and H_2O) that do not interfere with sorption reactions.

Several potential problems associated with addition of hydrazine to sorption measurement systems are recognized. Kelmers et al. (1984a and 1984b) have implied that radionuclide reactions with hydrazine may not yield the same reduced species as reactions with reducing agents present in the groundwater flow path. Although this may be true for some radionuclides with multiple lower oxidation states, most of the radionuclides of interest have only one stable reduced state that is soluble in aqueous solution. This reduced state can be predicted with confidence from studies reported in the literature (Table 4.1-23). Reduction kinetics for several of these reactions are also available. Additional evidence for reduction is the significant increase in sorption observed when hydrazine is present. For several radionuclides that cannot be reduced in aqueous solution (e.g., $^{90}Sr^{2+}$, $^{226}Ra^{2+}$, $^{137}Cs^{+}$), hydrazine actually decreases sorption due to ion exchange reactions shown in Equation 4.1-2 (Barney, 1984) as follows:

$$N_2H_5^+ + (^{\text{mineral}}_{\text{surface}}) - C_S = (^{\text{mineral}}_{\text{surface}}) - N_2H_5 + C_S^+ \qquad (4.1\text{-}2)$$

Kelmers et al. (1984a and 1984b) have also suggested that hydrazine may attack secondary minerals present in sorption experiments and alter their structures. However, if secondary minerals are altered to any significant extent, sorption of radionuclides that are not reduced by hydrazine, such as $^{241}Am(III)$, should also be affected. However, Barney (1984) has shown by statistically designed experiments that sorption of $^{241}Am(III)$ on interbed materials that contain secondary minerals is not significantly affected by the presence of hydrazine. It can be concluded that the mineral surfaces involved in radionuclide sorption are not significantly altered by the presence of hydrazine.

Kelmers et al. (1984a and 1984b) also point out that hydrazine is a base and will increase groundwater pH. In the BWIP sorption experiments, small amounts of hydrochloric acid were added to the synthetic groundwater solutions to neutralize the solutions to desired pH levels. Increased chloride concentration, due to addition of hydrochloric acid, does not affect radionuclides sorption reactions (Barney, 1984). The formation of hydrazine carbonate ($H_2NNHCOO^-$) by reaction of bicarbonate with hydrazine in experimental solutions (as suggested by Kelmers et al., 1984a and 1984b) seems

unlikely. The carbonate has only been prepared by reaction of carbon dioxide gas with hydrazine in strongly basic solution (Staal and Faurholt, 1951). This reaction product decomposes in water to form hydrazine and carbon dioxide.

An alternative method of radionuclide oxidation state control has been adopted by the BWIP because of the postulated problems associated with using hydrazine. The alternative method consists of removing enough oxygen from the groundwater and atmosphere above the groundwater-solid mixture so that the solids and dissolved redox couples (e.g., iron(II)/iron(III)) control oxidation states. The results of this new method will be used to confirm (or reject) the sorption results obtained by the above techniques.

In the alternative method, no chemical is added to the experimental system that does not naturally occur in groundwater. It is, however, more difficult to perform laboratory sorption measurements at very low oxygen concentrations. Oxygen must be removed from experimental systems to very low levels, and this requires the use of air-tight chambers and inert atmospheres of very low oxygen concentration. Also, this method of oxidation state control has limited usefulness because of very slow reaction rates at low temperature. Reactions between radionuclides and reducing species (such as iron(II) species) at the surface of the solids or dissolved from the solid into the groundwater are expected to be slow. Crushed basalt has been reported to control groundwater Eh at negative values (as measured by a platinum electrode) in deoxygenated synthetic groundwater (Jantzen, 1983) at 60 °C. However, the fresh, unaltered surfaces of crushed basalt are likely to be more reactive than solids found in the natural system.

A limited number of sorption experiments have been performed in an inert atmosphere glovebox using basalt to control the Eh at 60 °C (Ames and McGarrah, 1980b, pp. 14-19). The lowest oxygen concentrations attained in the glovebox were about 2.1 p/m. This corresponds to an oxygen fugacity of about 10^{-6} atm in solution, or a calculated Eh of +0.67 V at a pH of 8.0. This is much more oxidizing than the potential expected in deep basalt groundwaters (see Section 4.1.3.4.1). Not surprisingly under these relatively oxidizing conditions, the technetium, neptunium, and plutonium tracers in these sorption experiments were not reduced, and their sorption behavior was equivalent to that in air-saturated groundwaters. More recent results using higher temperatures (90 to 150 °C) indicate that technetium(VII), uranium(VI), and neptunium(V) can be reduced at a measurable rate by crushed basalt under an atmosphere containing low-oxygen concentrations. The rates of these reduction reactions are slow even at the higher temperatures (Barney et al., 1985, pp. 1-50). It is apparent that better oxygen removal techniques must be used to allow Eh control by the groundwater-solid system. These techniques are now being developed and are discussed in Sections 8.3.1.4.2.3 and 8.3.4.2.3.2.2.

Jantzen and Wicks (1985) have measured the redox potentials of argon-saturated synthetic Grande Ronde Basalt groundwater (see Section 4.1.2.10 for GR-4 composition), before and after contact with crushed Umtanum flow basalt, for 90 h at 60 °C in an argon atmosphere. Using a platinum electrode, redox potentials of +0.2 to +0.4 V and -0.34 to -0.40 V were measured before and

after adding the basalt, respectively. With no basalt present, the potential is probably controlled by the H_2O/O_2 couple due to the small amount of oxygen contamination expected in the experimental apparatus. When basalt is added, the platinum electrode apparently responds to reduced species (e.g., iron(II), sulfur(-II)) dissolved from the basalt more readily than to the oxidizing H_2O/O_2 couple. This seems reasonable since it is generally found that potentials of dissolved air in groundwater measured with platinum electrodes are more negative than expected due to a slow oxidation step and/or reaction of the oxygen with the electrodes platinum metal (Garrels and Christ, 1965, pp. 136-137). Because of the existence of competing redox couples in these solutions, it is difficult to predict which couple will control oxidation states of radionuclides. These oxidation states must be determined experimentally for a given set of conditions.

Control of groundwater pH is easier than control of redox conditions in sorption experiments since pH is established by the groundwater-rock system without special effort. Most basalt groundwaters are buffered over a narrow pH range by solids in contact with the groundwater. Intentionally induced changes in pH from this narrow range are usually undesirable because of the resulting changes in groundwater composition and unknown reactions at the solid surface. Such effects would make the interpretation and application of sorption data difficult. Although pH is always measured in these experiments, the solids present in the systems are allowed to control the pH of the groundwater.

4.1.3.2.4 Control and identification of radionuclide precipitation

The solubilities of many key radionuclides (mainly actinides, lanthanides, and transition elements) are severely limited in groundwater solutions used in performing sorption measurements (Early et al., 1984b, pp. 147-166). The high pH of these solutions (about 8.5 to 9.5) and their relatively high carbonate concentrations (50 to 250 mg/L) promote the formation of slightly soluble oxide, hydroxide, and carbonate compounds of these radionuclides. To avoid confusing sorption and precipitation processes, it was essential that radionuclide concentrations in sorption experiments be maintained below solubility limits. This was accomplished by determining sorption isotherms for each radionuclide (see Section 4.1.3.3.4). If precipitation occurred during sorption, the isotherm (as a Freundlich plot) began to curve upward to a solution concentration maximum due to the fact that all additional quantities of radionuclide added to the system went to the solid phase. All sorption data reported in Section 4.1.3.3.4 were obtained at radionuclide concentrations below this concentration maximum.

4.1.3.3 Sorption

The sorption and desorption behavior of key radionuclides in groundwater-geologic solid systems must be quantitatively described in models that predict radionuclide transport for safety assessment of a nuclear waste repository in basalt. Sorption is an important mechanism for preventing or retarding radionuclide transport via groundwater. Sorption processes will help determine whether or not federal regulations for long-term isolation of radioactive wastes from the environment (see Table 4.0-2) will be met by the proposed repository.

In the repository, sorption of radionuclides can occur on engineered barriers materials such as the container, packing material, tunnel backfill, shotcrete, concrete, or seal materials. Outside the repository, sorption on a variety of naturally occurring geologic materials can be important, depending on the flow path of contaminated groundwater. These geologic materials include basalt (entablature and flow-top materials), secondary minerals associated with basalt, interbed materials found between some of the basalt flows, and possibly the glaciofluvial sediments above the basalts. Secondary minerals are found lining and filling the vesicles, vugs, and fractures in the Columbia River basalts (see Section 4.1.1.3). Because fractures are the most probable initial pathway for groundwater movement in these formations, it is likely that secondary minerals found in this environment will be primary radionuclide-sorbing media outside the engineered barriers system. Secondary minerals are also important in transport along flow tops.

Most sorption data must, of necessity, be obtained from laboratory measurements in which the expected natural environmental conditions in the groundwater flow path are reproduced as accurately as possible. A summary of the available sorption data for representative geologic materials found in probable groundwater flow paths from a repository in the Columbia River basalts is presented in the following sections. Sorption data for engineered materials are presented in Chapter 7. Detailed descriptions and discussions of the sorption data can be found in Ames and McGarrah (1980a, pp. 1-95; 1980b, pp. 1-97; 1980c, pp. 1-20), Ames et al. (1981, pp. 1-127; 1984, pp. 1-27), Salter et al. (1981a, pp. 1-39; 1981b, pp. 1-38; 1982, pp. 1-48), Barney (1981a, pp. 1-28; 1981b, pp. 1-26; 1982, pp. 1-28; 1983, pp. 1-19; 1984, pp. 3-23), Barney et al. (1983, pp. 1-55; 1985, pp. 1-50), and Smith et al. (1980, pp. 2-311 to 2-344).

4.1.3.3.1 Materials used in sorption measurements

The compositions of groundwaters in the major water-bearing zones of the Columbia River basalts at the Hanford Site have been determined (Gephart et al., 1979, pp. II-128 to II-138, and Section 3.9.1.3). There are two distinct groundwater types (based on pH) present in the basalts: (1) a bicarbonate-buffered groundwater (pH about 8 at 25 °C) characteristic of the Saddle Mountains and Upper Wanapum Basalts and (2) a silicic acid-buffered groundwater (pH about 10 at 25 °C) characteristic of the lower Wanapum and

Grande Ronde Basalts. Synthetic groundwater compositions have been established that simulate these two groundwater types. The compositions of the synthetic groundwaters used in sorption experiments are given in Section 4.1.2.10. Synthetic groundwaters rather than actual groundwaters are used to ensure the availability of a stable, compositionally consistent groundwater unaffected by field sampling variables. Measurements using actual groundwaters will also be performed for confirmation (see Section 8.3.1.4).

The sorptive characteristics of a number of geologic solids from the Columbia River Basalt Group have been studied. Basalt entablature samples from candidate repository horizons (Umtanum and Cohassett flows), Umtanum flow-top material, secondary minerals from the Pomona flow, and interbed materials from the Mabton and Rattlesnake Ridge interbeds have been used in radionuclide sorption studies. A summary of experimental conditions used for sorption measurements on these materials is given in Table 4.1-24. The sources of these solids and references to detailed characterization of the materials are given in Table 4.1-25. Many of the geologic samples were obtained from outcrops of the listed stratigraphic units. These outcrops are expected to have a composition similar to the rock at depth. Plans for sorption studies with other geologic samples found along expected flow paths are described in Sections 8.3.1.4.2 and 8.3.1.4.2.3.

4.1.3.3.2 Sorption mechanisms

An understanding of radionuclide sorption mechanisms will allow greater confidence in predicting sorption behavior over the wide range of conditions expected along groundwater flow paths. Measurements of the effects of various factors affecting sorption (e.g., groundwater composition, temperature, mineral composition) can lead to mechanistic information. These studies also can identify additional factors that significantly affect sorption and allow more detailed measurements of these effects to be made. The mechanistic information that can be derived from these studies include the following:

- Extent of competition for sorption sites between radionuclides and major ions in the groundwater.
- Type of radionuclide bonding to the solid (ionic or covalent bonding).
- Extent of formation of complexes between groundwater components and radionuclides.
- Identification of oxidation states of multivalent radionuclides.
- Solubility limits for compounds of radionuclides.

Based on results reported in the references given in the introductory material for Section 4.1.3.3, several conclusions can be made concerning the mechanisms of radionuclide sorption reactions on basalt, secondary minerals,

and interbed materials. All evidence indicates that cesium, strontium, and radium are at least partially sorbed by ion exchange mechanisms since they can be partially desorbed by increasing concentrations of competing cations. Cations of similar ionic radii (K^+, Na^+, and Ca^{2+}) effectively compete with these radionuclides for exchange sites. A fraction of each of these radionuclides is irreversibly sorbed, however, due to processes other than ion exchange.

The sorption behavior of plutonium, neptunium, uranium, and technetium on basalts, secondary minerals, and interbed materials is strongly dependent on the oxidation states of their dissolved species. The reduced species are more strongly sorbed than oxidized species for each radioelement. Technetium exists in solution under oxidizing conditions as the anion TcO_4^- and is very poorly sorbed by these geologic solids. Plutonium, neptunium, and uranium are more strongly sorbed than technetium under oxidizing conditions. Based on thermodynamic evidence and the fact that they are not removed from the solids by ion exchange, each of these radionuclides are sorbed, at least partly, by chemisorption. Additional evidence for chemisorption mechanisms for these four radionuclides is the relatively large partial molar heats of sorption (ΔH^*) calculated for their sorption reactions on Mabton interbed material using the method described by Aly et al. (1980). Values of ΔH^* for plutonium, neptunium, uranium, and technetium are greater than 5 kilocalories per equivalent, which is larger than expected if ion exchange mechanisms are dominant.

Recent models of adsorption of hydrolyzable metal ions on oxides from aqueous solutions point to formation of surface complexes at the water-oxide interface (Schindler, 1981; Davis et al., 1978; Hsi and Langmuir, 1985). Coordinate bonding occurs between the surface oxygen ligands (e.g., from silicates or other mineral oxides) and the metal ion. For radionuclides such as neptunium, uranium, plutonium, and technetium, the stability of complexes with ligands containing oxygen is greater for the reduced species ((III) or (IV) oxidation state) than the oxidized species ((V), (VI), or (VII) oxidation state). This is consistent with observations that the reduced species of these radionuclides are more strongly sorbed than oxidized species.

Another possible sorption mechanism is exchange of dissolved waste radionuclides with naturally occurring isotopes contained in minerals existing along groundwater flow paths. An example is the exchange of $^{12}CO_3^{2-}$ in calcite for $^{14}CO_3^{2-}$

$$Ca^{12}CO_3 + {}^{14}CO_3^{2-} = Ca^{14}CO_3 + {}^{12}CO_3^{2-}.$$

This reaction has been found to cause significant sorption and retardation of radioactive carbon in laboratory experiments (Allard et al., 1981; Anderson et al., 1982; and Garnier, 1985).

4.1.3.3.3 Sorption kinetics

The rates of radionuclide reactions with the geologic substrate must be considered in measuring radionuclide sorption behavior. If sorption and desorption reactions are slow compared to groundwater velocity, the kinetics of these reactions will affect radionuclide transport rates. For the relatively short time scale of laboratory measurements (compared with repository operation), kinetic information must be obtained as follows:

- To determine the time required for batch sorption and desorption measurements to reach steady-state conditions.
- To establish required column residence times for flowthrough sorption experiments.
- To interpret the shapes of breakthrough and elution curves from flow-through sorption measurements (Schweich and Sardin, 1981, pp. 1-33; and Van Genuchten and Cleary, 1979, pp. 349-383).

Slow radionuclide sorption or desorption reactions (compared to practical experimental time scales) can result from the following:

- Slow reactions of the geologic solid substrate with the groundwater solution, resulting in alteration of the solid surface and changes in the groundwater composition.
- Slow redox reactions of the radionuclide with the solid that change the sorption behavior of the radionuclide.
- Slow diffusion of the radionuclide into (or out of) small pores in the solid substrate.
- Slow ion exchange or chemisorption reactions at the surface of the solid.

Radionuclide sorption reactions with fresh basalt surfaces are relatively slow to reach steady-state conditions, compared with all the other geologic materials studied. Measurements of radionuclide sorption and desorption rates have been performed for reactions with fresh basalt, altered flow-top basalt, secondary minerals (Barney et al., 1983, pp. 1-55; Barney, 1981a, pp. 6-8), and interbed materials. A comparison of the neptunium sorption rate curves for fresh, crushed basalts of the Cohassett and Umtanum flows with that of the Umtanum flow top is shown in Figure 4.1-14 as an example. Sorption of neptunium on the highly altered flow-top basalt reached 90% completion (90% of neptunium sorbed after reaching steady-state conditions) in less than 0.25 h, whereas sorption on the fresh basalts required 22 to 28 h to reach 90% completion. As shown in Table 4.1-26, sorption was much faster on flow-top material than on fresh basalt surfaces for both oxidizing and reducing conditions for each of eight different radionuclides studied. Detailed descriptions of rate equations and rate constants are given in Barney et al. (1983, pp. 1-55).

The slow sorption reactions with fresh basalt are probably a result of slow alteration of the fresh basalt surfaces by groundwater (Barney and Brown, 1980, pp. 290-298). The glassy mesostasis phase of fresh basalt is quite reactive, even at the low temperature (60 °C) of these sorption measurements. Dissolution of this glassy phase can change the composition of the groundwater and the composition of the surface of the basalt forming more highly sorbing phases. Materials from interbed and interflow zones of the basalt formation that have been in contact with groundwater for long time periods and contain highly sorbing secondary minerals are not likely to be altered measurably during sorption measurements. Thus, sorption reactions with these materials reach steady-state conditions relatively fast.

Rates of sorption reactions with fresh basalt surfaces may, in some cases, be controlled by reduction of the radionuclide at the basalt surface. Reduction at the surface is most likely to occur when the sorption reaction is performed under conditions of low oxygen concentration (anoxic conditions). Reduction of neptunium(V) (Meyer et al., 1984, pp. 18-37) and neptunium(VI) (Susak et al., 1983, pp. 266-270) on fresh basalt surfaces yields neptunium(IV), which is sorbed very strongly on the basalt. Technetium(VII) reduction on basalt surfaces is very sensitive to dissolved oxygen (Meyer et al., 1984, p. 35) and occurs at a very slow rate. The oxidation state of the sorbed technetium species has not been well characterized, but is thought to be technetium(IV). Since anoxic conditions are expected in the deep basalts (see Section 4.1.3.4.1), these reduction reactions will control the transport and chemical behavior of radionuclides that can be reduced.

Measurements of radionuclide desorption rates are difficult to perform because many sorption reactions with geologic solids are only slightly reversible, yielding concentrations of desorbed radionuclides that are too low to measure. Under reducing conditions, desorption of uranium, neptunium, and plutonium from crushed basalt and flow-top basalt was not measurable. However, under oxidizing conditions, desorption of these radionuclides for fresh basalt was measurable but slow. Desorption rate curves for neptunium desorption from basalt of the Cohassett flow entablature and Umtanum flow top are shown in Figure 4.1-15. Both sorption and desorption of neptunium from crushed basalt were slow to reach a steady state compared to the flow-top material. As shown in Table 4.1-27, desorption was extensive only for neptunium and uranium under oxidizing conditions from fresh basalt into GR-3 groundwater.

4.1.3.3.4 Sorption and desorption isotherms

The Freundlich isotherm (see Equation 4.1-1) was found to accurately describe sorption and desorption of most of the radionuclides studied except when precipitation of the radionuclide occurred. Although sorption capacity is not accounted for in the Freundlich equation, no sorption capacity limit has ever been observed. This is probably because the low solubility limits for radionuclides in deep basalt groundwaters does not allow saturation of sorption sites on the geologic solids.

Sorption and desorption isotherms were measured for geologic solids expected in groundwater flow paths in and adjacent to the repository isolation system. These geologic solids include basalt entablature, flow top, secondary minerals, and interbed materials.

Examples of Freundlich plots are given in Figures 4.1-6 through 4.1-23. Examples of Freundlich constants calculated from regression analyses of Freundlich plots (Barney, 1982, pp. 4-11) are presented in Tables 4.1-28 through 4.1-32.

Two types of error measurements are given in the isotherm constants that follow. The first, the standard error of estimate, is given by Equation 4.1-3:

$$\text{Standard Error of Estimate} = \sqrt{\frac{\Sigma(y-\hat{y})^2}{n-2}} \qquad (4.1\text{-}3)$$

where

n = number of data pairs

$\Sigma(y-\hat{y})^2$ = sum of the squares of differences between the experimental and computed log S values (y and $\hat{y}$, respectively).

It is a measure of dispersion about the straight line given by the regression equation (Eq. 4.1-4):

$$\log S = N \log C + \log K \qquad (4.1\text{-}4)$$

which is the log of Equation 4.1-1. The second type of error measurement is the coefficient of determination, r^2, which indicates the quality of fit achieved by the regression. Values of r^2 close to 1.0 indicate a better fit than values close to 0.0. Each value of K and N in Tables 4.1-28 through 4.1-32 is based on 12 to 15 measurements of radionuclide distribution between solid and solution phases. Triplicate measurements were performed for each initial concentration of radionuclide.

Statistical measurement of the correlation coefficient (r) for regression shows that the Freundlich equation accurately describes sorption of radionuclides on entablature basalt.

Examples of Freundlich plots (log S versus log C) are given in Figures 4.1-16 through 4.1-19 for cesium, uranium, radium, and strontium sorption on sandstone of the Rattlesnake Ridge interbed at 23, 60, and 85 °C. Examples of Freundlich plots for radionuclide sorption on entablature basalt of the Umtanum flow and secondary minerals are given in Figures 4.1-20 through 4.1-23. Freundlich constants calculated for radionuclide sorption on basalt

of the Umtanum and Cohassett flows and Umtanum flow top and secondary minerals from the Pomona flow (Ames and McGarrah, 1980b, pp. 21-75) are shown in Tables 4.1-29 through 4.1-31.

Freundlich constants for sorption of several radionuclides on interbed materials are given in Tables 4.1-31 and 4.1-32 for two temperatures (Barney, 1982, p. 10; 1983, pp. 8-14). The values for the coefficients of determination (r^2) are all near 1, which indicates that the data fit the Freundlich equation quite well.

The effects of temperature on sorption isotherms of several radionuclides can be determined by examination of the data presented in the foregoing figures and tables. Over the temperature range of 23 to 85 °C, several general observations can be made as follows:

- Cesium sorption appears to decrease significantly as the temperature increases.
- Strontium and radium sorption are only slightly affected over this temperature range.
- Uranium and selenium sorption increase with increasing temperature under both oxidizing and reducing conditions.
- Neptunium sorption is not appreciably affected.

Interpretation of the effects of temperature on sorption of these radionuclides is premature because of the complexities of the systems studied. Temperature affects most of the factors that control the sorption process (e.g., complex formation, redox reactions, groundwater composition, alteration of mineral surfaces). Sufficient data do not exist at the present time to identify, with confidence, those temperature-sensitive factors that control the sorption process. Plans for estimating these factors are given in Chapter 8.

The use of a single set of Freundlich constants to describe both sorption and desorption reactions requires the assumption that sorption reactions are reversible. However, a number of studies (Van Genuchten and Cleary, 1979, pp. 349-386; Koskinen et al., 1979, pp. 871-874; Elrashidi and O'Connor, 1982, pp. 27-31; Peek and Volk, 1985, pp. 583-586; Corwin and Farmer, 1984, pp. 507-514; Isaacson and Frink, 1984, pp. 43-48; Di Toro and Horzempa, 1982, pp. 594-602; Reddy and Perkins, 1974, pp. 229-231) have shown that K and N for both organic and inorganic solutes depend on sorption direction (i.e., whether sorption or desorption occurred). In each case, N was less and K was greater (see Eq. 4.1-1) for desorption than sorption; thus, a sorption hysteresis effect was observed.

Sorption hysteresis will, of course, affect radionuclide transport. For example, if hysteresis occurs during a column experiment in which a pulse of tracer is added to the influent, the effluent curve will show significant tailing and a reduction in peak concentration. Ignoring hysteresis effects

could cause significant, albeit conservative, errors in predicting radionuclide movement through the Hanford Site (Barney and Reed, 1985), since hysteresis will decrease radionuclide movement.

Reversibility of sorption reactions has been determined by comparing sorption and desorption isotherms for a given radioelement in the solid-groundwater systems. If the isotherms are identical, the sorption reaction is reversible. Most radionuclide sorption reactions studied thus far in systems relevant to radionuclide transport in basalt formations have been shown to be irreversible to some degree. These irreversible sorption reactions include reactions of complexed actinides and simple cations such as Cs^+ and Sr^{2+}. Specific examples of hysteresis are given in the following paragraphs.

Examples of sorption hysteresis

Desorption isotherms for selenium, technetium, neptunium, uranium, and radium have been measured for Mabton interbed materials under both oxidizing and reducing conditions at 60 °C using the Grande Ronde Basalt groundwater composition, GR-1A (see Section 4.1.2.10 for composition). The reason for measuring desorption isotherms is to determine whether or not the sorption reactions are reversible (i.e., exhibit hysteresis). An example of the results of desorption isotherm measurements is shown in Figure 4.1-24. These curves are Freundlich plots of the sorption and desorption data for neptunium at 60 °C under oxidizing and reducing conditions. The two desorption curves were obtained using different tracer loadings (initial S values). Both plots show hysteresis since the slopes of the desorption curves are less than the slopes of sorption curves. Hysteresis is more evident for neptunium sorption under reducing conditions; however, the ratio of Freundlich exponents N_s/N_d, where N_s and N_d are the measured exponents for sorption and desorption, respectively, is a measure of the magnitude of hysteresis. Larger values for N_s/N_d indicate greater hysteresis effects. For neptunium sorption under oxidizing conditions, N_s/N_d is approximately equal to 2, and for reducing conditions, N_s/N_d equals 435. The large value calculated for reducing conditions implies that neptunium will be strongly retained by Mabton interbed solids if reducing conditions persist in this interbed. Additional examples of desorption isotherm measurements are given in Figures 4.1-25 through 4.1-27 for selenium, technetium, and uranium.

These results illustrate the inadequacies of attempting to describe radionuclide sorption with a single Kd value. For a given set of conditions (groundwater composition, Eh, pH, temperature), both sorption and desorption isotherms are required. In addition, since the K values for Freundlich desorption isotherms are not unique but depend on radionuclide loading on the solid, the maximum S values must be calculated.

A summary of N_s/N_d values for each radionuclide sorption-desorption reaction with Mabton interbed material at 60 °C is given in Table 4.1-33. These data show that the reduced species of selenium, technetium, neptunium, and uranium are more irreversibly sorbed on Mabton interbed material than the oxidized species. The reducing environment expected in the interbed layers found in basalt formations at depth should significantly decrease the mobility

of these radionuclides and thus provide an additional safety factor for waste storage. The N_s/N_d values for sorption of cesium and strontium on basalt and secondary minerals (Table 4.1-34) indicate that even simple cations are irreversibly sorbed on these solids.

4.1.3.3.5 Values of Kd for modeling

As stated in Section 4.1.3.2.1, sorption of most radionuclides is complicated by nonlinearity of the sorption isotherms and irreversibility of sorption reactions. Because of these complications, an accurate description of sorption requires both sorption and desorption isotherms. At the present time, the BWIP performance assessment models are not equipped to use isotherm data but instead use a single-valued distribution coefficient (Kd) to describe sorption of each radionuclide. Van Genuchten and Wierenga (1974, pp. 22-29) have shown that incorporation of sorption and desorption isotherms into numerical transport models is not a difficult task. Alteration of performance assessment models by the BWIP to include these isotherms should be completed in the near future. In the meantime, if only conservative estimates of radionuclide transport are required (estimates that minimize the effects of sorption on transport), single-valued Kd values may be used. This is true because nonlinear isotherms and irreversible sorption reactions decrease the average transport velocity of radionuclides. The effect of nonlinear isotherms on transport is to sharpen the front of the radionuclide concentration peak and increase tailing. Irreversible sorption reactions will lower the radionuclide solution concentration peak height and also increase tailing.

Values of Kd used for modeling radionuclide transport in Umtanum flow basalt, secondary minerals, and interbed materials are given in Table 4.1-35. Measured ranges of Kd values (from references given in the introduction to Section 4.1.3.3) are also shown for comparison. The reference values selected for modeling were obtained by dividing the lowest average Kd value for either basalt or secondary minerals obtained under any conditions (e.g., oxidizing, reducing, temperature, groundwater) by a safety factor of five. This yields the conservative values of Kd given in Table 4.1-35. For several radionuclides (strontium, cesium, radium, and neptunium), more recent sorption data have extended the ranges of measured Kd values so that the conservative values given in the table (from a BWIP data package; Salter and Jacobs, 1983) are not exactly a factor of five less than the lowest measured value.

4.1.3.3.6 Sorption on colloids

Another possible mechanism for radionuclide transport from the repository is the sorption of dissolved radionuclides onto suspended colloidal particulates followed by colloid transport through porous, geologic media. The formation of colloidal hydrous oxides of radionuclides (e.g., polymeric transuranic hydrous oxides) by reaction of the waste form with water is also a

possibility. Particulates may arise from erosion of host rock material, mobilization of fine clay particles, or surface spalling of waste package materials in the repository (waste matrix, container, or packing material).

As radioactive particles move through the geologic formation, surrounding rock surfaces will compete for sorbed radionuclides. Also, particles and rock surfaces will interact to control the movement of particles. Several mechanisms can potentially remove particles from suspension in the groundwater (Apps et al., 1982, pp. 70-76). These include the following:

- o Physical filtration where pore sizes in the medium are too small for the particles to pass through.
- o Gravitational settling of particles, which depends on particle mass, size, and transport velocity.
- o Flocculation caused by Van der Waals forces or electrostatic attraction of particles.
- o Dissolution of the particle in groundwater.

Measurements of naturally occurring colloid concentrations in basalt groundwaters and their characterization have not yet been completed (see Section 4.1.2.7). Little information on colloids in deep groundwaters exists in the literature. Measurements reported by Neretnieks (1978, pp. 1-14) and Barnes (1975, pp. 177-191) indicate that particle concentrations in deep groundwaters are very low (about 1 to 3 p/b).

Preliminary laboratory studies have been completed that attempt to evaluate the capability of particulates to serve as carriers of sorbed radionuclides. Eichholz (1979, pp. 1-88) investigated the movement of labeled kaolin particles through columns of crushed basalt. Ames et al. (1984, pp. 1-27) examined the radionuclide sorption characteristics of bentonite and silica colloids and the transfer of radionuclides between these colloids and crushed basalt.

Obviously, the use of crushed basalt in these studies does not precisely duplicate actual conditions expected in basalt fractures. These fractures, which are important conduits of groundwater, contain secondary minerals that are not present in the laboratory experiments. However, for the purpose of measuring radionuclide distributions, the use of crushed basalt is probably conservative since any secondary minerals in fractures would only transfer more of the radionuclide from the colloid due to increased sorption on secondary minerals that have much higher surface areas. Abundant data exist to show that sorption on secondary minerals is greater than on crushed basalt (see Tables 4.1-28 and 4.1-30). Colloid transport and radionuclide distribution measurements in the presence of secondary minerals is expected to be difficult since some of these minerals contain colloidal-sized particles that often must be kept separate from the original colloids being studied.

Eichholz (1979, pp. 1-88) investigated the effects of salt concentration on kaolin particle transport through crushed basalt (40 to 50 mesh) columns at room temperature. Although kaolin is not expected in the basalt-groundwater system, it represents possible colloidal-sized particles in the system. The critical coagulation concentration (minimum concentration required to cause coagulation) for NaCl coagulation of kaolin in water was found to be about 1,000 mg/L (0.017M). Kaolin suspensions (mean particle size = 0.13 μm (5.1×10^{-6} in.)) containing 0, 500, 750, and 1,250 mg/L NaCl were passed through these columns, and the kaolin concentration in the effluents was measured. After about 14 pore volumes of solution had passed through the columns, the percent of the injected kaolin eluted was 1%, 84%, 45%, and 16%, respectively. Except for the suspension containing no salt, the suppression of kaolin transport with increasing salt concentration can be explained by physical filtration of kaolin agglomerates that form at the higher salt concentrations (near the critical coagulation concentration). The drastic change in kaolin particle behavior at zero salt concentration remains to be explained. These data indicate that even though the pore size of these crushed basalt columns is much greater than the pore size expected in actual groundwater flow paths, transport of colloidal-sized particles is significantly retarded.

Ames et al. (1984, pp. 1-27) measured radionuclide distributions in groundwater-colloid-basalt systems to determine the tendency of radionuclides to sorb onto colloids and to be transferred from colloids to basalt surfaces. Both of these processes are important to consider if radionuclide transport by colloids is significant. Two types of colloids were studied--a bentonite colloid representing a potential component of packing or backfill materials and a hydrated silica colloid that might represent colloids generated from a glass waste form. The radionuclide tracer was first sorbed onto the colloid from GR-3 synthetic groundwater and then crushed basalt was added to the mixture to determine if the sorbed radionuclide could be transferred to the basalt surfaces. The groundwater-colloid-basalt mixture was continuously agitated for 26 d. The colloid suspension was then separated from the crushed basalt by decanting, and the groundwater and colloids were separated by filtration. A summary of results from these measurements is given in Table 4.1-36.

The sorption behavior of the radionuclides was significantly different for the two types of colloids. Sorption on bentonite was generally less than on hydrated silica colloids. Also, most radionuclides were readily transferred to the basalt from bentonite colloids. The sole exception was neptunium under reducing conditions. For the hydrated silica colloids, sorbed uranium, neptunium, and selenium were not measurably transferred to the basalt under reducing conditions. However, radium was readily transferred. The behavior of radium and uranium was confirmed with column flow-through measurements (Ames et al., 1984, pp. 20-27). Based on these results, it can be concluded that colloid transport will be significant only for radionuclides that are strongly and irreversibly sorbed on the colloids. Reduced uranium, neptunium, and selenium appear to be irreversibly sorbed on hydrated silica colloids and thus, might be transported by these colloids.

To accurately assess the potential for radionuclide transport on colloids, more data are required. In particular, additional solids likely to be present in the contaminated groundwater flow path must be examined. These include waste package container corrosion products, packing material, backfill material, repository, intact basalt having natural fissures, and basalt flow-top solids. Experimental studies will address the stability of colloidal suspensions in groundwater as they pass through the above solids and the distribution of radionuclides among groundwater, colloids, and immobile solids. Plans for these studies are presented in Sections 8.___ and 8.3.4. In addition, plans for field testing colloidal transport are given in Section 8.3.1.4.

4.1.3.4 Processes affecting radionuclide concentrations and speciation in solution

A key factor in selecting the Columbia River basalts for consideration as a site for high-level nuclear waste disposal is the expectation that the site geochemistry itself will substantially limit the transport of radionuclides once they have been released from the waste package. This expectation is based on the moderately high pH (approximately 10), the reducing conditions found in the preemplacement environment, and the sorption properties of the minerals in the natural system.

Radionuclide transport through the natural system is primarily controlled by its concentration. The two primary factors controlling the concentration of radionuclides in the natural system are their rate of release from the waste package and their mobility through the natural system. Release from the waste package is expected to be limited by the solubility, sorption, and diffusion of the radionuclides in the packing material. This is discussed in greater detail in Section 7.4.4.

Factors that may affect the mobility of radionuclides during the controlled release period were identified in Table 4.0-3 as sorption, precipitation, basalt-water hydrothermal interaction, the oxidation/reduction environment, temperature, pressure, pH, and groundwater and solid composition. Additional topics discussed were complexation with species in the groundwater, ionizing radiation, and chemical substitution.

Of the factors listed above, only the oxidation/reduction environment, pH, complexation with species in the groundwater, and ionizing radiation are discussed in this section. The effect of chemical substitution and precipitation reactions is not considered important in the natural system. These reactions are expected to reduce rather than enhance radionuclide mobility. The hydrostatic pressure present at the mined geological disposal system will not significantly alter radionuclide mobility in the natural system. The effects of basalt-groundwater interactions, groundwater composition, and temperature on radionuclide transport in the natural system are discussed in Section 4.2.

4.1.3.4.1 Oxidation/reduction environment in the natural system

The oxidation/reduction (redox) environment of the natural system can substantially affect the transport of multivalent radionuclides. The reduction of radionuclides is characterized by high sorption, irreversible sorption, and low solubilities. The ability of the basaltic environment to reduce radionuclides received substantial attention in past experimental efforts (Sections 7.4.1 and 7.4.4) and is a key objective of experimental programs outlined in Section 8.3.4.3.4.

The redox environment of the natural system in the basalt flows of the Columbia Basin prior to the emplacement of high-level nuclear waste containers can be qualitatively described as a reducing environment (see Section 3.9.1.3.6). The evidence for this conclusion and its impact on the solubility and migration of radionuclides in the natural system are discussed in this section. The perturbation to this environment caused by the emplacement of nuclear waste is discussed in Section 4.2 and Section 7.4.1.1.

Oxidation potential (Eh)

The redox environment of a chemical or geochemical system is generally stated in terms of the oxidation potential (Eh). This is defined as the electrical potential of an oxidation half reaction relative to the potential of a standard hydrogen electrode.

Although Eh, in this section, is generally used to relate aqueous species, it is important to note that the redox couples present in solution are related in varying degrees to the mineralogy present. The role of basalt in establishing reducing conditions has been studied by the BWIP (see Section 7.4.4.1) and is discussed more generally elsewhere (White et al., 1985 and White and Yee, 1985).

The oxidation potential is theoretically related to the concentrations of the reduced and oxidized species by the Nernst equation (Eq. 4.1-5):

$$Eh = E^\circ + \frac{RT}{nF} \ln \frac{a_{ox}}{a_{red}} \qquad (4.1\text{-}5)$$

where

E° = oxidation potential when all reactants, the temperature, and the pressure are in their respective standard states

R = gas constant

T = temperature in degrees Kelvin

n = number of electrons transferred

F = Faraday's constant

a_{ox} = activities of the oxidized species

a_{red} = activities of the reduced species.

The redox reactions important in a saturated basalt environment will occur in the aqueous phase or at solids that are in contact with the aqueous phase. This theoretically imposes some limitations on the chemistry and stability of species in the basalt system. Specifically, redox processes are, in principal, limited by the oxidation (Eq. 4.1-6) and reduction (Eq. 4.1-7) of water:

$$\text{Oxidation:}\quad 2H_2O = 4H^+ + 4e^- + O_2(g) \qquad (4.1\text{-}6)$$

$$\text{Reduction:}\quad 2H_2O + 2e^- = H_2(g) + 2OH^- \qquad (4.1\text{-}7)$$

These reactions define the theoretical upper (oxidizing) and lower (reducing) stability limits for aqueous species.

In practice, the stability of an aqueous species will be determined by both the kinetics for the reaction of that species with water and the redox potential. Therefore, it is not possible to eliminate a half reaction from consideration solely because it has an Eh outside the theoretical stability limits of water. These limits (defined by Eq. 4.1-6 and 4.1-7) do, however, provide a qualitative indication of the significance of the various reaction processes being considered.

Applicability of Eh to natural systems

Although Eh is a very useful and widely applied construct, there are significant limitations in using a single Eh value (master Eh) to describe the redox environment of most real systems. This is especially true if the intent is to relate measured potentials to concentrations of aqueous species using the Nernst equation (see Eq. 4.1-5).

In a complex geochemical system, the two primary limitations to defining a master Eh are (1) redox couples in most real systems are not in thermodynamic equilibrium with each other, and (2) there are significant experimental difficulties in the measurement of redox potentials.

The very existence of a master Eh in natural groundwaters (indicating thermodynamic equilibrium between all aqueous species) has been frequently questioned in the chemical and geochemical literature (Morris and Stumm, 1967, pp. 270-285; Breck, 1971, pp. 121-139; Drever, 1982, pp. 257-258; Lindberg and Runnels, 1984, p. 926; Hostettler, 1984, p. 734). Even groundwaters that have been in isolation for long periods of time often are not at thermodynamic equilibrium. In effect, each redox couple appears to correspond to a different Eh.

The difficulties in relating the measured potential to solution concentrations have been discussed in detail elsewhere (Mann et al., 1974, pp. 727-732). In a complex system, the measured potential often corresponds to a combination of all the redox couples in solution. The contribution of each redox couple to the measured potential will depend on relative concentrations, the standard state potential, and the kinetics of the reaction at the electrode.

The measured potential will correspond to the predicted Nernstian thermodynamic potential only when the redox pair of interest is at thermodynamic equilibrium and reacts in a completely reversible manner with the sensing device (usually an ion-specific electrode). The occurrence of this in real systems is extremely rare.

In practice, an acceptable criterion for the reversibility of a redox reaction is that the Nernst equation (see Eq. 4.1-5) is obeyed. This will not occur if two species in a half reaction can react with each other via a different reaction mechanism. It is necessary to consider all significant redox reactions to properly interpret electrode behavior. Plans to address the question of the reversibility of redox reactions with respect to measured electrode potentials is discussed in Section 8.3.4.2. In any case, caution must be used in predicting electrode behavior based on potentials determined from thermodynamic data.

Evaluation of the redox environment in a basaltic system

Recognizing the limitations and problems concerning experimental determinations of the redox environment, efforts have been directed at evaluating the redox environment of Grande Ronde Basalt groundwater through four different approaches:

1. Identification of the secondary mineralogy in basalt flows.

2. Measurement of the concentration of both reduced and oxidized species of various redox couples.

3. Performance of hydrothermal basalt-groundwater experiments.

4. Direct measurement of the platinum electrode potentials.

Secondary mineralogy in basalt flows. The first key indicator of the preemplacement redox environment in Columbia River basalts is the secondary mineralogy. The assumption here is that these minerals were formed under conditions that reflect present day redox conditions. A trend from minerals characteristic of a reducing environment with some minerals characteristic of oxidizing conditions in the primary phases to minerals that are almost exclusively characteristic of reducing conditions in the secondary phases was interpreted to indicate that, in time, a more reducing environment was established.

Iron is the most abundant redox-sensitive element in basalt, and the various iron-bearing minerals are key indicators of redox conditions (Garrels and Christ, 1965, pp. 178-229). An Eh/pH diagram (for information on the meaning and derivation of these, see Stumm and Morgan, 1965, pp. 172-267) relevant to this system is shown in Figure 4.1-28.

A listing of redox half reactions of iron-bearing phases is presented in Table 4.1-37. This list is not complete and will be modified as more is understood about the geochemistry of a basaltic system. There is, unfortunately, a lack of thermodynamic data on iron-bearing clays in general (Deutsch et al., 1982b, pp. 1-37), and a specific absence of data relevant to clay with compositions similar to those found at the Hanford Site.

Primary titano-magnetite (Noonan et al., 1980, pp. 1-8) and, more recently, some primary hematite (only in the flow tops; see Section 4.1.1) are found to coexist with secondary iron-bearing alteration products including pyrite, nontronite, other smectites, and mixed ferrous-ferric oxyhydroxides (Benson and Teague, 1982, pp. 595-613). Notably, hematite and pure ferric hydroxide phases (which are generally formed under oxidizing conditions) have not been detected as secondary minerals. The predominant iron-bearing secondary phases that have been formed are iron-rich clays. However, pyrite (which is generally formed under reducing conditions) is typically observed as a secondary iron phase.

Although phases characteristic of oxidizing conditions have been identified as primary minerals in the natural system, there is no evidence that secondary minerals characteristic of an oxidizing environment are being formed. This finding is consistent with the general interpretation that, in time, increasingly reducing conditions were established in the natural system at or near repository depth. Further characterization of the secondary minerals in the Columbia River basalts is currently under way and is discussed in Section 8.3.1.2.

Concentration of both reduced and oxidized species of various redox couples. The second approach used to qualitatively evaluate the redox environment in the natural system was the direct measurement of the concentration of both the reduced and oxidized species in redox couples common to the basalt groundwater system. A list of reactions by which these couples are related is given in Table 4.1-38.

The concentrations corresponding to each redox couple is theoretically related to the oxidation potential by the Nernst equation (see Eq. 4.1-5). As previously discussed, the potential calculated using different redox couples will only be in agreement if the couples are in equilibrium with each other. However, the potentials calculated will, as a whole, provide qualitative information on the redox environment.

Either quantitative or qualitative concentration data are available for five redox couples: sulfide/sulfate, iron(II)/iron(III), methane/carbon dioxide, methane/inorganic carbon, and methane/carbon monoxide.

The sulfide (as either HS^- or $S^=$)/sulfate (as either $SO_4^=$ or HSO_4^-) couple has been commonly used as a redox indicator for natural groundwaters. At the ambient repository temperatures and pH values, the $HS^-/SO_4^=$ species will dominate (Garrels and Christ, 1965, pp. 213-218).

The kinetics of the uncatalyzed redox reaction between sulfide and sulfate are extremely slow at ambient repository conditions (Ohmoto and Lasaga, 1982, pp. 1727-1745). For this reason, the sulfate/sulfide couple may not be at equilibrium in the groundwater samples obtained. The presence of redox-sensitive mineral surfaces and certain bacteria may, however, help to catalyze this reaction. Examination of the sulfur isotope ratios of both HS^- and $SO_4^=$ (Ohmoto and Lasaga, 1982, pp. 1727-1945) could help to resolve this question (see Section 8.3.1.4).

Most of the sulfur occurs as sulfate in Grande Ronde Basalt groundwaters, with a typical value of 6×10^{-5} M in the reference repository location. Sulfide is not always detected, but concentrations of up to 1.3 p/m have been measured in Grande Ronde Basalt groundwater samples using an ion selective electrode (Dill et al., 1986, p. 10). The presence of sulfide in basaltic groundwater is strong evidence for reducing conditions.

The redox half reaction for the sulfate/sulfide couple is given as reaction 1 in Table 4.1-38. Eh calculated from concentration data available using the Nernst equation (Eq. 4.1-5) is listed in Table 4.1-39. The data listed show good agreement in the calculated Eh values with an average value of -0.4 V for Eh.

The second redox couple investigated was the iron(II)/iron(III) couple (Dill et al., 1986, p. 15). Half reactions relating the solid iron-bearing phases and aqueous iron species were listed in Table 4.1-37. The measurement of ferrous iron concentrations has only been recently initiated and little data have been obtained to date (see Section 8.3.1.4.2.3.2 for plans). These data are shown in Table 4.1-40.

Measured ferrous iron concentrations were obtained in wells that were associated with groundwaters at depths of less than 609 m (2,000 ft). At depths greater than 609 m (2,000 ft) (reference repository depth is 950 m (3,000 ft), significant concentrations of sulfide were measured, but only trace amounts of ferrous iron were detectable. When ferrous iron was present, it accounted for over 90% of total iron detected. This, along with the presence of sulfide (rather than ferrous iron) at depths greater than 609 m (2,000 ft), is qualitatively indicative of a reducing environment.

The third redox couple investigated was the equilibration between methane (CH_4) and carbon dioxide (CO_2). The half reaction for this couple was shown in Table 4.1-38 (reaction 3). The range of CO_2/CH_4 values measured in the reference repository location was 6 to 10^{-6}. These values correspond to reducing conditions. Again, the kinetics of this reaction are slow, and the concentrations measured may represent nonequilibrium conditions.

The fourth redox reaction investigated is dissolved methane/inorganic carbon (as carbonate or bicarbonate) shown as reaction 4 in Table 4.1-38. Average concentrations of methane and bicarbonate measured in groundwater samples are 0.044 mol/L and 0.0016 mol/L. The Eh calculated from these concentrations is -0.45 V. The region of the Eh/pH diagram corresponding to this Eh is indicated by the shaded area in Figure 4.1-28(a).

The last redox couple considered is carbon monoxide and methane. This can also be used to qualitatively suggest redox conditions, as shown by equation 5 of Table 4.1-38. Carbon monoxide is generally below detection limits (Gephart, 1983, p. I-196) in Grande Ronde Basalt groundwaters; therefore, the Eh values calculated using the Nernst equation (see Eq. 4.1-5) must represent upper Eh limits. The Eh of repository groundwaters presumably must be below the range for CO/CH_4. This couple has the same kinetic limitations as the CH_4/CO_2 couple.

The concentration data just discussed do not point to a single value for the redox potential of the natural system. Even the small differences in the calculated potentials reflect significant deviation from equilibrium concentrations for redox-sensitive species in basaltic groundwaters. However, the data consistently point to the existence of a reducing rather than oxidizing environment.

Hydrothermal basalt-groundwater experiments. The third approach used to establish the redox environment in the Columbia River basalts was the analysis of hydrothermal basalt-groundwater experiments with respect to the redox conditions established as a function of reaction progress. Although these experiments are more relevant to the hydrothermal conditions in the repository that will exist after waste emplacement, they do provide further evidence that the basaltic system is reducing.

Results reported in the hydrothermal testing program that are directly relevant to the redox conditions are summarized in this section. A more complete discussion of the results in these experiments is found in Section 7.4.1.1.

There are two experimental results reported by Lane et al. (1984, pp. 181-195) that apply to redox conditions in basaltic systems.

1. In time, in the temperature range of 150 to 300 °C, oxygen levels are reduced substantially when basalt is present.

2. Basalt-groundwater experiments spiked with arsenic at 300 °C attained an Eh of -400 ±100 mV (as calculated from the arsenic(III)/arsenic(V) couple) in 11 d.

Further evidence of a reducing environment in basaltic hydrothermal systems has been obtained by Moore et al. (1984, pp. 56-57) who observed hydrogen sulfide as a product in 200 and 300 °C basalt-groundwater experiments that initially contained only sulfate in the groundwater.

These experiments do not define the redox conditions present in the natural system prior to the emplacement of nuclear waste. They do, however, illustrate the tendency of Grande Ronde Basalt to remove oxidants from groundwater and reduce redox-sensitive species in the groundwater, which provides additional evidence for reducing conditions in the natural system.

Platinum electrode potentials. The fourth approach used to evaluate the redox environment in basalt groundwaters is the direct measurement of Eh with a platinum electrode. The range of values measured at the Hanford Site (+0.2 to -0.2 V) is presented in Figure 4.1-29.

The platinum electrode measurements reported are subject to question because the possibility of oxygen or sulfur poisoning cannot be eliminated. This type of electrode poisoning leads to spurious Eh values (Garrels and Christ, 1965, pp. 135-139; Morris and Stumm, 1967, pp. 282-283; Langmuir, 1971, pp. 518-621; Whitfield, 1969, pp. 547-549; Whitfield, 1974, pp. 857-865). These data also reflect measurements of repository groundwaters at the Earth's surface, not at repository depth.

Exposure of the sample to the more oxidizing surface environment (atmospheric oxygen and contamination of the groundwater with drilling muds) will potentially lead to more oxidizing measurements and may explain the wide range of measured Eh values. Since the electro-active species in basaltic groundwater have not been identified, an alternative explanation of the range of Eh values measured is variability in the composition of the groundwater (sulfide content, iron content, etc.).

The expectation is, therefore, that all directly measured Eh values are more oxidizing (i.e., displaced toward more positive values) than actual Eh values of groundwaters at the Hanford Site. This displacement cannot be quantified because of the uncertainties in electrode response and the possibility of sample contamination (which cannot be quantified). The recorded Eh values, however, can be used in a qualitative manner. The predominance of negative Eh values in Figure 4.1-29 (i.e., reducing conditions) is clearly shown. Furthermore, the skewed shape of the histogram is what would be expected if the majority of groundwater samples were not significantly contaminated.

Summary of evidence for reducing conditions in the natural system. Combining the results of the platinum electrode measurements, calculations of Eh from the concentrations of redox couples, results from hydrothermal experiments, and the observed secondary mineralogy of the natural system, it is clear that the redox environment of basalt groundwaters is reducing. In fact, the majority of electrode measurements and calculations of the oxidation potential place this potential in the range of -0.4 to -0.1 V. This does not establish a master Eh for basalt groundwaters but indicates that many of the aqueous species in the groundwater are responding, to some extent, to the reducing conditions present in the basaltic environment.

Control of the redox environment in the natural system

The capacity of the basalt and alteration phases in the natural system to maintain the reducing conditions present in the groundwater is an important question because a possible result of waste emplacement will be a more oxidizing environment in the part of the natural system nearest the waste package. The capacity of basalt to reinstate an ambient reducing environment may be important in establishing solubility limits and the sorption properties of redox-sensitive radionuclides.

The existence of a single redox buffer has the same limitations as the concept of a master Eh in that a specific redox couple may not be affected by solid/liquid interactions that readily oxidize or reduce a different couple. For the most part, the capacity of a basalt system to maintain a reducing environment will be determined experimentally in the waste-rock-barrier interaction testing outlined in Section 8.3.4.3.

There is some evidence that the reducing conditions in Grande Ronde Basalt are related to the dissolution of the mesostasis (Noonan et al., 1980, pp. 1-8) that is found to react with groundwater to a greater degree than other phases of the basalt (Apted and Myers, 1982, pp. 1-78; Benson and Teague, 1982, pp. 595-613). This glass contains approximately a 3-mol% fraction of an iron-pyroxene component (Noonan et al., 1980, pp. 1-8).

Hydrolysis of the glass could lead to the redox reaction as described in reaction 3 of Table 4.1-37 in which the iron-pyroxene component of the glass undergoes dissolution, followed by an iron(II)/iron(III) redox reaction and subsequent precipitation of secondary magnetite and silica (quartz-pyroxene-magnetite reaction). Reaction 3 of Table 4.1-37 is an irreversible reaction that provides a possible redox control mechanism. The silica-saturated Grande Ronde Basalt groundwaters, and the presence of amorphous silica and magnetite as alteration phases (Benson and Teague, 1982, pp. 595-613) in Grande Ronde Basalt, qualitatively supports the role of the quartz-pyroxene-magnetite reaction in controlling the redox environment.

A similar reaction involving primary clinopyroxene (with a 30-mol% fraction of $FeSiO_3$) could also be applied as a possible buffering reaction, given the observation of Benson and Teague (1982, pp. 595-613) that clinopyroxene has experienced the greatest degree of alteration of the primary mineral (nonglassy) phases. The assumption of a crystalline iron-pyroxene rather than a glass $FeSiO_3$ component does not appreciably change reaction 3 in Table 4.1-37.

The existence of alteration minerals lining basalt fractures may prevent access of groundwater to fresh basalt inhibiting any redox control the basalt may have. However, recent surface studies (Petrovic, 1976, pp. 1509-1521; Berner, 1978, pp. 1235-1252; Holdren and Berner, 1979, pp. 1161-1171; Aagaard and Helgeson, 1982, pp. 237-285) of hydrothermally reacted minerals indicate secondary minerals do not prevent direct contact between the solution and

primary solid. It is also likely that the secondary phases formed will act to maintain reducing conditions. Further testing in systems containing basalt are planned (Section 8.3.4.3) to establish this in the natural system.

The effect of Eh on radionuclide concentration and speciation in solution

A key advantage of placing a high-level nuclear waste repository in a reducing environment is the expectation that the radionuclides will also be reduced as they interact with the geochemical system. The extent to which this occurs in the waste package will be established experimentally (see Section 8.3.4.3.4) in the waste-rock-barrier interaction testing program.

In the natural system, the importance of the redox environment is its effect on the transport of radionuclides. A reducing environment will potentially limit radionuclide mobility in the two following ways:

1. Radionuclides that were released from the waste package in their reduced state (see Section 7.4.6 for discussion of reducing conditions in the waste package) will not be reoxidized. This will help maintain low radionuclide mobility throughout the repository site.

2. Radionuclides released from the waste package may undergo further reduction, thereby decreasing their mobility.

The expectation that the reducing environment in a basaltic system will reduce radionuclides is based, in part, on the thermodynamics of some radionuclide systems. Calculations based on a published procedure for Eh-pH plots (Drewes, 1983) are shown in Figure 4.1-30 for uranium and neptunium. These diagrams qualitatively predict that both of these radionuclides will be redox sensitive.

In the natural system, the important process affecting radionuclide speciation and concentration is their sorption onto the solids present. The redox environment can affect this process in two ways. First, it will, to some extent, determine the concentrations of aqueous species that complex radionuclides. This will either enhance or decrease radionuclide sorption (see Section 4.1.3.4.4). Second, it will affect the concentration of radionuclides is the redox chemistry. Qualitatively, a reducing environment (relative to an oxidizing environment) favors the reduction of radionuclide species. The reduced radionuclide, in general, undergoes both sorption and precipitation more readily than species in higher oxidation states. The sorption characteristics of various radionuclides in their reduced and oxidized form were discussed in Section 4.1.3.7.

The effect of the redox environment on the concentration and speciation of radionuclides in solution, however, must be established experimentally. This has not yet been done in a basalt-groundwater system. The primary reason for this is the general lack of both solubility and thermodynamic data on radionuclides under conditions expected in a basalt repository (reducing conditions at a high pH).

In view of this, the BWIP has initially approached the question of how radionuclides will respond to the basaltic environment by conducting laboratory experiments under repository relevant conditions. In these experiments, radionuclides are placed in the basalt-groundwater system at various temperatures. Their concentration and oxidation states are monitored as a function of time. These are, by design, scoping experiments that will establish general trends in radionuclide behavior and identify aspects of radionuclide systems that require more detailed studies.

Preliminary results have been obtained for technetium (Wood et al., 1986; Jones et al., 1986) and plutonium in a basaltic system. In both cases, the radionuclides were reduced by the conditions established experimentally by basalt resulting in low aqueous concentrations and high sorption. In the case of technetium, reduction of technetium(VII) (pertechnetate ion) to technetium(IV) dramatically affects its sorption and solubility behavior making technetium essentially immobile in a basaltic system. The two results just mentioned are not conclusive. They do, however, suggest that there is good reason to expect that the reduction of radionuclides will occur in a basaltic system.

In conclusion, the effect of the redox environment on radionuclide speciation must be established for each radionuclide of interest experimentally. The reduction of radionuclides involves specific chemical reactions that may be kinetically inhibited under the conditions expected in the repository (temperature, pH pressure, etc.). In this sense the primary effect of the redox environment on radionuclide speciation is through the aqueous species and solid surfaces present that can either catalyze or directly facilitate the reduction of radionuclides. This is primarily a kinetic question involving specific redox reactions between the radionuclide and aqueous species and the primary and secondary phases in the basalt. This question will be addressed in the hydrothermal testing with waste forms in a basalt-groundwater system currently planned (Section 8.3.4.3).

4.1.3.4.2 pH in the natural system

The pH of a geochemical system is a key parameter in determining the speciation of aqueous species and the stability of the solid phases present. In a basaltic system, the concentration of many of the radionuclides is determined by complexation with the hydroxide ion or solubility of hydroxy or mixed hydroxy phases.

This section discusses pH in the natural system before the emplacement of high-level nuclear waste. The two main objectives are as follows:

1. Summarize the pH data for basaltic groundwater in the natural system in the vicinity of the reference repository location.

2. Discuss processes important in controlling the pH of the natural system.

The effect of pH on the radionuclide speciation (with respect to the source term) is discussed in Section 7.4.4.1; the effect of emplacement on the pH is discussed in Section 4.2 for the natural system and Section 7.4.4.1 for the waste package.

pH of basaltic groundwater in the natural system

The pH is routinely measured in all the groundwater samples taken from basalts at the Hanford Site. A summary of data for the entire Hanford Site was shown in Figure 3.9.1-17 and discussed in Section 3.9.1.3.6. Data for the pH of the Grande Ronde Basalt was given in Figure 4.1-4. A more comprehensive source of this data is the hydrochemical data base for the Hanford Site (Early et al., 1986, pp. 1-347).

Acid-base reactions in solution are generally reversible and very fast. The pH values measured, therefore, correspond to systems that are at equilibrium with respect to the homogeneous acid/base reaction of the aqueous species present. The major difficulty in obtaining accurate pH values at depth is that the sampling process necessarily imposes temperature and pressure changes on the sample (Garrels and Christ, 1965, pp. 129-132; Stumm and Morgan, 1981, pp. 481-489). There is an additional error introduced by inconsistent sample handling in transporting the sample from the field to the laboratory. For this reason, the experimental error in measuring pH at depth introduces an uncertainty of $\pm$0.5 pH units to the values reported. This uncertainty was estimated from the scatter in observed measurements.

The pH values measured range from 7.2 to 10.8 throughout the natural system. There is a systematic increase in the pH with groundwater depth even within a particular basalt flow. This trend is typical of groundwaters in a high-silica system that are progressively isolated from the atmosphere (as depth increases).

In the Grande Ronde Basalt, field measurement of the pH are significantly higher than those obtained site-wide. Measurements range from a pH of 8.5 to 10.8, with an average value of 9.5 (measured at 25 °C). The Cohassett flow (currently the location of the reference repository location) in the Grande Ronde Basalt has measured pH values in the range of 8.7 to 10.3, with an average of 9.3. There is no significant difference between the pH values measured in the other members of the Grande Ronde Basalt and the Cohassett flow.

In summary, the field pH for the natural system in the vicinity of the proposed repository is 9.5 $\pm$0.5 (at 25 °C). Correcting this to the ambient temperature, using the geochemical code EQ3NR, gives a pH of 9.2 $\pm$ 0.5 (at 55 °C).

Control of pH in the natural system

The pH of groundwater in the Hanford Site basalts is characteristic of geologic formations with high-silica minerals that are isolated from the atmosphere. In this system, the pH is determined by the temperature and interaction between the groundwater and specific mineralogy of the Hanford Site.

The increase in temperature caused by the emplacement of high-level nuclear waste will potentially change the pH of the natural system. This temperature increase will lower the pKw of water and facilitates hydrothermal alteration of the minerals and groundwater in the natural system. This effect is not addressed in this section but is discussed in Section 4.2 for the natural system and Section 7.4.4.1 for the waste package.

The subject of this section is the two general types of processes that are expected to control the pH in the Hanford Site basalts. These are as follows:

1. Homogeneous equilibria with aqueous species; the buffering of the groundwater by weak acids/bases already in solution.

2. Heterogeneous reactions between the minerals present and groundwater.

The buffering capacity of species in the groundwater determines the ability of the system to respond to rapid changes in the pH whereas the solids present will determine the long term response of the basaltic system to induced changes in the pH.

Homogeneous pH buffering. The immediate pH controls in the Hanford Site groundwater are the weak acids found in the groundwater. In the basaltic groundwater, the two most important of these are silicic acid/silicate ion (pKa = 9.7 at 25 °C) and bicarbonate/carbonate (pKa = 10.25 at 25 °C) equilibria.

A qualitative idea of the buffering capacity of basaltic groundwater can be obtained by calculating the buffer capacity of basaltic groundwater using 25 °C acid dissociation constants. The buffer intensity of the groundwater, as defined by Stumm and Morgan (1981, pp. 160-161), is 0.0016 based on measured inorganic ion concentrations. The neutralizing capacity (Stumm and Morgan, 1981, pp. 162-164) of the groundwater is 9.6×10^{-4} mol/L with respect to acid and 2.1×10^{-3} mol/L with respect to base.

The buffering capacity of the groundwater, although small compared to the capacity of basaltic minerals to control the pH through hydrothermal processes, is potentially an important property of the Hanford Site. This capacity will minimize localized pH effects induced by effects such as ionizing radiation and will act to reestablish the initial pH of the Hanford Site in the long term as fresh groundwater flows into or through the repository.

Heterogeneous pH buffering. The heterogeneous rock-groundwater reactions provide the greatest potential for pH control in natural groundwaters that are isolated from the atmosphere (Stumm and Morgan, 1981, pp. 558-561). The most important heterogeneous processes that control the pH in Hanford Site basalts are as follows:

- o Hydrolysis of silicates.
- o Ion exchange reactions.
- o Precipitation of minerals.

The first of these processes is the effect of silicate hydrolysis on the pH of geochemical systems. This has been well established in the geochemical literature (Krauskopf, 1979, pp. 113-116) and has been previously discussed as the pH controlling mechanism by Smith et al. (1980, pp. 2-119 to 2-124) for Hanford Site basalts.

Minerals with a high-silica content will, given enough time, drive the pH to alkaline values in almost all natural systems (e.g., pH = 8.0 for Tuff groundwater, 7.0 for granite, 7.6 or rhyolite). This is reflected in the alkaline pH values found throughout the Hanford Site basalts. The alkalinity will be limited by the dissolution and dissociation of silicic acid to a pH of approximately nine. This indicates that the pH of Grande Ronde Basalt groundwater is at or near the upper pH limit of a high-silica system.

The actual pH of the groundwater in a basaltic system, within the alkaline pH range established by the high-silica content, depends primarily on the specific mineralogy (type of silicates present, etc.) and temperature. These will determine the stoichiometry of hydrolysis reactions, the positioning of ions between the solid and liquid phases (ion-exchange reactions) and the precipitation of minerals, all of which may remove hydroxide ions from solution or generate hydronium ions in solution.

Evidence for the mechanism that controls the pH of a basaltic system has been obtained in three areas of study: (1) studies of Icelandic basalts that are an analog of Hanford Site basalts, (2) studies reported in the literature on basalt-seawater hydrothermal systems, and (3) basalt-groundwater interaction testing performed under contract to the BWIP. Although there are substantial differences between the systems considered in these studies, the general mechanisms identified as controlling the pH appear to be similar.

The Icelandic geothermal systems are discussed in greater detail elsewhere (Section 4.3). Arnorsson et al. (1978, pp. 523-536) have determined that pH in this system was determined by the positioning of cation exchange equilibria between the aqueous and solid phase of the basalt, which was mostly a function of temperature. There was, in general, a minor dependence of pH on the mineralogy within the Icelandic system.

Basalt-seawater hydrothermal interactions have been the subject of several studies (Seyfried and Bischoff, 1981, pp. 135-147; Seyfried and Mottl, 1981, pp. 985-1002; Seyfried and Bischoff, 1979, pp. 1937-1947; Mottl and Holland, 1978, pp. 1103-1115). The general conclusion is that initially, for the lower temperature experiments (less than 200 °C), there was a rapid pH drop followed by a slower rise in the pH. The fast drop was attributed to the precipitation of magnesium hydroxide, and the slow rise was the hydrolysis of the silicates in the basalt. These processes clearly depended on the temperature and rock-groundwater ratio of the experiments.

The results of a series of hydrothermal experiments that have been done under contract to the BWIP, using crushed basalt from the Umtanum and Cohassett flow, have indicated that a similar mechanism to the basalt-seawater is controlling the pH (Ulmer and Granstaff, 1984, pp. 3-41). A temperature-dependent rapid decrease in the pH followed by a slower rise in the pH was observed. This mechanism is discussed more fully in Section 7.4.4.1. A correlation between the aqueous concentration of Na^+ and the initial drop in pH has been noted. It appears, based on this, that the pH is being lowered as the result of a rapid precipitation of sodium minerals. It is still not certain what accounts for the slow rise in the pH but, by analogy with the basalt-seawater interaction results, it is likely that it represents the hydrolysis of silicates present in the glassy phase of the basalts.

The mechanism that controls the pH of the groundwater in Hanford Site basalts is still not fully understood. Further data pertinent to the mechanisms discussed here will be generated by the hydrothermal testing program (Section 8.3.4 and Section 7.4.4.1). There does, however, seem to be sufficient evidence that points to contributions from the three primary processes just discussed.

Summary: pH in the natural system. The pH in the natural system ranges from 7.0 to 10.8 in 25 °C field measurements. There is a systematic increase in pH as the depth at which the groundwater is sampled increases. In the vicinity of the repository location (Grande Ronde Basalt) the pH is 9.0 $\pm$ 0.5.

The groundwater itself, because of the silicic acid and bicarbonate ion present, has a small buffering capacity. The pH observed at depth appears to be established by contributions from three processes: (1) hydrolysis of silicates present in the basalt, (2) precipitation of minerals, and (3) ion exchange equilibria between the liquid and solid phases present. Further work is needed to establish the specific minerals and mechanisms controlling the pH (see Section 8.3.4).

4.1.3.4.3 Effect of ionizing radiation on radionuclide concentrations and speciation in solution

The effect of ionizing radiation on the concentrations and speciation of radionuclides in the natural system is, for the most part, insignificant. The

primary reason for this is the dilution factor as distance is increased from the waste container and the slow release of radionuclides expected from the waste package.

Ionizing radiation can potentially affect the concentration and speciation of radionuclides in two ways. First, it can change the chemical environment of the radionuclide by altering the pH, redox environment, and concentration of complexants in the groundwater. Second, it also generates highly reactive intermediates that are strongly oxidizing or reducing. These may react directly with the radionuclide species to oxidize or reduce that species resulting in significant changes in solubility and sorption behavior.

In the waste package, these processes may be significant because the expected radiation dose rate is considerably higher than in the natural system. This possibility and the data that have been obtained on radiolytic effects are discussed in Section 7.4.

In the natural system, however, the radionuclides released from the waste package during the isolation period will be greatly diluted. The resulting dose rates will be extremely small. This will cause an insignificant change in the groundwater chemistry and have no significant affect on radionuclide speciation.

4.1.3.4.4 Radionuclide complexes

Grande Ronde Basalt groundwaters contain a number of inorganic and organic ligands that could form soluble complexes with the key radionuclides. Potential inorganic ligands are carbonate/bicarbonate, hydroxyl, sulfate, fluoride, and chloride ions. The concentrations of these anions vary depending on the location of the groundwater (see Section 4.1.2.2). Potential organic ligands are humic acids, fatty acids, and phenols (Means, 1982, pp. 1-22). Although the total organic concentration is low (less than 1 mg/L), its effect on radionuclide speciation is not known (see Section 8.3.1.4.3.3.1 for plans to evaluate radionuclide reactions with organic materials).

Thermodynamic formation constants (measured or estimated) for actinide complexes have been compiled by Apps et al. (1982, pp. 110-118) and Allard (1982, pp. 553-580). According to these values, hydroxide and carbonate complexes would be expected to predominate in basalt groundwaters. Fluoride, sulfate, and chloride complexes should be present at very low concentrations (orders of magnitude less than hydroxyl or carbonate complexes) and will have negligible influence on sorption or transport.

The identity of dominant radionuclide species in groundwaters will, of course, influence radionuclide sorption behavior. For example, if a dissolved metal ion is sorbed only as a hydrated species such as M^{2+}, but forms carbonate complexes by the reactions,

$$M^{2+} + CO_3^{2-} = MCO_3 \qquad (4.1\text{-}8)$$

and

$$MCO_3 + CO_3^{2-} = M(CO_3)^{2-}, \qquad (4.1\text{-}9)$$

then sorption will decrease as the carbonate concentration in groundwater increases.

Information on radionuclide complex formation can be obtained indirectly by varying the composition of the groundwater and measuring effects on sorption (Barney, 1981a, pp. 8-22; 1982, pp. 7-28; 1984, pp. 16-22). The effects of major components of basalt groundwater (Na^+, Ca^{2+}, K^+, Mg^{2+}, Cl^-, F^-, CO_3^{2-}, HCO_3^-, and SO_4^{2-}) on radionuclide sorption on basalt, secondary minerals, and interbed materials have been determined. Because of the large number of variables to be studied, it was necessary to use statistical methods to design the experiments. The details of experimental design and procedures are given in Barney (1981a, pp. 8-31; 1982, pp. 7-28, App. B and C). The concentrations of components used in these experiments covered those ranges measured in groundwater samples obtained from water-bearing zones in basalt. The significant groundwater variables for sorption of several radionuclides are given in Table 4.1-41. Groundwater cations compete for sorption sites with ^{137}Cs, ^{85}Sr, and ^{226}Ra. Neptunium in both (V) and (IV) oxidation states forms complexes with carbonate, causing decreased neptunium sorption. Americium sorption appears to be affected by small pH variations over the range where CO_3^{2-} or HCO_3^- are the dominant carbonate species.

Based on the available thermodynamic data and the results of measuring effects of groundwater composition on sorption, several generalizations can be made concerning complex formation by key radionuclides:

- Actinides should exist mainly as either hydroxyl or carbonate complexes (or as mixed ligand complexes containing both anions). Fluoride, sulfate, chloride, and phosphate complexes should be present at very low concentrations (orders of magnitude lower than hydroxide and carbonate complexes) and should have little influence on sorption. These conclusions are consistent with observed effects of groundwater components on sorption that are described above.

- Radionuclides that exist only as anions in solution should be weakly sorbed (or even repelled by the solids) due to the negatively charged surfaces of minerals at pH values of basalt groundwaters. This behavior has been observed for iodine, technetium (oxidized form), carbon, and selenium, which probably exist as anions in

sorption experiments. Results from recent work (Paquette and Lawrence, 1985; Barney et al., 1985) indicate that reduced technetium is strongly sorbed and forms soluble complexes with carbonate.

- Cesium will exist as the simple hydrated cation, Cs^+, in basalt groundwater solutions. Formation constants for zirconium, samarium, and tin indicate that hydroxyl species of these elements will probably predominate (Early et al., 1984b, pp. 153-163). The dissolved species of the remaining key radionuclide, palladium, is sensitive to the presence of reduced sulfur species (S^{2-}, HS^-). If sulfide is absent, the predominant solution species are hydroxyl complexes.

4.1.3.5 Matrix diffusion

Diffusion of radionuclides into the host basalt rock can, potentially, retard their transport by groundwater, especially if diffusion is slow compared to groundwater advective flow. Diffusion into microfractures and pores in the basalt and into pores and layered silicates in secondary minerals and interbed minerals are considered to be the most significant diffusion processes affecting radionuclide transport. Pores and microfractures contain stagnant or immobile water zones that act as sinks to molecular diffusion during the displacement process and, thus, lead to incomplete displacement. This results in retardation of the dissolved radionuclide with respect to the flux of groundwater in the flow path.

Diffusion of radionuclides in groundwater flow paths expected for the natural system are strongly scale dependent. This is a result of the nonhomogeneous distribution of fractures and pore sizes expected in the flow paths. Thus, laboratory-scale measurements of diffusion cannot be used with confidence in radionuclide transport models. Diffusion effects, however, may be accounted for, along with other nonequilibrium effects, in a value for the effective dispersivity used to analyze solute breakthrough curves for field tracer tests (Grisak et al., 1984). Plans for these tests are described in Section 8.3.1.4.2.3.

Laboratory-scale radionuclide diffusion measurements with the packing material component of the waste package can be applied to transport predictions because of the expected homogeneity and smaller scale of the packing material. Results of these diffusion measurements are described in Section 7.4.3.

4.1.3.6 Radionuclide transport

Estimation of radionuclide transport in the natural system requires a thorough understanding of radionuclide behavior in the applicable groundwater flow path. This, in turn, requires identification and quantification of all

processes that influence transport. These processes include chemical reactions such as sorption, desorption, complexation, and redox reactions; and physical processes such as advective flow, diffusion, mechanical dispersion, radioactive decay, and colloid transport.

The following discussion presents an example of how chemical and physical processes are quantitatively related to radionuclide transport calculations.

The general one-dimensional convective-dispersive radioactive solute transport equation as given by Bear (1972, p. 242) for saturated flow in porous media is as follows (Eq. 4.1-10):

$$\frac{\partial C}{\partial t} = D\frac{\partial^2 C}{\partial x^2} - V\frac{\partial C}{\partial x} - \frac{\rho}{\theta}\frac{\partial S}{\partial t} - \lambda\left(C + \frac{\rho}{\theta}S\right) \qquad (4.1\text{-}10)$$

(dispersion) (advection) (sorption) (radioactive decay)

where:

C = groundwater solute concentration (M/L^3)

S = sorbed solute concentrations (M/M)

D = hydrodynamic dispersion coefficient (L^2/T)

V = average pore velocity (L/T)

ρ = bulk density of the media (M/L^3)

θ = volumetric water content (L^3/L^3)

t = time (T)

x = distance (L)

λ = radioactive decay constant.

Radionuclide sorption is represented by the term

$$\frac{\rho}{\theta}\frac{\partial S}{\partial t} \qquad (4.1\text{-}11)$$

For many of the radionuclides of interest, equilibrium (or steady-state) sorption can be described by the Freundlich equation (Eq. 4.1-1) as shown in Section 4.1.3.3. Differentiating the Freundlich equation with respect to time gives:

$$\frac{\partial S}{\partial t} = KNC^{(N-1)} \frac{\partial C}{\partial t} \qquad (4.1\text{-}12)$$

Substituting Equation 4.1-12 into Equation 4.1-10 yields:

$$\frac{\partial C}{\partial t} = \frac{1}{R_f} \left[\frac{D \partial^2 C}{\partial x} - \frac{V \partial C}{\partial x} - \lambda \left(C + \frac{\rho}{\theta} S \right) \right] \qquad (4.1\text{-}13)$$

where:

$$R_f = 1 + \frac{\rho}{\theta} KNC^{(N-1)} \qquad (4.1\text{-}14)$$

The retardation factor, R_f, can be calculated from the Freundlich constants of both sorption and desorption isotherms (obtained from batch experiments) if sorption hysteresis is important. The concentration, C, in Equation 4.1-14 can be estimated by methods given in Van Genuchten and Wierenga (1974, pp. 24-28) when $N \neq 1$.

When the rate of sorption is slow compared to the groundwater flow rate, sorption kinetics must be described by:

$$\frac{\partial S}{\partial t} = f(C,S) \qquad (4.1\text{-}15)$$

Van Genuchten and Cleary (1979, p. 351) give a number of possible rate equations for sorption. A first order rate equation that has been successfully used is:

$$\frac{\partial S}{\partial t} = k \left(KC^N - S \right) \qquad (4.1\text{-}16)$$

where k is a rate constant.

Detailed plans for incorporating radionuclide transport models in performance assessment analyses of the natural system are given in Section 8.3.5.2.3.

4.1.3.7 Geochemical retardation in the host rock and surrounding units--expected and unexpected conditions

Summary descriptions of (1) conditions that influence radionuclide retardation, (2) expected retardation processes, and (3) expected retardation behavior for individual key radionuclides (listed in Section 4.1.3.1) are presented in this section. These descriptions are based on currently available data that are incomplete for some important radionuclides. Most variables that influence retardation have been examined over a wide range of values, and in many cases these ranges exceed expected values. Thus, information for both expected and unexpected conditions has been obtained.

4.1.3.7.1 Expected conditions

The expected flow path for groundwater transport of waste radionuclides from the repository to the accessible environment is through basalt flows and along flow tops and interbeds. The dense interiors of basalt flows have low groundwater permeabilities compared to flow tops and interbeds. Thus, dense interiors tend to act as confining units for groundwater contained in the flow tops and interbeds. This permeability contrast promotes two-dimensional, horizontal movement of groundwater in flow tops and interbeds and one-dimensional, vertical movement through dense interiors. The top of the Cohassett flow is a likely early segment of the flow path because of a slightly upward hydraulic head gradient across the flow. The remainder of the flow path in the natural system consists of basalt flow interiors, relatively porous flow tops, and sedimentary interbeds above the repository horizon in the primary isolation zone.

Radionuclide retardation processes depend on the characteristics of the minerals and groundwaters along the flow path. In dense interiors, radionuclides will mainly contact secondary minerals that line fissures and vesicles in the basalt. These minerals consist mostly of smectitic clays, zeolites, and silica although smaller quantities of numerous additional minerals have been identified. They have high surface areas and are effective sorbants for most radionuclides. Flow tops consist of brecciated and vesicular basalt layers about 1 to 4 m thick above the dense flow interiors. The breccia and associated rubble are typically composed of clasts 1 to 6 cm in diameter imbedded in a matrix filled with clay, zeolite, or basalt. The porous flow-top materials have high surface areas and strongly sorb most radionuclides. Most sedimentary interbeds are located in the Saddle Mountains Basalt, approximately 400 m (1,312 ft) above the repository horizon. Radionuclide retardation in these interbeds is only of secondary importance since they are above the upper buffer zone. They range from less than 1 m (3.2 ft) to about 40 m (131 ft) thick. These interbeds consist mostly of tuffaceous siltstone with lesser amounts of quartz sandstone, conglomerate, and well-sorted vitric tuff. They are porous and the high-surface-area minerals in the interbeds strongly sorb most radionuclides.

Groundwater composition varies as a function of depth. Concentrations of sodium, chloride, and fluoride increase with depth while potassium and calcium concentrations decrease. Concentration ranges for major inorganic components are sodium (less than 50 to 450 mg/L), potassium (less than 4 to 36 mg/L), calcium (less than 2 to 18 mg/L), magnesium (less than 2 to 12 mg/L), silicon (less than 25 to 175 mg/L), chloride (less than 50 to 550 mg/L), fluoride (less than 5 to 55 mg/L), and sulfate (less than 25 to 250 mg/L). Measured pH values range from 7.2 to 10.8, but most are in the range of 9.2 to 9.8. Concentrations of dissolved organic carbon in Grande Ronde Basalt are less than 1 mg/L. The major dissolved gas in Grande Ronde Basalt groundwaters is methane (350 to 700 mg/L).

The groundwater components that have the greatest influence on retardation of key radionuclides are hydrogen ion, carbonate, and possibly dissolved organics. At the pH values found for these groundwaters, most radionuclide metal ions (actinides, technetium, zirconium, tin, samarium, and palladium) exist mainly as hydroxyl or carbonate complexes. The formation of these species (and organic complexes if they also form) control the retardation behavior of these radionuclides.

Oxidation states of the key radionuclides are important in determining their retardation behavior. The preponderance of evidence indicates that conditions in the natural system are reducing. Radionuclides, therefore, will be present in lower oxidation states. Most radionuclides are more strongly retarded in reduced form.

The temperature of the Columbia River Basalt Group increases with increasing depth. Measured fluid temperatures range from about 55 °C at repository depth to about 20 °C at 100 m (328 ft). However, temperature increases due to waste emplacement may reach as high as 100 °C at 200 m (656 ft) above the repository (see Section 4.2.1). Data on retardation processes must cover this temperature range to be applicable.

4.1.3.7.2 Retardation processes

Radionuclides that are sorbed onto minerals in the flow path will move at a slower velocity than the groundwater. Diffusion and hydrodynamic dispersion of radionuclides will also retard their transport. These are the significant retardation processes expected in the natural system.

Sorption of key radionuclides occurs by chemisorption and ion exchange reactions with minerals in the groundwater flow path. The extent of sorption is controlled by the following:

- Mineral composition, surface area, and ion exchange capacity of the geologic solids.
- Groundwater composition and pH.

- o Redox potential of the groundwater-mineral systems.
- o Radionuclide identity and concentration.
- o Temperature and time.

For a given set of the above conditions, steady-state sorption and desorption can be accurately described by the Freundlich isotherm equation (see Section 4.1.3.2). Desorption isotherms for most radioelements are different than the sorption isotherms. In these cases, desorption is inhibited compared to sorption. This hysteretic effect is important to radionuclide transport calculations since it can lower peak radionuclide concentrations in groundwater and delay transport. Both sorption and desorption isotherm data can be incorporated into radionuclide transport models by using the isotherms to calculate retardation factors as described in Section 4.1.3.6.

Radionuclide diffusion and dispersion processes retard transport by a spreading or dissipation mechanism that results in dilution of radionuclide concentrations along the flow path. These processes depend on the physical structure (pore structure, particle size, and distribution) of the flow path. Other important factors affecting diffusion and dispersion are temperature and groundwater-flow velocity. Radionuclide transport models account for diffusion and dispersion processes by combining them in the dispersion coefficient term (see Section 4.1.3.6).

4.1.3.7.3 Retardation behavior of key radionuclides

The retardation behavior of key radionuclides is summarized below. The radionuclides are listed in approximate order of decreasing inventory/EPA release limit, 1,000 yr after of the repository (see Table 4.1-22).

Americium

Americium is one of the most strongly sorbed radionuclides studied. Distribution coefficients for americium sorption on basalt, secondary minerals, and interbed materials are relatively high (230 to 3,000 mL/g) under all conditions studied. The predominant solution species in basalt groundwaters will be carbonate or hydroxyl complexes of americium(III). Americium is sorbed by a chemisorption reaction with basalt and interbed materials rather than ion exchange since sorption is not decreased by addition of competing cations. All retardation data obtained thus far indicate that americium will be immobile over a wide range of possible conditions in the natural system. Because of these observations, future investigations of americium transport by groundwaters have been deemphasized.

Plutonium

The sorption behavior of plutonium is critically dependent on its oxidation state. In air-saturated groundwaters, plutonium(V) is the dominant oxidation state and is more weakly sorbed than lower oxidation states. Distribution coefficients on basalt, secondary minerals, and interbed materials in air-saturated conditions range from about 18 to 3,000 mL/g. Under reducing conditions, plutonium(IV) or plutonium(III) is formed and is more strongly sorbed (distribution coefficients range from about 400 to less than 10,000 mL/g). Basalt appears to be able to reduce higher oxidation states of plutonium to plutonium(IV) or plutonium(II). Plutonium species in basalt groundwater solutions are probably either hydroxyl or carbonate complexes. The dominant sorption mechanism is chemisorption. Major groundwater components appear to have little influence on sorption. Plutonium should be relatively immobile in basalt-groundwater systems, especially if lower oxidation states are maintained. Desorption from basalt does not occur to any measurable extent. Further plutonium sorption studies will be required to determine the likely oxidation states of plutonium in natural system groundwaters and to further evaluate desorption isotherms.

Neptunium

Sorption of neptunium(V) on basalt is relatively slow and is likely controlled by reduction to neptunium(IV) by the basalt surfaces. The neptunium(IV) is sorbed more strongly (distribution coefficients range from about 60 to 1,000 mL/g) than neptunium(V). Both oxidation states of neptunium form strong carbonate complexes. Increased carbonate concentrations in groundwater decrease sorption. Other groundwater components have negligible effects on sorption. Chemisorption is the dominant sorption mechanism since sorption is not affected by changes in ionic strength. Desorption measurements show that sorption hysteresis is a significant phenomenon for both neptunium(V) and neptunium(IV). Neptunium is not expected to be significantly mobile in the natural system. However, additional work is required to better define those processes that can affect mobility, especially carbonate complexation and redox reactions.

Uranium

In the natural system environment, uranium(IV) and uranium(VI) will be the most important oxidation states. As for the other actinides, the (IV) species will be more strongly sorbed than the (VI) species. Distribution coefficients for uranium(VI) sorption on basalt, secondary minerals, and interbed materials range from about 2 to 1,500 mL/g, and for uranium(IV), about 50 to 1,200 mL/g. The reduction of uranium(IV) at basalt surfaces appears to be an important process in uranium sorption. The reaction is slow and results in increased sorption over long time periods in laboratory experiments. The dominant solution species of uranium are carbonate complexes. The presence of carbonate in the groundwaters decreases sorption of uranium. Like other actinides, uranium is sorbed by a chemisorption reaction, rather than by ion exchange. Sorption hysteresis is important for both uranium(IV) and uranium(VI). Uranium transport in groundwater is

expected to be strongly retarded by sorption in the natural system, especially if the reduced state is maintained in this system. Additional work on uranium sorption will emphasize the need for a better understanding of redox reactions that uranium can undergo in the natural system and of effects of carbonate complexation on sorption.

Carbon and iodine

Carbon-14 and iodine are not measurably sorbed by any of the geologic solids studied thus far. Probable chemical species in the natural system groundwaters are CO_3^{2-} and I^-. Since the anion exchange capacity of geologic solids is very low at ambient pH values, little interaction is observed. Diffusion and dispersion are the only likely retardation mechanisms for these radionuclides, although isotopic exchange of $^{14}CO_3^{2-}$ with naturally occurring carbonate solids may be significant. Future work with these radionuclides will concentrate on determining whether or not isotopic exchange of ^{14}C is a significant process.

Curium, zirconium, and tin

Little information is available on retardation of these radionuclides under conditions of the natural system. Curium behavior is expected to be analogous to that of americium because of similar chemical behavior. Therefore, curium should be immobile in the natural system. Zirconium is strongly sorbed on fresh basalt surfaces and on flow-top basalt (distribution coefficients of 70 to 320 mL/g and 650 to greater than 10,000 mL/g, respectively, were measured). Tin sorption on Mabton interbed materials was so extensive that it could not be detected in the groundwater solution (distribution coefficients were greater than 10,000 mL/g). Each of these radionuclides is expected to be immobile under natural system conditions. Future work with these radionuclides will include sorption studies on a wider range of geologic solids.

Technetium

The negatively charged pertechnetate ion, TcO_4^-, is the most stable technetium species in solution under oxidizing conditions. This anion is not appreciably sorbed by geologic solids in the natural system. Pertechnetate ion, however, can be reduced by basalt surfaces if oxygen is removed to very low levels. The reduced species (probably technetium(IV)) is strongly sorbed on basalt, secondary minerals, and interbed materials. Distribution coefficients range from about 11 to 360 mL/g under reducing conditions. A strong sorption hysteresis effect is observed for technetium. Sorption occurs by a chemisorption mechanism rather than ion exchange. The dominant solution species under reducing conditions is probably a carbonate complex of technetium(IV). The presence of carbonate in groundwater solution significantly decreases sorption of the reduced species. An accurate prediction of the oxidation state of technetium in the natural system is essential to determine its mobility. Future field and laboratory measurements will provide an understanding of the redox behavior of technetium in the natural system.

Samarium and palladium

No information is available on retardation of these elements in the natural system. Future sorption studies will include these radionuclides.

Selenium

In the deep groundwaters of the Hanford Site, selenium can exist as either SeO_3^{2-} or HSe^-, depending on redox conditions. Elemental selenium also may be present but is insoluble. Unlike other nonmetallic anions, selenium is significantly sorbed from solution onto basalts, secondary minerals, and interbed materials. Distribution coefficients range from about 0.3 to 10 mL/g for SeO_3^{2-} and from about 3 to 40 mL/g for HSe^-. Reduction of SeO_3^{2-} by basalt has not been observed even at 90 °C in the absence of oxygen. Sorption of both anions must be by a chemisorption mechanism since the anion exchange capacity of the geologic experiments is very low under conditions of these measurements and they will not exchange with other anions. The presence of calcite in the solids appears to enhance sorption of both SeO_3^{2-} and HSe^-. Insoluble calcium compounds containing these anions are known. A strong sorption hysteresis effect is observed for HSe^-. To assess selenium mobility, its oxidation state in the natural system must be determined. Selenite ion will be more mobile than HSe^-. Both selenium species will be more mobile than radionuclides that are metal ions. Future retardation studies with selenium will concentrate on understanding redox reactions that control the selenium species and on measuring selenium sorption on a wider range of site geologic solids.

Cesium

Cesium is extensively sorbed on basalt, secondary minerals, and interbed materials. Distribution coefficients range from about 20 to 14,000 mL/g. Cesium will exist as the simple hydrated cation in natural system groundwaters. It is at least partly sorbed by an ion-exchange mechanism since Na^+ and K^+ compete for sorption sites with Cs^+. Because it is not expected to be mobile, and since a large amount of information already exists on cesium retardation, only a minimal effort will be made in future on cesium sorption studies.

4.2 GEOCHEMICAL EFFECTS OF WASTE EMPLACEMENT

This section discusses the geochemical effects of waste emplacement on the host basalt environment. Effects of increased temperatures in the natural system due to decay heat from the wastes on several geochemical processes (hydrothermal alteration of basalt, changes in groundwater chemistry, and radionuclide migration) are estimated.

Computer models show the temperature at the wall of the borehole containing the waste package peaks at 186 °C 12 yr after waste emplacement; the peak temperature then slowly propogates outward and diminishes (Section 4.2.1). Preliminary basalt-groundwater experiments show heating can decrease pH, lead to reducing conditions, increase the concentration of some radionuclide-complexing anions but not others, and influence which alteration minerals are produced (Section 4.2.2). Preliminary experiments also show the rate of radionuclide diffusion in a basaltic system increases with temperature (Section 4.2.3.1), but the effect of temperature on radionuclide sorption depends on the specific chemistry of the radionuclide (Section 4.2.3.2). Plans to collect more data are given in Section 8.3.4.

4.2.1 ANTICIPATED THERMAL CONDITIONS RESULTING FROM WASTE EMPLACEMENT

The emplacement of nuclear wastes in a mined geologic disposal system in basalt will cause the temperature of the engineered barrier system to rise as heat is evolved from the waste containers. Initially, the source of heat is the decay of short-lived fission products in the nuclear waste (gamma and beta radiation). Later, the primary contributors to decay heat are the longer lived actinides that decay primarily by the emission of alpha particles. Following the initial period of heat generation by the fission products of the wastes, temperatures in the natural system will gradually fall, approaching ambient temperatures after about 10,000 yr.

Reactions between the groundwater and host rock will occur as a result of this heating and will modify the geochemical environment surrounding the waste packages. Because the nature of these reactions are strongly dependent on temperature, it is important to understand how temperatures evolve in the host

rock throughout the lifetime of the repository. The thermal evolution of a mined geologic disposal system in basalt can be modeled using thermal analysis codes like HEATING5 (Turner et al., 1977, pp. 1-107) together with data on the thermal properties of the repository. These data include the types and ages of nuclear fuel, container design, thermal conductivity of the waste package and basalt, and repository design (spacing of the waste containers). The source term for the decay heat from waste containers is calculated from radionuclide inventories computed from information on the power history of the fuel assemblies (see Section 7.4.6.3.3.2.2).

Results of the thermal evolution calculations are reviewed below. A detailed discussion of the thermal modeling that has been conducted to date is given in Section 7.4.6.3.3.2.1. Therefore, in the following discussion, only the results of this modeling effort that are applicable to the host rock surrounding the waste packages are presented. The results are based on the current understanding of repository design and characteristics. The data will be revised as new information becomes available.

The thermal evolution of the host rock for a repository in basalt has been investigated as part of the analysis by Yung et al. (1986, pp. 1-6), as discussed in Section 7.4.6.3.3.2.1. The HEATING5 code, which was used in the analysis, solves the heat conduction equation for both steady-state and transient conditions. In the modeling effort by Yung et al. (1986, pp. 1-6), heat flow from the waste form to the waste package and into the surrounding basalt is modeled in three dimensions using an integrated model that accounts for mathematical continuity at the interfaces in the system (waste form-container-packing material-basalt) and for transient effects and heat capacity. All waste packages are assumed identical and, by invoking geometric symmetry based on the distribution of the waste packages in the repository, a single representative region of the repository (see Figures 7.4.6.3-1 and 7.4.6.3-2) can be modeled. The region that was modeled by Yung et al. (1986, pp. 1-6) is bounded by the ground surface where the temperature is 15 °C and a surface located 1,000 m (3,280 ft) below the repository where the temperature, 105 °C, is fixed by the observed geothermal gradient (see Figure 7.4.6.3-3). Heat transport by circulating groundwater is assumed to be negligible due to the expected low flow rates of groundwater near the repository. The model and the assumptions and data used in the thermal analysis are discussed in Yung et al. (1986, pp. 1-6) and in Section 7.4.6.3.3.2. The integration of the subsystems of the repository in the model by Yung et al. (1986, pp. 1-6) and its capability of modeling heat flow in three dimensions provides better estimates of the thermal evolution of the repository than those generated in earlier analyses (Altenhofen, 1981, pp. 33-48; King et al., 1981, pp. 16-24; Osnes et al., 1984, pp. 39-115) that linked multidimensional heat flow models for the host rock with quasi-steady one-dimensional models for the waste package. For these reasons, the analysis by Yung et al. (1986) is preferred. The results of their analysis are reviewed below for the basalt environment surrounding waste packages.

Thermal conditions in the host rock near the waste packages are shown in Figure 4.2-1 for the first 50 yr following waste emplacement (which is the period of most extreme changes in temperature near the waste packages). In

the analysis by Yung et al. (1986, pp. 1-6), it was assumed that consolidated spent fuel alone is emplaced. The distribution of temperatures shown in the figure is within a plane oriented normal to the axis of the waste containers (see Figures 7.4.6.3-1 and 7.4.6.3-2). Maximum temperatures at the wall of the boreholes in which the wastes are emplaced peak at 186 °C 12 yr after waste emplacement. Thereafter, peak temperatures are propogated slowly outward into the host rock and are diminished so that, for example, after 24 yr, at a distance 1.6 m (5.2 ft) into the host rock from the borehole wall, a maximum temperature of 150 °C is predicted. Temperature gradients are steep by the first year following waste emplacement but decrease significantly within 50 and 10,000 yr. Temperatures in the basalt 1.6 m (5.2 ft) from the borehole surface fall from about 140 °C to about 110 °C after 10,000 yr (see Figure 7.4.6.3-4).

An expanded view of temperature distributions in the host rock, encompassing the upper and lower boundaries of the model by Yung et al. (1986, pp. 1-6), is shown in Figure 4.2-2 for a duration up to 1,000 yr after waste emplacement. The temperature distribution in this figure is within the same plane as shown for Figure 4.2-1. As shown in the figure, even after 1,000 yr temperature 500 m (1,640 ft) above and below the level of the repository will be increased by the radiogenic heat from the waste forms. Although the volume of rock that is affected by this heating is continually increased with time, temperatures throughout the rock mass continually decline from the peak value of 186 °C at the borehole interface. When considering geochemical interactions between the basalt and groundwater, therefore, a range of temperatures between 52 °C (the ambient temperature in the host rock at the level of the repository; see Section 4.1.2.9), and 186 °C is indicated by the thermal analyses.

4.2.2 HYDROTHERMAL ALTERATION AND CHANGES IN GROUNDWATER CHEMISTRY DUE TO THE THERMAL PULSE

The thermal pulse resulting from waste emplacement could possibly affect radionuclide isolation through changes in pH, redox environment, anion concentrations, colloid formation, and secondary phases.

The effect of temperature on the mineralogy and groundwater chemistry of the natural system is more fully discussed in the section on hydrothermal reactions involving basalt and groundwater (Section 7.4.1.1). The following is a summary of the observations made in hydrothermal basalt-groundwater experiments at 100 to 300 °C. This temperature range corresponds approximately to the temperature range predicted for the natural system by the thermal analyses discussed above. Experiments conducted at 300 °C are included in the discussion even though they exceed, by 114 °C, the maximum temperatures predicted in the thermal analyses because it is expected that these higher temperature experiments will more closely approach equilibrium than experiments conducted at temperatures of 200 °C and lower. The attainment of equilibrium in the hydrothermal experiments is discussed in Section 7.4.1.1. Experimental investigation of basalt-groundwater

interactions at temperatures less than 100 °C have not been attempted, in part because of the sluggish reaction rates at low temperatures but also because the best information on these systems is provided by Hanford Site hydrochemical investigations (see Section 4.1.2). All of the experiments discussed below were conducted at a pressure of 30 MPa. Sections 4.2.2 and 4.2.3 of the SCP annoted outline (DOE, 1985b) have been combined here in Section 4.2.2.

The four characteristics of principal interest in the solution chemistry of basaltic groundwaters are the pH, redox state, concentrations of radionuclide-complexing ligands (most of which are anions) and colloid formation. These characteristics of the solutions are controlled by basalt-groundwater reactions. Sorption and solubility control of radionuclide migration is strongly influenced by the pH, redox state, and ligand concentrations in solution. Alteration minerals resulting from hydrothermal interactions between basalt and groundwater are important adsorbing substrates for many radionuclides.

The pH in the natural system before waste emplacement is approximately 9.7 at 25 °C. The at-temperature pH resulting from basalt-groundwater reactions in experiments at 100 to 300 °C tends to drop initially and then rises slowly as the experiments progress. (The pH at the temperature of the experimental system is calculated from the compositions of the solutions sampled during the runs, using chemical speciation codes like EQ3NR (Wolery, 1983, pp. 1-191).) Typical pH values at the termination of experiments run for several thousand hours are 7.0 to 7.6 at all temperatures up to 300 °C. Variable water/rock mass ratios have little effect on the final pH. Although the pH in the experiments is nearly the same in all of the experiments at temperatures between 100 to 300 °C, the solutions become less alkaline at the higher temperatures because pH decreases as temperature increases in the temperature range of the experiments. The control of pH values in the experiments appears to involve interactions between the mesostasis of the basalt, cations in solution, and secondary minerals. The mechanism for pH control in the experiments is discussed more fully in Section 7.4.1.1.

Redox conditions in the natural system before repository construction appear to be generally reducing, but quantification of the redox state of the fluids is difficult to determine due to an apparent lack of overall equilibrium among redox reactions. The redox conditions in ambient Hanford Site groundwaters is discussed more fully in Section 4.1.3.4.

The effects of temperature on the redox conditions in basalt-groundwater systems has been investigated experimentally to 300 °C. Slow reaction kinetics have prevented a determination of the redox conditions in basalt-groundwater systems in experiments conducted at temperatures of 200 °C and less. At 300 °C, changes in the redox state of solutions contacting basalt have been monitored by measuring changes in the concentrations of oxidized and reduced species of sulfur. Measurements of the concentration of hydrogen gas in these experiments have also been used to infer the redox state of the fluids in these experiments. The results indicate that the solutions become reducing after contacting the basalt for several tens of hours. At the

termination of the runs (several thousand hours), log fO_2 values are computed to be about -30 to -32 (Eh approximately -0.7 V). Redox controlling reactions in these experiments have not yet been identified. The status of redox investigations in basalt-groundwater systems is discussed more fully in Section 7.4.1.1. Plans for characterizing the redox conditions in these systems, especially at the lower temperatures expected in the repository, are discussed in Section 8.3.4.2.

The concentrations of anions in basalt groundwaters are of interest because of their potential to complex radionuclides and increase their migration through the natural system. The major inorganic anions in the groundwater are chloride, fluoride, carbonate/bicarbonate, sulfate, and $H_3SiO_4^-$.

Fluoride and chloride concentrations do not vary significantly in the hydrothermal basalt-groundwater experiments completed as of January 31, 1986. Total inorganic carbon concentrations typically rise during the initial phases of a run then decrease and approach (approximately) their initial values. Sulfate concentrations do not change significantly during the experiments at all temperatures up to 200 °C. At 300 °C, sulfide concentrations increase, possibly as a result of sulfate reduction. Total silica concentrations increase with increasing temperatures. However, because the pH of the solutions also decreases in the hydrothermal experiments compared to the pH in the natural system (9.7), the concentration of $H_3SiO_4^-$ is also expected to decrease. Anion concentrations in the hydrothermal experiments are discussed further in Section 7.4.1.1.

The effect of temperature on the colloidal properties of basalt groundwaters has not been well documented. Preliminary results show a slight tendency for an increase in the concentration of colloids at 100 to 300 °C. Further data are needed before conclusions can be made (see Section 8.3.4.3).

The alteration minerals resulting from basalt-groundwater experiments at all temperatures include smectites, zeolites, illite, and potassium feldspar. Cristobalite and tridymite have been identified in experiments at 300 °C, and cristobalite has also been identified in experiments at 200 °C. Magnetite and an iron oxyhydroxide have been identified in the 300 °C experiments, and iron oxyhydroxide has been identified in experiments at 200 °C. At 100 °C, an iron sulfide (possibly pyrrhotite) has been identified. The alteration mineralogy observed in the hydrothermal experiments completed as of January 31, 1986, is discussed in more detail in Section 7.4.1.

4.2.3 THE EFFECT OF THE THERMAL PULSE ON RADIONUCLIDE MIGRATION

In the natural system, the most important effect on radionuclide migration caused by the emplacement of high-level nuclear waste is the increase in the temperature. As discussed in Section 4.2.1, temperatures in the natural system will be elevated by as much as 65 °C 50 m from the waste package during the controlled release period.

The increase in temperature will affect radionuclide mobility by increasing the rate of diffusion of nonsorbed radionuclides through the natural system and by altering the sorption characteristics of radionuclides. The overall effect on radionuclide mobility is complex and not well understood.

The two major objectives of this section are as follows:

- o Briefly describe the effect of temperature on diffusion measured in the BWIP laboratory.
- o Discuss and present some preliminary data on the effect of temperature on sorption in a basaltic system.

The general topic of the sorption of radionuclides in the natural system was discussed in Section 4.1.3.3; the expected mineral alteration was discussed in Section 4.2.2 (mineral alterations in the natural system are not expected to significantly change sorption); experimental efforts in this area are summarized in Section 7.4.4.__; and future plans for work relating to the sorption of radionuclides are discussed in Sections 8.3.1.4.2 and 8.3.4.

4.2.3.1 The effect of temperature on diffusion in a basaltic system

In a geochemical system with a low groundwater flow rate, the rate-limiting step for the transport of nonsorbing radionuclides is diffusion. The diffusion constant, because it depends on the viscosity of the medium, will be affected by the temperature pulse in the natural system.

The general effect of temperature on diffusion has been well established in dilute aqueous media. The activation energy of the diffusion constant for a low molecular weight solute in water is approximately 2 kcal/mol with a diffusion coefficient on the order of 1×10^{-9} m^2/s (at 25 °C). The diffusion constant, therefore, is relatively insensitive to changes in temperature (it will double for every 75 °C increase in temperature at temperatures near 25 °C).

In a basalt environment, the additional interaction between nonsorbing solutes and the solids present is expected to affect their rate of diffusion. Charge-charge and charge-dipole interaction is expected between the migrating solute and the solid surface and absorbed ions. Therefore, it is important to measure diffusion under conditions that closely resemble those found in the repository. Although no work has been done in basalt alone, diffusion experiments have been conducted in packing material (which is 75% basalt and 25% sodium bentonite) on tritiated water and chloride by Relyea et al. (1986, pp. 317-323) over the temperature range of 20 to 90 °C.

The diffusion data obtained for tritiated water are shown plotted as a function of temperature in Figure 4.2-3. The data were found to fit the

following empirical equation (Eq. 4.2-1):

$$\log(D) = -5.513 - \frac{1,120}{T} - 0.338 \text{ (clay density)} \qquad (4.2\text{-}1)$$

where D is the diffusion constant, T is the temperature in °K and the clay density is in Mg/m^3. The activation energy derived from this equation was 5.2 kcal/mol. The diffusion constant calculated at various temperatures is shown in Table 4.2-1. The effect of raising the temperature in the natural system from 55 to 150 °C, assuming that the lower temperature diffusion data can be extrapolated, increases the diffusion constant by a factor of six for tritium.

The diffusion constant for chloride in packing material was not as strongly dependent on the temperature as was tritiated water. The diffusion constant as a function of temperature is given by the following empirical equation (Eq. 4.2-2):

$$\log(D) = -6.807 - \frac{547.5}{T} - 1.195 \text{ (clay density)} \qquad (4.2\text{-}2)$$

The units are as previously defined. The activation energy for this solute is 2.4 kcal/mol, which is approximately that expected for solutes in a pure water system. The diffusion constant as a function of temperature is shown in Table 4.2-1. The calculated effect of raising the temperature from 55 to 150 °C was to increase the diffusion coefficient by a factor of 2.4.

In summary, the rate of diffusion in a basalt environment is slower and more sensitive to temperature than in a pure aqueous system. The increase observed by raising the temperature from 55 and 150 °C is approximately a factor of 2.4 for negatively charged species and a factor of five for neutral species. The actual extent to which this occurs depends on the temperature increase which is a function of time and distance from the waste package.

4.2.3.2 The effect of temperature on radionuclide sorption in a basaltic system

The effect of temperature on the adsorption of radionuclides in a basalt environment is not yet well understood. The major reason for this is the complexity of the process (as discussed in Section 4.1.3.3.3) and the strong dependency of radionuclide chemistry on temperature. The principal goal of this section is to briefly present data that reflect the current understanding of the effect of temperature on sorption of key radionuclides in a basalt medium.

The apparent sorption of radionuclides, determined experimentally, is expected to be strongly influenced by temperature. No general trend with

respect to temperature has been observed in a basalt system. The effect of temperature on sorption, therefore, must be established for each radionuclide.

Major temperature-dependent processes that will affect sorption parameters are as follows:

- o Radionuclide redox reactions.
- o Irreversible sorption/hysteresis.
- o Ion exchange.
- o Chemisorption.
- o Precipitation reactions.
- o Hydrothermal alteration of solid surface.

Because these processes are frequently interdependent, caution must be used in the interpretation of sorption data reported.

Data that have been obtained on the effect of temperature on radionuclide sorption in a basalt environment have been discussed in greater detail elsewhere (Ames and McGarrah, 1980c, pp. 1-24; Salter et al., 1981b, pp. 13-17; Barney, 1982, pp. 4-13). In these studies, the effect of temperature on the sorption of strontium, cesium, technetium, selenium, uranium, americium, radium, neptunium, and plutonium on basalt were examined.

Of all the radionuclides studied, general agreement has been reached on only cesium and strontium. For these, there appears to be no complexity introduced in their chemistry as temperature was increased. The effect of temperature on Kd for cesium is shown in Figure 4.2-4. As can be seen, the Kd decreases as a function of temperature, goes through a minimum at approximately 150 °C, and increases beyond that temperature. The Kd for strontium was not significantly affected by temperature in the range of 25 to 85 °C.

The effect of temperature on the sorption of the rest of the radionuclides studied is not clearly understood. In most of the experiments, it was difficult to interpret the data obtained because of complexities introduced by slow kinetics, precipitation, reduction, or possibly changes in the sorption mechanism as the temperature was varied. The general trends observed, given the limitations just identified, were the following:

- o Radium exhibits complex behavior as a function of temperature and solution concentration but is in general not greatly affected by temperature.
- o Selenium and technetium both are precipitated at higher temperatures and have sorption properties that are very sensitive to redox conditions. In general, higher temperature facilitates their removal from solution.
- o Kd for uranium appears to increase significantly as a function of temperature.

- Neptunium sorption is not significantly affected by temperature.

- Plutonium and americium exhibit complex behavior as a function of temperature but are, in general, removed from solution as the temperature is increased (mostly due to reduction/precipitation rather than a real increase in Kd).

In conclusion, the general effect of temperature on sorption of radionuclides in a basaltic environment depends on the specific chemistry of that radionuclide. Therefore, increased temperatures in the natural system caused by the temperature pulse will enhance the mobility of some radionuclides and decrease the mobility of others. Experiments to provide a more definitive answer to the effect of temperature on sorption are outlined in Section 8.3.4.

4.3 NATURAL ANALOGS AND RELATED FIELD STUDIES

Results from studying natural analogs and from field tests can supplement information from laboratory experiments. Laboratory experiments are conducted for a limited time under artificial conditions, but natural analogs represent natural experiments over geologic time. Similarly, laboratory tests are small-scale representations in an artificial environment of large-scale processes in the natural environment; field tests can more accurately represent processes in the natural system.

This section presents the current natural analog and field test data relevant to radionuclide isolation in a mined geologic disposal system in basalt, which include the following:

- Studies of native copper deposits in northern Michigan show that copper (a backup material for the waste package) is stable in a geochemical environment similar to the geochemical environment expected in the repository (Section 4.3.1.1).

- Field studies show that the alteration minerals formed during laboratory experiments with heated groundwater and basalt are nearly identical to the secondary phases found in the controlled area study zone (Section 4.3.1.2). Therefore, the results of the laboratory experiments probably apply to the natural system.

- The only available field test of solute chemistry and radionuclide transport shows that a portion of the reactive tracer (K^+) migrates through the flow system at the same rate as a nonreactive tracer (SCN^-) (Section 4.3.2.2).

- Field tests in Sweden of reactive tracers show that field tests may have to last longer than the one mentioned above to get accurate results (Section 4.3.2.3).

Plans for further studies of natural analogs and more field tests are given in Sections 8.3.1.4 and 8.3.4.2.

4.3.1 NATURAL ANALOGS

Natural analog studies can be used as indicators of processes that may occur in a mined geologic disposal system in basalt over long periods of time. Results from analog investigations can be compared with laboratory experiments that simulate expected repository conditions. The advantage of studying natural analogs is that they represent natural experiments over geologic time periods that are similar to or even longer than those called out in Federal regulatory criteria. Thus, they can demonstrate the long-term behavior of elements and the long-term persistence of certain mineral phases in natural systems, something that cannot be accomplished with laboratory experiments alone.

A possible limitation to the application of natural analogs to materials behavior in a mined geologic disposal system in basalt is that no natural analog can be shown, or is likely to be shown, to exactly reproduce all the various environmental conditions expected in a mined geologic disposal system in basalt. Nonetheless, the value of these studies for demonstrating the behavior of a hydrothermal system over repository-relevant lengths of time should not be underestimated.

Examples of several natural analogs that have been investigated previously by the BWIP are presented in this section. Areas that have not been studied but which are potentially analogous to a mined geologic disposal system are considered in Section 8.3.4.2. The natural analogs stuided to date include the following:

- Native copper deposits of northern Michigan as a natural analog for the evaluation of the long-term stability of copper container material.

- Field studies of existing secondary phases within the basalt at the Hanford Site as a natural analog for evaluation of the long-term stability of alteration minerals that form during waste-barrier-rock hydrothermal interaction test.

Future planned natural analog studies will include examination of basalt cores from the geothermal fields of Iceland and other similar hydrothermal systems, active and fossil, in basalt (Section 8.4.3.2.2.2.3). In this system, fresh groundwater has interacted with hot basalt to produce secondary phases that have remained stable for thousands of years. The predominant rock that has been altered by the hydrothermal fluids is a tholeiitic basalt, similar in composition to the tholeiite basalts of the Hanford Site. Secondary phases common to both Iceland and the Hanford Site include K-feldspar, zeolites, smectite, and anhydrite (Arnorsson et al., 1982, pp. 1513-1532). The natural occurrence of these minerals in the basalt-groundwater system in Iceland is an ideal analog for the long-term stability of these minerals.

4.3.1.1 Native copper deposits of northern Michigan as a natural analog for copper container corrosion

Although copper is not currently the primary material for container fabrication, it is currently a backup material. The native copper deposits in the Portage Lake Volcanics of northern Michigan provide a natural analog for the evaluation of the long-term stability of copper containars in a repository at the Hanford Site.

The Michigan copper deposits occur in tholeiitic flood basalts that are similar in general chemical characteristics to those of the Columbia Plateau (Mason and Berry, 1968, pp. 209-211; Jolly and Smith, 1972, p. 2; Jolly, 1974, pp. 1118-1125). The native copper, which is believed to have precipitated from higher temperature hydrothermal solutions (200 to 300 °C) between 500 and 800 m.y.B.P., has remained relatively unaltered in the Portage Lake basalt-groundwater system. This illustrates the stability of copper in groundwater of pH (7.5 to 9), low to moderate Eh (+ 100 to -250 mV), and low total dissolved solids including sulfur, chloride, and carbon, similar to Hanford Site groundwater (Chrisman and Jacobs, 1982).

The large stability field of native copper, which falls largely within the range of expected repository conditions in Eh-pH space, is of particular interest. The stability relationships among copper compounds in the system Cu-H_2O-O_2 at 25 °C and 0.1 MPa total pressure are shown in Figure 4.3-1 (Garrels and Christ, 1965, p. 239). (No data are available on the system at higher-temperatures.) Although this is a simple system, the stability of metallic copper indicates that a reasonable possibility exists that this material is stable under repository conditions. Because the data are for the simple system, other factors must be considered, such as the effect of complexants (i.e., S^{--}, Cl^{-}, CO_3^{--}) on the position of the phase boundaries in the diagram.

In the presence of chloride, for example, stability fields are created for a series of copper chloride complexes that are stable under low pH and high Eh conditions--conditions that correspond to those in the upper left of Figure 4.3-1. These do not affect the positions of the boundaries for native copper stability under alkaline and low Eh conditions (Rose, 1976).

The presence of carbonate creates stability fields for hydrous copper carbonate phases such as malachite and azurite, but these phases are stable only under oxidizing conditions and do not affect the stability field of metallic copper.

In the presence of sulfide, stability fields for a host of copper sulfide phases are created (such as covellite (CuS) and chalcocite (Cu_2S)). At low sulfide concentration, these phases are stable only at low pH, but their stabilities extend across the Eh-pH field as the concentration of total dissolved sulfur species increases. The reference groundwater (GR-4) contains 4.2 mg/L sulfate, a concentration that effects the stability of metallic copper only under extremely low pH conditions.

Whereas the 90-10 cupronickel alloy is currently a backup material, the data in the figure considers pure copper. This has no deleterious effects on the applicability of the data because copper and nickel form a binary isomorphous phase system in which the two species combine to form a continuous solid solution series with the same structure from pure copper to pure nickel. The addition of 10% nickel to the copper will lower the free energy of the material and increase the thermodynamic stability of the metal, thus expanding the area of Eh-pH space where the metallic phase is stable.

A study of the copper-bearing basalts in Michigan indicates that similarities exist between that system and the basalt-groundwater system at the Hanford Site (Crisman and Jacobs, 1982, pp. 1-71). These similarities include similar pH ranges, low Eh, and low total dissolved solids. (This is not an unexpected conclusion, since the chemistry of the groundwater will be controlled largely by the material in which it is contained (in both these cases by basalts with very similar petrochemistry).) Preliminary calculations indicate that copper should be stable with respect to copper oxides under the expected temperature, pressure, Eh, and pH conditions in a repository at the Hanford Site.

4.3.1.2 Field studies of existing secondary phases at the Hanford Site

In a mined geologic disposal system in basalt, heat release from the emplaced waste will cause hydrothermal interactions to occur between the heated groundwater and the basalt. These interactions will result in changes in the composition of the groundwater and the formation of secondary phases. The formation and long-term stability of these secondary phases, is of key concern in the design of the nuclear waste repository. These minerals can potentially incorporate radionuclides either by coprecipitation or sorption, thus limiting the release of radionuclides from the repository.

Experiments using basalt plus groundwater reacted at temperatures of 200 and 300 °C and pressures of 30 MPa (4,410 lbf/in^2) (Apted and Myers, 1982, pp. 15-34) identified a suite of alteration minerals that include smectite, iron oxyhydroxide, silica, and zeolites. These are of particular importance since they have excellent sorptive capacity for certain dissolved waste components. The long-term stability of these alteration minerals, however, is not certain. They may be metastable phases that will eventually break down to form a more stable assemblage. This uncertainty can be addressed by an investigation of the natural secondary phases that exist in the basalt underlying the Hanford Site. Investigations of the distribution and composition of secondary phases in the Pasco Basin determined that the principal components of secondary mineral assemblages found are iron-rich smectite, zeolite, and several forms of silica (see Section 4.1.1.3).

The secondary phases found at the Hanford Site are compared in Table 4.3-1 with those alteration minerals observed to form during basalt-groundwater hydrothermal experiments performed at 100 to 300 °C. This

comparison suggests that the major alteration minerals that form during hydrothermal interaction experiments are, in some cases, virtually identical to the natural secondary phases. It is, therefore, valid to assume that the smectite, zeolite, and iron oxyhydroxide observed to form in basalt-groundwater experiments will persist (stably or metastably) in the repository environment for a time period equal to or exceeding the lifetime of the repository.

4.3.2 RELATED FIELD TESTS

Field testing is an integral part of site characterization activities conducted by the BWIP. Most of the field testing to date has focused on characterization of hydrologic parameters, but solute chemistry and transport can be characterized as well. The latter is the subject of this section and Sections 8.3.1.4.1.3 and 8.3.1.4.2.3. Field testing, as used in this section, refers specifically to those tests that are directed at solute chemistry and transport.

Field tests considered in this section involve placing a tracer in a specific groundwater flow zone and monitoring its change in speciation (both oxidation state or ligand association) or its arrival at a distant position. The latter test, traditionally called a tracer test, is the only type of field test that has been conducted by the BWIP; therefore, this is the only type of field test that will be discussed here.

4.3.2.1 Field testing rationale

The BWIP rationale for conducting field tests is based on the following four concepts.

- The application of sorption parameters to large-scale field problems can be scale dependent even though the sorption parameters themselves are not scale dependent.
- Natural system solute transport calculations are conducted for discrete parts of the system, ranging in size from tens to hundreds of meters; therefore, sorption parameters must be quantified at those scales.
- Basalt flow tops, through which most of the deep groundwaters flow, may act like a fractured geologic media; therefore, laboratory-scale tests using crushed geologic samples may yield only relative rather than absolute estimates of radionuclide retardation.
- Some kinetically influenced retardation mechanisms are flow-system specific as well as scale dependent.

The rationale presented is based principally on the inability to adequately describe the spatial distribution of the solid phases present in the flow system. Therefore, any extrapolation of laboratory-derived data that are based on mass, surface area, or volume relationships may be in error, in an absolute sense, to the degree that the sorptive surfaces are inaccurately quantified in space. Field tests conducted at tens to hundreds of meters yield integrated estimates of tracer reactivity with the formation as it naturally exists. These estimates are averaged over the microenvironment variabilities along the flow path associated with mineral types and their distribution, the quantity of reactive surface area, and solution compositions. Mineral types and solution compositions can be quantified and incorporated into laboratory studies so that reaction mechanisms can be identified and, in a relative sense, quantified. Quantifying reactivity on an absolute basis requires either knowledge of the reactive surface area of the formation or a measurement of reactivity on the formation itself. The later is estimated via tracer tests.

Reaction kinetics must be taken into account to calculate realistic estimates of solute travel time. Reaction kinetics, as used in this section, involve any process that results in a departure from steady-state conditions if sufficient time has not elapsed for the process to proceed to completion. The kinds of kinetic processes that are important from a solute transport standpoint are matrix diffusion, migration of the solute to a reactive surface, changes in speciation, and the sorption reaction itself. The importance of the first two processes is formation specific and, at least in the natural system, can be characterized only in the field. The second two processes can be characterized in the laboratory.

The degree of solute retardation depends on both the quantity and availability of reactive surfaces in the formation. These are in turn dependent on the type and distribution of formation materials and groundwater flow characteristics. Kinetic processes will also be affected by the groundwater flow rate. These formation-specific parameters can be accounted for in field tests.

4.3.2.2 Field tests at the Hanford Site

Field tests at the Hanford Site range in type from planned tests in deep and shallow aquifers to observations of radionuclide transport in the unconfined aquifer resulting from defense waste disposal operations. Because of differing geochemical conditions (e.g., major ion chemistry, redox status) between the unconfined and confined aquifers, radionuclide behavior observed in the unconfined groundwaters may not be representative of the behavior associated with a deep basalt system. Therefore, in this section, only tests conducted in deep basalt systems will be discussed.

Only one deep basalt tracer test has been conducted at the Hanford Site in which the behavior of a reactive solute has been monitored. The test, documented in Leonhart et al. (1984), was designed primarily to evaluate

longitudinal dispersivity and effective flow thickness, but fortuitous selection of an ionic tracer provided limited information about ion exchange processes in the formation. These data indicate how an element such as cesium may behave in the test zone and, equally important, how the formation itself behaves. Because the test was not designed as a reactive tracer test, no pretest laboratory studies were conducted to quantify the extent of cationic reactivity. Plans for this type of study to be conducted in the future are discussed in Section 8.3.1.4.2.3.

The test consisted of a two-well recirculating design using boreholes DC-7 and DC-8 (Figure 4.1-2). The tracer used was potassium thiorganate, KSCN. The test was conducted in the McCoy Canyon flow top with a borehole separation of approximately 16.8 m (55 ft) at the test interval. Borehole DC-7 was pumped at 3.8 L/min (1 gal/min) and the tracers were monitored at the ground surface in borehole DC-8.

Breakthrough curves for SCN^-, K^+, and Na^+ are presented in Figure 4.3-2. The curves of SCN^- and K^+ by themselves indicate that SCN^-, a nonreactive (conservative) tracer (Leonhart et al., 1984), and K^+, a reactive (nonconservative) tracer, migrated through the flow system at approximately the same rate. This is indicated by their peak concentrations arriving at the monitoring well at the same time. When the Na^+ peak is considered, it appears that considerable potassium exchanged with sodium and remained in the formation. Further support for this conclusion is indicated by the mass balance presented in Table 4.3-2. Of the original tracer injected, 60% of the thiocyanate was recovered but only 11% of the potassium was detected at the monitoring borehole. In order to maintain the electroneutrality of the groundwater, sodium replaced potassium in solution. The displaced sodium then migrated through the formation at the same rate as the thiocyanate as indicated by the sodium breakthrough curve. The mass balance indicates that the cation-anion balance for the test was within 15%.

This test indicates that a small fraction of a reactive tracer (K^+) migrated through the flow system without any retardation. This could be due to a number of reasons including:

- Saturation of available sorption sites for K^+ (by injected or naturally occurring K^+).
- Flow through highly transmissive flow paths with little available reactive surface.
- Sorption on particulates that migrated rapidly through the flow system.

Whatever the reason, an important conclusion is that, at this scale, a small fraction of a reactive tracer may migrate through the flow path just as fast as the water. This conclusion points out the need to conduct further tests of this type to determine the behavior of specific elements and to determine formation-specific parameters.

4.3.2.3 Field tests at other potential repository sites

Reactive tracer tests in crystalline rock have been conducted in a number of countries and are summarized in Grisak et al. (1984). It is beyond the scope of this section to provide a detailed review of those studies, but the results of one study in Sweden will be discussed in light of its significance on the completed Hanford Site test and future tests that will be conducted by the BWIP.

Results of tracer tests conducted at Studsvik, Sweden, are presented in Landstrom et al. (1983). The tests consisted of a pulse injection, two-well, convergent design and were conducted in a fractured gneiss at about 100 m (328 ft) below ground surface. Flow path lengths ranged from 11.8 to 22.6 m. The tracers used were ^{131}I, ^{85}Sr, ^{134}Cs, and ^{3}H. Breakthrough curves for ^{3}H (a nonreactive tracer) and ^{85}Sr (a reactive tracer) for two flow paths are presented in Figure 4.3-3. The importance of these curves is that a fraction of the ^{85}Sr appeared in the monitoring well at the same time as the ^{3}H, but the bulk of the ^{85}Sr appeared much later. The rapid appearance of the first strontium peak was attributed to a possible particulate transport mechanism, but no filtration studies were reported to confirm this hypothesis nor did ^{134}Cs behave similarly. Whatever the mechanism, it was specific to strontium. In light of this information, the breakthrough curve for potassium in the Hanford Site test may represent an early breakthrough peak, while the bulk of potassium remained in the formation. If this conclusion is true, future reactive tracer tests conducted at the Hanford Site will have to be conducted for a longer period of time in order to determine retardation parameters.

Landstrom et al. (1983) also present comparisons between laboratory and field data. They report field derived retardation factors for strontium of 17 and 30 as compared to laboratory-column retardation-factors values of 30 to 35. The field retardation factors were calculated by considering only the second peaks where the bulk of the strontium appeared. This indicates reasonable agreement between field estimates of retardation and estimates made using crushed geologic samples obtained from core. This type of comparison cannot be made for the Hanford Site test because laboratory-derived potassium sorption data were not collected. These types of laboratory data will be collected in future studies and are described in Section 8.3.1.4.2.3.

4.4 GEOCHEMICAL STABILITY

4.4.1 Potential man-induced effects
4.4.2 Potential effects of natural changes

Geochemical stability is important to waste isolation because changes in geochemistry could lead to changes in the processes controlling radionuclide transport to the accessible environment. Neither man-induced changes (Section 4.4.1) nor natural changes (Section 4.4.2) are expected to affect the geochemistry enough to influence radionuclide transport.

4.4.1 POTENTIAL MAN-INDUCED EFFECTS

Large-scale perturbations of the Hanford Site geochemistry due to human activities such as recovery of natural resources or injection disposal of wastes are considered to be improbable at depths that could affect waste isolation. There are no known metalliferous or petroliferous natural resources that have, or are projected to have, a value great enough to be considered commercially extractable at the reference repository location. Industrial rocks and minerals of relatively low-unit value (peat, diatomaceous earth, permicite, quarry rock, and sand and gravel) occur but would be extracted from surface mining operations. No commercial coal production has been recorded within 100 km (62 mi) of the Hanford Site. Geothermal gradients at the Hanford Site are less than 45 °C/km, which is considered too low for extraction of space heating energy. Deep groundwaters within the reference repository location contain fluoride concentrations much greater than safe drinking water limits and high-sodium and high-salinity concentrations. The inaccessability of these deep strata and the poor water quality of deep aquifers (see Section 3.8) for agricultural, industrial, or domestic use make deep groundwater withdrawal unlikely.

The potential for extraction of oil and gas in sedimentary strata underlying the Columbia Plateau at depths in excess of 3,000 m (9,842 ft) is, at best, speculative (see Section 1.7). Although natural gas has been recovered, all wells drilled in this area have been deemed noncommercial. Possible future activities to recover oil and gas outside the controlled area are not expected to significantly perturb the Hanford Site geochemistry.

The potential for past defense waste water disposal affecting the hydrochemistry of the deep basalt groundwaters is considered low. This is concluded from three lines of evidence including the lack of tritium in deep waters, distinct hydrochemical differences existing with depth, and an increase in hydraulic heads in the deep basalts compared to the shallower formations. This last item means that groundwater movement is upward. Some contamination (e.g., tritium and iodine-129) is present in shallow basalts across portions of the Hanford Site. Studies are planned to determine the

source and movement of these contaminants and to establish a more complete radiological status of the deep basalt waters (see Section 8.3.1.3).

The only likely mechanisms for shallow disposal waters to reach the deep basalts are by the following:

- o Movement along or within boreholes.
- o Introduction near anticlines or where paleochannels were eroded into the basalts.
- o Any past deep-well injection.

4.4.2 POTENTIAL EFFECTS OF NATURAL CHANGES

It appears likely that, over the relatively short time period (compared to geologic time) when the repository must function, no significant changes in the natural system geochemistry will occur. The geochemical stability of the natural system can be estimated by examining effects of geochemical processes that have occurred in the basalts over the 6 to 16.5 m.y. since their eruption. Alteration of these basalts by groundwaters to form secondary phases is probably the most significant geochemical process that has taken place over this time period. Primary phases in the basalts are, of course, inherently unstable thermodynamically in the aqueous environment of the basalt flows. However, the relatively small quantities of secondary phases now found in these basalts show that basalt-groundwater reactions have been very slow. For example, the total volume of secondary phases in the Cohassett and Umtanum flow interiors is less than about 0.27% (see Section 4.1.1.3.4.1).

The planned development of a mineralogy-petrology model (see Section 8.3.1.2.2.5) based on past and present geochemical processes will allow reliable predictions of future geochemical environments in the basalts. This model will integrate information obtained from mineralogic and petrologic characterization of basalts, secondary phases, and sedimentary interbeds using standard geologic, geochemical, and petrologic methods. Past and present geochemical conditions will be projected into the future using kinetic and thermodynamic considerations and by comparisons with analog geochemical situations. Predictions will take into consideration (1) continuation of present-day geochemical changes and their rates and (2) perturbation of present-day changes in the physicochemical environment.

Tectonic or volcanic activity could conceivably affect the natural system geochemistry, although the probabilities of events serious enough to significantly affect geochemistry at depth are low (see Sections 1.5.1 and 1.5.2).

Variations in the climate at the Hanford Site are not expected to affect geochemical conditions in the deep basalts since they are currently saturated with groundwater and groundwater velocities in the basalts are low (Chapter 3).

4.5 SUMMARY

This section presents a synopsis of the significant results recorded in Chapter 4 in terms of how the geochemical data are to be used and what data are available. Also additional data needs required for site characterization are identified in this section.

4.5.1 SUMMARY OF SIGNIFICANT RESULTS

4.5.1.1 Mineralogy and petrology

Characterization of natural system mineralogy and petrology is necessary to (1) assess current and future changes in natural system composition, (2) provide input to hydrochemical models, (3) provide compositions of relevant geologic solids to be used in radionuclide transport experiments, and (4) determine intraflow structure and stratigraphic correlation. All of this information is necessary to predict the long-term performance of a repository in basalt. Geologic solids present in potential pathways to the accessible environment are characterized in this chapter. These materials include Grande Ronde Basalt, Wanapum Basalt, secondary minerals associated with these basalts, and interbed materials.

The major mineral composition of the dense interiors of the primary isolation zone (in modal %) ranges from 0% to 35% pyroxene, 25% to 48% plagioclase, 0% to 6% iron-titanium oxides, 0% to 3% olivine and 20% to 65% mesostasis. Less abundant phases include apatite, orthopyroxene, pigeonite, and sulfide blebs. The mesostasis phase is mainly composed of glass, the most reactive primary phase in the basalt.

The concentrations of most major element oxides and trace elements are relatively consistent throughout the dense interiors of the primary isolation zone. The ratio of $FeO/(FeO+Fe_2O_3)$ varies from about 0.76 to 0.79. Therefore, the rock mass is highly reduced in the flow interiors. Preliminary investigations of flow tops have identified hematite in minute blebs disseminated throughout the groundmass and as inclusions in plagioclase phenocrysts. The hematite was probably formed during the primary crystallization as suggested by its presence in basalt fragments and absence from secondary infillings.

Secondary minerals are found in fractures, vesicles, and vugs in the repository isolation system. These minerals are mainly smectite clays, zeolites, and silica. Other secondary minerals have been identified but are present in much lower amounts. The presence of secondary pyrite in these basalts provides strong evidence for reducing conditions in the natural system.

At present, little is known about the petrology of sedimentary interbeds. They consist mainly of tuffaceous siltstone with lesser amounts of quartz sandstone, conglomerate, and well-sorted vitric tuff. Most of these sediments are friable, but some are cemented with calcite, clay, opal, and zeolite.

The primary phases of the basalts are not in equilibrium with the present physicochemical environment. They are metastably persistent, however, because the kinetics of alteration are slow at the ambient low temperatures of the basalts. Most primary crystals remain unaltered or slightly altered. Most of the reported secondary phases may be in equilibrium or are metastably persistent based on geologic evidence. However, the lack of reliable thermodynamic data on secondary minerals prevents a rigorous evaluation of their stability.

Many aspects of the petrology of the controlled area study zone need further study. This is particularly true for secondary mineralogy and geochemistry and interbed mineralogy and geochemistry. Plans for these investigations are presented in detail in Section 8.3.1.2.2.5.

4.5.1.2 Groundwater geochemistry

Hydrochemical Characterization of groundwaters along potential flow paths from the repository to the accessible environment is necessary to provide appropriate compositional parameters for experimental studies on radionuclide transport and on degradation of engineered barriers components. Hydrochemical data are also used as input to hydrologic models that describe groundwater flow directions and velocities. Compositions of groundwaters in the Grande Ronde and the Frenchman Springs Member of the Wanapum Basalts are described in terms of major inorganic components, trace elements, organic components, dissolved gases and background radioactivity, and particulates and colloids.

Major inorganic components of these groundwaters are sodium (27.6 to 439 mg/L), potassium (less than 1 to 35.4 mg/L), calcium (less than 1 to 17.8 mg/L), magnesium (less than 1 to 9.6 mg/L), silicon (22 to 109 mg/L), chloride (4.3 to 508 mg/L), fluoride (less than 1 to 50 mg/L), and sulfate (less than 1 to 229 mg/L). Measured pH values range from 7.45 to 10.6 (most are in the range of 9.2 to 9.8). Alkalinity (as $CaCO_3$) ranges from 52.3 to 211 mg/L. Both vertical and lateral variations of major element compositions are observed. Concentrations of sodium, chloride, and fluoride increase with increasing depth while potassium and calcium concentrations decrease. Higher concentrations of sodium and chloride are observed in the reference repository location than outside it.

Information on the organic content of the groundwaters is limited. Analyses of total organic carbon in groundwaters from boreholes that have been extensively pumped (to eliminate drilling fluid contamination) suggest that the natural background level is less than 1 mg/L. Detailed analysis of one groundwater sample from the Grande Ronde Basalt gave a concentration of 0.34 mg/L of dissolved organic carbon. Approximately 2.5 µg/L of the organic carbon was in the form of fatty acids and phenols. The remainder of the organic carbon for this sample consisted of fulvic acids that have molecular weights in the range of 300 to 1,000. No humic acids were found. Additional information on natural organics in groundwaters must be obtained to determine their radionuclide complexing ability and to provide assurance that analyzed samples are not contaminated with organics from drilling fluids (see Section 8.3.1.4.1.3).

The major dissolved gas found in groundwaters within the reference repository location is methane. Minor amounts of nitrogen, argon, and carbon dioxide are also present. Estimates of methane concentrations range from 102 to 1,222 mg/L for groundwaters in Grande Ronde Basalt within the reference repository location. The source of the methane in this region is under investigation, but additional work must be completed to determine whether the methane is of thermocatalytic or biogenic origin. Also, measurements of dissolved gases in groundwaters outside the reference repository location are needed. Plans for these studies are given in Section 8.3.1.4.1.

Indirect information on background radioactivity in groundwaters is available from measurements of tritium, carbon-14, chlorine-36, uranium, and decay chain daughters of uranium and thorium. These data are, however, subject to errors caused by potential contamination of groundwater samples by drilling fluids. This contamination also impedes analyses of naturally occurring particulates in the groundwater. Plans to address these sampling problems are given in Section 8.3.1.4.

Geochemical modeling of groundwater-mineral equilibrium reactions has helped to determine the degree of saturation of basalt groundwaters with solid phases found in the basalt system under ambient conditions. Preliminary results of modeling several dozen spring samples and more than 100 groundwater analyses suggest that amorphous silica and allophane are at or near saturation in the shallow confined aquifers. Groundwaters from the Grande Ronde and Wanapum Basalts are generally undersaturated with these phases. Calcite and

fluorite are generally undersaturated in the shallow groundwaters but reach saturation with increasing depth. Clays and zeolites appear to be oversaturated in all the groundwaters examined, although the lack of appropriate thermodynamic data for these phases is a problem. In general, the models can only give inferences as to the equilibrium state of these groundwater-mineral systems.

4.5.1.3 Geochemical retardation

In the natural system, sorption is the most important geochemical retardation process for radionuclides dissolved in groundwater. Calculations of repository performance must include sorption parameters that describe the sorption behavior of key radionuclides. The sorption and desorption isotherms presented in Section 4.1.3.3.4 will be input to radionuclide transport models (e.g., Barney and Reed, 1985) that predict radionuclide releases to the accessible environment. These predictions will be compared to Federal regulatory performance criteria to determine the suitability of a nuclear waste repository in basalt.

Sorption of key radionuclides occurs by chemisorption and ion exchange reactions with minerals in the groundwater flow path. Actinides are strongly sorbed by each of the geologic solids studied (basalt, secondary minerals, and interbed materials), as are radionuclides that exist in solution as hydrated metal ions. Sorption of these elements can be accurately described using the Freundlich isotherm equation, which can be used to represent sorption reactions in transport models. Nonmetallic radionuclides such as ^{129}I and ^{14}C exist only as anions in solution and are not measureably sorbed. Selenium-79 is also anionic, but is sorbed significantly by a chemisorption mechanism.

Most radionuclide sorption reactions are at least partially irreversible under conditions expected in basalt groundwaters. Sorption and desorption isotherms for a given radioelement are non-single-valued and show a significant degree of sorption hysteresis. This hysteretic effect is important to radionuclide transport calculations since it can lower peak radionuclide concentrations in groundwater and delay transport.

Migration of radionuclides as particulates suspended in groundwater is not likely to be a significant transport mechanism. The porous media through which radionuclides must travel (container corrosion products, packing material, and clay-filled fractures in basalt) will have small pores and low groundwater velocities in the pores. Under these conditions, physical filtration and gravitational settling will remove colloids from suspension. To confirm these expectations, additional transport data on colloids must be obtained under conditions expected in radionuclide flow paths.

The chemical species of radionuclides in the natural system will influence their retardation behavior. Speciation, in turn, depends on the oxidation state of the radionuclide and on the presence of complexing ligands.

The preponderance of evidence indicates that conditions in the natural system are reducing. It is expected, therefore, that radionuclides will be present in lower oxidation states. For example, both neptunium(V) and technetium(VII) have been shown to be reduced by basalt to the (IV) oxidation state. Most radionuclides are less mobile (more strongly sorbed and less soluble) in reduced form. In basalt groundwaters, carbonate and hydroxyl complexes of radionuclides will predominate. The formation of carbonate complexes by neptunium and uranium has been shown to decrease sorption. Other potential ligands such as chloride, fluoride, and sulfate form much weaker complexes and are not expected to significantly affect behavior.

A large quantity of radionuclide sorption and desorption data have been obtained that can be used in performance assessment models for a repository in basalt. A wide range of experimental conditions have been examined in these measurements in an attempt to duplicate the variety of possible conditions expected in the natural system. Because of uncertainties in groundwater composition, oxidation states of some radionuclides, and composition of geologic solids in groundwater flow paths, attempts have been made to determine the sensitivity of radionuclide sorption to these parameters. As a result of these efforts, most existing sorption information was obtained at the extremes of expected conditions (oxidation states, groundwater compositions, etc.). Although this may be adequate for certain radionuclides, additional data are needed for radionuclides that are highly sensitive to these sorption parameters. Plans for collecting additional sorption data for the natural system are presented in Section 8.3.1.4.2.

4.5.1.4 Geochemical effects of waste emplacement

Emplacement of nuclear waste in a repository in deep basalt formations can potentially alter geochemical conditions in the host rock. These changes can subsequently affect the performance of the repository. Since the release and transport of radionuclides from the repository are strongly controlled by geochemical parameters, changes in these parameters due to waste emplacement must be estimated so that the long-term safety of the repository can be accurately determined. Potential effects in the natural system include alteration of minerals in the host rock, changes in the groundwater chemistry, and changes in radionuclide migration. Each of these changes is the result of an increase in temperature from ambient (the thermal pulse) due to radiogenic heating by decay of waste radionuclides.

The magnitude of the thermal pulse in the natural system depends on the distance and direction from the repository, time after waste emplacement, radionuclide inventory in the waste, and the design of the repository. The preemplacement temperature of the rock (55 °C at the repository horizon) is, of course, perturbed most strongly near the repository. However, some calculations indicate that temperatures of greater than 100 °C can be reached at a distance of 200 m (656 ft) above the repository horizon after about 3,000 yr. The thermal maximum will occur at a longer time after emplacement and at a lower temperature as distance from the repository increases.

The effect of this thermal pulse on groundwater-rock reactions in the natural system is expected to be small. The maximum temperatures expected in the natural system (52 to 186 °C) are in the low-temperature region where many geochemical reactions proceed at very slow rates. The limited data available on low temperature groundwater-basalt reactions indicate that the pH of the groundwater may be lowered slightly, that anion concentrations are essentially unchanged, and that silica concentrations increase as the temperature increases. The primary mineral alteration product of reactions at 200 °C and below is iron smectite, which also occurs naturally as an alteration product in Hanford Site basalts.

Effects of groundwater-rock reactions on radionuclide transport in the natural system is complex and depends on the chemistry of the specific radionuclide involved. For radionuclides that can be reduced by basalt (uranium(VI), neptunium(V), plutonium(V), technetium(VII), etc.) higher temperatures will generally facilitate reduction reactions and lower the mobility of the radionuclide since the lower oxidation states are more strongly sorbed. The slightly lower pH values at higher temperatures will decrease the tendency of some radionuclides (e.g. technetium(IV), neptunium(IV)) to form hydroxyl and carbonate complexes and, thus, increase their sorption on rock surfaces. Immobilization of radionuclides by incorporation into alteration phases of the rock is also expected to be more significant at the higher temperatures. Diffusion rates of radionuclides in the natural system are expected to increase at higher temperatures and may increase the mobility of some radionuclides. The magnitude of this effect for the radionuclides is not known.

Estimates of the magnitude of the thermal pulse in the natural system will be refined as more accurate data are obtained from site characterization. Thermal conductivities of waste package components, basalt flows, and interbeds will be measured more accurately as described in Section 8.3.__. Effects of groundwater flow and repository resaturation time have not been considered in current models but will be included in future models. Inhomogeneities in basalt flows and basalt formations will also be considered (see Section 8.3.___). The models will also improve as the final repository design is better understood and the types and quantities of wastes to be placed in the repository are more accurately known.

Additional measurements of temperature effects on geochemical processes must be performed to estimate effects of the thermal pulse on radionuclide transport. Low-temperature groundwater-rock reactions will be better defined (see Section 8.3.___). Effects of temperature on radionuclide sorption (Section 8.3.___), solubility (Section 8.3.___), and rates of reduction by basalt will be determined.

4.5.1.5 Natural analogs and related field tests

Studies of natural analogs can be used to substantiate laboratory evidence for geochemical processes that may affect the performance of

a nuclear waste repository. The advantage of studying natural analogs is that they represent the results of processes that have occurred over long time periods and under in situ conditions that may be difficult to duplicate in laboratory experiments. Federal regulations for repository performance require predictions of geochemical processes over thousands of years. Extrapolation of laboratory data over these long time periods can be accomplished with more confidence if natural analog information is available.

Two natural analogs have been investigated thus far: (1) native copper deposits in northern Michigan as a natural analog for evaluation of the long-term stability of copper containers in a repository in basalt and (2) field studies of existing alteration minerals in Columbia River basalts as natural analogs for evaluation of the long-term stability of alteration products of groundwater-basalt reactions.

Results of the copper analog study (Crisman and Jacobs, 1982) show that the native copper (estimated to have been deposited 500 to 800 m.y.B.P.) has remained relatively unaltered in the basalt-groundwater system in which it is found. The groundwater characteristics (near-neutral pH, reducing Eh, low dissolved solids concentration) at the Michigan site are similar to Hanford Site groundwater. This information leads to the conclusion that copper waste containers placed in a repository in Hanford Site basalt will not be corroded over the time period required for isolation of the waste.

Alteration minerals formed during hydrothermal reactions of basalts with Hanford Site groundwaters in laboratory experiments were compared with naturally occurring secondary minerals found in Hanford Site basalts. Results of this comparison suggest that the identity of alteration minerals from both sources are virtually identical. It can be assumed, therefore, that the smectite, zeolite, and iron oxyhydroxide phases produced in laboratory hydrothermal experiments will persist (stably or metastably) in the repository environment for a time period exceeding the repository lifetime. Since these minerals can potentially incorporate some radionuclides in their chemical structures, transport and release of these radionuclides will be lowered.

Additional information on basalt alteration mineral stability will be obtained by examination of basalt cores from the geothermal fields of Iceland and other similar hydrothermal systems. In the Iceland system, fresh groundwater has interacted with heated basalt to produce alteration minerals that have remained stable for thousands of years. Plans for obtaining these data are presented in Section 8.3.4.2.2.

Field studies provide large-scale estimates of geochemical parameters that are used in repository performance analysis. These estimates complement laboratory data and provide an evaluation of the effects of scale on these parameters. A groundwater tracer test has been conducted in a deep basalt flow top (McCoy Canyon). Results from this test provide limited information about sorption processes in this formation. The test consisted of a two-well recirculating design using a nonreactive tracer (SCN^-) and a reactive tracer (K^+). Analysis of tracer breakthrough curves showed that part of the potassium was sorbed by the formation and part migrated though the flow system

without any retardation. The sorption of potassium was caused by ion exchange with Na^+ on mineral surfaces. The small fraction of potassium not retarded can be explained by either slow sorption reactions compared with the time allowed for the test or by transport of potassium as particulates suspended in the groundwater. Plans for additional field testing of transport parameters are discussed in Section 8.3.1.4.

4.5.1.6 Geochemical stability

The geochemical stability of the natural system over the isolation period required by Federal regulations (10,000 yr) must be estimated because geochemical factors strongly influence radionuclide containment and release. Alteration of basalts by groundwaters to form secondary minerals is probably the most significant geochemical process that has occurred since eruption of the basalt flows (6 to 16.5 m.y.B.P.). This process has been very slow since the total volume percentage of secondary minerals now found in several flow interiors is less than 0.27%. These slow alteration reactions are expected to continue over the isolation period. No large-scale perturbations of the natural system are expected due to climate variations or intrusion by man. This is because of the inaccessibility of these deep strata and lack of natural resources in the deep basalts (see Section 3.8).

A mineralogy-petrology model will be developed that will allow reliable predictions of future geochemical environments in the basalts. Past and present geochemical conditions will be projected into the future using kinetic and thermodynamic considerations and by comparisons with geochemical analogs. Plans for development of the model are presented in Section 8.3.1.2.2.5.

4.5.2 RELATION TO DESIGN

The geochemical environment surrounding the repository has a strong influence on the design of the repository. Components of the subsurface facilities must be able to function properly in the geochemical environment of basalt formations for thousands of years. Materials chosen for repository components must be compatible with existing groundwater compositions, minerals in the basalts, and elevated temperatures due to radiogenic heating by radionuclides in the waste. Laboratory and natural analog studies of engineering materials are performed to determine the long-term stability of these materials.

In the waste package, corrosion of the waste container by Hanford Site groundwaters is an important factor in container design. The composition of these groundwaters is a critical factor in choosing a metal container that can resist corrosion and completely contain the waste for 300 to 1,000 yr. Important groundwater characteristics include oxygen concentration, cation and anion concentrations, and pH. Discussion of the effects of these factors on container corrosion is presented in Section 7.4.2.

Hydrothermal interactions among Hanford Site groundwaters, the packing material component, and the waste form component of the waste package must be considered in design. The packing material must act as a barrier to groundwater flow for thousands of years by retaining its initial low permeability. Groundwater composition will be an important factor in determining whether or not hydrothermal reactions will occur and, if they do, what reaction products will form. Studies of hydrothermal stability of candidate packing materials are discussed in Section 7.4.3. Similar considerations must be made for the backfill material placed in underground openings in the repository. Geochemical interactions of backfill with the repository environment are discussed in Section 6.3.3.6. Chemical reactions of the waste form with groundwater will partially control the release of radionuclides from the waste package. The solubility of the radionuclides will be affected by groundwater characteristics such as pH, redox conditions, and ion concentrations. These chemical interactions influence the selection of materials for each of the waste package components (see Section 7.4.4).

The chemical stability of cementitious materials used for strengthening openings in the basalt and of sealing materials for shafts and boreholes in the basalt geochemical environment is an important consideration in design. Reactions of these materials over long time periods is an important material selection criterion. Descriptions of plans for obtaining information on the long-term chemical stability of sealing materials are presented in Sections 8.3.3.1.2.1 and 8.3.3.3.1.

4.5.3 IDENTIFICATION OF INFORMATION NEEDS

This chapter is a summary of the geochemical data obtained during investigation of the Hanford Site. Additional data must be obtained during site characterization to fill gaps that exist in the current geochemical data base and to reduce uncertainties in the data so that assessment of the performance of the natural system can be made with more confidence. This section briefly identifies geochemical information needs and outlines additional studies planned to meet these information needs. These studies are presented in much greater detail in Sections 8.3.1.2.4.6, 8.3.1.2.2.5, and 8.3.4.2.2. Information needs are presented under the following subheadings:

- Mineralogy and petrology.
- Groundwater geochemistry.
- Radionuclide retardation.
- Natural analogs.
- Field tests.

Priorities regarding information needs have not yet been established, but work is in progress to determine these priorities. Prioritization must include consideration of the following: (1) importance of various kinds of information in estimating the performance of the repository; (2) scheduling, personnel, and budgetary restraints; and (3) hierarchy of studies where some studies must be completed prior to initiation of subsequent studies.

4.5.3.1 Mineralogy and petrology

The objective of mineralogy and petrology studies is to provide mineralogic and geochemical characterization of the basalt flows and interbeds in the reference repository location and surrounding region. This information is necessary to develop geochemical and hydrochemical models of basalt-groundwater systems, assess current and future changes in the natural system, determine intraflow structure and stratigraphic correlations, and identify mineral distributions that influence radionuclide transport.

Data that are required to meet these objectives are mineralogic and petrologic characterization of the following:

- o Primary minerals.
- o Secondary infilling minerals.
- o Interbeds.
- o Fault infilling minerals.
- o Pervasively altered basalt.

The characterization methods include optical or analytical identification of phases, descriptions of mineral and rock textures, modal analysis, determination of bulk chemical compositions, and determination of the chemical compositions of individual minerals.

The current data base consists mainly of analyses of dense interiors of unaltered flows. These include more than 10,000 major element analyses of whole-rock basalt, about 400 minor and trace element analyses, about 700 electron probe analyses of primary phases, and about 50 detailed modal analyses. Relatively little work has been completed on secondary infilling minerals in the basalts. The existing data on secondary minerals contain inconsistencies that must be resolved in future work. Characterization of sedimentary interbeds has also received only slight attention. Analyses of interbed samples are preliminary because they do not allow definitive, qualitative or quantitative description of some phases. No work has been done on fault infilling mineralogy or pervasively altered basalt.

Development of a mineralogy-petrology model is currently in a conceptual state. Plans for obtaining these data are presented in Section 8.3.1.4. Further model development requires more data.

4.5.3.2 Groundwater geochemistry

Characterization of groundwater geochemistry has two objectives. The first is to provide a comprehensive data base that will be used in support of conceptual hydraulic flow models. Understanding the hydrochemistry of groundwaters, the reactions controlling their composition, and evidence of groundwater age and aquifer communication can provide important constraints on a hydrologic flow model (see Chapter 3). The second objective is to estimate

geochemical conditions in groundwaters that can affect repository performance and radionuclide transport. Groundwater parameters such as pH, redox potential, and chemical composition are important in determining the mobility of waste radionuclides.

Data that are required to meet these objectives are as follows:

- o Major and trace inorganic components of groundwater.
- o Concentration and identification of dissolved organic components.
- o Dissolved gases.
- o Stable and radioactive isotopes.
- o Redox conditions, pH.
- o Geochemical models.
- o Temperature.

The current hydrochemical data base contains the results of nearly 500 chemical analyses of groundwaters sampled from boreholes on the Hanford Site. In general, the quantity of data decreases with increasing depth and gaps in the areal distribution of the data exist. Major inorganic components of the groundwater have been routinely determined; however, the data base for organic components, dissolved gases, and radioactive isotopes is more limited.

An alternative approach to determining in situ groundwater redox conditions, in addition to platinum electrode measurements, is needed. A more reliable method is measurement of relative quantities of naturally occurring dissolved redox couples. By studying a variety of redox couples, it will be possible to determine if they are in equilibrium (i.e., if calculated Eh values for different couples converge to a narrow range). Promising naturally occurring redox couples include HS^-/SO_4^{2-}, iron(II)/iron(III), arsenic(III)/arsenic(V), uranium(IV)/uranium(VI), and HSe^-/SeO_3^{2-}.

Improved methods for groundwater sampling and analysis are also needed. Downhole sampling equipment and procedures must be developed to prevent contamination of samples and loss of dissolved gases caused by pumping the sample to the top of the borehole. Analyses of groundwaters from boreholes drilled without drilling fluid (e.g., boreholes drilled using air-mist techniques) must be performed so that the groundwater samples are not contaminated. In addition, more accurate analytical techniques must be developed for analysis of dissolved gases, organics, isotopic ratios, and minute quantities of various redox species. Because of the fragile nature of groundwater samples, some analyses (pH, alkalinity, dissolved oxygen, etc.) must be performed at the borehole site in a mobile laboratory.

4.5.3.3 Radionuclide retardation

The objective of radionuclide retardation studies is to quantify the retardation characteristics of expected groundwater flow paths between the repository and the accessible environment. Laboratory measurements of

radionuclide retardation must attempt to duplicate as closely as possible the geochemical conditions present in the flow paths. Retardation parameters for each key radionuclide obtained from these measurements are used in transport models that evaluate the ability of the natural system to isolate waste radionuclides.

Laboratory-scale radionuclide retardation data needed to meet the above objective are as follows:

- Sorption and desorption coefficients and isotherms for key radionuclides.
- Kinetics of sorption and desorption reactions.
- Elution and breakthrough curves for flowthrough experiments.
- Effects of solid type on sorption parameters.
- Effects of groundwater composition on sorption parameters.

Data needs from field-scale retardation studies are described in Section 4.5.3.5.

The current radionuclide retardation data base consists of results from thousands of batch sorption and desorption measurements for a wide range of groundwater compositions but is limited to a small number of geologic solid types that are relevant to retardation in the natural system. Additional sorption studies using solids from major flow zones in the Wanapum and Grande Ronde Basalts are required (mainly flow-top samples). Very little data from flowthrough sorption measurements are available. Flowthrough experiments will more closely simulate field conditions and will provide confirmation for batch sorption and desorption experiments.

Improved methods for preparation of samples of geologic solids will be developed. The effects of crushing core samples of flow-top materials on sorption results will be examined. Composite reference flow-top samples from Cohassett, Rocky Coulee, and Umtanum flows and Wanapum Basalt samples will be prepared from core samples.

4.5.3.4 Natural analogs

Studies of natural analogs will provide qualitative information on geochemical processes that can affect waste isolation. Results from these studies will be used in concert with laboratory tests and repository performance models to help evaluate the long-term geochemical stability of the natural and engineered barriers systems. Since laboratory measurements are limited to short time durations (several years at most), compared to the

length of time that a repository must continue to function (10,000 yr or more), natural geologic settings where geologic processes have evolved for long periods of time can yield information on the stability of repository materials. The natural geologic conditions must, of course, simulate repository conditions as closely as possible.

Two natural analog studies are planned. The first is investigation of the secondary mineralogy present in naturally altered basalts at two different locations--the geothermal fields of Iceland and the Columbia River basalts. The second is investigation of the stability of bentonite in the hydrothermal environment of a site yet to be determined. Both of these studies will help verify the results of short-term laboratory hydrothermal experiments in which groundwater is reacted with basalts and packing materials containing bentonite. The physicochemical behavior of these materials in the natural environment will be compared to those of the laboratory experiments.

One natural analog study has been completed thus far. The native copper deposits in northern Michigan were used to evaluate the long-term stability of copper containers in a repository in basalt.

4.5.3.5 Field test

Field-scale tests of radionuclide retardation, while not comprehensive and almost totally empirical in nature, can provide retardation estimates at the scale required in performance assessment calculations and under conditions that are close to ambient conditions in likely groundwater flow paths.

No field tests of reactive tracers have yet been performed. Planned tests include measurements of the following retardation parameters:

- Retardation factors as determined in field tracer tests and inferred from natural radionuclide concentrations.
- Natural particulate concentrations and characteristics.

The laboratory studies described in Section 4.5.3.3 and the field tests will be conducted in an iterative manner with feedback between. This will assure that each type of test will be conducted in a manner that yields the maximum amount of information.

Measurements of retardation factors from field-scale tests involve the introduction of a reactive tracer into an established flow regime and monitoring its arrival at a known distance from the injection point. This information allows determination of the retardation behavior of the tracer in that flow path. Particulate transport in flow paths will be studied using similar methods. Development of the techniques required for these tests are summarized in Section 8.3.1.4.3.3.1.

Calculation of retardation factors by measuring distributions of naturally occurring radionuclides (e.g., decay series for ^{238}U and ^{232}Th) may yield in situ values on a time scale that is comparable to residence times of the radionuclides in the flow system. The validity of this method will be explored as described in Section 8.3.1.4.3.3.1.

4.5.4 RELATION TO REGULATORY GUIDE 4.17

The content of this chapter follows the annotated outline for site characterization plans developed by the DOE from Regulatory Guide 4.17 (NRC, 1983). The most significant change from Regulatory Guide 4.17 (NRC, 1983) is that the information requested on chemical interactions between the waste package and the emplacement environment has been moved from Chapter 4 to Chapter 7. This allows a more cohesive presentation in Chapter 7 for support of the waste package design program. Other minor changes involve reorganization of the material and expansion of several topics.

4.6 REFERENCES

Aagaard, P. and H. C. Helgeson, 1982. "Thermodynamic and Kinetic Constraints on Reaction Rates Among Minerals and Aqueous Solutions, I. Theoretical Considerations," American Journal of Science, Vol. 282, pp. 237-285. [MF 2000; V; C-1; HC]

Allard, B., 1982. "Solubilities of Actinides in Neutral or Basic Solutions," N. M. Edelstein (ed.), Actinides in Perspective, Pergamon Press Inc., Elmsford, New York, pp. 553-580. [MF 1202; V; C-6; HC]

Allard, B., B. Torstenfelt, and K. Andersson, 1981. "Sorption Studies of $H^{14}CO_3^-$ on Some Geologic Media and Concrete," Procedings of American Chemical Society Meeting, San Francisco. [MF 347; V; C-6; HC]

Allen, C. C., R. B. Kasper, D. L. Lane, R. G. Johnston, and S. A. Rawson, 1985. Experimental Approaches to Determining the Extent of Equilibrium in a Basaltic Hydrothermal System, RHO-BW-SA-436 P, Rockwell Hanford Operations, Richland, Washington. [MF 3703; NV; C-N; NHC]

Allen, C. C., and M. B. Strope, 1983. Microcharacterization of Basalt--Considerations for a Nuclear Waste Repository, RHO-BW-SA-294 P, Rockwell Hanford Operations, Richland, Washington. [MF 2357; NV; C-N; NHC]

Altenhofen, M. K., 1981. Waste Package Heat Transfer Analysis: Model Development and Temperature Estimates for Waste Packages in a Repository Located in Basalt, RSD-BWI-ST-18, Rockwell Hanford Operations, Richland, Washington. [MF 0702; NV; C-N; NHC]

Aly, M. I., N. Bakry, F. Kishk, and A. H. El-Sebae, 1980. "Carbaryl Adsorption on Calcium-Bentonite and Soils," Soil Science Society of America Journal, Vol. 44, pp. 1213-15. [MF 3465; NV; C-99; NHC]

Ames, L. L., 1980. Hanford Basalt Flow Mineralogy, PNL-2847, Pacific Northwest Laboratory, Richland, Washington. [MF 2006; V; C-N; HC]

Ames, L. L., and J. E. McGarrah, 1980a. Basalt Radionuclide Distribution Coefficient Determinations FY 1979 Annual Report, PNL-3146, Pacific Northwest Laboratory, Richland, Washington. [MF 2008; V; C-N; HC]

Ames, L. L., and J. E. McGarrah, 1980b. Investigation of Basalt-Radionuclide Distribution Coefficients: Fiscal Year 1980 Annual Report, RHO-BWI-C-108/PNL-3462, Pacific Northwest Laboratory for Rockwell Hanford Operations, Richland, Washington. [MF 0500; V; C-N; HC]

Ames, L. L., and J. E. McGarrah, 1980c. High-Temperature Determination of Radionuclide Distribution Coefficients for Columbia River Basalts, RHO-BWI-C-111/PNL-3250, Pacific Northwest Laboratory for Rockwell Hanford Operations, Richland, Washington. [MF 0501; V; C-N; HC]

Ames, L. L., J. E. McGarrah, and B. A. Walker, 1981. Basalt-Radionuclide Reactions: FY-1981 Annual Report, RHO-BWI-CR-127 P/PNL-3992, Pacific Northwest Laboratory for Rockwell Hanford Operations, Richland, Washington. [MF 3497; NV; C-N; NHC]

Ames, L. L., J. E. McGarrah, M. J. Smith, and B. A. Walker, 1984. Transport of Radionuclides by Bentonite and Silica Colloids in a GR-3 Synthetic Groundwater--Interim Report, SD-BWI-TI-182, Rockwell Hanford Operations, Richland, Washington. [MF 0400; V; C-N; HC]

Anderson, D. M., and R. C. Reynolds, 1966. "Umiat bentonite: An unusual montmorillonite from Umiat, Alaska," The American Mineralogist, Vol. 51, pp. 1443-1456. [MF 1678; V; C-38; HC]

Anderson, K., B. Torstenfelt, and B. Allard, 1982. "Sorption Behavior of Long-Lived Radionuclides in Igneous Rock," Environmental Migration of Long-Lived Radionuclides of International Symposium, 1981, IAEA-SM-257/20, pp. 111-131. [MF 3473; NV: C-___; NHC]

Andrews, A. J., 1980. "Saponite and celadonite in layer 2 Basalts, DSDP Leg 37," Contributions to Mineralogy and Petrology, Vol. 73, pp. 323-340. [MF 1679; V; C-16; HC]

Aoyagi, K., and T. Kazama, 1980. "Transformational changes of clay minerals, zeolites and silica minerals during diagenesis," Sedimentology, Vol. 27, pp. 179-188. [MF 1680; NV; C-6; NHC]

Åpps, J. A., C. L. Carnahan, P. C. Lichter, M. L. Michel, P. Perry, R. J. Silva, O. Weres, and A. F. White, 1982. Status of Geochemical Problems Relating to the Burial of High-Level Radioactive Waste, 1982, LBL-15103, Lawrence Berkeley Laboratory, Berkeley, California. [MF 0201; V; C-N; HC]

Apted, M. J., 1983. Laboratory and Field Data Needs for Site-Specific Repository Modeling, RHO-BW-SA-321 P, Rockwell Hanford Operations, Richland, Washington. [MF 0503; V; C-N; HC]

Apted, M. J., and J. Myers, 1982. Comparison of the Hydrothermal Stability of Simulated Spent Fuel and Borosilicate Glass in a Basaltic Environment, RHO-BW-ST-38 P, Rockwell Hanford Operations, Richland, Washington. [MF 2014; NV; C-N; NHC]

Arnorsson, S., K. Gronvold, and S. Sigurdsson, 1978. "Aquifer Chemistry of Four High-Temperature Geothermal Systems in Iceland," Geochimica et Cosmochimica Acta, Vol. 42, pp. 523-536. [MF 3478; ___; C-6; ___]

Arnorsson, S., S. Sigurdsson, and H. Svavarsson, 1982. "The Chemistry of Geothermal Waters in Iceland, I. Calculation of Aqueous Speciation from 0 to 370 °C," Geochimica et Cosmochimica Acta, Vol. 46, pp. 1513-1532. [MF 0505; V; C-6; HC]

Barnes, R. B., 1975. "The Determination of Specific Forms of Aluminum in Natural Water," Chemical Geology, Vol. 15, pp. 177-191. [MF 2025; V; C-17; HC]

Barney, G. S. and D. T. Reed, 1985. Effects of Sorption Hysteresis on Radionuclide Releases from Waste Packages, RHO-BW-SA-508 P, Rockwell Hanford Operations, Richland, Washington. [MF 3400; NV; C-N; NHC]

Barney, G. S., 1981a. Radionuclide Reactions with Groundwater and Basalts from Columbia River Basalt Formations, RHO-SA-217, Rockwell Hanford Operations, Richland, Washington. [MF 0013; V; C-N; HC]

Barney, G. S., 1981b. Evaluation of Methods for Measurement of Radionuclide Distribution in Groundwater/Rock Systems, RHO-BWI-LD-47, Rockwell Hanford Operations, Richland, Washington. [MF 0508; V; C-N; HC]

Barney, G. S., 1982. FY 1981 Annual Report--Radionuclide Sorption on Basalt Interbed Materials, RHO-BW-ST-35 P, Rockwell Hanford Operations, Richland, Washington. [MF 2026; V; C-N; HC]

Barney, G. S., 1983. Radionuclide Sorption and Desorption Reactions with Interbed Materials from the Columbia River Basalt Formation, RHO-BW-SA-291 P, Rockwell Hanford Operations, Richland, Washington. [MF 2027; V; C-N; HC]

Barney, G. S., 1984. "Radionuclide Sorption and Desorption Reactions with Interbed Materials from the Columbia River Basalt Formation," G. S. Barney, J. D. Navratil, and W. W. Schulz (eds.), Geochemical Behavior of Disposed Radioactive Waste, American Chemical Society Symposium Series 246, Washington, D.C. [MF 0509; V; C-22; HC]

Barney, G. S., and G. E. Brown, 1979. "The Kinetics and Reversibility of Radionuclide Sorption Reaction with Rocks--Progress Report for Fiscal Year 1979," J. F. Relyea (ed.), Waste Isolation Safety Assessment Program, Task 4, Third Contractor Information Meeting, CONF-7910160, Vol. II, PNL-SA-8571, Pacific Northwest Laboratory, Richland, Washington. [MF 0510; V; C-N; HC]

Barney, G. S., L. L. Ames, J. E. McGarrah, and B. A. Walker, 1983. Radionuclide Sorption Kinetics and Column Sorption Studies with Columbia River Basalts, SD-BWI-TI-168, Rockwell Hanford Operations, Richland, Washington. [MF 0401; V; C-N; HC]

Barney, G. S., D. L. Lane, C. C. Allen, and T. E. Jones, 1985. Sorption and Desorption Reactions of Radionuclides with a Crushed Basalt-Bentonite Packing Material, RHO-BW-SA-416 P, Rockwell Hanford Operations, Richland, Washington. [MF 1709; NV; C-N; NHC]

Bear, J., 1972. Dynamics of Fluids in Porous Media, Elsevier Science Publishing Co., Inc., New York, New York. [MF 3479; ___; C-17; ___]

Beeson, M. H., K. R. Fecht, S. P. Reidel, and T. L. Tolan, 1985. "Regional Correlations within the Frenchman Springs Member of the Columbia River Basalt Group: New Insights into the Middle Miocene Techtonics of Northwest Oregon," Oregon Geology, Vol. 47, pp. 87-96. [MF 1713; NV; C-N; NHC]

Benson, L. V., and L. S. Teague, 1979. A Study of Rock-Water-Nuclear Waste Interactions in the Pasco Basin, Washington, LBL-9677, Lawrence Berkeley Laboratory, Berkeley, California. [MF 0512; NV; C-N; NHC]

Benson, L. V., and L. S. Teague, 1982. "Diagenesis of Basalts from the Pasco Basin, Washington - I. Distribution and Composition of Secondary Mineral Phases," Journal of Sedimentary Petrology, Vol. 52, No. 2, pp. 595-613. [MF 0016; V; C-44; HC]

Benson, L. V., C. L. Carnahan, J. A. Apps, C. A. Mouton, D. J. Corrigan, C. J. Frisch, and L. K. Shomura, 1978. Basalt Alteration and Basalt-Waste Interaction in the Pasco Basin of Washington State, LBL-8532, Lawrence Berkeley Laboratory, Berkeley, California. [MF 0511; V; C-N; HC]

Benzing, W. C., J. B. Conn, J. V. Magee, and E. J. Sheehan, 1958. "Synthesis of Selenides and Tellurides. I. The Reduction of Selenites by Hydrazine," American Chemical Society Journal, Vol. 80, pp. 2657-59. [MF 1716; NV; C-22; NHC]

Berner, R. A., 1971. Principles of Chemical Sedimentology, McGraw-Hill Book Company, New York, New York, pp. 202-208. [MF 1681; V; C-59; HC]

Berner, R. A., 1978. "Rate Control of Mineral Dissolution under Earth Surface Conditions," American Journal of Science, Vol. 278, pp. 1235-1252. [MF 0513; V; C-1; HC]

Bish, D. L., 1984. "Effects of exchangeable cation composition on the thermal expansion/contraction of clinoptilolite," Clays and Clay Minerals, Vol. 32, No. 6, pp. 444-451. [MF 1682; V; C-65; HC]

Bish, D. L., D. T. Vaniman, F. M. Byers, Jr., and B. E. Broxton, 1982. Summary of the Mineralogy--Petrology of Tuffs of Yucca Mountain and the Secondary-Phase Thermal Stability in Tuffs, LA-19321-MS, Los Alamos National Laboratory, Los Alamos, New Mexico. [MF 3480; ___; C-N; ___]

Boles, J. R., 1972. "Composition, optical properties, cell dimensions, and thermal stability of some heulandite group zeolites," Amer. Miner., Vol. 57, pp. 1463-1493.

Boles, J. R., 1981. "Zeolites in low-grade metamorphic rocks," F. A. Mumpton (ed.), "Mineralogy and geology of natural zeolites," Mineralogical Society of America Reviews in Mineralogy, Vol. 4, pp. 103-135. [MF 2051; V; C-38; HC]

Borchardt, G. A., 1977. "Montmorillonite and other smectite minerals," m J. B. Dixon, and S. B. Weed (eds.), "Minerals in Soil Environments," Soil Science Society of America, Madison, Wisconsin, pp. 293-330. [MF 1895; NV; C-99; NHC]

Breck, W. G., 1971. "Redox Potentials by Equilibration," Journal of Marine Research, Vol. 30, pp. 121-139. [MF 0518; V; C-14; HC]

Brigatti, M. F., 1982. "Hissingerite: A review of its crystal chemistry," H. Van Olphen, and F. Veniale (eds.), Developments in Sedimentology, 35, International Clay Conference 1981, Proceedings of the VII International Clay Conference, Bologna and Parris, Italy, September 6-12, pp. 97-110. [MF 2065; V; C-17; HC]

Brindley, G. W., 1980. "Order-disorder in clay mineral structures," G. W. Brindley, and G. Brown (eds.), "Crystal structures of clay minerals and their x-ray identification," Mineralogical Society Monograph No. 5, Mineralogical Society, London, England, pp. 125-195. [MF 2066; NV; C-__; NHC]

Brown, P. R. L., and A. J. Ellis, 1970. The Ohaki-Broadlands hydrothermal area, New Zealand; mineralogy and related geochemistry," American Journal of Science, Vol. 269, pp. 97-131. [MF 1683; NV; C-1; NHC]

Burnham, C. W., 1979. "The importance of volatile constituents," H. S. Yoder, Jr. (ed.), The evolution of the Igneous Rocks: Fiftieth Anniversity Perspectives, Princeton University Press, Princeton, New Jersey, pp. 437-482. [MF 1684; NV; C-75; NHC]

Carmichael, I. S. E., F. J. Turner, and J. Verhoogen, 1974. Igneous Petrology, McGraw-Hill Book Company, New York, New York, p. 739. [MF 2077; NV; C-59; NHC]

Chen, Chao-Hsia, 1975. "A method of Estimation of Standard Free Energies of Formation of Silicate Minerals at 298.15 °K," American Journal of Science, Vol 275, pp. 801-817. [MF 1685; NV; C-1; NHC]

Clark, S. P., Jr., 1966. "Composition of Rocks," S. P. Clark, Jr. (ed.), Handbook of Physical Constants, Geological Society of America Memoir 97, pp. 1-5. [MF 2082; NV; C-13; NHC]

Clifton, P. M., 1986. Groundwater Travel Time Analysis for the Reference Repository Location at the Hanford Site, SD-BWI-TI-303, Rockwell Hanford Operations, Richland, Washington. [MF 3481; ___; C-N; ___]

Corwin, D. L., and W. J. Farmer, 1984. "Nonsingle-Valued Adsorption-Desorption of Bromacil and Diquast by Freshwater Sediments," American Chemical Society, Environmental Science and Technology, Vol. 18, pp. 507-514. [MF 3405; V; C-22; HC]

Cremer, M., H. N. Elsheimer, and E. E. Escher, 1972. "Microcoulometric Measurement of H_2O in Minerals," Analytical Chimica Acta, Vol. 60, pp. 183-192. [MF 2093; V; C-17; HC]

Crisman, D. P., and G. K. Jacobs, 1982. Native Copper Deposits of the Portage Lake Volcanics, Michigan: Their Implications with Respect to Canister Stability for Nuclear Waste Isolation in the Columbia River Basalts Beneath the Hanford Site, Washington, RHO-BW-ST-26 P, Rockwell Hanford Operations, Richland, Washington. [MF 2094; V; C-N; HC]

Cross, R. W., 1983. Deep borehole stratigraphic correlation charts and structure cross sections, SD-BWI-DP-035, Rockwell Hanford Operations, Richland, Washington, p. 142. [MF 0407; V; C-N; HC]

Davis, J. A., R. O. James, and J. O. Leckie, 1978. "Surface Ionization and Complexation at the Oxide/Water Interface," Journal of Colloid Interface Science, Vol. 63, p. 480. [MF 3482; NV; C-N; NHC]

Deer, W. A., R. A. Howie, and J. Zussman, 1966. An Introduction the Rock-forming Minerals. Longman Group Limited, London, England, p. 180. [MF 1687; V; C-__; HC]

Deere et al., 1963. Table 4.1-18.

Deutsch, W. J., E. A. Jenne, and K. M. Krupka, 1980. "Solid Phases Limiting the Concentration of Dissolved Constituents in Basalt Aquifers of the Columbia Plateau in Eastern Washington," Proceedings of the 1981 National Waste Terminal Storage Program Information Meeting, DOE/NWTS-15, U.S. Department of Energy, Washington, D.C., pp. 245-247. [MF 3467; V; C-N; HC]

Deutsch, W. J., E. A. Jenne, and K. M. Krupka, 1982a. Computed Solid Phases Limiting the Concentration of Dissolved Constituents in Basalt Aquifers of the Columbia Plateau in Eastern Washington, PNL-4089, Pacific Northwest Laboratory, Richland, Washington. [MF 2106; V; C-N; HC]

Deutsch, W. J., E. A. Jenne, and K. M. Krupka, 1982b. "Solubility Equilibria in Basalt Aquifers: The Columbia Plateau, Eastern Washington, U.S.A.," Chemical Geology, Vol. 36, pp. 15-34. [MF 0832; V; C-17; HC]

Di Toro, D. M., and L. M. Horzempa, 1982. "Reversible and Resistant Components of PCB Adsorption-Desorption: Isotherms," American Chemical Society Environmental Science and Technology, Vol. 16, pp. 594-602. [MF 2112; V; C-22; HC]

Dibble, W. E., Jr., and W. A. Tiller, 1981. "Kinetic model of zeolite paragenesis in tuffaceous sediment," Clays and Clay Minerals, Vol. 29, pp. 323-330. [MF 0712; V; C-65; HC]

Diediker, L. D., 1983. Borehole DC-16A Report, SD-BWI-TI-135, Rockwell Hanford Operations, Richland, Washington. [MF 0409; V; C-N; HC]

Dill, J. A., T. E. Jones, A. D. Marcy, M. O. Boechler, and J. R. Payne, 1984. An Evaluation of the Stability of Synthetic Groundwater Formulations GR-3 and GR-4, SD-BW-TD-013, Rev. 03, Rockwell Hanford Operations, Richland, Washington. [MF 3400; V; C-N; HC]

Dill, J. A., T. E. Jones, A. D. Marcy, and M. H. West, 1986. Limitations in Determining Redox Chemistry in Basalt Groundwaters at the Hanford Site, RHO-BW-ST-76 P, Rockwell Hanford Operations, Richland, Washington. [MF 2110; NV; C-N; HC]

Donner, H. E., and W. C. Lynn, 1977. "Carbonate, halide, sulfate, and sulfide minerals," m J. B. Dixon, and S. B. Weed (eds.), Minerals in Soil Environments, Soil Science Society of America, Madison, Wisconsin, pp. 75-98. [MF 1689; NV; C-99; NHC]

DOE, 1982. Site Characterization Report for the Basalt Waste Isolation Project, DOE/RL 82-3, U.S. Department of Energy, Washington, D.C. [MF 2119; ___; C-N; ___]

DOE, 1984. "General Guidelines for the Recommendation of Sites for the Nuclear Waste Repositories; Final Siting Guidelines," Title 10 Code of Federal Regulations, Part 960, Federal Register, Vol. 49, No. 236, pp. 47714-47770.

DOE, 1985a. Annotated Outline for Site Characterization Plans, OGR/B-5, U.S. Department of Energy, Washington, D.C.

DOE, 1985b. Mission Plan for the Civilian Radioactive Waste Management Program, DOE/RW-0005, U.S. Department of Energy, Washington, D.C. [MF ___; ___; C-N; ___]

Drever, J. I., 1982. The Geochemistry of Natural Waters, Prentice-Hall, Inc., Englewood Cliffs, New Jersey. [MF 2131; V; C-60; HC]

Drewes, D. R., 1983. EHPH Users Guide, RHO-BW-ST-62 P, Rockwell Hanford Operations, Richland, Washington. [MF 2131; V; C-N; HC]

Early, T. O., 1986. Concentrations of Dissolved Methane (CH_4) and Nitrogen (N_2) in Groundwaters from the Hanford Site, Washington, SD-BWI-TI-296, Rev. 0, Rockwell Hanford Operations, Richland, Washington. [MF 3409; NV; C-N; NHC]

Early, T. O., C. C. Allen, and W. J. Anderson, 1983. "Characteristics of the Waste Package Environment Expected in a Repository Located in the Rocky Coulee, Cohassett, McCoy Canyon, or Umtanum Flows," P. E. Long (ed.), Repository Horizon Identification Report, Vol. I; Comparative Evaluation of Candidate Repository Horizons within the Reference Repository Location, SD-BWI-TY-001, Rev. 0-0, Rockwell Hanford Operations, Richland, Washington, pp. I-143 to I-207. [MF 2136; NV; C-N; NHC]

Early, T. O., J. Myers, and E. A. Jenne, 1984a. "Applications of Geochemical Modeling to High-Level Nuclear Waste Disposal at the Hanford Site, Washington," G. K. Jacobs and S. K. Whatley (eds.), Proceedings of the Conference on the Application of Geochemical Models to High-Level Nuclear Waste Repository Assessment, October 2-5, NUREG/CP-0062, ORNL/TM-9585, Oak Ridge, Tennessee, pp. 104-108. [MF 3413; V; C-N; HC]

Early, T. O., G. K. Jacobs, and D. R. Drewes, 1984b. "Geochemical Controls on Radionuclide Releases from a Nuclear Waste Repository in Basalt, Estimated Solubilities for Selected Elements," G. S. Barney, J. D. Navratil, and W. W. Schulz (eds.), Geochemcial Behavior of Disposed Radionuclide Waste, American Chemical Society Symposium Series 246, Washington, D.C. [MF 1336; V; C-22; HC]

Early, T. O., M. D. Mitchell, and G. D. Spice, 1986. A Hydrochemical Data Base for the Hanford Site, Washington, SD-BWI-DP-061, Rev. 1, Rockwell Hanford Operations, Richland, Washington. [MF 3411; V; C-N; HC]

Eberl, D., G. Whitney, and H. Khoury, 1978. "Hydrothermal reactivity of smectite," American Mineralogist, Vol. 63, pp. 401-409. [MF 1342; V; C-38; HC]

Eichholz, G. G., 1979. "Subsurface Migration of Radioactive Waste Materials by Particulate Transport," Annual Progress Report 1978-79, School of Nuclear Engineering, Georgia Institute of Technology, Atlanta, Georgia. [MF 2146; V; C-62; HC]

Elders, W. A., J. R. Hoagland, and A. E. Williams, 1981. "Distribution of hydrothermal mineral zones in the Cerro Prieto geothermal field of Baja California, Mexico," Geothermics, Vol. 10, pp. 245-253. [MF 1670; NV; C-6; NHC]

Elrashidi, M. A., and G. A. O'Connor, 1982. "Boron Sorption and Desorption in Soils," Soil Science Society of America Journal, Vol. 46, pp. 27-31. [MF 3414; V; C-99; HC]

EPA, 1985. "Environmental Protection Agency, 40 CFR Part 191, Environmental Standards for the Measurement and Disposal of Spent Nuclear Fuel, High-Level and Transuranic Radioactive Wastes," Federal Register, Vol. 50, No. 182, pp. 38066-38089. [MF 1906; V; C-N; HC]

Felmy, A. R., S. M. Brown, Y. Onishi, S. B. Yabusaki, and R. S. Argo, 1984a. MEXAMS--The Metals Exposure Analysis Modeling System, EPA-600/3-84-031, Pacific Northwest Laboratory for the U.S. Environmental Protection Agency, Washington, D.C. [MF 3415; NV; C-N; NHC]

Felmy, A. R., D. C. Girvin, and E. A. Jenne, 1984b. "MINTEQ--A Computer Program for Calculating Aqueous Geochemical Equilibria. EPA-600/3-84-032, Report to U.S. Environmental Protection Acency by Pacific Northwest Laboratories. [MF 3416; NV; C-N; NHC]

Gardner, J. N., M. G. Snow, and K. R. Fecht, 1981. Geology of the Wallula Gap Area, Washington, RHO-BWI-LD-9, Rockwell Hanford Operations, Richland, Washington. [MF 2181; V; C-N; HC]

Garnier, J. M., 1985, "Retardation of Dissolved Radiocarbon Through a Carbonated Matrix," Geochimica et Cosmochimica Acta, Vol. 49, pp. 683-693. [MF 3474; V; C-6; HC]

Garrels, R. M., and C. L. Christ, 1965. Solutions, Minerals, and Equilibria, Cooper Freeman and Company, San Francisco, California. [MF 2183; V; C-5; HC]

Gephart, R. E., 1983. "Geohydrology," P. E. Long (ed.), Repository Horizon Identification Report, Vol. I; Comparative Evaluation of Candidate Repository Horizons within the Reference Repository Location, SD-BWI-TY-001 Rev. 0-0, Rockwell Hanford Operations, Richland, Washington, pp. I-208 to I-226. [MF 2186; NV; C-N; NHC]

Gephart, R. E., R. C. Arnett, R. G. Baca, L. S. Leonhart, and F. A. Spane, Jr., 1979. Hydrologic Studies within the Columbia Plateau, Washington: An Integration of Current Knowledge, RHO-BWI-ST-5, Rockwell Hanford Operations, Richland, Washington. [MF 0041; V; C-N; HC]

Goles, G. G., 1977. "Instrumental Methods of Neutron Activation Analysis," Zussman et al. (eds.), Determinative Methods in Physical Mineralogy, John Wiley and Sons, pp. 343-369. [MF 2191; NV; C-24; NHC]

Gottardi, G., and E. Galli, 1985. Natural Zeolites, Springer-Verlag, Inc., New York, p. 409. [MF 3483; ___; C-16; ___]

Graham, D. L., R. W. Bryce, and D. J. Halko, 1985. A Field Test to Assess the Effects of Drilling Fluids on Groundwater Chemistry Collected from Columbia River Basalts, RHO-BW-SA-370 P, Rockwell Hanford Operations, Richland, Washington. [MF 1767; V; C-N; HC]

Grisak, G. E., G. M. Thompson, K. Stetzenbach, and R. M. Smith, 1984. Field Sorption Testing: The Basalt Waste Isolation Project Position, SD-BWI-CR-021 Rev. 03, Rockwell Hanford Operations, Richland, Washington. [MF 1692; V; C-N; HC]

Halko, D. J., 1984. Chemical Analysis of Drilling Fluid and Drilling Fluid Additives used in a Cleanup Test in Borehole DC-14, SD-BWI-TD-012, Rockwell Hanford Operations, Richland, Washington. [MF 2205; V; C-N; HC]

Hawkins, D. B., R. A. Sheppard, and A. J. Gude, 3rd, 1978. "Hydrothermal synthesis of clinoptilolite and comments on the assemblage phillipsite-clinoptilolite-mordenite," L. B. Sand, and F. A. Mumpton (eds.), Natural Zeolites: Occurrence, Properties, Use, Pergamon Press, Oxford, England, pp. 337-343. [MF 2221; V; C-6; HC]

Hay, R. L. and R. A. Sheppard, 1981. "Zeolites in Open Hydrologic Systems," F. A. Mumpton, (ed.), Mineralogy and Geology of Natural Zeolites, Reviews in Mineralogy, Vol. 4, Mineralogical Society of America, Bookcrafters, Inc., Chelsea, Michigan, pp. 93-102. [MF 1693; V; C-38; HC]

Hearn, P. P. and W. C. Steinkampf, 1984. Chemical Evolution of Groundwater in Basalt Aquifers of the Columbia River Plateau, Washington State, Abstracts with Programs, Geological Society of America, 97th Annual Meeting, Reno, Nevada, p. 536. [MF 3476; NV; C-___; NHC]

Helgeson, G. C., J. M. Delany, H. W. Nesbitt, and D. K. Bird, 1978. "Summary and Critique of the Thermodynamic Properties of Rock-Forming Materials," American Journal of Science, Vol. 278-A, p. 229.

Hoffman, J., and J. Hower, 1979. "Clay mineral assemblages as low grade metamorphic geothermometers: Application to the trust faulted disturbed belt of Montana, U. S. A.," P. A. Scholle, and P. R. Schluger (eds.), Aspects of Diagenesis, Society of Economic Paleontologists and Mineralogists Special Publication, No. 26, pp. 55-79. [MF 2233; NV; C-44; NHC]

Holden, G. S., and P. R. Hooper, 1976. "Petrology and chemistry of a Columbia River basalt section, Rocky Canyon, west-central Idaho," Geological Society of America Bulletin, Vol. 87, pp. 215-225. [MF 1914; V; C-13; HC]

Holdren, G. R., Jr., and R. A. Berner, 1979. "Mechanism of Feldspar Weathering I. Experimental Studies," Geochimica et Cosmochimica Acta, Vol. 43, pp. 1161-1171. [MF 2234; V; C-6; HC]

Horton, D. G., 1985. Status Report on Secondary Minerals in Rocky Coulee and Cohassett Flow Tops, SD-BWI-TI-302 Rev. 0-0, Rockwell Hanford Operations, Richland, Washington. [MF 3420; V; C-N; HC]

Hostettler, J. D., 1984. "Electrode, Electrons, Aqueous Electrons, and Redox Potentials in Natural Waters," American Journal of Science, Vol. 284, p. 731. [MF 3421; NV; C-1; NHC]

Hsi, C. K. D., and D. Langmuir, 1985. "Adsorption of Uranyl onto Ferric Oxyhydroxides: Application of the Surface Complexation Site-Binding Model," Geochimica et Cosmochimica Acta, Vol. 49, pp. 1931-1941. [MF 3484; ___; C-6; ___]

Isaacson, P. J., and C. R. Frink, 1984. "Nonreversible Sorption of Phenolic Compounds by Sediment Fractions: The Role of Sediment Organic Matter," American Chemical Society, Environmental Science and Technology, Vol. 18, pp. 43-48. [MF 3422; V; C-22; HC]

Jantzen, C. M., 1983. Methods of Simulating Low Redox Potential (Eh) for a Basalt Repository, DP-MS-83-59X, Savannah River Laboratory, Aiken, South Carolina. [MF 2255; NV; C-N; NHC]

Jantzen, C. M., and G. G. Wicks, 1985. "Control of Oxidation Potential for Basalt Repository Simulation Tests," C. M. Jantzen, J. A. Stone, and R. C. Ewing (eds.), Scientific Basis for Nuclear Waste Management VIII, Materials Research Society, Pittsburgh, Pennsylvania, pp. 29-35. [MF 3494; ___; C-8; ___]

Jolly, W. T., 1974. "Behavior of Cu, Zn, and Ni During Prehnite--Pumpellyite Rank Metamorphism of the Keweenawan Basalts, Northern Michigan," Economic Geology, Vol. 69, pp. 1118-1125. [MF 2261; V; C-86; HC]

Jolly, W. T., and R. E. Smith, 1972. "Degradation and Metamorphic Differentiation of the Keweenawan Tholeiitic Lavas of Northern Michigan, U.S.A.," Journal of Petrology, Vol. 13, p. 2. [MF 2262; V; C-50; HC]

Jones, T. E., 1982. Reference Material Chemistry--Synthetic Groundwater Formulation, RHO-BW-ST-37 P, Rockwell Hanford Operations, Richland, Washington. [MF 2265; V; C-N; HC]

Jones, T. E., D. G. Coles, and R. C. Britton, 1986. "Development and Evaluation of a Tracer-Injection Hydrothermal Technique for Studies of Waste Package Interactions," Proceedings of Material Research Society Meeting. [MF ____; ___; C-___; ___]

Kalnins, I., and G. Gibson, 1959. "The Interaction of Uranyl Chloride with Hydrazine, Ammonia, and Amines," Journal of Inorganic Nuclear Chemistry, Vol. 11, pp. 115-123. [MF 1780; V; C-___; HC]

Keller, C., 1971. The Chemistry of the Transuranium Elements, Verlag Chemie GmbH, Weinheim/Bergstr., Germany, p. 299. [MF 1781; V; C-EA; HC]

Kelmers, A. D., J. H. Kessler, W. D. Arnold, R. E. Meyer, N. H. Cutshall, G. K. Jacobs, and S. Y. Lee, 1984a. Progress in Evaluation of Radionuclide Geochemical Information Developed by DOE High-Level Nuclear Waste Repository Site Projects - Report for October-December 1983, NUREG/CR-3851, Vol. 1, ORNL/TM-9191/VI, Oak Ridge National Laboratory for the U.S. Nuclear Regulatory Commission, Washington, D.C. [MF 1782; V; C-N; HC]

Kelmers, A. D., J. H. Kessler, W. D. Arnold, R. E. Meyer, N. H. Cutshall, G. K. Jacobs, and S. Y. Lee, 1984b. Progress in Evaluation of Radionuclide Geochemical Information Developed by DOE High-Level Nuclear Waste Repository Site Projects - Report for October-December 1983, NUREG/CR-3851, Vol. 2, ORNL/TM-9191/V2, Oak Ridge National Laboratory for the U.S. Nuclear Regulatory Commission, Washington, D.C. [MF 1983; V; C-N; HC]

King, I. P., D. B. McLaughlin, W. R. Norton, R. G. Baca, and R. C. Arnett, 1981. Parametric and Sensitivity Analysis of Waste Isolation in a Basalt Medium, RHO-BWI-C-94, Rockwell Hanford Operations, Richland, Washington. [MF 0722; V; C-N; HC]

Koltunov, V. S., and M. F. Tikhonov, 1973. "Kinetics of Reduction of Neptunium by Hydrazine," Radiokhimiya, Vol. 15, p. 789. [MF 1784; V; C-90; HC]

Koltunov, V. S., and G. I. Zhuravleva, 1974. "Kinetics of Reduction of Plutonium by Hydrazine. II. Reduction of Pu(IV)," Radiokhimiya, Vol. 16, pp. 84-88. [MF 1785; V; C-90; HC]

Koskinen, W. C., G. A. O'Connor, and H. H. Cheng, 1979. "Characterization of Hysteresis in the Desorption of 2,4,5-T from Soils," Soil Science Society of America Journal, Vol. 43, pp. 871-874. [MF 3429; NV; C-99; NHC]

Koster van Groos, A. F., and S. Guggenheim, 1984. "The effect of pressure on the dehydration reaction of interlayer water in Na-montmorillonite (SWy-1)," American Mineralogist, Vol. 69, No. 5, 9, and 10, pp. 872-879. [MF 1695; V; C-38; HC]

Krauskopf, K. B., 1979. Introduction to Geochemistry, McGraw-Hill Book Company, New York, New York. [MF 2281; V; C-59; HC]

Kristmannsdottir, H., 1975. "Hydrothermal alteration of basaltic rocks in Icelandic geothermal areas," Proc. Second U. N. Symposium on the Development and Use of Geothermal Resources, Vol. 1, San Francisco, California, pp. 441-445. [MF 2282; V; C-N; HC]

Kristmannsdottir, H., 1976. "Types of clay minerals in hydrothermally altered basaltic rocks, Reykjavik, Iceland," Jokull, Vol. 26, pp. 30-39. [MF 2283; V; C-___; HC]

Kristmannsdottir, H. 1979. "Alteration of Basaltic Rocks by Hydrothermal Activity at 100-300 °C," M. M. Mortland and V. C. Farmer (eds)., Proceedings, International Clay Conference 1978, Elsevier, New York, New York. [MF 3485; ___; C-17; ___]

Landon, R. D., 1984. X-Ray Fluorescence Data from Deep Boreholes in the Pasco Basin, SD-BWI-DP-043, Rockwell Hanford Operations, Richland, Washington, 80 pp. [MF 0419; V; C-N; HC]

Landon, R. D., 1985. Deep Borehole Stratigraphic Correlation Charts, SD-BWI-DP-035, Rockwell Hanford Operations, Richland, Washington. [MF 1789; V; C-N; HC]

Landstrom, O., C. E. Klockars, O. Persson, E. L. Tullborg, S. A. Larsson, K. Andersson, B. Torstenfelt, and B. Allard, 1983. Migration Experiments in Studsvik, KBS 83-18, Studsvik Energiteknik AB, Nykoping, Sweden. [MF 1697; V; C-___; HC]

Lane, D. L., M. J. Apted, C. C. Allen, and J. Meyers, 1984. "Basalt/Water System: Consideration for a Nuclear Waste Repository," Material Research Society Symposium Proceedings, Vol. 26, pp. 95-103. [MF 1455; V; C-8; HC]

Langmuir, D., 1971. "Eh-pH Determination," R. E. Carver (ed.), Procedures in Sedimentary Petrology, Wiley Interscience, New York, New York, pp. 597-635.

Laul, J. C., M. R. Smith, V. G. Johnson, and R. M. Smith, 1985. Disequilibrium of Natural Radionuclides in Hanford Site Groundwaters, RHO-BW-SA-496, Rockwell Hanford Operations, Richland, Washington. [MF 3431; NV; C-N; NHC]

Leonhart, L. S., R. L. Jackson, D. L. Graham, L. W. Gelhar, G. M. Thompson, B. Y. Kanehiro, and C. R. Wilson, 1984. Analysis and Interpretation of a Recirculating Tracer Experiment Performed on a Deep Basalt Flow Top, RHO-BWI-SA-300 P, Rockwell Hanford Operations, Richland, Washington. [MF 1066; V; C-N; HC]

Lindberg, J. W., 1986. Width and Infilling of Fractures in Four Grande Ronde Basalt Flows Beneath the Reference Repository Location, SD-BWI-TI-282, Rockwell Hanford Operations, Richland, Washington. [MF 1797; V; C-N; HC]

Lindberg, R. D., and D. D. Runnells, 1984. "Ground Water Redox Reactions: An Analysis of Equilibrium State Applied to Eh Measurements and Geochemical Modeling," Science, Vol. 225, pp. 925-927. [MF 1798; V; C-20; HC]

Liou, J. G., 1971. "Analcime equilibria," Lithos, Vol. 4, pp. 389-402. [MF 3434; NV; C-___; NHC]

Long, P. E., and B. J. Wood, 1986. "Structures, Textures, and Cooling Histories of Columbia River Basalt Flows," Geological Society of America Bulletin, Vol. 97, pp. 144-1155. [MF 3436; V; C-13; HC]

Long, P. E., and M. B. Strope, 1983. "Composition of Augite and Pigeonite in Basalt Flows That are Candidates for a Nuclear Waste Repository," Microbeam Analysis - 1983, R. Gooley (ed.), San Francisco Press, San Francisco, California, pp. 57-60. [MF 3435; NV; C-___; NHC]

Long, P. E., and N. J. Davidson, 1981. "Lithology of the Grande Ronde Basalt with Emphasis on the Umtanum and McCoy Canyon Flows," Subsurface Geology of the Cold Creek Syncline, C. W. Myers and S. M. Price (eds.), RHO-BWI-ST-14, Rockwell Hanford Operations, Richland, Washington. [MF 0055; NV; C-N; NHC]

Long, P. E., R. D. Landon, R. W. Cross, K. R. Fairchild, and M. A. Chamness, 1984. "Geology of Candidate Repository Horizons," Repository Horizon Identification Report, P. E. Long and Woodward-Clyde Consultants (eds.), SD-BWI-TY-001, Rockwell Hanford Operations, Richland, Washington. [MF 0057; V; C-N; HC]

MacEwan, D. M. C., 1972. "Montmorillonite Minerals," The X-ray Identification and Crystal Structures of Clay Minerals, G. Brown (ed.), Mineralogical Society, London, England, pp. 143-207. [MF 2310; NV; C-___; NHC]

Mamy, J., and J. P. Gaultier, 1975. "Etude de l'evolution del'ordre cristallin dans la montmorillonite en relation avec la diminution d'echangeabilite du potassium," Proc. Internat. Clay Conf. 1975, Applied Publishing Ltd., Wilmette, Illinois, pp. 149-156. [MF 3495; ___; C-___; ___]

Mann C. K., T. J. Vickers, and W. M. Gulick, 1974. Instrumental Analysis, Harper & Row Publishers, New York.

Mason, B., and L. G. Berry, 1968. Elements of Mineralogy, W. H. Freeman and Company, San Francisco, California. [MF 2317; NV; C-___; NHC]

Mattigod S. V., and G. Sposito, 1978. "Improved Method for Estimating the Standard Free Energies of Formation (ΔG_f°, 298.15) of smectites," Geochimica et Cosmochimica Acta, Vol. 42, pp. 1753-1762. [MF 2674; NV; C-6; NHC]

McDowell, S. D. and W. A. Elders, 1980. "Authigenic layer silicate minerals in borehole Elmore 1, Salton Sea geothermal field, California, U.S.A," Contributions to Mineralogy and Petrology, Vol. 74, pp. 293-310. [MF 3438; NV; C-16; NHC]

McKee, E. H., D. A. Swanson, and T. L. Wright, 1977. "Duration and volume of Columbia River basalt volcanism, Washington, Oregon and Idaho," Geological Society of America, Abstracts with Programs, Vol. 9, No. 4, p. 463.

McKee, E. H., P. R. Hooper, and W. D. Kleck, 1981. "Age of Imnaha Basalt - Oldest Basalt Flows of the Columbia River Basalt Group, Northwest United States," Isochron/West, No. 31, pp. 31-33.

McKinley, J. P., 1986. Microprobe Analysis of Pyrite Samples from Hanford Site Boreholes, SD-BWI-TI-277, Rockwell Hanford Operations, Richland, Washington, 25 pp. [MF 3441; NV; C-N; NHC]

McKinley, J. P., and S. A. Rawson, 1985. Intraflow Compositional and Morphological Variation of Fe-Ti Oxide minerals in Columbia River Basalts, RHO-BW-SA-515 P, Rockwell Hanford Operations, Richland, Washington, 4 pp. [MF 3442; NV; C-N; NHC]

McKinley, J. P., S. A. Rawson, and D. G. Horton, 1986. Forms and Composition of Secondary Mineralization in Fractures in Columbia River Basalts, RHO-BW-SA-565 P, Rockwell Hanford Operations, Richland, Washington. [MF 3486; ___; C-N; ___]

Means, J. L., 1982. The Organic Geochemistry of Deep Ground Waters, ONWI-268, Battelle's Columbus Laboratories, Columbus, Ohio. [MF 2327; V; C-N; HC]

Meyer, R. E., W. D. Arnold, and F. I. Case, 1984. Valence Effects on Sorption of Nuclides on Rocks and Minerals, NUREG/CR-3389, ORNL-5978, Oak Ridge National Laboratory, Oak Ridge, Tennessee. [MF 2330; V; C-N; HC]

Moore, E. L., G. C. Ulmer, and D. E. Grandstaff, 1984. Hydrothermal Interaction of Columbia Plateau Basalt from the Umtanum Flow with Its Coexisting Groundwater, SD-BWI-TI-228, Rockwell Hanford Operations, Richland, Washington, 58 p. [MF 1494; V; C-N; HC]

Morris, J. C., and W. Stumm, 1967. "Redox Equilibria and Measurements of Potential in the Aquatic Environment," W. Stumm (ed.), Equilibrium Concepts in Natural Water System, American Chemical Society Series #67, Washington, D.C., pp. 270-285. [MF 0561; V; C-22; HC]

Mottl, M. J., and H. D. Holland, 1978. "Chemical Exchange during Hydrothermal Alteration of Basalt by Seawater - I. Experimental Results for Major and Minor Components of Seawater," Geochimica et Cosmochimica Acta., Vol. 42, p. 1103. [MF 3444; NV; C-6; NHC]

Myers, C. W., 1973. Yakima Basalt flows near Vantage, and from core holes in the Pasco Basin, Washington, Ph.D. Dissertation, University of California, Santa Cruz, California.

Nathan, Y., and A. Flexer, 1977. "Clinoptilolite, paragenesis and stratigraphy," Sedimentology, Vol. 24, pp. 845-855. [MF 2677; NV; C-6; NHC]

Neretnieks, I., 1978. Some Aspects on Colloids as a Means for Transporting Radionuclides, KBS Technical Report 103, Karn-Bransle-Sakerhet, Stockholm, Sweden. [MF 2361; NV; C-45; NHC]

Noble, D. C., V. C. Smith, and L. C. Peck, 1967. "Loss of Halogens from Crystallized and Glassy Silicic Volcanic Rocks," Geochimica et Cosmochimica Acta, Vol. 31, pp. 215-223. [MF 3487; ___; C-6; ___]

Noonan, A. F., C. K. Fredrickson, and J. Nelen, 1980. Phase Chemistry of the Umtanum Basalt: A Reference Repository Host in the Columbia Plateau, RHO-BWI-SA-77, Rockwell Hanford Operations, Richland, Washington. [MF 1047; V; C-N; HC]

Nriagu, J. O., 1975. "Thermochemical Approximations for Clay Minerals," American Mineralogist, Vol. 60, pp. 834-839. [MF 2583; NV; C-38; NHC]

NRC, 1983. Standard Format and Content of Site Characterization Plans for High-Level-Waste Geologic Repositories, Draft Regulatory Guide 4.17, U.S. Nuclear Regulatory Commission, Washington, D.C.

NRC, 1985. Disposal of High-Level Radioactive Wastes in Geologic Repositories, Title 10 Code of Federal Regulations Part 60, U.S. Nuclear Regulatory Commission, pp. 563-593. [MF 1986; ___; C-N; HC]

Ohmoto, H. and A. C. Lasaga, 1982. "Kinetics of Reactions Between Aqueous Sulfates and Sulfides in Hydrothermal Systems," Geochimica et Cosmochimica Acta, Vol. 46, pp. 1727-1745. [MF 0302; V; C-6; HC]

Osmond, J. K., 1980. "Uranium Disequilibrium in Hydrologic Studies," P. Fritz and J. C. Fontes (eds.), Handbook of Environmental Isotope Geochemistry, - The Terrestrial Environment, A, Vol. 1 Elsevier, New York, New York, pp. 259-282. [MF 2385; V; C-17; HC]

Osnes, J. D., G. K. Coates, K. B. DeJonge, M. C. Loken, and R. A. Wagner, 1984. Expected Repository Environments in Granite: Thermal Environment, RE/SPEC, Inc., BME/OCRD-7, Battelle Memorial Institute, Office of Crystalline Repository Development, Columbus, Ohio. [MF 2642; ___; C-N; HC]

Palmer, R. A., G. D. Aden, R. G. Johnston, T. E. Jones, D. L. Lane, and A. F. Noonan, 1982. Characterization of Reference Materials for the Barrier Materials Test Program, RHO-BW-ST-27 P, Rockwell Hanford Operations, Richland, Washington. [MF 2390; V; C-N; HC]

Palmer, R. A., R. G. Johnston, and M. I. Wood, 1983. Determination of an Upper Temperature Limit for Bentonite as a Backfill Component in a Nuclear Waste Repository in Basalt, RHO-BW-ST-47 P, Rockwell Hanford Operations, Richland, Washington, p. 27. [MF 1519; V; C-N; HC]

Paquette, J., and W. E. Lawrence, 1985. "A Spectrochemical Study of the Technetium(IV)/Technetium(III) Couple in Bicarbonate Solutions," Canadian Journal of Chemistry, Vol. 63, pp. 2369-2373. [MF 3489; ___; C-N; ___]

Parkhurst, D. L., D. C. Thorstenson, and L. N. Plummer, 1980. "PHREEQE, A Computer Program for Geochemical Calculations," Water Recources Investigations 80-96, U.S. Geological Survey, Washington, D.C. [MF 2392; NV; C-N; NHC]

Peek, D. C., and V. V. Volk, 1985. "Fluoride Sorption and Desorption in Soils," Soil Science Society of America Journal, Vol. 49, pp. 583-586. [MF 3447; NV; C-99; NHC]

Perry, E. A., Jr., 1975. "Submarine smectite genesis as an oceanic magnesium sink," Proc. Internat. Clay Conf. 1975, Applied Publishing Ltd., Wilmette, Illinois, pp. 287-295. [MF 2584; NV; C-___; NHC]

Petrovic, R., 1976. "Rate Control in Feldspar Dissolution--II: The Protective Effect of Precipitates," Geochimica et Cosmochimica Acta, Vol. 40, pp. 1509-1521. [MF 2397; V; C-6; HC]

Philpotts, A. R., 1982. "Compositions of Immiscible Liquids in Volcanic Rocks," Contributions to Mineralogy and Petrology, Vol. 80, pp. 201-218. [MF 2400; V; C-16; HC]

Plummer, L. N., D. L. Parkhurst, and D. C. Thorstenson, 1983. "Development of Reaction Models for Groundwater Systems," Geochimica et Cosmochimica Acta., Vol. 47, pp. 665-686. [MF 0308; V; C-6; HC]

Rawson, S. A., 1986a. X-Ray Diffraction Study of Selected Cohassett and Rocky Coulee Flow Tops, SD-BWI-TI-269, Rockwell Hanford Operations, Richland, Washington. [MF 3449; V; C-N; HC]

Rawson, S. A., 1986b. Xrd Determination of the Secondary Mineralogy of Selected Flow Top Samples from the Saddle Mountains, Wanapum, and Grande Ronde Formation, SD-BWI-TI-330, Rockwell Hanford Operations, Richland, Washington. [MF 3450; NV; C-N; NHC]

Reddy, M. R., and H. F. Perkins, 1974. "Fixation of Zinc by Clay Minerals," Soil Science Society of America Proceedings, Vol. 38, pp. 229-231. [MF 3451; NV; C-99; NHC]

Reidel, S. P., 1983. "Stratigraphy and Petrogenesis of the Grande Ronde Basalt from the Deep Canyon Country of Washington, Oregon, and Idaho," Geological Society of America Bulletin, Vol. 94, pp. 519-542. [MF 1003; V; C-13; HC]

Reidel, S. P., 1978. Stratigraphy and petrogenesis of the Grande Ronde Basalt in the Lower Salmon and adjacent Snake River Canyons, Ph.D Disseration, Washington State University, Pullman, Washington. [MF 2417; NV; C-25; NHC]

Reidel, S. P., M. E. Ross, and P. E. Long, 1978. Orthopyroxene Fractionation in the Grande Ronde Basalt, Columbia River Group, RHO-BWI-SA-5A, Rockwell Hanford Operations, Richland, Washington.

Relyea, J. F., D. P. Trott, C. V. McIntyre, and C. G. Rieger, 1986. "Diffusion of Tritiated Water and Chloride in Basalt-Bentonite Mixtures," Nuclear Technology, Vol. 74, pp. 317-323. [MF 3490; ___; C-97; ___]

Roddy, J. W., H. L. Clairborne, R. L. Ashline, P. J. Johnson, and B. T. Rhyne, 1985. Physical and Decay Characteristics of Commercial LWR Spend Fuel, ORNL/TM-9591/V1, Oak Ridge National Laboratory, Oak Ridge, Tennessee. [MF 3496; ___; C-N; ___]

Rose, Arthur W., 1976. "The Effect of Cuprous Chloride Complexes in the Origin of Red-Bed Copper and Related Deposits," Economic Geology, Vol. 71, pp. 1036-1048. [MF 2585; NV; C-___; NHC]

Ross, M. E., 1978. Stratigraphy, Structure, and Petrology of Columbia River Basalt in a Portion of the Grande Ronde River - Blue Mountains Area of Oregon and Washington, RHO-SA-58, Rockwell Hanford Operations, Richland, Washington. [MF 0009; V; C-N; HC]

Salter, P. F., and G. K. Jacobs, 1983. BWIP Data Package for Reference Solubility and K_d Values, SD-BWI-DP-001, Rockwell Hanford Operations, Richland, Washington. [MF 1562; NV; C-N; HC]

Salter, P. F., L. L. Ames, and J. E. McGarrah, 1981a. Sorption of Selected Radionuclides on Secondary Minerals Associated with the Columbia River Basalts, RHO-BWI-LD-43, Rockwell Hanford Operations, Richland, Washington. [MF 2448; V; C-N; HC]

Salter, P. F., L. L. Ames, and J. E. McGarrah, 1981b. The Sorption Behavior of Selected Radionuclides on Columbia River Basalt, RHO-BWI-LD-48, Rockwell Hanford Operations, Richland, Washington. [MF 0010; V; C-N; HC]

Salter, P. F., L. L. Ames, G. S. Barney, and J. E. McGarrah, 1982. The Sorption Behavior of Selected Radionuclides on Columbia River Basalts and Associated Interbed Materials, RHO-BW-ST-40, Rockwell Hanford Operations, Richland, Washington. [MF 2449; V; C-N; HC]

Schiffman, P., and G. E. Lofgren, 1982. "Dynamic Crystallization Studies on the Grande Ronde Pillow Basalts, Central Washington," Journal of Geology, Vol. 90, pp. 49-78. [MF 0328; V; C-6; HC]

Schindler, P. W., 1981. "Surface Complexes at Oxide-Water Interfaces," M. A. Anderson and A. J. Rubin (eds.), Adsorption of Inorganics at Solid-Liquid Interfaces, Ann Arbor Science Publishers, Inc., Ann Arbor, Michigan. MF 3491; ___; C-___; ___]

Schmincke, H. U., 1964. Petrology, paleocurrents, and stratigraphy of the Ellensburg Formation and interbedded Yakima basalt flows, south-central Washington, Ph.D. Dissertation, Johns Hopkins University, Baltimore, Maryland, p. 425.

Schweich, D., and M. Sardin, 1981. "Adsorption, Partition, Ion Exchange and Chemical Reaction in Batch Reactors or in Columns--Review," Journal of Hydrology, Vol. 50, pp. 1-33.

Seyfried, W. E., Jr., and J. L. Bischoff, 1979. "Low Temperature Basalt Alteration by Seawater: An Experimental Study at 70 and 150 °C," Geochimica et Cosmochimica Acta, Vol. 43, p. 1937. [MF 3454; V; C-6; HC]

Seyfried, W. E., Jr., and J. L. Bischoff, 1981. "Experimental Seawater-Basalt Interaction at 300 °C, 500 bars, Chemical Exchange, Secondary Mineral Formation and Implications for the Transport of Heavy Metals," Geochemica et Cosmochimica Acta., Vol. 45, p. 135. [MF 0589; V; C-6; HC]

Seyfried, W. E., and M. J. Mottl, 1981. "Hydrothermal Alteration of Basalt by Seawater Under Seawater-Dominated Conditions," Geochimica et Cosmochimica Acta, Vol. 46, No. 63, p. 985. [MF 3455; V; C-6; HC]

Seyfried, W. E., W. C. Shanks, and J. L. Bischoff, 1976. "Alteration and vein formation in Site 321 basalts," Initial Reports of the Deep Sea Drilling Project, T. L. Vallier (ed.), Vol. XXXIV, U.S. Government Printing Office, Washington, D.C., pp. 385-392. [MF 2587; V; C-N; HC]

Sheppard, R. A., 1971. "Zeolites in Sedimentary Deposits of the United States-A Review," Molecular Sieve Zeolites - I, E. M. Flanigen, and L. B. Sand (eds.), American Chemical Society, Advances in Chemistry Series 101, Washington, D.C., pp. 279-310. [MF 2588; V; C-22; HC]

Sheppard, R. A., and A. J. Gude, 3rd, 1973. Zeolites and associated authigenic silicate minerals in tuffaceous rocks of the Big Sandy Formation, Mohave County, Arizona, Professional Paper 830, U.S. Geological Survey, Washington, D.C. [MF 2589; NV; C-N; NHC]

Smith, M. J., G. J. Anttonen, G. S. Barney, W. E. Coons, F. N. Hodges, R. G. Johnston, J. D. Kaser, R. M. Manabe, S. C. McCarel, E. L. Moore, A. F. Noonan, J. E. O'Rourke, W. W. Schulz, C. L. Taylor, B. J. Wood, and M. I. Wood, 1980. Engineered Barrier Development for a Nuclear Waste Repository Located in Basalt: An Integration of Current Knowledge, RHO-BWI-ST-7, Rockwell Hanford Operations, Richland, Washington. [MF 0069; V; C-N; HC]

Spane, F. A., 1986. Hydraulic Head Relationships and Inferred Lateral Groundwater Flow Direction for Horizons Monitored at DC-19, -20, -22, SD-BWI-TI-332, Rockwell Hanford Operations, Richland, Washington. [MF 3468; ___; C-N; ___]

Spitsyn, V. I., S. V. Kryuchkov, and A. F. Xugina, 1983. "Reduction of Pertichnetate Ions in Nitric Acid Solution by Hydrazine," Radiokhimiya, Vol. 25, pp. 497-502. [MF 1856; V; C-90; HC]

Staal, E., and C. Faurholt, 1951. "Carbonates. IV. The Carbonate of Hydrazine," Dansk. Tids. Farm., Vol. 25, pp. 1-12. [MF 1859; V; C-___; HC]

Stumm, W. and J. J. Morgan, 1965. Aquatic Chemistry, John Wiley & Sons, Inc., New York

Stumm, W., and J. J. Morgan, 1981. Aquatic Chemistry, 2nd Ed., John Wiley and Sons, New York, New York. [MF 1071; V; C-24; HC]

Sula, M. J., J. M. V. Carlile, K. R. Price, and W. D. McCormack, 1983. Environmental Surveillance at Hanford for CY 1982, PNL-4657, Pacific Northwest Laboratory, Richland, Washington. [MF 3458; NV; C-N; NHC]

Surdam, R. C., 1981. "Zeolites in closed hydrologic systems," F. A. Mumpton (ed.), Mineralogy and geology of natural zeolites. Mineralogical Society of America Reviews in Mineralogy, Vol. 4, pp. 65-91. [MF 1605; V; C-38; HC]

Susak, N. J., A. Friedman, S. Fried, and J. C. Sullivan, 1983. "The Reduction of Neptunium (VI) by Basalt and Olivine," Nuclear Technology, Vol. 63, pp. 266-270. [MF 0350; V; C-97; HC]

Swanson, D. A., T. L. Wright, P. R. Hooper, and R. D. Bentley, 1979. "Revisions in Stratigraphic Nomenclature of the Columbia River Basalt Group," U.S. Geological Survey Bulletin, 1457-G, p. G59. [MF 2505; V; C-N; HC]

Swanson, D. A., and T. L. Wright, 1981. "Guide to Geologic Field Trip between Lewiston, Idaho and Kimberly, Oregon, Emphasizing the Columbia River Basalt Group," D. A. Johnston and J. Donnelly-Nolen, (eds.), Guides to Some Volcanic Terrains in Washington, Idaho, Oregon, and Northern California, U.S. Geological Survey Circular 838.

Tardy, Y., and R. M. Garrels, 1974. "A method of Estimating the Gibbs Energies of Formation of Layer Silicates," Geochimica et Cosmochimica Acta, Vol. 38, pp. 1101-1116. [MF 2590; V; C-6; HC]

Taylor, T. L., 1976. The Basalt Stratigraphy and Structure of the Saddle Mountains of South-Central Washington, M.S. Thesis, Washington State University, Pullman, Washington. [MF 3459; NV; C-25; NHC]

Teague, L. S., 1980. Secondary Minerals Found in Cores DC2-A1 and DC2-A2 Taken from Grande Ronde Basalt Formation, Pasco Basin, Washington, LBL-10387, Lawrence Berkeley Laboratory, Berkeley, California. [MF 0355; V; C-N; HC]

Truesdell, A. H., and B. F. Jones, 1974. "WATEQ, A Computer Program for Calculating Chemical Equilibria of Natural Waters," J. Research, U.S. Geological Survey, Vol. 2, pp. 233-248.

Turner, W. D., D. C. Elrod, and I. I. Simon-Tov, 1977. HEATING5-An IBM 360 Heat Conduction Program, ORNL/CSD/TM-15, Union Carbide Corp., Oak Ridge, Tennessee. [MF 2591; NV; C-N; NHC]

Ulmer, G. C., and D. E. Granstaff, 1984. Icelandic Basaltic Geothermal Field: A Natural Analog for Nuclear Waste Isolation in Basalt, SD-BWI-TI-257, Rockwell Hanford Operations, Richland, Washington. [MF 1943; V; C-N; HC]

Van Genuchten, M. Th. and P. J. Wierenga, 1974. Simulation of One-Dimensional Solute Transfer in Porous Media, Bulletin 628, New Mexico State University Agricultural Experiment Station, Las Cruces, New Mexico. [MF 0365; V; C-N; HC]

Van Genuchten, M. Th., and R. W. Cleary, 1979. "Movement of Solutes in Soil: Computer-Simulated and Laboratory Results," G. H. Bolt (ed.), Soil Chemistry B. Physico-Chemical Models, Elsevier Scientific Publishing Company, New York, New York, pp. 349-386. [MF 0364; V; C-17; HC]

Van Genuchten, M. Th., J. M. Davidson, and P. J. Wierenga, 1974. "An Evaluation of Kinetic and Equilibrium Equations for the Prediction of Pesticide Movement Through Porous Media," Soil Science Society of America, Proceedings, Vol. 38, pp. 29-35. [MF 2536; V; C-99; HC]

Warner, S. D., N. C. Krothe, G. C. Solomon, and W. C. Steinkampf, 1986. Modeling the Geochemical Evolution of Groundwater within the Grande Ronde Basalt, Columbia Plateau, Washington, Abstracts with Programs, Geological Society of America, 99th Annual Meeting, San Antonio, Texas, p. 782. [MF 3475; NV; C-___; NHC]

Weaver, C. E., 1984. "Shale-slate metamorphism in southern Appalachians," Developments in Petrology No. 10, Elsevier Scientific Publishing Company, New York, N. Y., pp. 239. [MF 2593; NV; C-17; NHC]

White, A. F., and A. Yee, 1985. "Aqueous Oxidation-Reduction Kinetics Associated with Coupled Electron-Cation Transfer from Iron-Containing Silicates at 25 °C," Geochimica et Cosmochimica Acta, Vol. 49, pp. 1263-1275.

White, A. F., A. Yee, and S. Flexser, 1985. "Surface oxidation-reduction kinetics associated with experimental basalt-water reaction at 25 °C," Chemical Geology, Vol. 49, pp. 73-86.

Whitfield, M., 1969. "Eh as an Operational Parameter in Stuarine Studies," Limnology and Oceanography, Vol. 19, pp. 857-865. [MF 0376; V; C-___; HC]

Whitfield, M., 1974. "Thermodynamic Limitations on the Use of the Platinum Electrode in Eh Measurements," Limnology and Oceanography, Vol. 19, pp. 857-865. [MF 2558; V; C-___; HC]

Wilson, A. D., 1955. "A new method for the determination of ferrous iron in rocks and Minerals," Great Britian Geologic Surveillance Bulletin, Vol. 9, pp. 56-58. [MF 2565; V; C-N; HC]

Wintczak, T. M., 1983. Principal Borehole Report, Borehole RRL-2, SD-BWI-TI-113, Rockwell Hanford Operations, Richland, Washington. [MF 0443; V; C-N; HC]

Wise, W. S., and H. P. Eugster, 1964. "Celadonite: Synthesis, thermal stability and occurrence," American Mineralogist, Vol. 49, pp. 1031-1083. [MF 2594; NV; C-38; NHC]

Wolery, T. J., 1979. Calculation of Chemical Equilibrium Between Aqueous Solutions and Minerals: The EQ316 Software Package, UCRL-52658, Lawrence Livermore National Laboratory, Livermore, California. [MF 2575; V; C-N; HC]

Wolery, T. J., 1983. EQ3NR, A Computer Program for Geochemical Aqueous Speciation - Solubility Calculations: Users Guide and Documentation, UCRL-53414, Lawrence Livermore National Laboratory, Livermore, California. [MF 3463; V; C-N; HC]

Wood, M. I., L. L. Ames, and J. E. McGarrah, 1986. "Tc Behavior in the Basalt-Synthetic Groundwater System as a Function of Temperature and Initial Oxygen Content," Proceedings of Material Research Society Meeting.

Wright, T. L., D. A. Swanson, R. T. Helz, and G. R. Byerly, 1979. "Major Oxide, Trace Element, and Glass Chemistry of Columbia River Basalt Samples Collected Between 1971 and 1977," U.S. Geol. Survey Open File Report 79-711, p. 146. [MF 3492; ___; C-N; ___]

Yeh, H. and S. M. Savin, 1977. "Mechanism of burial metamorphism of argillaceous sedimentd: 3. O-isotope evidence," Geol. Soc. Am. Bull., Vol. 88, No. 7, pp. 1321-1330. [MF 3493; V; C-___; HC]

Yung, S. C., R. T. Toyooka, and T. B. McCall, 1986. Thermal Analysis of Waste Package Preliminary Reliability Assessment, RHO-BW-SA-509, Rockwell Hanford Operations, Richland, Washington. [MF 3464; V; C-N; HC]

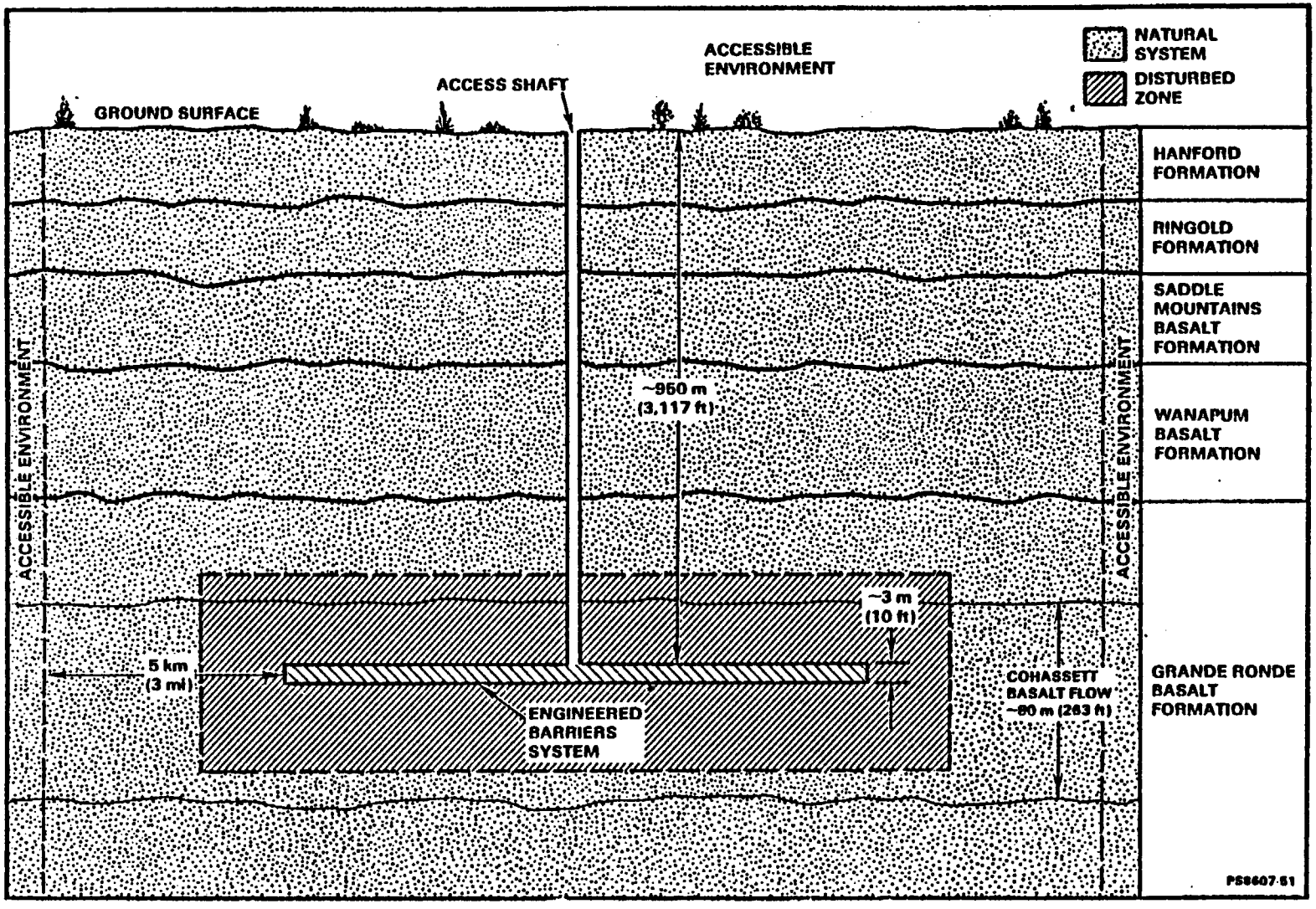

Figure 4.0-1. Regions of a nuclear waste repository in basalt.

PS 8607-51

FORMATION	MEMBER OR SEQUENCE	SEDIMENT STRATIGRAPHY OR BASALT FLOW	UNIT THICKNESS RANGES (m)		
	SURFICIAL UNITS	LOESS, SAND DUNES, ALLUVIUM ALLUVIAL FANS, LANDSLIDE, TALUS, COLLUVIUM	<3[a]		
HANFORD	TOUCHET BEDS / PASCO GRAVELS		64[a] / ≤5[a]		
		PLIO-PLEISTOCENE UNIT	26[a]		
RINGOLD		UPPER RINGOLD	0-33[a]		
		MIDDLE RINGOLD	55-100[a]		
		LOWER RINGOLD	0-17[a]		
		BASALT RINGOLD	6-60[a]		
SADDLE MOUNTAINS BASALT	ELEPHANT MOUNTAIN MEMBER	ELEPHANT MOUNTAIN FLOW	0-39.0		
		RATTLESNAKE RIDGE INTERBED	0-34.4		
	POMONA MEMBER	POMONA FLOW	0-59.0		
		SELAH INTERBED	0-30.8		
	ESQUATZEL MEMBER	GABLE MOUNTAIN FLOW	0-36.3		
		COLD CREEK INTERBED	0-36.6		
	UMATILLA MEMBER	UMATILLA FLOW	20.7-73.2		
		SILLUSI FLOW (DISCONTINUOUS)			
		MABTON INTERBED	25.6-51.8		
WANAPUM BASALT	PRIEST RAPIDS MEMBER	LOLO FLOW	39.3-55.2	UPPER BUFFER ZONE	REPOSITORY ISOLATION SYSTEM
		ROSALIA FLOW	16.5-33.5		
		QUINCY INTERBED (DISCONTINUOUS)	0-0.5		
	ROZA MEMBER	ROZA FLOW (2 COOLING UNITS)	42.1-59.4		
		SQUAW CREEK INTERBED (DISCONTINUOUS)	0-0.9		
	FRENCHMAN SPRINGS MEMBER	SENTINEL GAP FLOW	50.9-64.6		
		SAND HOLLOW FLOWS (2 FLOWS)	32.6-54.4		
		SILVER FALLS FLOWS (1 TO 3 FLOWS)	19.8-47.9		
		GINKGO FLOWS (2-3 FLOWS)	68.0-100.9		
		UNNAMED INTERBED (DISCONTINUOUS)	0-3.7		
		PALOUSE FALLS FLOW	9.1-25.0		
		VANTAGE INTERBED	0-9.1		
GRANDE RONDE BASALT	SENTINEL BLUFFS SEQUENCE	FLOW 1	5.3-23.1	PRIMARY ISOLATION ZONE	
		FLOW 2	15.9-34.9		
		ROCKY COULEE FLOW	40.2-57.0		
		LEVERING FLOW (DISCONTINUOUS)	0-28.0		
		COHASSETT FLOW	65.8-8.14		
		BIRKETT FLOW	34.1-43.3		
		FLOW 7	9.0-19.8		
		FLOW 8	11.6-24.4		
		McCOY CANYON FLOW	32.3-45.0		
	SCHWANA SEQUENCE	UMTANUM FLOW	60.5-75.0		
		VERY HIGH Mg FLOW	0-22.6	LOWER BUFFER ZONE	
		AT LEAST 3 FLOWS[b]	93.5[a]		
		N_2-R_2 PALEOMAGNETIC CONTACT GREATER THAN 10 FLOWS	>1,750 TO BASE OF BASALT		

ELLENSBURG FORMATION

[a] THICKNESS RANGE FOR THE REFERENCE REPOSITORY LOCATION ONLY
[b] VALUE IS A MINIMUM ONLY, (ONLY ONE BOREHOLE PENETRATED TO BASE OF LOWER BUFFER ZONE)

609-1655

Figure 4.1-1. Idealized stratigraphy of the reference repository location within the controlled area study zone.

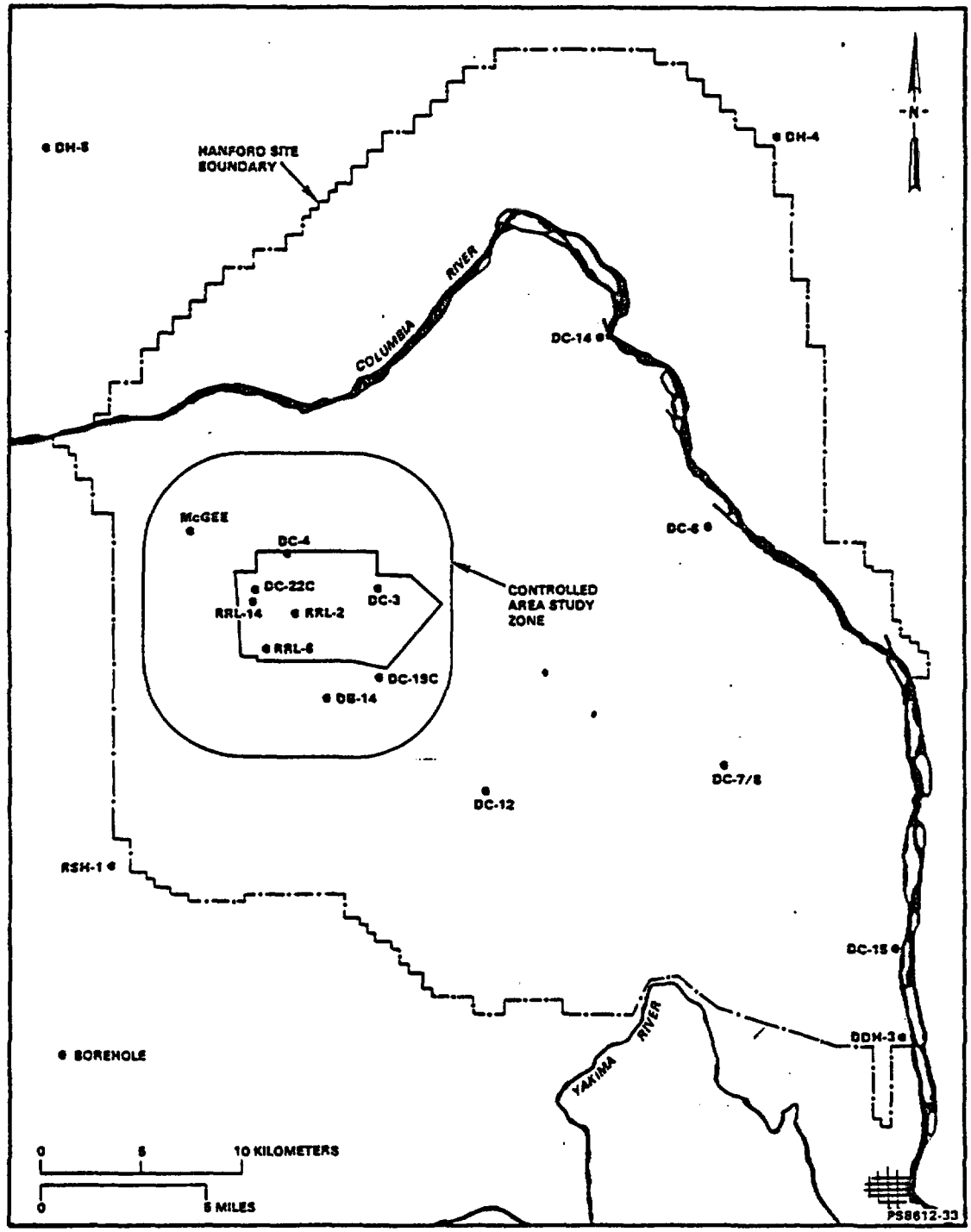

Figure 4.1-2. Locations of the controlled area study zone, reference repository location, and sample boreholes.

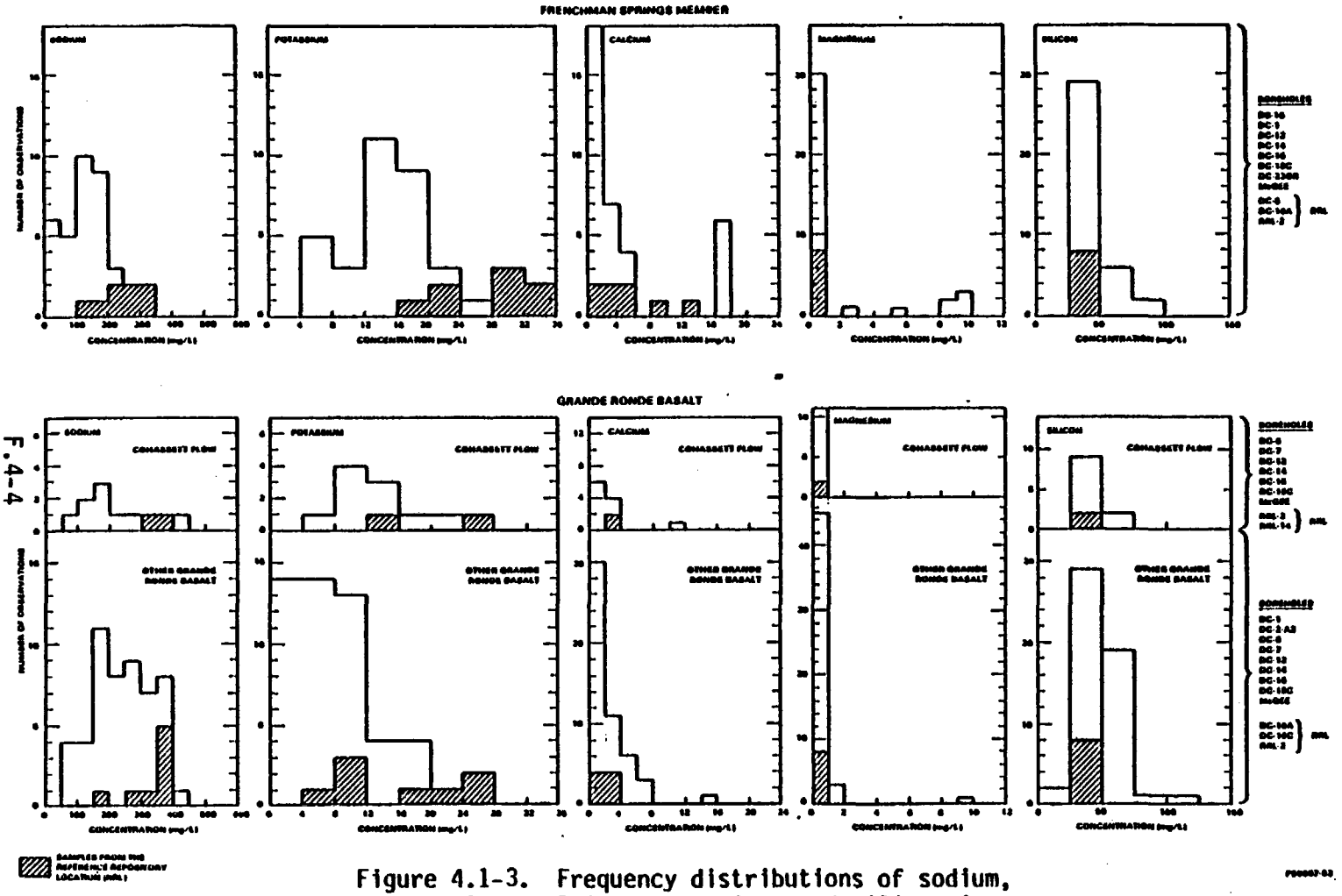

F.4-4

Figure 4.1-3. Frequency distributions of sodium, potassium, calcium, magnesium, and silicon in groundwaters from the Frenchman Springs Member and Grande Ronde Basalt. (One calcium value for a Grande Ronde Basalt groundwater lies outside the range of the figure.)

FOLDOUT PS8607-53

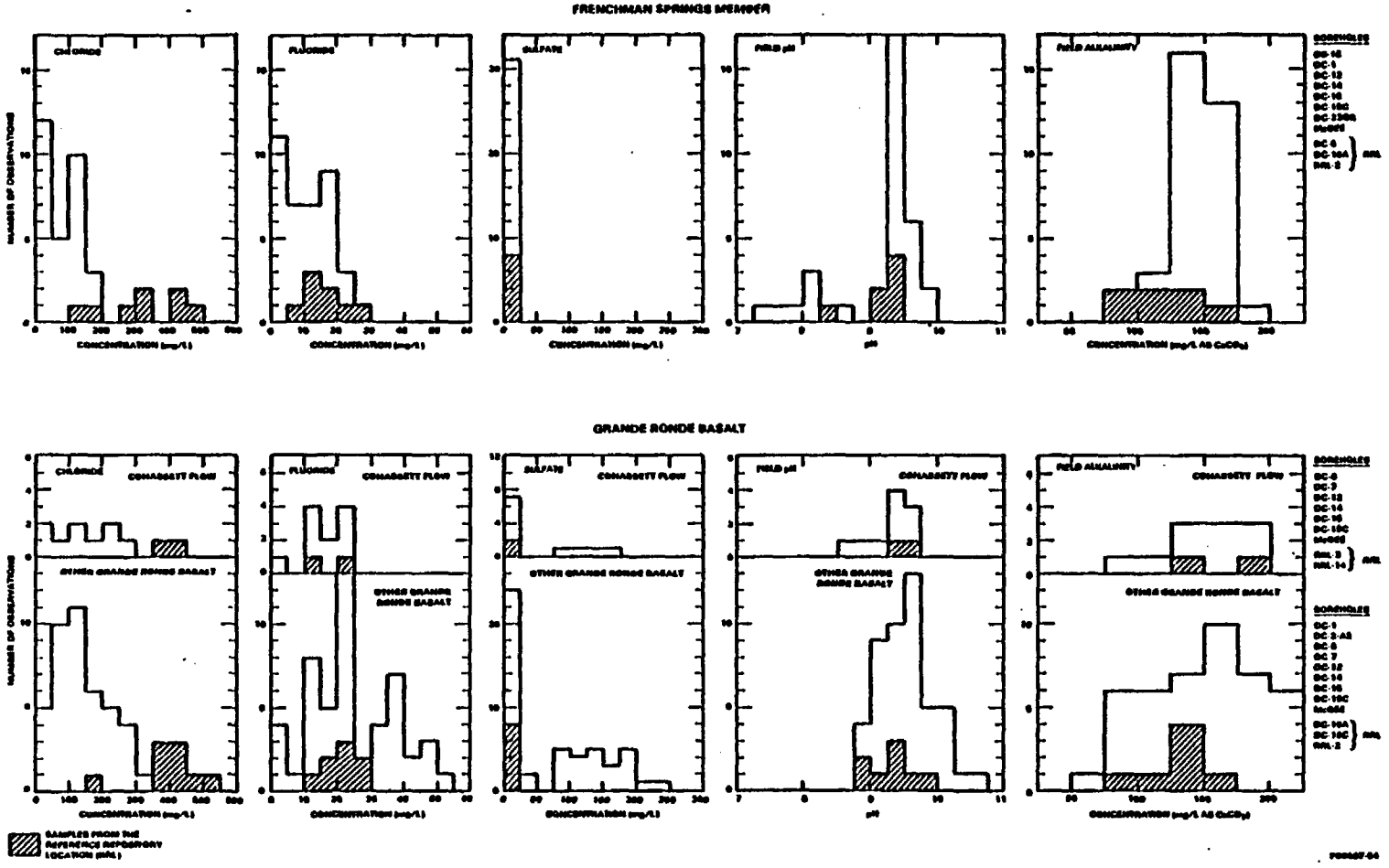

Figure 4.1-4. Frequency distributions of chloride, fluoride, sulfate, field ph and field alkalinity in groundwaters from the Frenchman Springs Member and Grande Ronde Basalt. (One field alkalinity value for a Grande Ronde Basalt groundwater lies outside the range of the figure.)

FOLDOUT PS8607-54

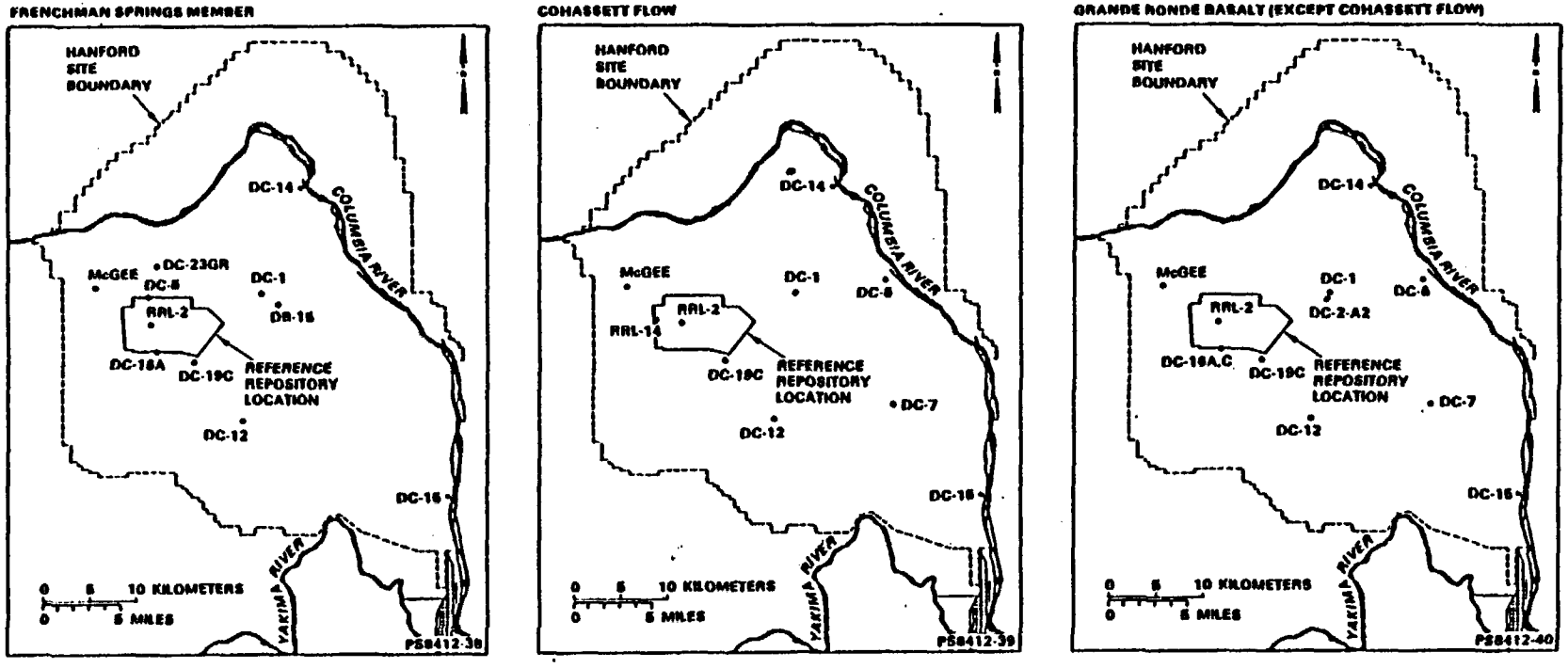

Figure 4.1-5. Location of boreholes with hydrochemical data for major inorganic constituents.

PS8412-38, -39, -40

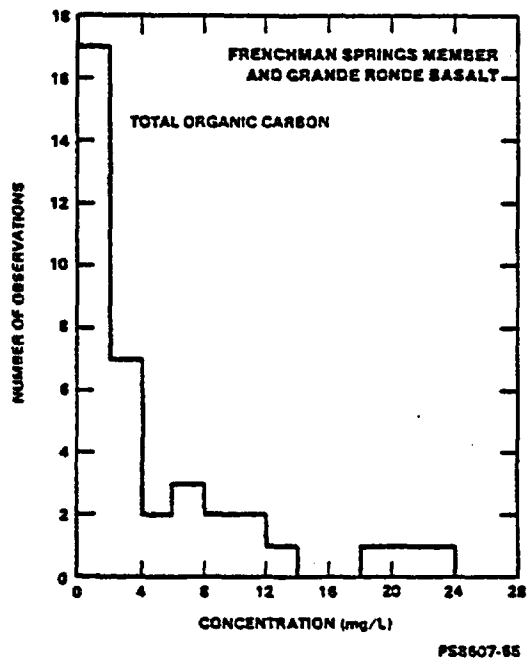

Figure 4.1-6. Frequency distribution of observed total organic carbon concentrations in groundwaters from the Frenchman Springs Member and Grande Ronde Basalt. (Two samples with total organic carbon concentrations greater than 20 mg/L are not plotted in the interest of producing a compact figure.)

PS8407-55

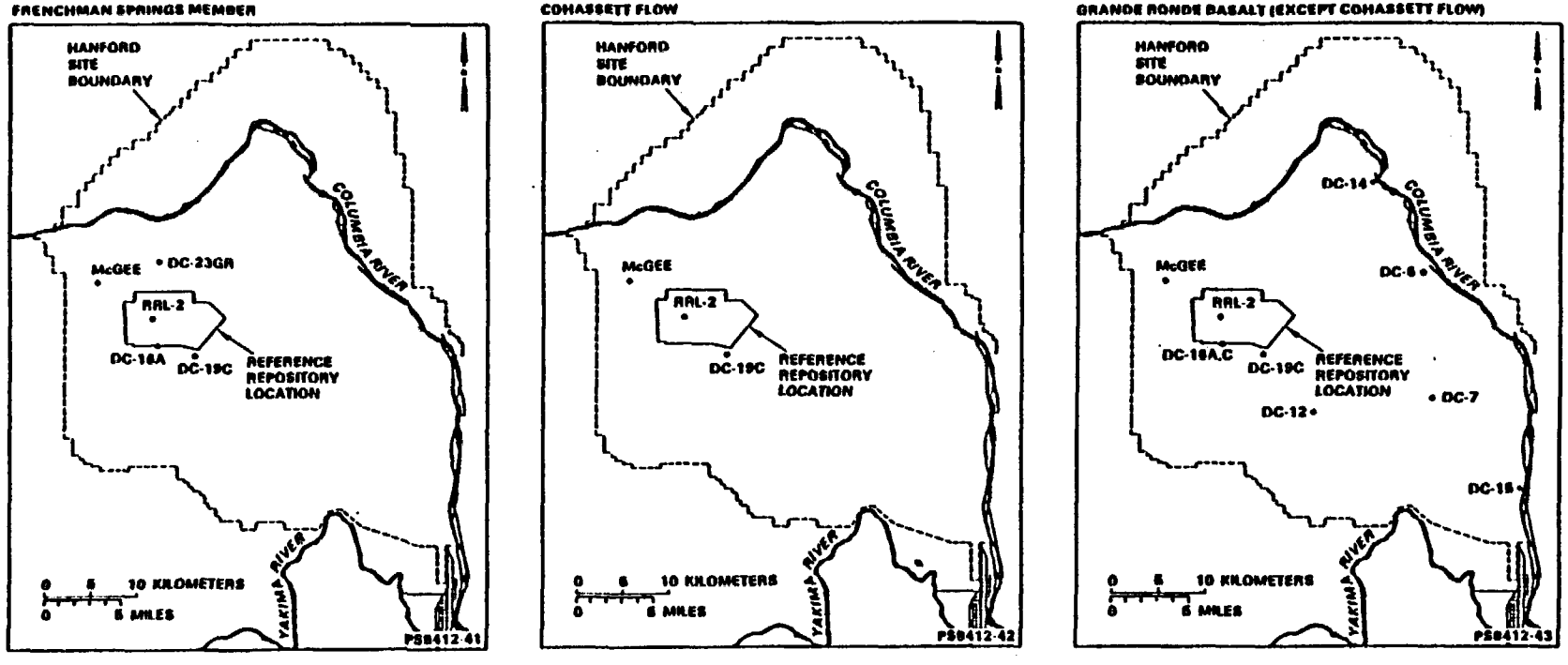

Figure 4.1-7. Location of boreholes from which total organic carbon data are used.

PS8412-41, -42, -43

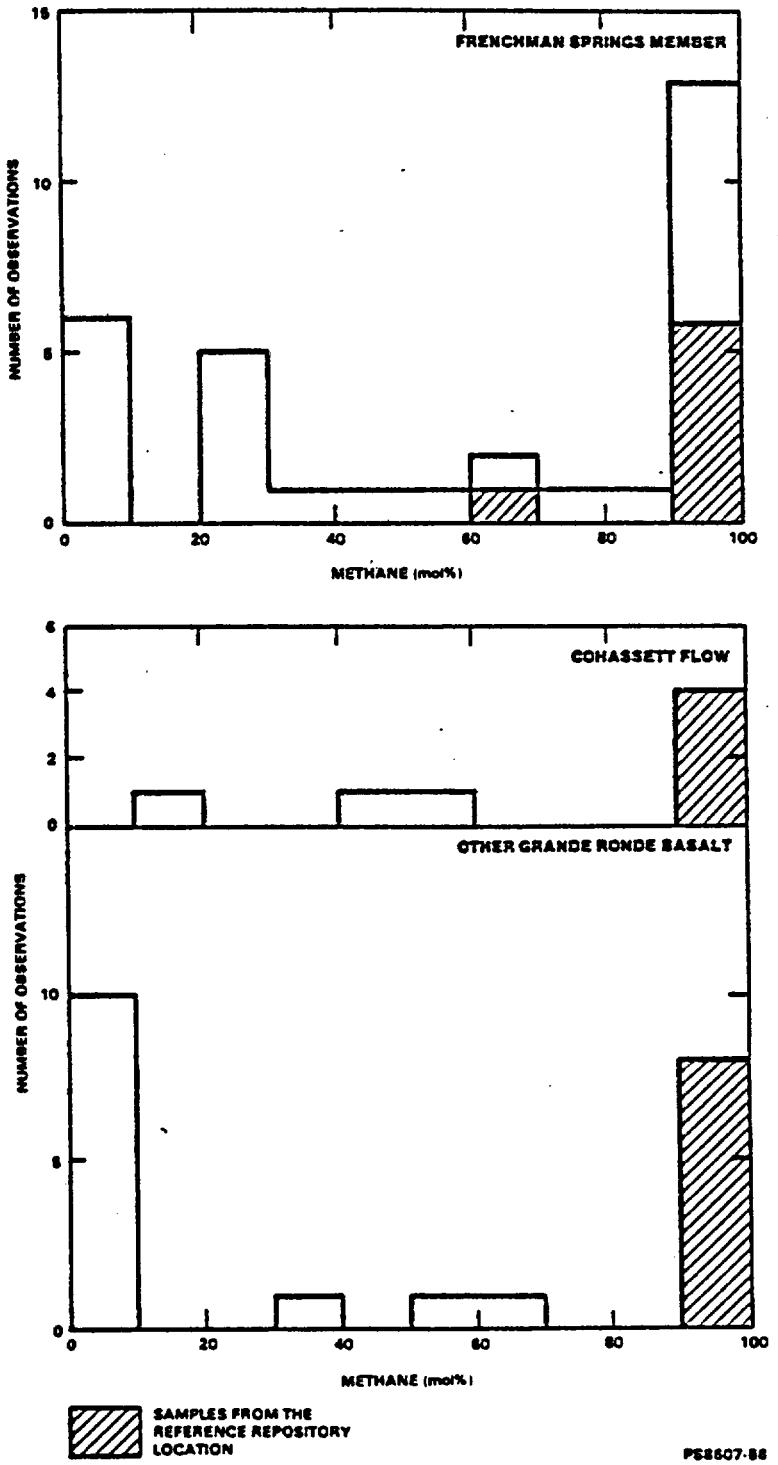

Figure 4.1-8. Frequency distributions of dissolved methane in groundwaters from the Frenchman Springs Member and Grande Ronde Basalt.

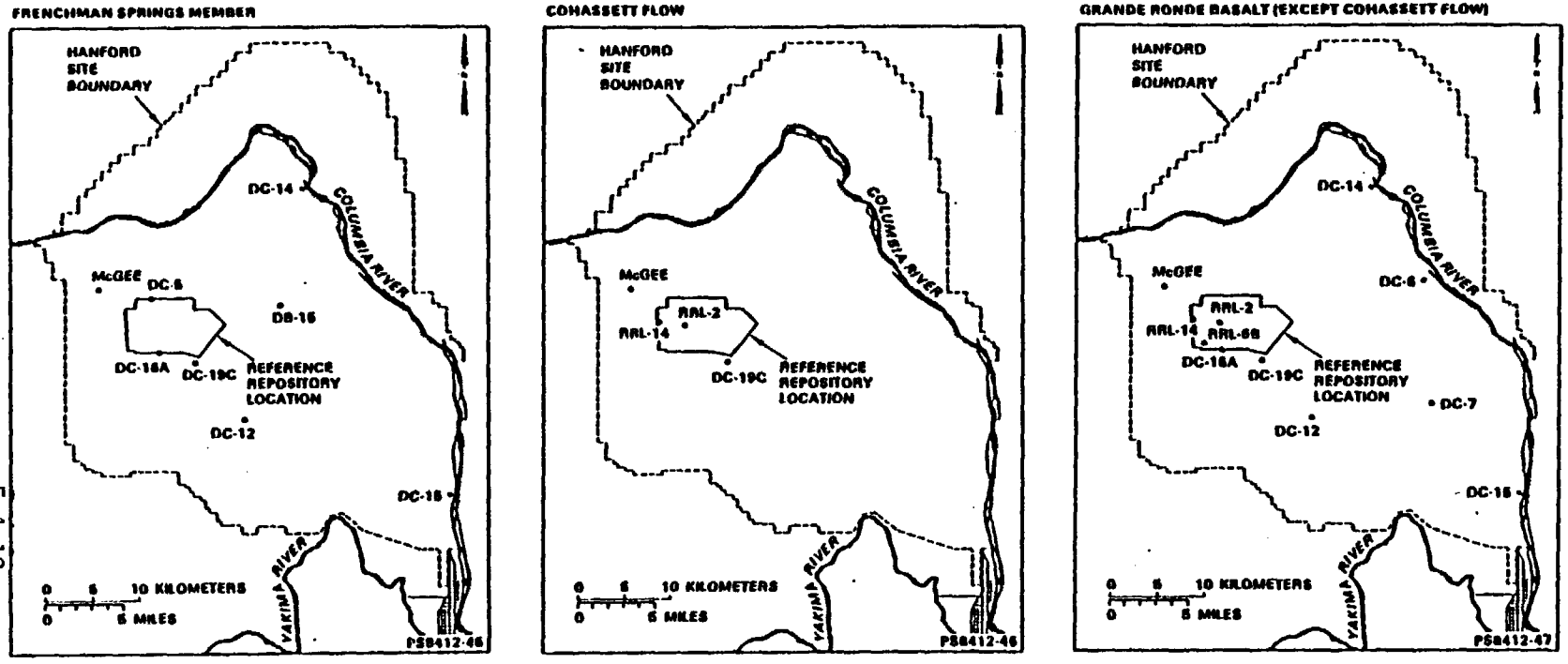

Figure 4.1-9. Location of boreholes from which dissolved gas data are used.

PS8412-45, -46, -47

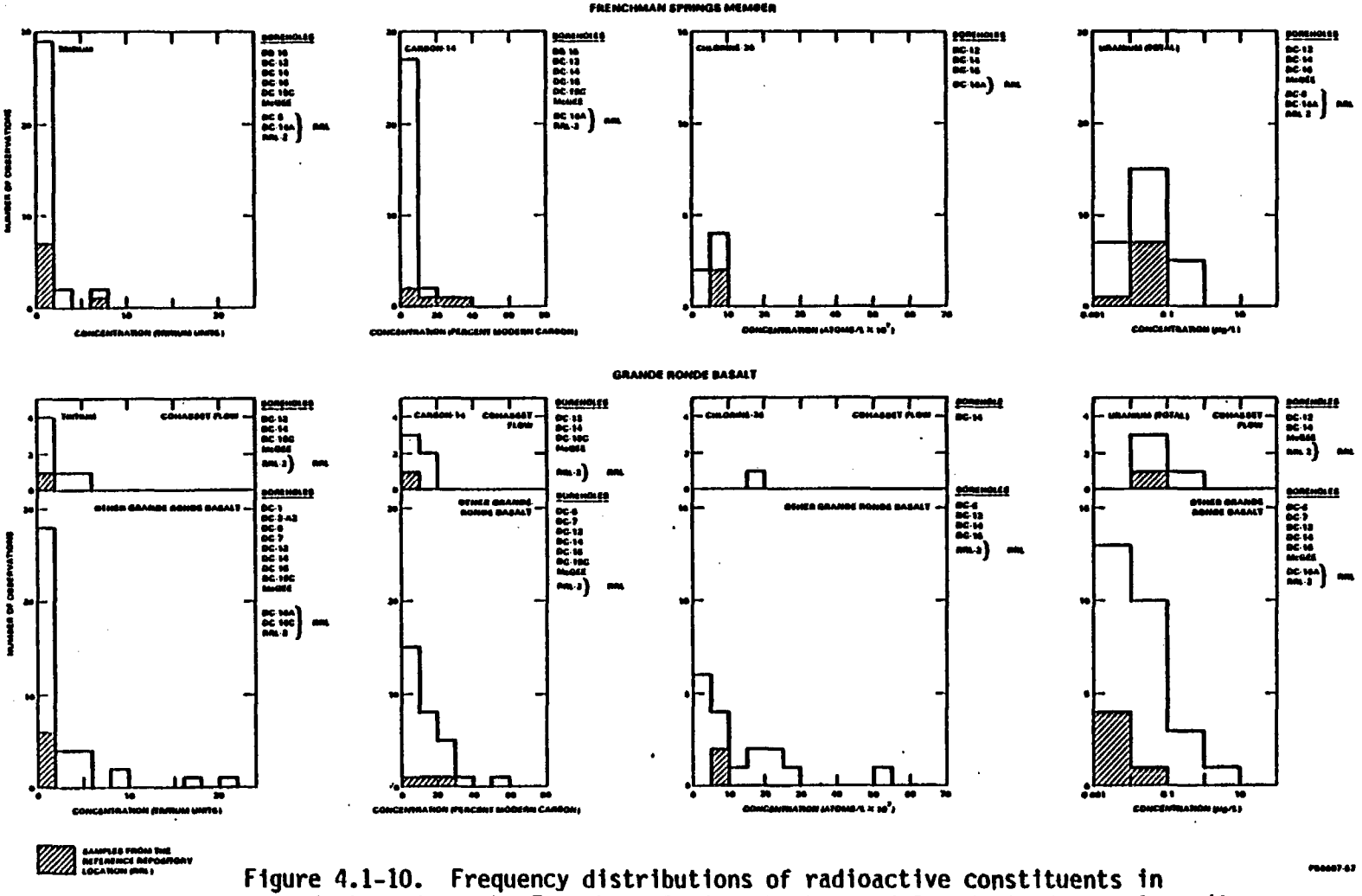

Figure 4.1-10. Frequency distributions of radioactive constituents in groundwaters from the Frenchman Springs Member and Grande Ronde Basalt. (One tritium value from a Frenchman Springs Member groundwater lies outside the range of the figure. See Fig. 4.1-5 for the location of sampled boreholes.)

FOLDOUT PS8607-57

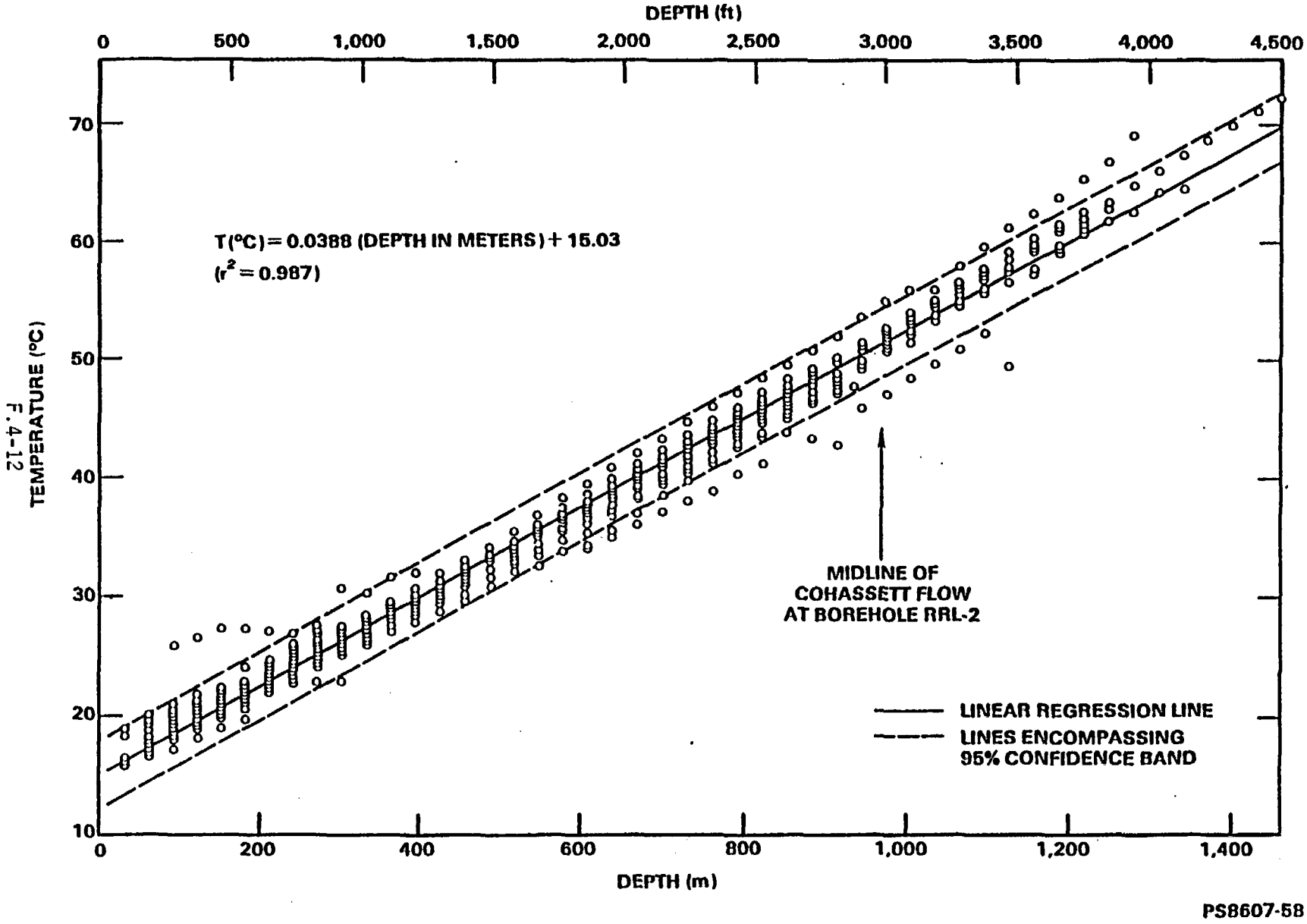

Figure 4.1-11. Measured fluid temperature versus depth in boreholes from the Hanford Site. (See Fig. 4.1-12 for borehole locations.)

F.4-12

CONTROLLED DRAFT 0
DECEMBER 22, 1986

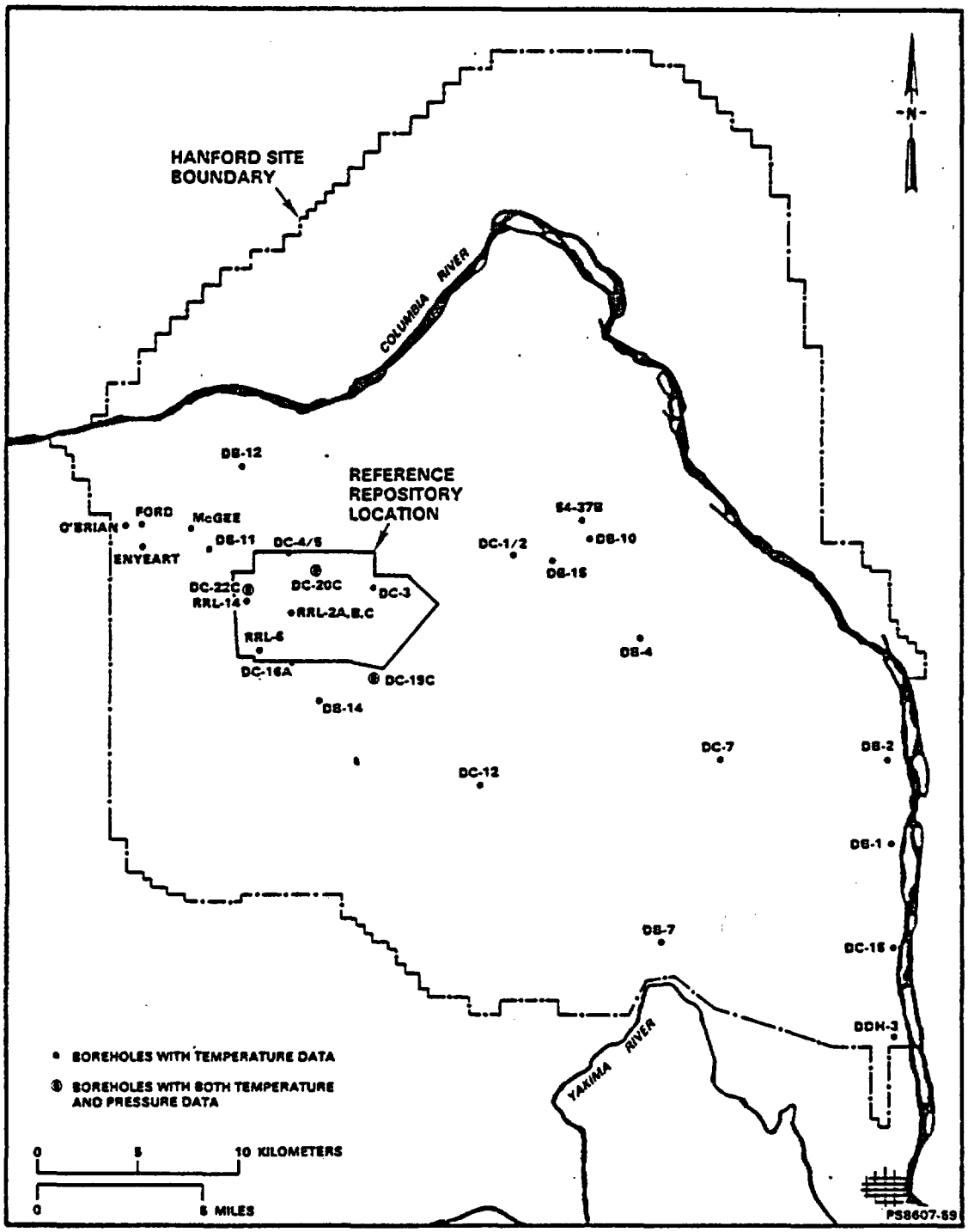

Figure 4.1-12. Locations of boreholes from which available temperature and pressure data are used.

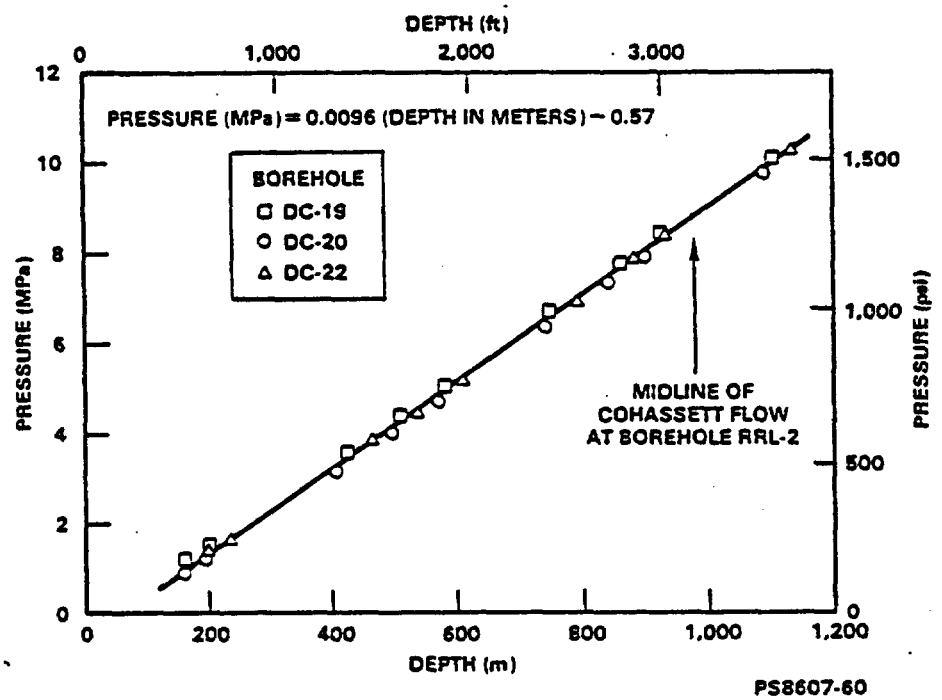

Figure 4.1-13. Measured hydrostatic pressure versus depth in piezometers from the vicinity of the reference repository location. (The line represents a linear regression fit to borehole pressure data. See Fig. 4.1-12 for borehole locations.)

PS8607-60

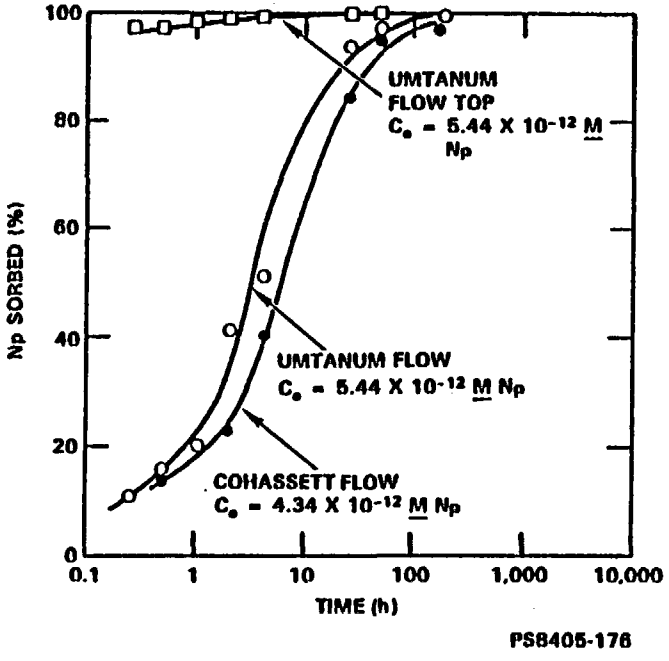

Figure 4.1-14. Sorption of neptunium on basalt of the Umtanum and Cohassett flow entablature and Umtanum flow top from reducing (0.1M hydrazine) GR-3 groundwater at 60 °C. (C_0 is the initial concentration.)

PS8405-176

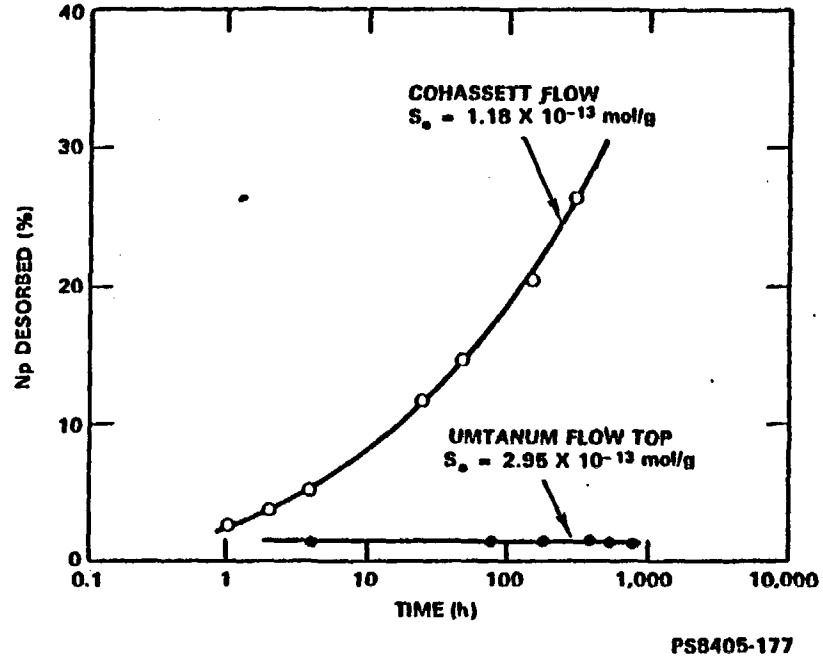

Figure 4.1-15. Desorption of neptunium from basalt of the Cohassett flow entablature and Umtanum basalt flow top into oxidizing GR-3 groundwater at 60 °C. (S_o is the initial sorbed concentration.)

PS8405-177

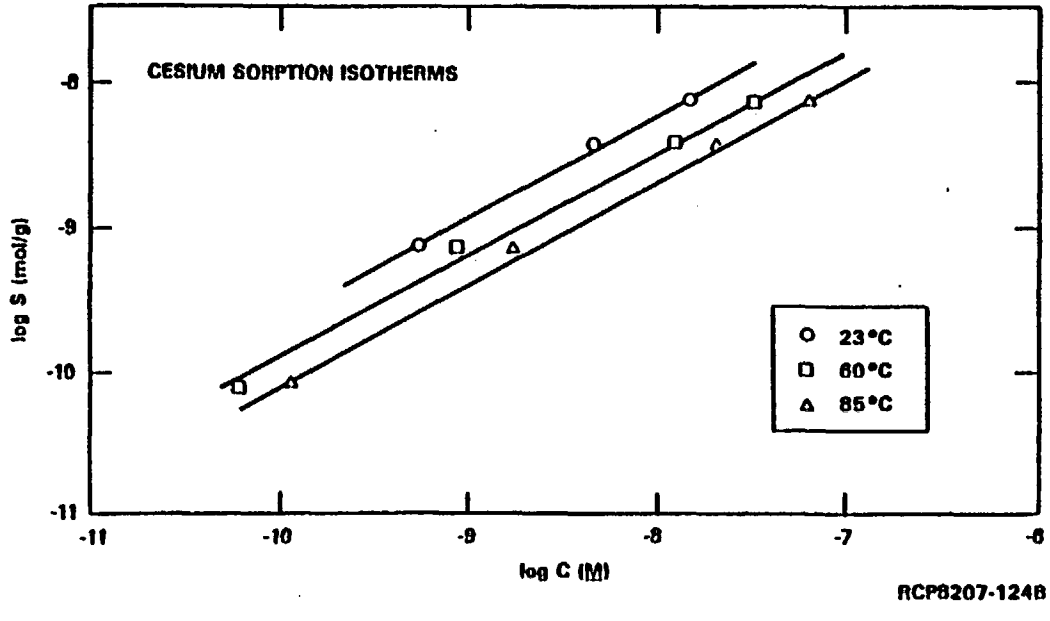

Figure 4.1-16. Cesium isotherms for sorption on sandstone of the Rattlesnake Ridge interbed under oxidizing conditions.

RCP8207-124B

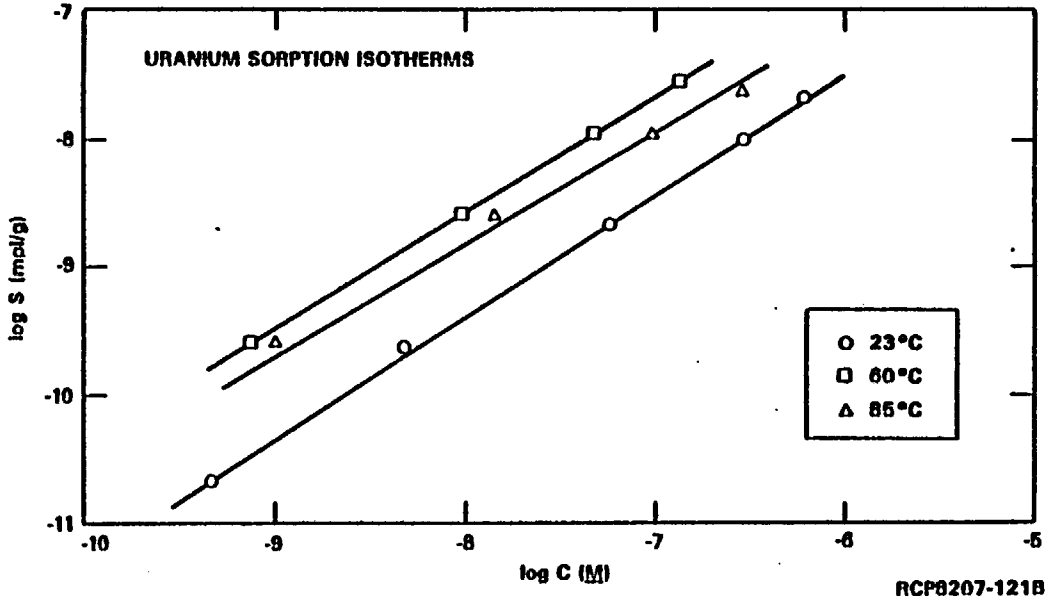

Figure 4.1-17. Uranium isotherms for sorption on sandstone of the Rattlesnake Ridge interbed under reducing conditions (0.05M hydrazine).

RCP8207-121B

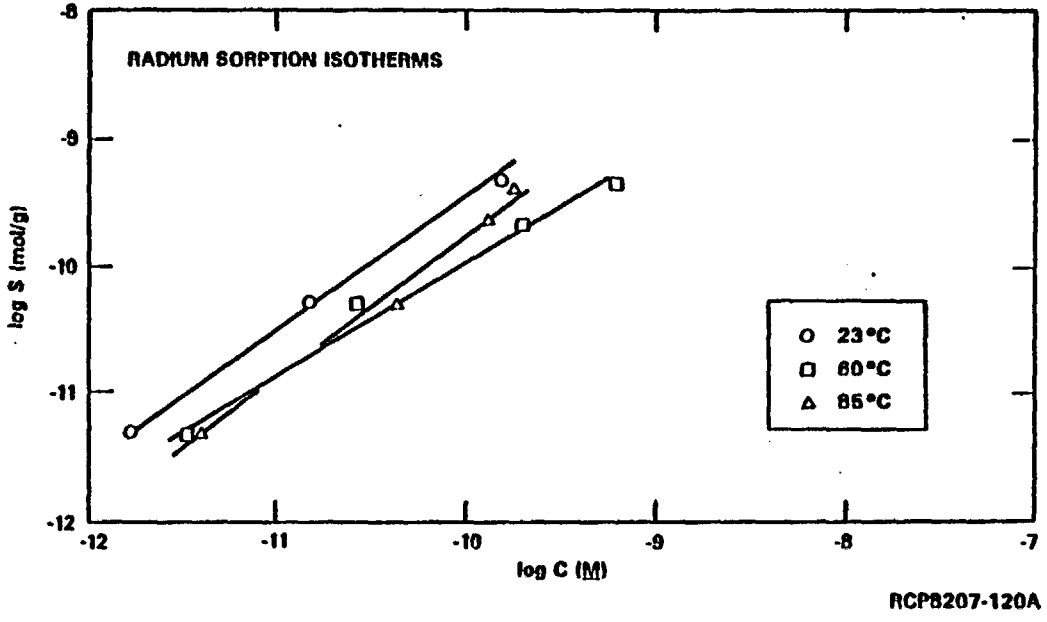

Figure 4.1-18. Radium isotherms for sorption on sandstone of the Rattlesnake Ridge interbed under oxidizing conditions.

RCP8207-120A

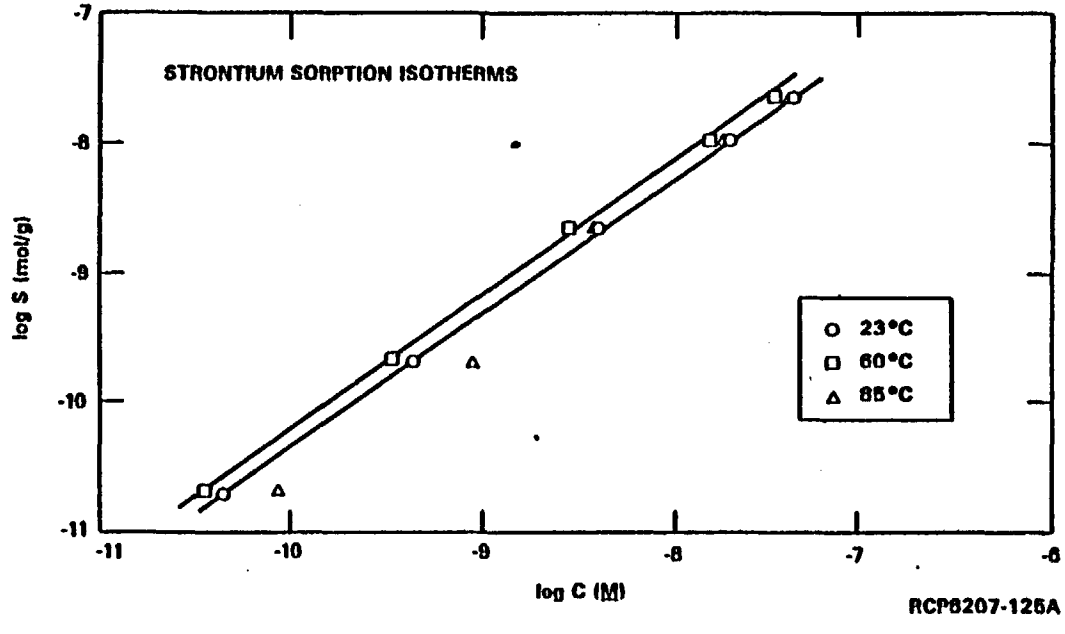

Figure 4.1-19. Strontium isotherms for sorption on sandstone of the Rattlesnake Ridge interbed under oxidizing conditions.

RCP8207-125A

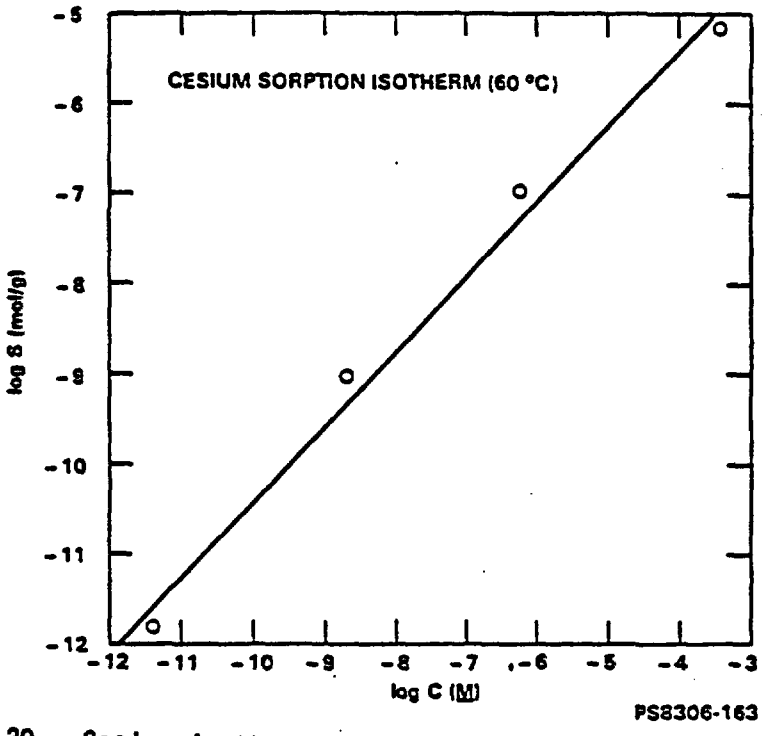

Figure 4.1-20. Cesium isotherms for sorption on basalt of the Umtanum flow under oxidizing conditions.

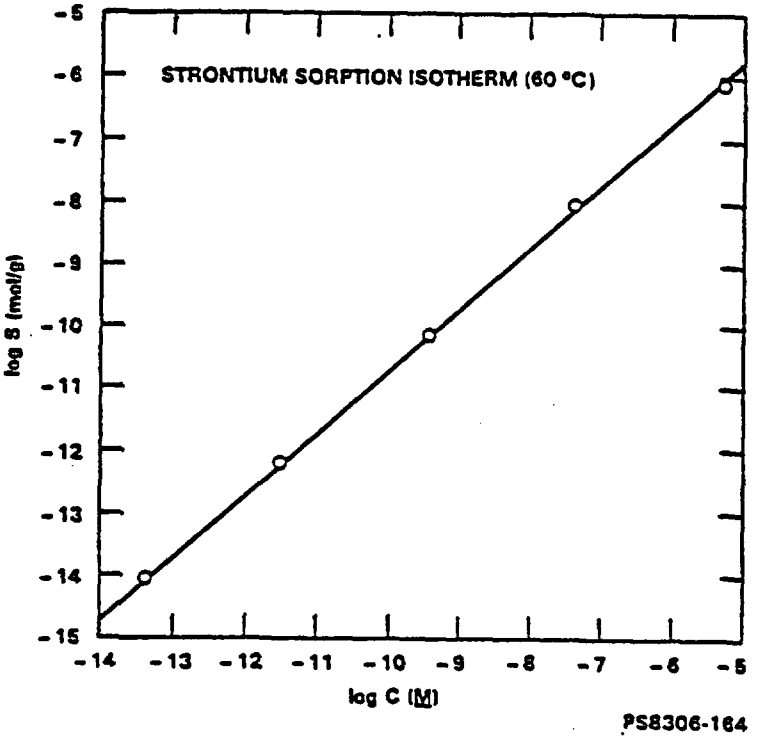

Figure 4.1-21. Strontium isotherms for sorption on basalt of the Umtanum flow under oxidizing conditions.

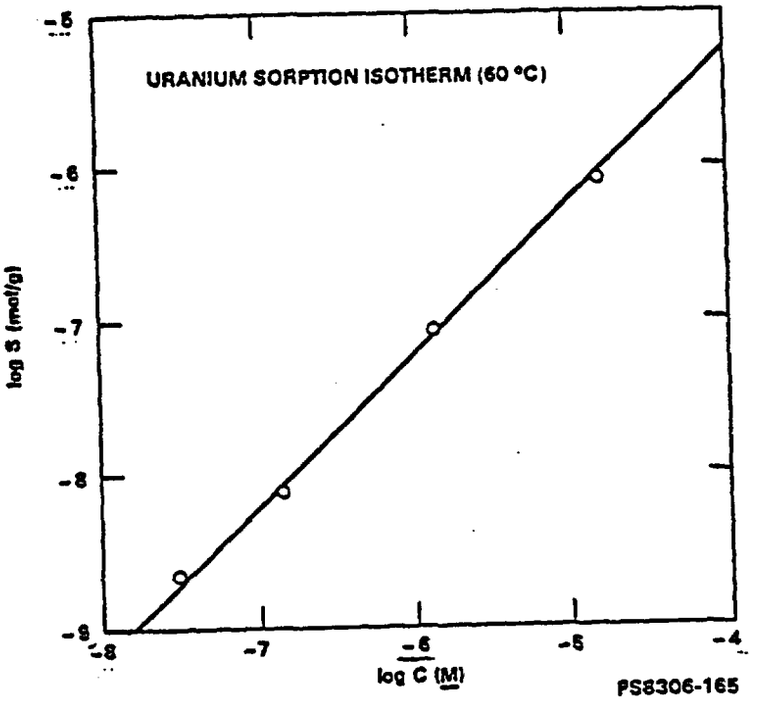

Figure 4.1-22. Uranium isotherms for sorption on basalt of the Umtanum flow under reducing conditions (0.1M hydrazine).

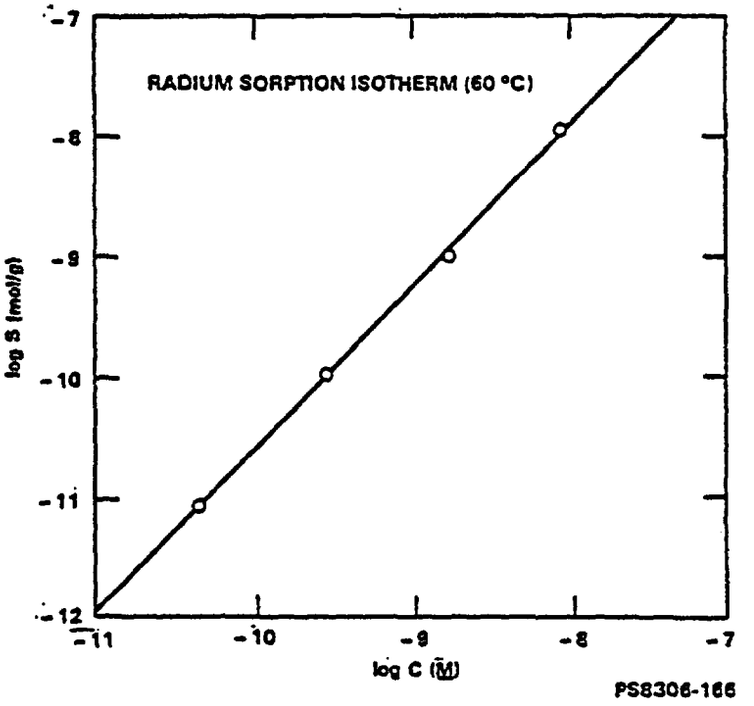

Figure 4.1-23. Radium isotherms for sorption on basalt of the Umtanum flow under oxidizing conditions.

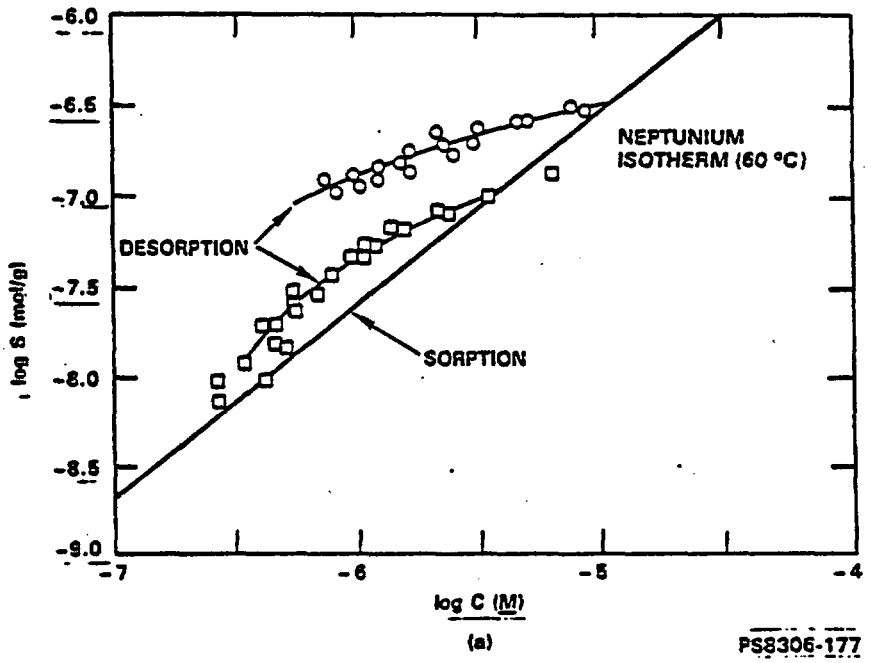

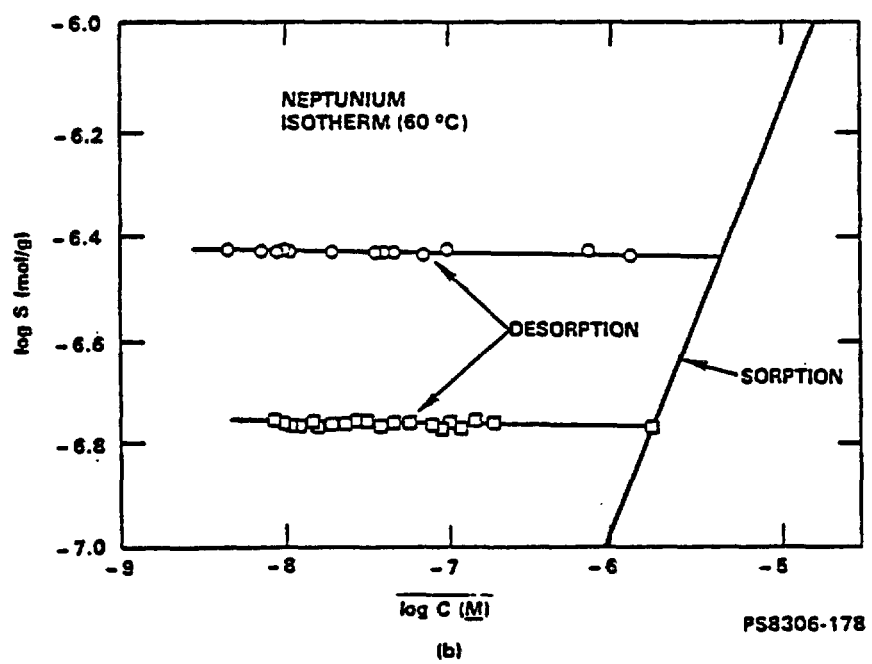

Figure 4.1-24. Sorption and desorption isotherms for neptunium on Mabton interbed solids under (a) oxidizing and (b) reducing conditions. (The O and □ symbols indicate different levels of radionuclide loading.)

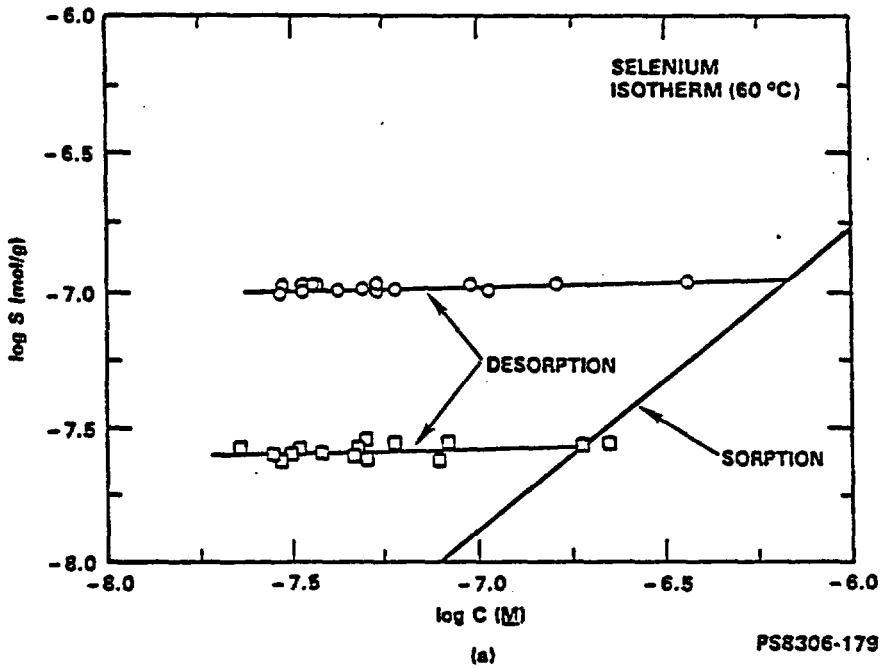

Figure 4.1-25. Sorption and desorption isotherms for selenium on Mabton interbed solids under reducing conditions. (The O and □ symbols indicate different levels of radionuclide loading.)

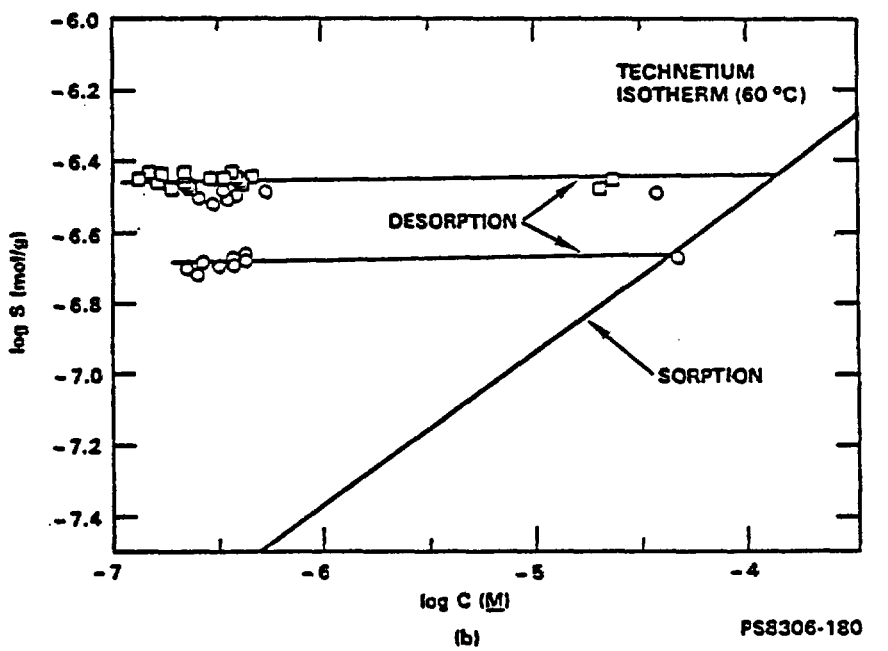

Figure 4.1-26. Sorption and desorption isotherms for technetium on Mabton interbed solids under reducing conditions. (The O and □ symbols indicate different levels of radionuclide loading.)

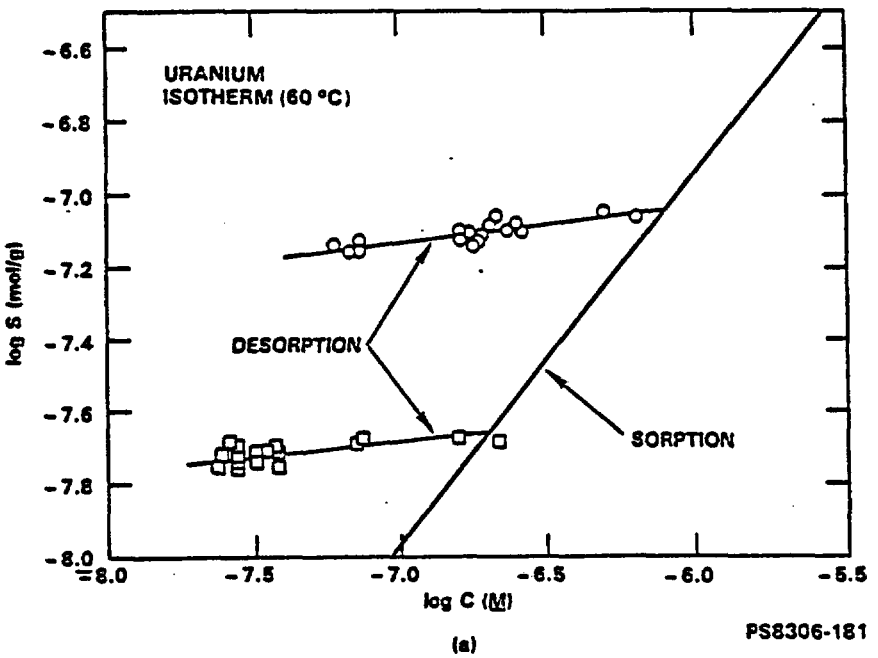

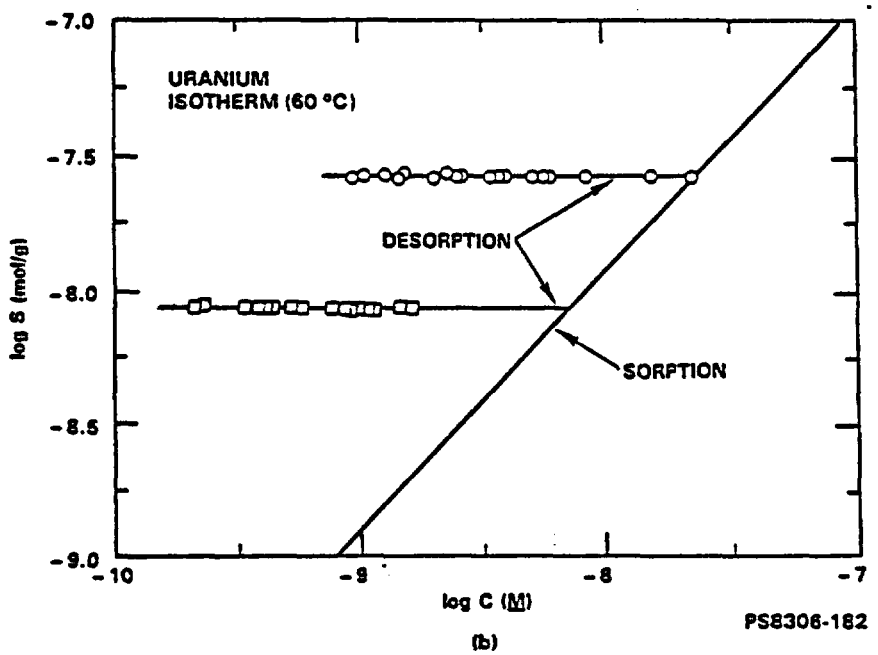

Figure 4.1-27. Sorption and desorption isotherms for uranium on Mabton interbed solids under (a) oxidizing, and (b) reducing conditions. (The O and □ symbols indicate different levels of radionuclide loading.)

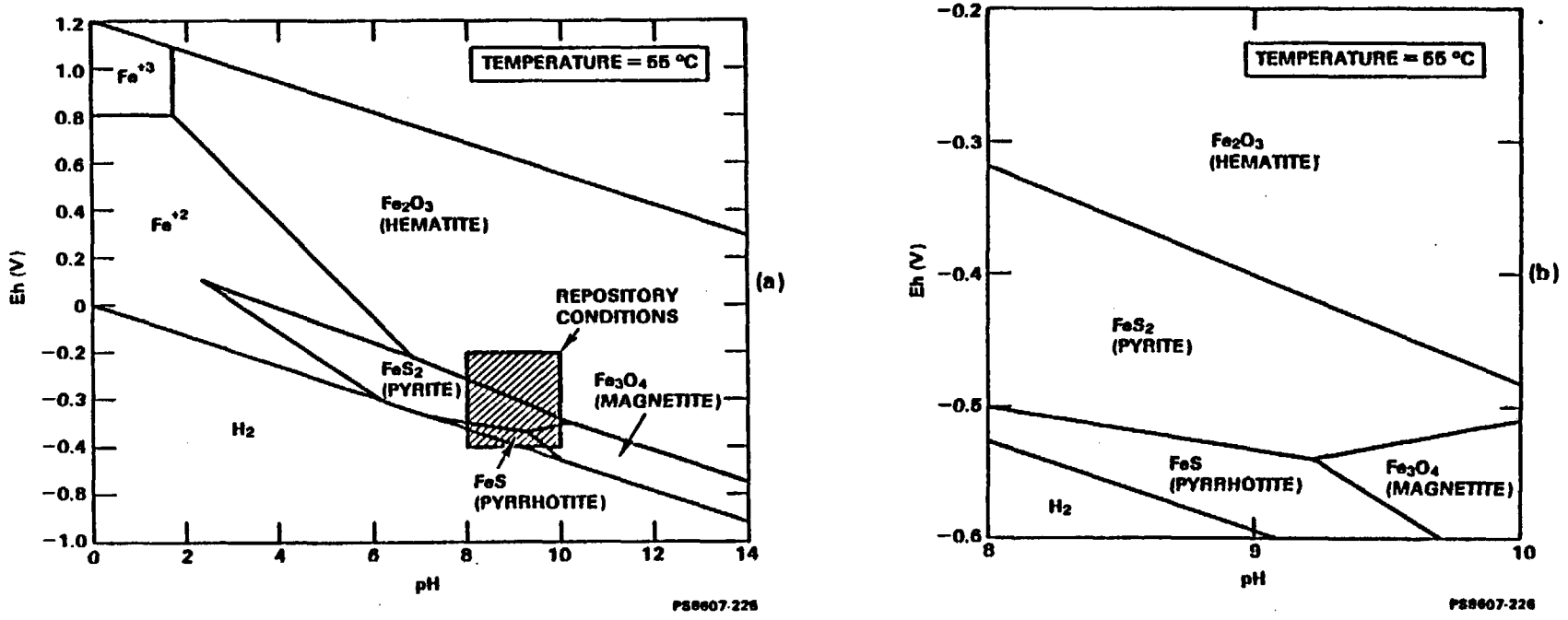

Figure 4.1-28. Eh-pH diagram for the Fe-H_2O-S system relating the various iron phases. Entire field is shown in Figure a. The area marked repository conditions is expanded and shown in Figure b. Diagrams were constructed assuming (total S) = $10^{-4.5}$ m, with HS^- and SO_4^{2-} at equilibrium, (total Fe) = 10^{-6} m at the solution solid boundary and the following source of thermodynamic data: solids and gases (Helgesen et al., 1978); water (Helgeson and Kirkham, 1974); HS^-, SO_4^{2-} (Helgeson et al., 1981); Fe^{2+}/Fe^{3+} (Helgeson, 1985); $H_2S \pm H^+ + HS^-$ (Helgeson, 1969).

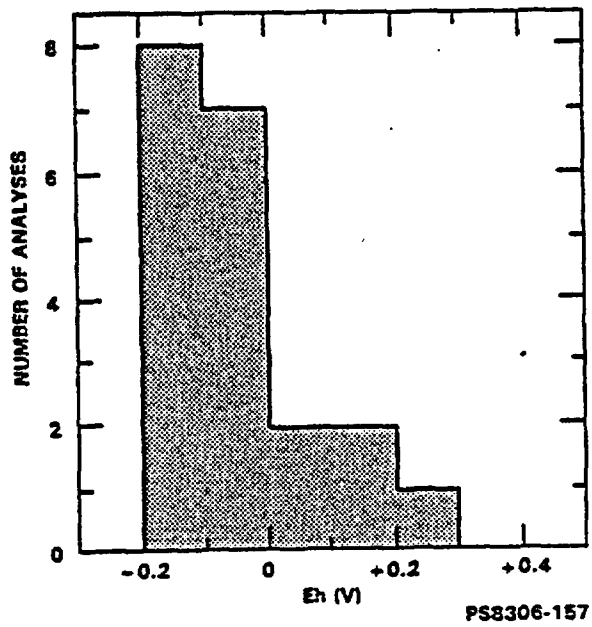

Figure 4.1-29. Histogram of measured Eh values (using a platinum electrode) for Grande Ronde Basalt groundwaters sampled at the Hanford Site in boreholes DC-6, -7, -12, -14, and -15.

PS8306-157

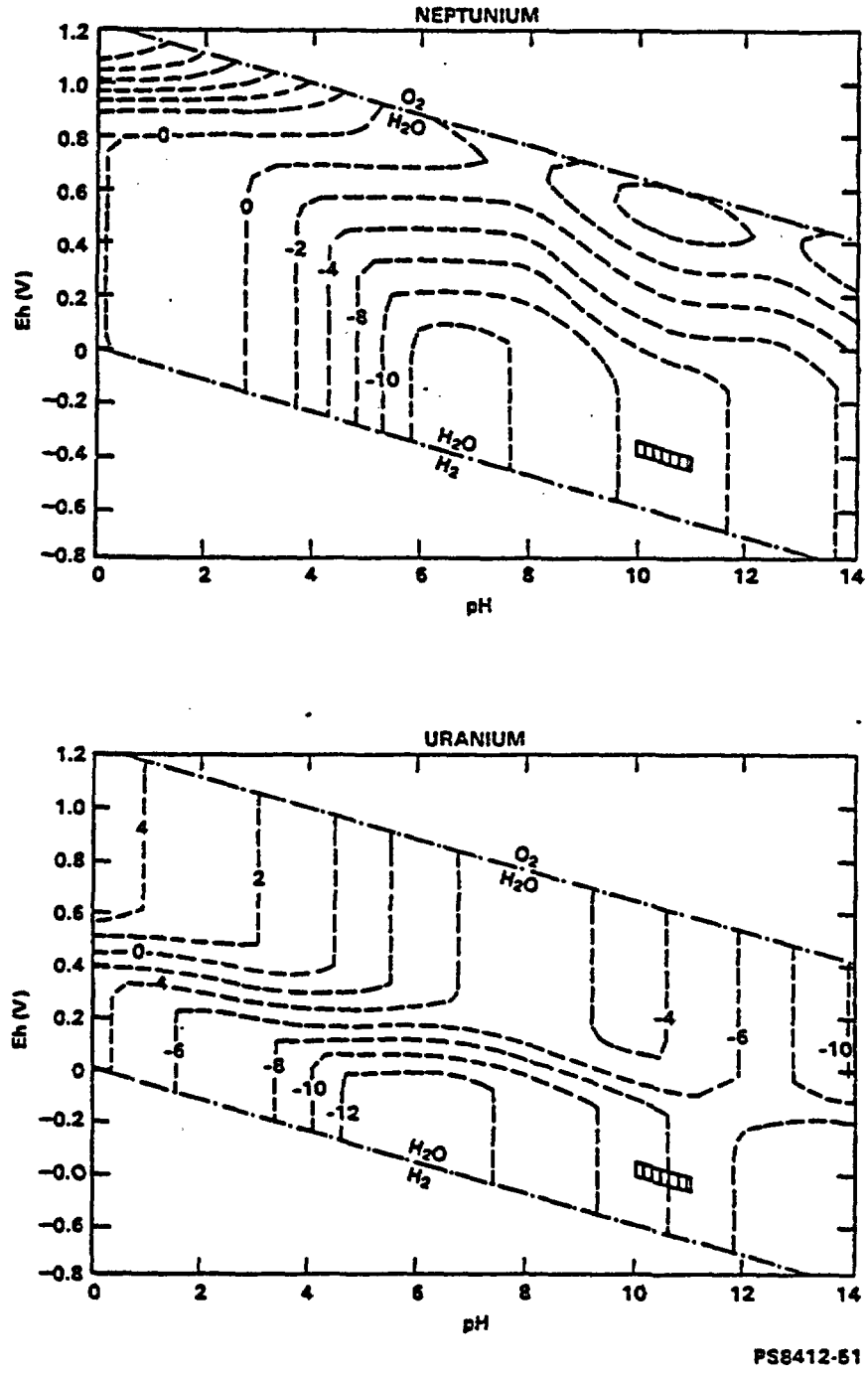

Figure 4.1-30. Eh-pH diagrams for uranium and neptunium.

PS8412-51

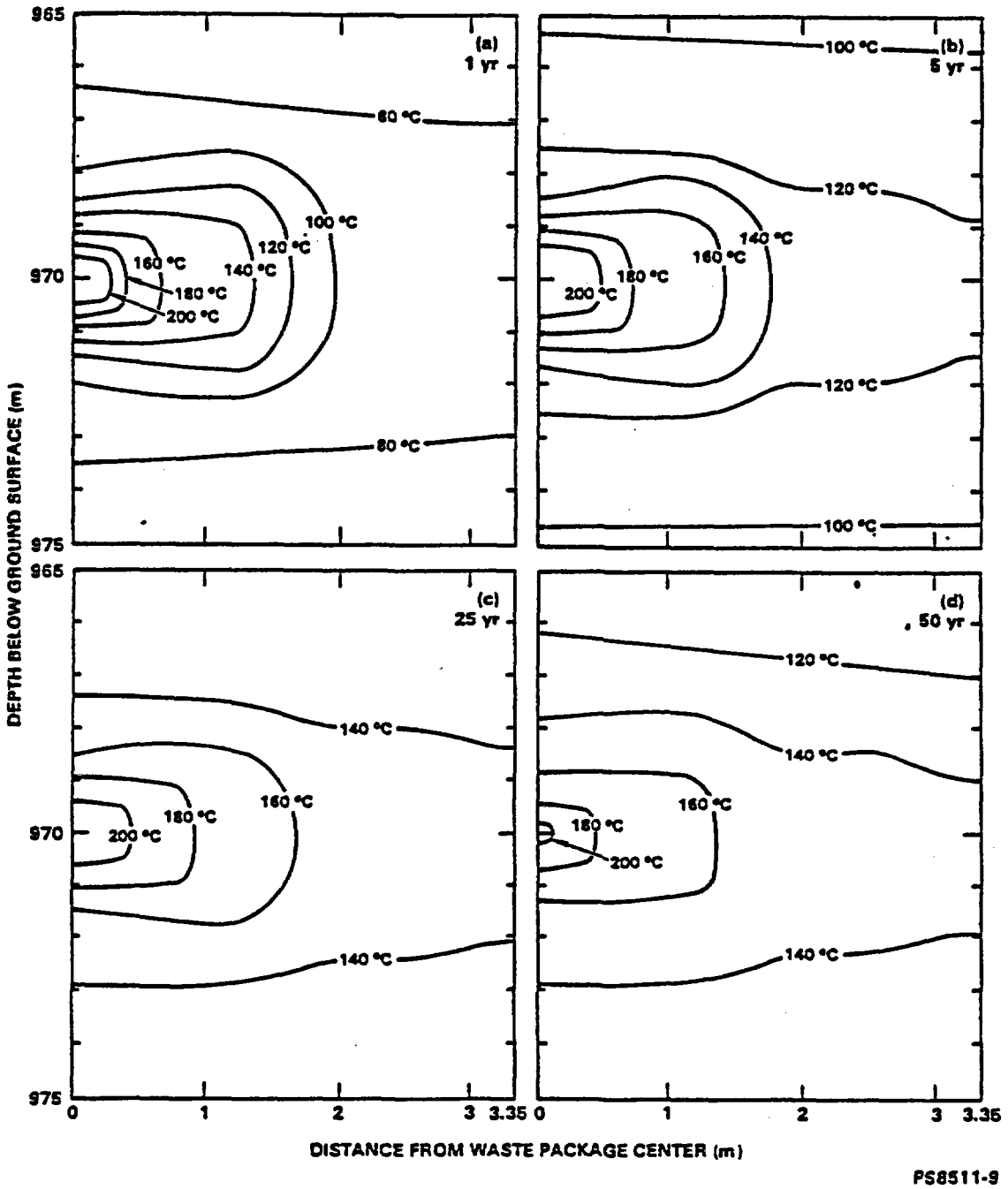

Figure 4.2-1. Isotherms in a waste-package bisecting plane (which is oriented perpindicular to the long axis of the waste container) at 1, 5, 25, and 50 years (Yung et at., 1986, pp. 1-6).

PS8511-9

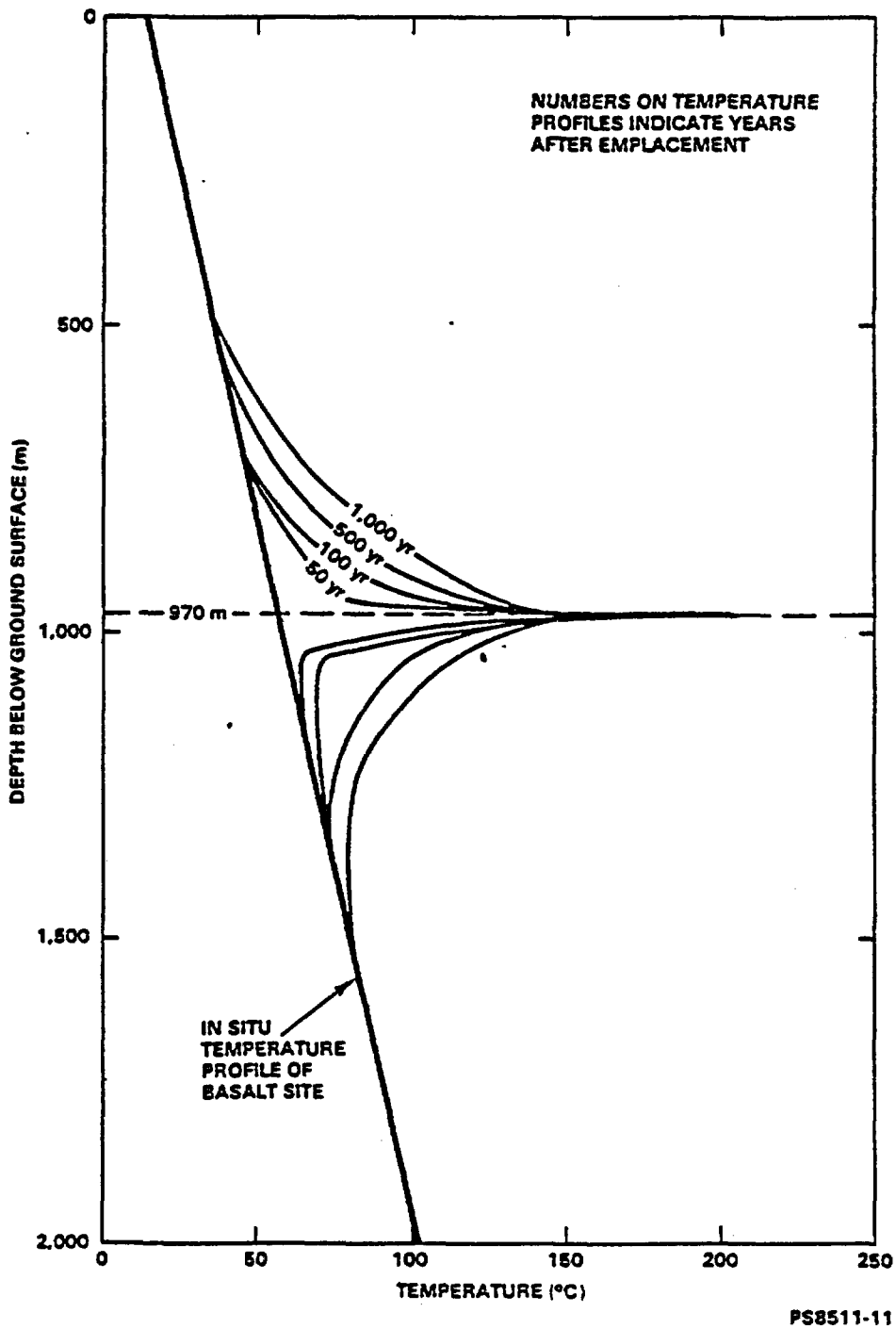

Figure 4.2-2. Temperature profiles in basalt at 50, 100, 50, and 1,000 years (Yung et al., 1986, pp. 1-6). (The orientation of the plane shown here is the same as shown in Fig. 4.2-1.)

PS8511-11

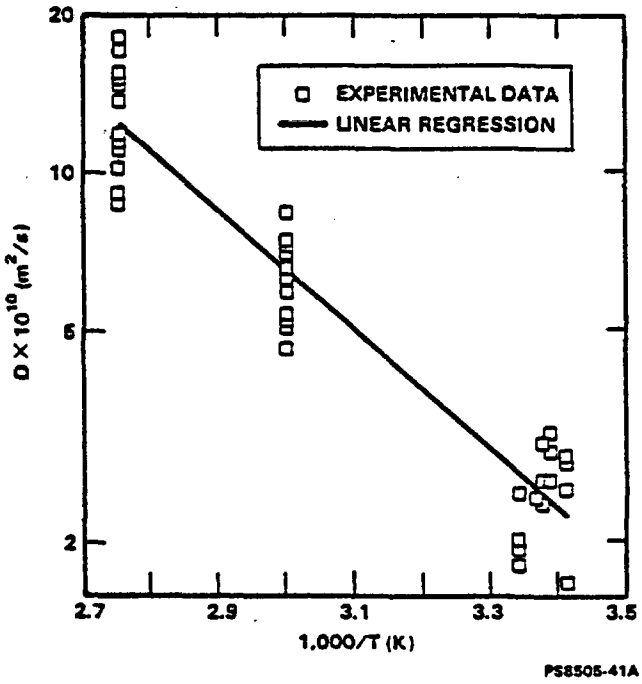

Figure 4.2-3. Tritium diffusion coefficients are plotted on a logarithmic scale versus the inverse of temperature.

PS8505-41A

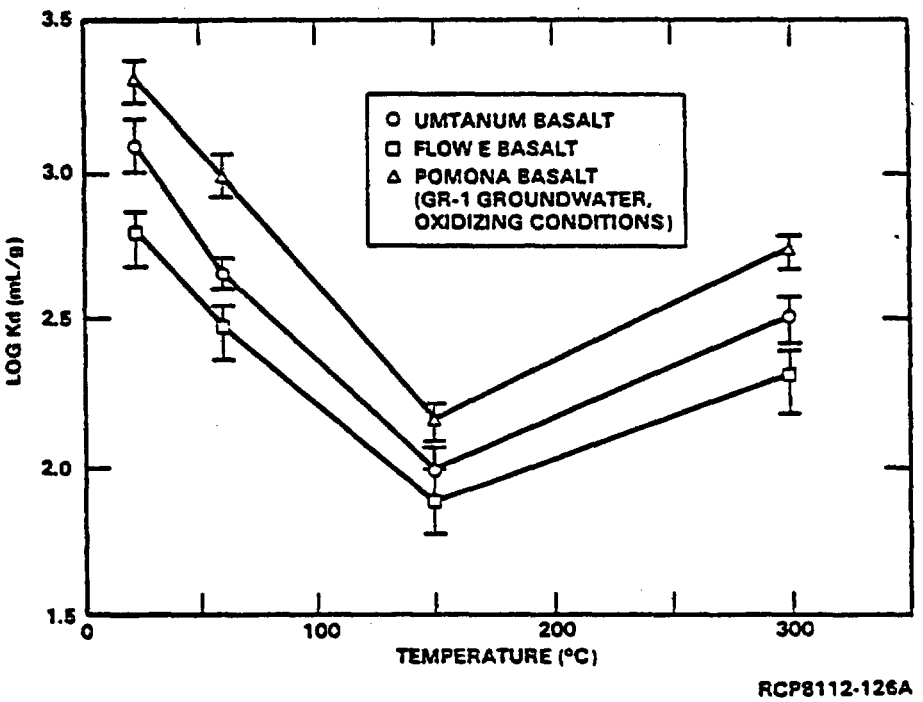

Figure 4.2-4. Kd dependence on temperature for ^{137}Cs.

RCP8112-126A

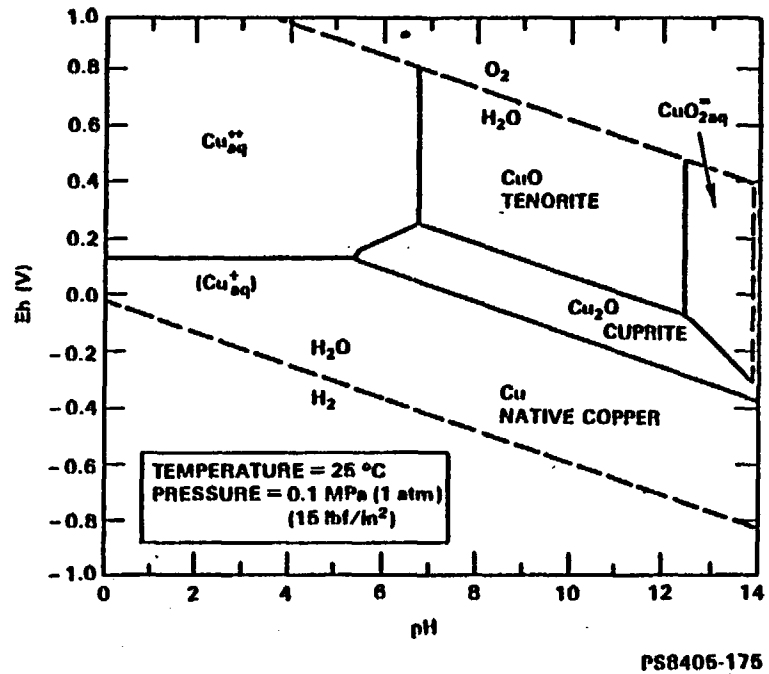

Figure 4.3-1. Stability relations among copper compounds in the system Cu-H_2O-O_2 at 25 °C and 1 atmosphere total pressure (from Garrels and Christ, 1965, p. 239).

PS8405-175

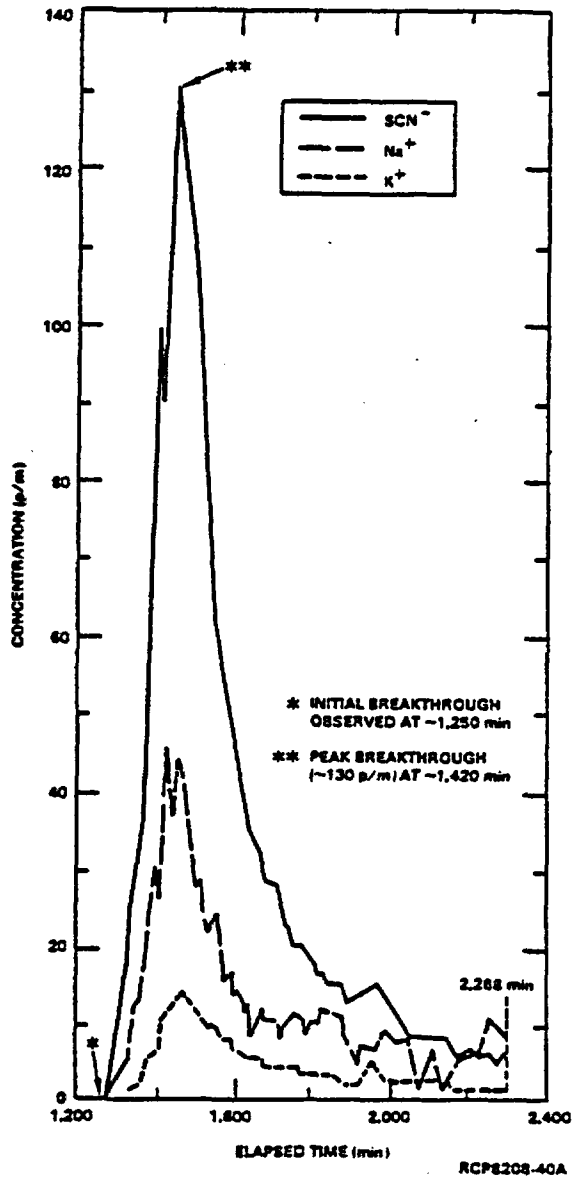

Figure 4.3-2. Tracer breakthrough curves for the Hanford Site tracer test.

RCP8208-40A

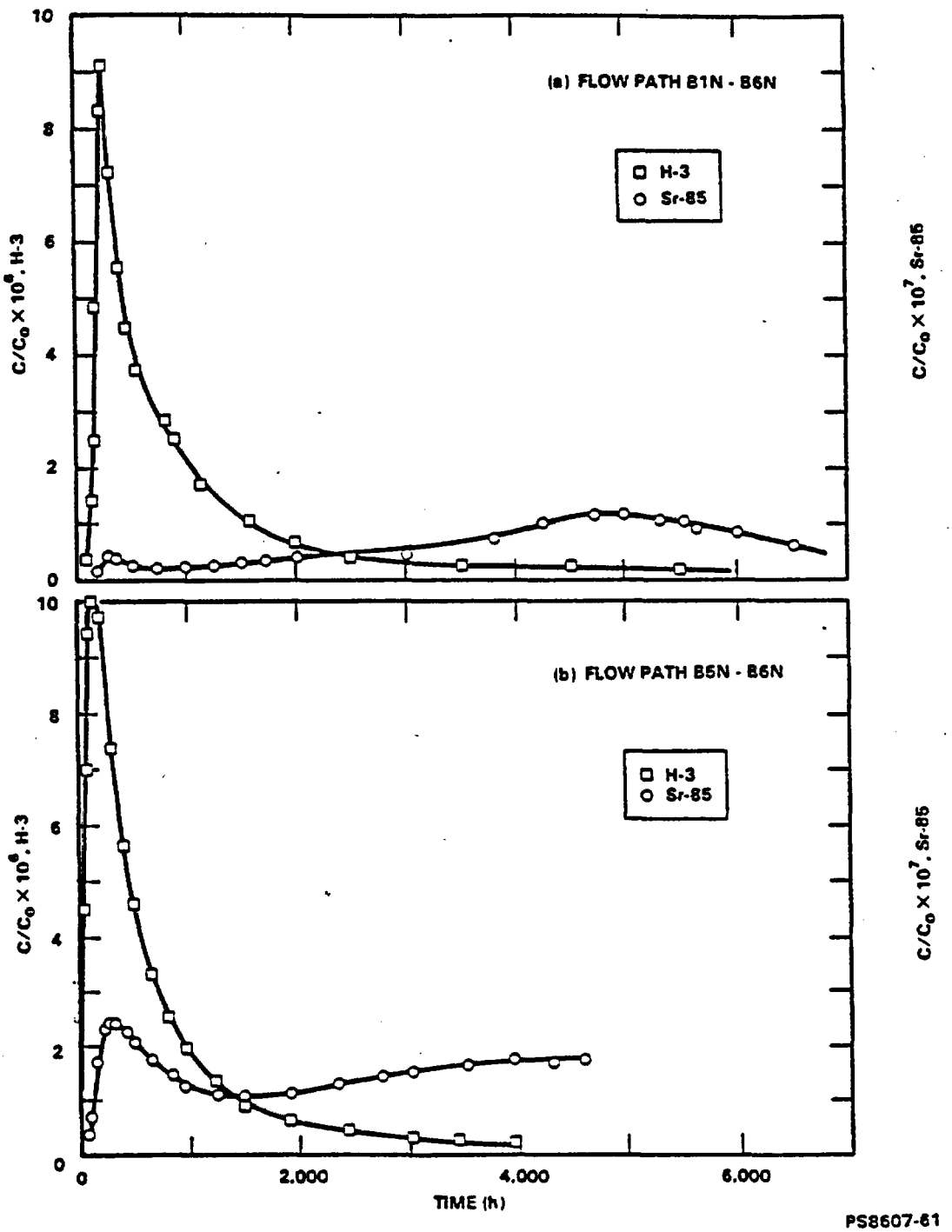

Figure 4.3-3. Tracer breakthrough curves for the Swedish tracer tests (Landstrom et al., 1983).

Table 4.0-1. Federal regulatory performance criteria that require geochemical information (sheet 1 of 3)

Regulatory performance criteria	Required geochemical information
10 CFR 60 (NRC, 1985, pp. 563-593)	
Section 60.112 Overall system performance objective for the geologic repository after permanent closure. The geologic setting shall be selected and the engineered barrier system and the shafts, boreholes and their seals shall be designed to assure that releases of radioactive materials to the accessible environment following permanent closure conform to such generally applicable environmental standards for radioactivity as may have been established by the Environmental Protection Agency with respect to both anticipated processes and events and unanticipated processes and events. Section 60.113 Performance of particular barriers after permanent closure. (a) General provisions. (1) Engineered barrier system. (i) The engineered barrier system shall be designed so that assuming anticipated processes and events: (A) Containment of HLW will be substantially complete during the period when radiation and thermal conditions in the engineered barrier system are dominated by fission product decay, and (B) any release of radionuclides from the engineered barrier system shall be a gradual process which results in small fractional releases to the geologic setting over long times. For disposal in the saturated zone, both the partial and complete filling with groundwater of available void spaces in the underground facility shall be appropriately considered and analyzed among the anticipated processes and events in designing the engineered barrier system. (ii) In satisfying the preceding requirement the engineered barrier system shall be designed assuming anticipated processes and events, so that: (A) Containment of HLW within the waste package will be substantially complete for a period to be determined by the Commission taking into account the factors specified in Sec. 60.113(b) provided that such period shall not be less than 300 years nor more than 1,000 years after permanent closure of the geologic repository; and	The repository performance criteria are essentially radionuclide containment time, release rates (from the waste package and to the accessible environment), and groundwater travel time. Geochemical parameters influence processes that control containment time and release rates. In addition, geochemical data can provide supportive evidence for estimating groundwater travel time. The geochemical parameters that control containment processes (saturation of packing material, container corrosion, waste form leaching, radionuclide dissolution and precipitation, radionuclide sorption on waste package materials, hydrothermal alteration of packing material, radionuclide diffusion, and radiolysis) are: 1. Groundwater composition a. Major and trace inorganic components b. Organic components c. Dissolved gases 2. pH 3. Redox potential 4. Colloid concentration and composition 5. Composition of waste package components a. Mineralogy b. Surface area c. Cation exchange capacity d. Redox capacity Geochemical parameters that control radionuclide release processes (radionuclide sorption on geologic minerals, radionuclide precipitation, radionuclide diffusion, and hydrothermal alteration of host rock) to the accessible environment are the same as those listed above, except that the composition of geologic solids in the flow path must be included. The rates of each of these processes must also be estimated. Geochemical information that may be used in estimating groundwater travel times include isotopic concentrations of ^{14}C, ^{36}Cl, and ^{4}He.

Table 4.0-1. Federal regulatory performance criteria that require geochemical information (sheet 2 of 3)

Regulatory performance criteria	Required geochemical information
10 CFR 60 (NRC, 1985, pp. 563-593)	
Section 60.113 Performance of particular barriers after permanent closure. (Continued) (B) The release rate of any radionuclide from the engineered barrier system following the containment period shall not exceed one part in 100,000 per year of the inventory of that radionuclide calculated to be present at 1,000 years following permanent closure or such other fraction of the inventory as may be approved or specified by the Commission; provided that this requirement does not apply to any radionuclide which is released at a rate less than 0.1% of the calculated total release rate limit. The calculated total release rate limit shall be taken to be one part in 100,000 per year of the inventory of radioactive waste originally emplaced in the underground facility that remains after 1,000 years of radioactive decay. (2) Geologic setting. The geologic repository shall be located so that prewaste-emplacement groundwater travel time along the fastest path of likely radionuclide travel from the disturbed zone to the accessible environment shall be at least 1,000 years or such other travel time as may be approved or specified by the Commission.	The above information applies here also.
40 CFR 191 (EPA, 1985, pp. 38066-38089)	
Section 191.13 Containment Requirements. (a) Disposal systems for spent nuclear fuel or high-level or transuranic wastes shall be designed to provide a reasonable expectation, based upon performance assessments, that the cumulative releases of waste to the accessible environment for 10,000 years after disposal from all significant processes and events that may affect the disposal system shall: (1) have a likelihood of less than one chance in 10 of exceeding the quantities calculated according to Table 1	The repository performance criteria are essentially radionuclide containment time, release rates (from the waste package and to the accessible environment), and groundwater travel time. Geochemical parameters influence processes that control containment time and release rates. In addition, geochemical data can provide evidence for estimating groundwater travel time. The geochemical parameters that control containment processes (saturation of packing material, container corrosion, waste form

Table 4.0-1. Federal regulatory performance criteria that require geochemical information (sheet 3 of 3)

Regulatory performance criteria	Required geochemical information
40 CFR 191 (EPA, 1985, pp. 38066-38089)	
Section 191.13 Containment Requirements. (Continued) (Appendix A), and (2) have a likelihood of less than one chance in 1,000 of exceeding 10 times the quantities calculated according to Table 1 (Appendix A).	leaching, radionuclide dissolution and precipitation, radionuclide sorption on waste package materials, hydrothermal alteration of packing material, radionuclide diffusion, and radiolysis) are: 1. Groundwater composition a. Major and trace inorganic components b. Organic components c. Dissolved gases 2. pH 3. Redox potential 4. Colloid concentration and composition 5. Composition of waste package components a. Mineralogy b. Surface area c. Cation exchange capacity d. Redox capacity Geochemical parameters that control radionuclide release processes (radionuclide sorption on geologic minerals, radionuclide precipitation, radionuclide diffusion, and hydrothermal alteration of host rock) to the accessible environment are the same as those listed above, except that the composition of geologic solids in the flow path must be included. Geochemical information that may be used in estimating groundwater travel times include isotopic concentrations of ^{14}C, ^{36}Cl, and ^{4}He.

Table 4.0-2. Natural system geochemical information required by Federal siting criteria compared with that given in Chapter 4 and related studies from Chapter 8 (sheet 1 of 2)

Federal regulations	Summary of regulations	Chapter 4 information	Studies from Chapter 8
10 CFR 60, Section 60.122(a)(1) (NRC, 1985, pp. 563-593) and 10 CFR 960, Section 960.4-2-2(b) (DOE, 1984, pp. 47761)	Siting criteria require that favorable conditions of the geologic setting must be sufficient to provide reasonable assurance that performance objectives of waste isolation will be met. Favorable conditions include:		
	1. The rate and nature of geochemical processes operating during the Quaternary Period would not affect (or would favorably affect) waste isolation	Geochemical processes occurring in the natural system that could affect waste isolation are addressed in Section 4.2 and 4.4. Natural analogs that represent long-term processes are presented in Section 4.3.1. The paragenesis of basalt secondary minerals is discussed in Section 4.1.1.3.2.2.2, and projected rates of geochemical processes are addressed in Section 4.1.1.4.	Mineralogic and Petrologic Characterization (Section 8.3.1.2.3) Basalt/Groundwater Interactions (Section 8.3.4.2.2.3.1) Geochemical Environment Analysis (Section 8.3.4.2.2.3.2) Groundwater Flow System Hydrochemistry (Section 8.3.1.4.2.3.1)
	2. Geochemical conditions that promote precipitation or sorption of radionuclides and inhibit formation of particulate colloids, and organic complexes that increase the mobility of radionuclides	Effects of groundwater composition, geologic solid type, colloids, and other variables on radionuclide sorption are given in Section 4.1.3.3.	Radionuclide Retardation Behavior (Section 8.3.1.4.3.3.1) Radionuclide Solubility/Sorption and Speciation Behavior (Section 8.3.4.3.5.3.1)
	3. Mineral assemblages that will retain their capacity to inhibit radionuclide migration after the thermal period.	The stability of mineral assemblages in the site system is addressed in Sections 4.1.1.4 and 4.4. Alteration products from basalt diagenesis and weathering are described in Sections 4.1.1.3.2.2.2 and 4.3.1.	Mineralogic and Petrologic Characterization (Section 8.3.1.2.3) Radionuclide Retardation Behavior (Section 8.3.1.4.3.3.1)

Table 4.0-2. Natural system geochemical information required by Federal siting criteria compared with that given in Chapter 4 and related studies from Chapter 8 (sheet 2 of 2)

Federal regulations	Summary of regulations	Chapter 4 information	Studies from Chapter 8
10 CFR 60, Section 60.122(a)(1) (NRC, 1985, pp. 563-593) and 10 CFR 960, Section 960.4-2-2(c) (DOE, 1984, pp. 47761)	Siting criteria require that potentially adverse conditions must be adequately investigated to show that they do not compromise the performance of the repository. Potentially adverse conditions include:		
	1. Geochemical processes that would reduce sorption of radionuclides or degrade rock strength	Effects of groundwater composition, geologic solid type, colloids, and other geochemical variables on radionuclide sorption are given in Section 4.1.3.3.	Radionuclide Retardation Behavior (Section 8.3.1.4.3.3.1) Basalt/Groundwater Interactions (Section 8.3.4.2.2.3.1)
	2. Groundwater conditions in the host rock that are not reducing	Redox conditions expected in the host rock environment are given in Section 4.1.3.4.	Redox Characterization of Groundwater (Section 8.3.1.4.2.3.2)
	3. Groundwater conditions in the host rock that could affect the solubility or chemical reactivity of the engineered barriers system so that the expected repository performance could be compromised.	Expected groundwater conditions are given in Sections 4.1.2 (composition, temperature, pressure) and 4.1.3.4 (pH, redox potential, complexing species).	Groundwater Flow System Hydrochemistry (Section 8.3.1.4.2.3.1) Chemical Stability (Section 8.3.4.3.4.3.1) General Corrosion (Section 8.3.4.3.3.3.1)
10 CFR 60, Section 60.113(b)(3) (NRC, 1985, pp. 563-593)	The Commission may approve or specify a radionuclide release rate, containment time, or groundwater travel time, based on a number of factors including the geochemical characteristics of the host rock, surrounding strata, and groundwater.	Geochemical characteristics of the host rock and groundwater are given in Sections 4.1.1 and 4.1.2, respectively.	Mineralogic and Petrologic Characterization (Section 8.3.1.2.3) Groundwater Flow System Hydrochemistry (Section 8.3.1.4.2.3.1)

Table 4.0-3. Listing of important geochemical processes and environmental parameters for demonstrating performance compliance with repository criteria

Region	Pre-emplacement	Preclosure operational and containment	Isolation
Engineered barriers system	NA[a]	Saturation	Precipitation
		Corrosion	Colloid formation
		Packing/water interaction	Complexation
			Packing/water interaction
			Sorption
		Gamma radiolysis	Alpha radiolysis
		Composition of engineered barriers	Composition of engineered barriers
Disturbed zone	Basalt/water interaction	Basalt/water interaction	Basalt/water interaction
	Composition of basalts	Gamma radiolysis	Sorption
		Composition of basalts	Complexation
			Precipitation
			Composition of basalts
Natural system	Basalt/water interaction	Basalt/water interaction	Sorption
			Basalt/water interaction
	Composition of basalts	Composition of basalts	Composition of basalts

Source: Apted (1983, p. 4).

NOTE: Important geochemical parameters common to all regions and time periods are:

pH
redox potential
temperature
pressure
groundwater composition

[a]Not applicable.

Table 4.1-1. Chemical and textural characteristics of primary phases in Grande Ronde Basalt in the primary isolation zone

Characteristic phase	Abundance (modal %)	Compositional range	Compositional zoning	Grain size (mm)	Texture	Special features
Plagioclase (Long et al. 1984, p I-101; Schiffmann and Lofgren 1982, pp. 49-78)	25 - 48	An_{45} to An_{65}	General moderate, normal. Locally reversed and/or oscillatory	0.02 - 6.0, Average 0.12	Lath shaped	Microphenocrysts common; contains glass inclusions and symmetrically arranged pyroxene inclusion.
Augite* (Long and Strope 1983, pp. 57-60)	20 - 32	(Wo_{40} En_{40} Fs_{20}) to (Wo_{30} En_{30} Fs_{40})	Moderate, normal intergrown with pigeonite, some iron-rich rims	0.01 - 5.0, Average 0.08	Euhedral to subhedral prismatic grains	
Pigeonite* (Long and Strope 1983, pp. 57-60)	0 - 10	(Wo_{13} En_{50} Fs_{27}) to (Wo_{9} En_{64} Fs_{29})	Intergrown with augite, occurs as rims on some clinopyroxene or orthopyroxene grains	ND	Anhedral, equant	Mode of occurrence and textures suggest limited stability range in certain flows.
Orthopyroxene* (Reidel et al. 1978, pp. 148-163)	0 - trace	(Wo_{4} En_{61} Fs_{35}) to (Wo_{6} En_{75} Fs_{19})	Unzoned to slight normal zoning	~2	Subhedral, prismatic, commonly embayed	Resorption textures and reaction rims indicated instability at 0.1 MPa (14.5 lbf/in^2) (surface pressure).
Iron-titanium oxide (Noonan et al. 1980, pp. 1-7)	0 - 6	Dominantly titanium-magnetite with TiO_2 = 28 - 32 wt%. Ilmenite occurs in some samples.	Unzoned (?)	0.02 - 0.4 Average 0.08	Octahedral, cruciform, dendritic or blade shaped	Oxidation lamellae occur in colonnade samples.
Olivine (Schiffmann and Lofgren 1982, pp. 49-78)	0 - 3	Fo_{67} to Fo_{47}	Moderate, normal zoning	0.05	Adhedral to subhedral, equant	Commonly absent from Grande Ronde Basalt flows. Occurrence limited to glassy rind of some flows.
Apatite (Long and Davidson 1981, pp. 5-33 to 5-40; Allen and Strope 1983, pp. 2-7)	0 - 2	ND	ND	0.01 - 0.06 (apparent); true lengths of some needles may be 0.03	Acicular	Occurs both as discrete grains and minute crystal aggregates within blebs in mesostasis of entablature samples.
Mesostasis (Long and Davidson 1981, pp. 5-33 to 5-40; Noonan et al. 1980, pp. 1-7; Allen and Strope 1983, pp. 2-7; Long et al. 1984, p. I-101)	20 - 65	SiO_2 = 60 - 74 wt%	Compositional variation apparent adjacent to magnetite and clinopyroxene grains	0.01 - 0.65 Average 0.17	Intersertal to interstitial, with or without abundant tachylitic inclusions	Immiscible liquid blebs common. Highly tachylitic in entablature, relatively inclusion-free in colonnade.

Source: Based principally on Table I-17 of Long et al. (1984, pp. I-101).

Note: ND = Not determined.

*Pyroxene.

Table 4.1-2. Major-element composition of Grande Ronde Basalt flows in the primary isolation zone (sheet 1 of 3)

Oxide	Mean	Standard deviation	Minimum value	Maximum value
		Rocky Coulee flow (N = 30)		
SiO_2	54.19	0.63	53.12	56.88
Al_2O_3	15.19	0.39	14.30	15.85
FeO	11.37	0.30	10.76	11.98
MgO	4.81	0.21	4.36	5.08
CaO	8.45	0.27	7.62	9.03
Na_2O	2.40	0.36	1.56	2.81
K_2O	1.14	0.08	1.00	1.33
TiO_2	1.76	0.07	1.60	1.87
P_2O_5	0.31	0.02	0.26	0.35
MnO	0.20	0.01	0.19	0.22
		Levering flow (N = 15)		
SiO_2	53.51	0.56	52.43	54.68
Al_2O_3	15.02	0.29	14.65	15.50
FeO	11.67	0.33	11.11	12.42
MgO	5.00	0.29	4.31	5.44
CaO	8.82	0.30	8.30	9.33
Na_2O	2.58	0.20	2.21	2.86
K_2O	0.90	0.14	0.71	1.19
TiO_2	1.80	0.03	1.76	1.86
P_2O_5	0.28	0.01	0.26	0.29
MnO	0.22	0.01	0.19	0.24
		Cohassett flow (N = 55)		
SiO_2	53.43	0.48	51.47	54.21
Al_2O_3	15.14	0.41	14.16	15.91
FeO	11.67	0.39	10.98	13.32
MgO	5.02	0.22	4.45	5.44
CaO	8.70	0.30	8.09	9.27

Table 4.1-2. Major-element composition of Grande Ronde Basalt flows in the primary isolation zone (sheet 2 of 3)

Oxide	Mean	Standard deviation	Minimum value	Maximum value
Na_2O	2.50	0.29	1.44	2.92
K_2O	1.04	0.11	0.51	1.28
TiO_2	1.82	0.08	1.68	2.07
P_2O_5	0.29	0.04	0.24	0.39
MnO	0.21	0.01	0.19	0.24
Birkett flow (N = 32)				
SiO_2	53.33	0.44	51.74	54.03
Al_2O_3	15.04	0.30	14.56	15.74
FeO	12.06	0.32	11.39	12.58
MgO	4.92	0.16	4.67	5.30
CaO	8.72	0.24	8.31	9.30
Na_2O	2.48	0.34	1.59	3.17
K_2O	0.89	0.15	0.59	1.41
TiO_2	1.88	0.08	1.74	2.04
P_2O_5	0.29	0.02	0.26	0.32
MnO	0.21	0.01	0.20	0.23
McCoy Canyon flow (N = 38)				
SiO_2	53.67	0.46	52.89	54.79
Al_2O_3	14.95	0.32	14.40	15.81
FeO	12.61	0.68	11.89	14.45
MgO	4.59	0.24	3.85	5.38
CaO	8.37	0.24	7.48	8.81
Na_2O	2.41	0.40	1.43	3.09
K_2O	1.04	0.23	0.70	2.21
TiO_2	1.97	0.08	1.80	2.26
P_2O_5	0.29	0.02	0.25	0.36
MnO	0.22	0.01	0.19	0.29

Table 4.1-2. Major-element composition of Grande Ronde Basalt flows in the primary isolation zone (sheet 3 of 3)

Oxide	Mean	Standard deviation	Minimum value	Maximum value
Umtanum flow (N = 52)				
SiO_2	54.68	0.87	51.26	56.03
Al_2O_3	14.68	0.29	14.08	15.37
FeO	13.08	0.79	12.21	15.35
MgO	3.55	0.22	3.15	4.45
CaO	7.17	0.34	6.69	8.59
Na_2O	2.57	0.37	1.66	3.19
K_2O	1.50	0.17	0.96	2.22
TiO_2	2.22	0.08	2.06	2.43
P_2O_5	0.35	0.02	0.30	0.38
MnO	0.22	0.01	0.19	0.29
All other high-magnesium chemical type flows in the primary isolation zone (N = 120)				
SiO_2	53.78	0.64	52.03	55.52
Al_2O_3	15.12	0.40	14.18	16.13
FeO	13.54	0.58	11.96	14.69
MgO	4.84	0.25	3.89	5.35
CaO	8.58	0.30	7.43	9.43
Na_2O	2.45	0.33	1.12	2.99
K_2O	1.00	0.26	0.67	3.08
TiO_2	1.81	0.12	1.52	2.06
P_2O_5	0.28	0.02	0.19	0.35
MnO	0.21	0.01	0.16	0.25

Source: Statistical parameters derived from data in Landon (1984).
NOTE: Values are in wt%.

Table 4.1-3. Trace element concentrations (p/m) for basalt in the primary isolation zone (sheet 1 of 2)

Element	Number of samples	Mean	Standard deviation	Minimum value	Maximum value
Low-magnesium chemical type					
Scandium	10	33.2	2.5	28.5	36.1
Chromium	3	7.3	1.0	6.4	8.3
Cobalt	10	36.8	1.2	35.0	38.2
Rubidium[a]	6	44.7	5.3	38.3	51.1
Strontium[a]	6	319.0	10.2	309.4	355.0
Zirconium[a]	6	189.0	8.2	181.5	201.2
Niobium	6	16.1	1.4	13.9	18.1
Cesium	4	1.16	0.37	0.62	1.45
Barium[a]	9	607	75	512	770
Lanthanum	10	22.9	2.8	15.2	25.0
Cerium[a]	10	52.2	3.0	48.0	56.6
Samarium	10	6.80	0.33	6.37	7.26
Europium	10	2.05	0.13	1.90	2.32
Terbium	7	1.11	0.24	0.75	1.35
Ytterbium	10	3.76	0.36	3.10	4.36
Lutetium	10	0.57	0.08	0.47	0.70
Hafnium	10	5.05	0.19	4.76	5.30
Tantalum	9	0.81	0.10	0.61	0.99
Thorium	10	5.82	0.55	4.99	6.59
Uranium	2	1.48	0.32	1.25	1.70

Table 4.1-3. Trace element concentrations (p/m) for basalt in the primary isolation zone (sheet 2 of 2)

Element	Number of samples	Mean	Standard deviation	Minimum value	Maximum value
High-magnesium chemical type					
Scandium	42	35.2	2.6	28.2	39.1
Chromium	39	35.5	8.0	19.0	48.0
Cobalt	42	38.0	3.2	28.4	43.5
Rubidium[a]	23	32.4	8.3	17.1	61.0
Strontium[a]	23	308.7	13.7	269.3	323.4
Zirconium[a]	23	166.6	44.3	147.4	328.0
Niobium	23	14.2	2.2	11.6	21.2
Cesium	20	0.85	0.19	0.44	1.14
Barium[a]	31	468	141	300	1,020
Lanthanum	42	19.2	4.2	16.2	39.7
Cerium[a]	42	43.1	9.0	33.0	87.4
Neodymium	1	41.0	NA	NA	NA
Samarium	42	5.92	1.12	5.18	11.62
Europium	42	1.81	0.19	1.42	2.31
Terbium	37	0.98	0.23	0.57	1.76
Ytterbium	40	3.47	0.53	2.54	5.73
Lutetium	42	0.51	0.12	0.37	0.99
Hafnium	42	4.29	0.89	3.18	8.60
Tantalum	41	0.74	0.15	0.44	1.36
Thorium	39	3.78	1.23	0.94	9.17
Uranium	8	1.19	0.46	0.71	2.00

NOTE: All data used to obtain satistical parameters for trace element concentrations are from BRMC Index Record No. B062365-68, B062301-03, B062287-91, B062293.

[a]Concentrations for these elements were determined by x-ray fluorescence and instrumental neutron activation analysis; concentrations for all other elements were determined by instrumental neutron activation analysis only.

NA = not applicable.

Table 4.1-4. Structural water (H_2O+), absorbed water (H_2O-), and total water contents for samples of selected flow interiors in the primary isolation zone

Flow	Number of analyses	Structural water (H_2O+)		Absorbed water (H_2O-)		Total water	
		Mean value	Standard deviation	Mean value	Standard deviation	Mean value	Standard deviation
Rocky Coulee	4	0.72	0.13	1.13	0.43	1.85	0.40
Cohassett	10	0.67	0.24	0.78	0.34	1.45	0.35
McCoy Canyon	6	0.80	0.10	0.88	0.38	1.68	0.42
Umtanum	8	1.04	0.15	0.66	0.18	1.70	0.11

Source: Long et al. (1984, p. I-E-1).
NOTE: Values are in wt%.

Table 4.1-5. The FeO and Fe_2O_3 for selected flow interiors in the primary isolation zone

Flow	FeO			Fe_2O_3			Fe_2O_3
	Number of analyses	Mean value	Standard deviation	Number of analyses	Mean value	Standard deviation	$Fe_2O_3 + FeO$
Rocky Coule	2	8.98	0.15	2	2.72	0.80	0.23
Cohassett	6	9.15	0.65	5	2.22	0.53	0.20
McCoy Canyon	5	9.51	0.62	5	2.87	1.12	0.23
Umtanum	9	9.73	0.89	9	3.03	1.16	0.24

Source: From Long et al. (1984, p. I-F-1).
NOTE: All values are in wt%.

Table 4.1-6. Relative proportions of secondary minerals in Grande Ronde Basalt, Pasco Basin

Mineral	Vesicles	Fractures
Smectite	~32	~75
Zeolite[a]	~43	~20
Silica	~25	~5

Source: From Benson and Teague (1979, pp. 31-41).

NOTE: Values are in percent by volume of total amount present.

[a]Dominantly clinoptilolite.

Table 4.1-7. Average compositions (wt %) for smectites in the primary isolation zone (sheet 1 of 2)

Oxide	Mean	Standard deviation	Minimum value	Maximum value
Early smectite (N = 13)				
SiO_2	44.87	2.06	42.28	48.63
Al_2O_3	7.27	1.24	5.94	9.83
TiO_2	0.57	1.27	0.38	0.75
FeO	25.40	2.19	20.33	28.02
MnO	0.22	0.04	0.17	0.28
CaO	2.02	0.42	1.37	3.05
MgO	4.89	0.50	3.18	5.55
K_2O	2.26	0.45	1.57	2.88
Na_2O	1.27	0.45	0.77	2.31
Intermediate smectite (N = 89)				
SiO_2	44.82	4.78	32.36	54.43
Al_2O_3	6.65	1.64	3.16	11.43
TiO_2	0.83	1.40	0.08	9.65
FeO	18.18	5.84	6.84	28.37
MnO	0.15	0.08	0.00	0.35
CaO	1.66	0.71	0.55	4.49
MgO	7.67	2.73	4.64	13.15
K_2O	2.05	1.03	0.50	4.90
Na_2O	0.93	0.38	0.00	1.80

Table 4.1-7. Average compositions (wt %) for smectites in the primary isolation zone (sheet 2 of 2)

Oxide	Mean	Standard deviation	Minimum value	Maximum value
		Late smectite (N = 6)		
SiO_2	45.16	3.28	42.05	49.60
Al_2O_3	3.31	0.12	3.13	3.50
TiO_2	0.14	0.07	0.06	0.23
FeO	27.67	2.15	25.36	29.77
MnO	0.53	0.09	0.42	0.64
CaO	1.32	0.06	1.24	1.39
MgO	3.60	0.13	3.46	3.81
K_2O	0.73	0.49	0.23	1.24
Na_2O	0.44	0.22	0.21	0.75

NOTE: (1) All values are in wt%.
(2) Statistical parameters derived from data in BRMC Index Record No. B088328.

Table 4.1-8a. Average composition (wt%) for clinoptilolite in the primary isolation zone (for 29 samples)

Oxide	Mean[a]	Standard deviation
SiO_2	68.51	2.28
Al_2O_3	12.34	0.45
TiO_2	NA	NA
Fe_2O_3[b]	0.13	0.07
MnO	NA	NA
BaO	0.42	0.10
CaO	1.13	0.50
MgO	NA	NA
K_2O	3.02	0.99
Na_2O	3.09	0.62

Source: Benson and Teague (1979).

Table 4.1-8b. Average composition (wt%) for clinoptilolite in the primary isolation zone

Oxide	Mean[a]	Standard deviation	Minimum value	Maximum value
SiO_2	70.55	2.26	64.06	78.60
Al_2O_3	13.07	0.90	8.47	14.66
TiO_2	0.04	0.09	0.00	0.61
Fe_2O_3[b]	0.18	0.17	0.00	1.03
MnO	0.01	0.02	0.00	0.12
BaO	ND	ND	ND	ND
CaO	2.17	1.20	0.71	7.82
MgO	0.03	0.03	0.00	0.19
K_2O	2.70	1.24	1.09	5.64
Na_2O	1.31	0.48	0.36	2.31

Source: BRMC Index Record No. B088328.
NOTE: All values are in wt%.
NA = Not available.
ND = Not determined.
[a]Values do not total 100% because analyses of some oxides and H_2O are not available.
[b]Total iron as Fe_2O_3.

Table 4.1-9. Average composition of silica in the primary isolation zone

Oxide	Mean[a]	Standard deviation	Minimum value	Maximum value
		Colored silica (N = 13)		
SiO_2	54.72	17.94	30.85	96.25
Al_2O_3	1.65	3.42	0.38	13.03
TiO_2	0.07	0.04	0.00	0.12
FeO*	2.23	1.97	0.08	5.47
MnO	0.04	0.04	0.00	0.10
CaO	0.18	0.23	0.06	0.93
MgO	0.50	0.29	0.04	0.86
K_2O	0.70	1.24	0.09	4.74
Na_2O	0.25	0.26	0.00	0.93
		Colorless silica (N = 11)		
SiO_2	84.34	6.63	77.13	97.08
Al_2O_3	0.62	0.08	0.52	0.74
TiO_2	0.02	0.03	0.00	0.10
FeO*	0.98	0.11	0.00	0.39
MnO	0.01	0.02	0.00	0.04
CaO	0.10	0.03	0.05	0.13
MgO	0.01	0.02	0.00	0.04
K_2O	0.17	0.08	0.09	0.28
Na_2O	0.27	0.14	0.00	0.38

NOTE: (1) Statistical parameters derived from data in BRMC Index Record No. B088328.
(2) All values are in wt%.

[a]Values do not total 100% because analyses of some oxides and H_2O are not available.

Table 4.1-10. Average composition of celadonite from the central Pasco Basin

Oxide	Mean[a]	Standard deviation	Minimum value	Maximum value
		Celadonite (N = 13)		
SiO_2	42.34	6.26	34.23	51.92
Al_2O_3	4.07	0.52	2.80	4.82
TiO_2	0.53	0.09	0.35	0.63
Fe_2O_3[b]	13.16	2.04	8.71	15.57
MnO	0.14	0.04	0.08	0.21
CaO	0.24	0.03	0.17	0.28
MgO	6.51	0.92	3.98	7.53
K_2O	6.59	1.27	4.57	8.19
Na_2O	0.43	0.12	0.21	0.62

NOTE: (1) Statistical parameters derived from data in BRMC Index Record No. B088328.
(2) All values are in wt%.

[a]Values do not total 100% because analyses of some oxides and H_2O are not available.

[b]Total iron as Fe_2O_3.

Table 4.1-11. Relative proportions of secondary minerals in the primary isolation zone in the controlled area study zone

Flow	RRL-2[a]				RRL-2, RRL-6, RRL-14, DC-16[b]					
	Clay[c]	Zeolite	Silica	Pyrite	Clay[c]	Zeolite	Silica	Pyrite	Void	Unknown
Rocky Coulee					81	5	13	<1	<1	<1
Cohassett	89	9	1	<1	88	6	4	<1	<1	<1
McCoy Canyon					81	5	11	<1	<1	1
Umtanum	53	37	9	~1.5	59	30	10	<1	<1	<1

[a]Data are from Long et al. (1984, p. I-124) and are averages of more than 200 visual estimates from each flow.

[b]Data are from Lindberg (1986, p. 48) and are visual estimates of percentages of 3,194 fractures in which indicated mineral dominates the secondary assemblage.

[c]Dominantly smectite.

Table 4.1-12. Average chemical compositions of basalt in the lower buffer zone (sheet 1 of 2)

Oxide	Mean	Standard deviation	Minimum value	Maximum value
Very-high magnesium chemical type (N = 31)				
SiO_2	52.35	0.86	50.74	55.63
Al_2O_3	15.28	0.32	14.79	16.30
FeO*	11.70	0.41	10.46	13.03
MgO	5.66	0.27	4.71	6.39
CaO	9.49	0.73	6.63	10.43
Na_2O	2.56	0.38	1.71	3.07
K_2O	0.61	0.50	0.22	3.11
TiO_2	1.69	0.06	1.57	1.79
P_2O_5	0.27	0.02	0.17	0.30
MnO	0.21	0.02	0.16	0.30
High-magnesium chemical type (N = 12)				
SiO_2	53.26	0.57	52.13	53.95
Al_2O_3	14.98	0.41	14.30	15.50
FeO*	12.76	0.39	12.06	13.42
MgO	4.84	0.30	4.38	5.35
CaO	8.70	0.33	8.23	9.18
Na_2O	2.05	0.43	1.57	2.90
K_2O	0.77	0.26	0.33	1.14
TiO_2	1.90	0.05	1.83	2.03
P_2O_5	0.32	0.01	0.30	0.33
MnO	0.21	0.01	0.19	0.23
Low-magnesium chemical type (N = 69)				
SiO_2	55.10	1.07	52.63	57.68
Al_2O_3	15.02	0.38	14.23	15.93
FeO*	12.17	0.71	11.20	13.59

Table 4.1-12. Average chemical compositions of basalt in the lower buffer zone (sheet 2 of 2)

Oxide	Mean	Standard deviation	Minimum value	Maximum value
MgO	3.60	0.17	3.12	4.17
CaO	7.20	0.29	6.24	7.78
Na_2O	2.62	0.43	1.51	3.75
K_2O	1.57	0.33	0.94	2.61
TiO_2	2.01	0.14	1.79	2.34
P_2O_5	0.32	0.02	0.27	0.36
MnO	0.20	0.01	0.18	0.24

Source: Data from Landon, 1984.
NOTE: All values are in wt%.
*Total iron as FeO.

Table 4.1-13. Trace element concentrations for basalt in the lower buffer zone (sheet 1 of 3)

Element	Number of samples	Mean	Standard deviation	Minimum value	Maximum value
High-magnesium chemical type					
Scandium	6	37.0	1.7	35.5	39.2
Chromium	6	36.7	6.1	31.1	46.8
Cobalt	6	38.4	0.8	37.5	39.2
Rubidium*	2	27.0	3.0	24.8	29.1
Strontium*	2	338.0	11.3	330.0	346.0
Zirconium*	2	134.0	2.6	132.2	135.9
Niobium	2	12.6	0.4	12.3	12.8
Cesium	3	0.61	0.40	0.24	1.04
Barium*	3	405	53	350	460
Lanthanum	6	17.5	0.6	16.8	18.4
Cerium*	6	38.7	2.5	34.1	40.8
Neodymium	0	NA	NA	NA	NA
Samarium	6	5.34	0.14	5.09	5.50
Europium	6	1.78	0.08	1.69	1.91
Terbium	6	0.94	0.09	0.85	1.10
Ytterbium	6	3.20	0.31	2.76	3.60
Lutetium	4	0.45	0.03	0.42	0.48
Hafnium	6	3.71	0.14	3.59	3.95
Tantalum	6	0.56	0.05	0.48	0.62
Thorium	6	2.85	0.11	2.76	3.04

Table 4.1-13. Trace element concentrations for basalt in the lower buffer zone (sheet 2 of 3)

Element	Number of samples	Mean	Standard deviation	Minimum value	Maximum value
	Low-magnesium chemical type				
	40	30.2	1.9	27.4	34.6
	35	8.1	2.8	5.1	19.5
	40	35.7	2.3	32.3	43.7
	30	46.7	13.0	17.6	68.3
	13	326.2	14.2	310.4	365.0
	13	183.6	3.8	177.0	191.1
	13	14.8	1.7	11.6	17.5
	31	1.32	0.49	0.56	2.43
	38	581	91	400	850
	40	23.5	2.0	14.8	26.7
	40	49.0	5.7	29.6	58.1
	2	34.0	8.5	28.0	40.0
	40	6.25	0.53	4.24	7.19
	39	1.92	0.11	1.57	2.14
	40	1.02	0.09	0.84	1.21
	40	3.53	0.36	2.90	4.59
	39	0.54	0.09	0.38	1.00
	40	4.90	0.34	4.22	5.80
	36	0.79	0.14	0.50	1.39
	40	5.59	0.87	3.75	7.27
	15	1.52	0.35	0.92	2.50

Table 4.1-13. Trace element concentrations for basalt in the lower buffer zone (sheet 3 of 3)

Element	Number of samples	Mean	Standard deviation	Minimum value	Maximum value
Very high-magnesium chemical type					
Scandium	12	39.4	1.6	36.9	41.8
Chromium	12	110.6	10.8	90.0	130.0
Cobalt	12	42.3	3.6	38.0	50.0
Rubidium*	9	13.0	5.2	6.4	24.2
Strontium*	8	356.2	15.9	344.7	394.0
Zirconium*	8	120.5	5.4	112.1	130.2
Niobium	8	29.7	46.2	10.2	144.1
Cesium	6	0.56	0.24	0.37	1.03
Barium*	9	385	55	307	470
Lanthanum	12	14.9	1.7	12.9	19.5
Cerium*	12	33.8	5.3	28.3	48.8
Neodymium	1	19.7	NP	NP	NP
Samarium	12	4.92	0.21	4.58	5.27
Europium	12	1.67	0.16	1.44	2.06
Terbium	12	0.85	0.20	0.49	1.22
Ytterbium	12	3.01	0.45	2.24	3.68
Lutetium	12	0.47	0.05	0.37	0.54
Hafnium	12	3.38	0.28	2.98	3.92
Tantalum	11	0.55	0.14	0.36	0.83
Thorium	12	2.13	0.22	1.79	2.44
Uranium	0	NP	NP	NP	NP

NOTE: (1) All values are in p/m.
(2) All data used to obtain statistical parameters for trace-element concentrations are from BRMC Index Record No. B062365-68, B062301-03, B062297-99, B062294-95, B062287-91, B062293.
(3) NA = not analyzed or below detection limits.
(4) NP = not applicable.

*Concentrations for these elements were determined by x-ray fluorescence and instrumental neutron activation analysis; concentrations for all other elements were determined only by instrumental neutron activation analysis.

Table 4.1-14. Petrographic modes for the very high-magnesium flow in the lower buffer zone

Sample	Mean (%)	Standard deviation	Mean (%)	Standard deviation
	RRL02-3870.8		RRL02-3878.4	
Plagioclase	43.57	1.77	45.99	1.38
Pyroxene	22.83	0.88	25.07	1.88
Mesostasis	10.24	0.58	9.26	0.43
Iron-titanium oxides	2.87	0.38	3.10	0.32
Alteration products	20.11	2.10	16.01	0.93
Other	0.38	0.04	0.48	0.23
Olivine	0.00	0.00	0.01	0.12
	RRL06-3176.2		RRL14-3939.3	
Plagioclase	43.77	1.36	43.15	1.02
Pyroxene	26.00	1.48	23.41	0.96
Mesostasis	12.25	1.47	9.74	0.60
Iron-titanium oxides	2.72	0.23	2.47	0.19
Alteration products	13.05	1.75	20.09	0.95
Other	2.17	0.36	1.05	0.26
Olivine	0.03	0.04	0.10	0.07
	RRL14-3972.4		RRL06-3991.3	
Plagioclase	47.57	0.97	46.72	0.91
Pyroxene	26.83	1.29	27.12	1.01
Mesostasis	9.13	0.15	10.03	0.54
Iron-titanium oxides	2.32	0.31	2.28	0.51
Alteration products	13.58	0.84	12.95	0.80
Other	0.55	0.30	0.85	0.18
Olivine	0.03	0.04	0.05	0.05

Source: Data from BRMC Index Record No. B052882-B052887.

Table 4.1-15. Chemical composition for basalt in the upper buffer zone (sheet 1 of 2)

Oxide	Mean	Standard deviation	Minimum value	Maximum value
		Priest Rapids Member (N = 52)		
SiO_2	49.93	6.58	49.12	51.81
Al_2O_3	14.10	0.39	13.28	14.94
FeO*	14.64	0.75	12.10	16.64
MgO	4.76	0.52	3.48	5.67
CaO	8.63	0.48	6.69	9.53
Na_2O	2.44	0.18	2.08	3.10
K_2O	1.05	0.20	0.59	1.58
TiO_2	3.35	0.22	2.99	3.89
P_2O_5	0.67	0.06	0.62	1.04
MnO	0.24	0.02	0.20	0.28
		Roza Member (N = 43)		
SiO_2	50.62	0.44	49.67	51.72
Al_2O_3	14.64	0.32	14.02	15.37
FeO*	15.50	0.67	13.50	16.44
MgO	4.56	0.21	3.83	4.99
CaO	8.58	0.20	8.18	9.05
Na_2O	2.56	0.19	2.06	2.91
K_2O	1.12	0.12	0.64	1.27
TiO_2	3.05	0.09	2.89	3.27
P_2O_5	0.55	0.02	0.52	0.63
MnO	0.23	0.02	0.16	0.25

Table 4.1-15. Chemical composition for basalt in the upper buffer zone (sheet 2 of 2)

Oxide	Mean	Standard deviation	Minimum value	Maximum value
	Frenchman Springs Member (N = 220)			
SiO_2	51.31	0.64	50.07	56.79
Al_2O_3	14.28	0.42	12.83	16.39
FeO*	14.39	0.58	11.87	16.05
MgO	4.15	0.31	1.54	5.08
CaO	8.18	0.55	0.96	8.93
Na_2O	2.53	0.28	0.28	3.17
K_2O	1.20	0.17	0.68	1.83
TiO_2	3.00	0.11	0.58	3.29
P_2O_5	0.54	0.07	0.10	0.75
MnO	0.23	0.02	0.17	0.43

Source: Data from Landon, 1984.
NOTE: Values are in wt%.
*Total iron as FeO.

Table 4.1-16. Trace element concentrations for basalt in the upper buffer zones

Element	Number of samples	Mean	Standard deviation	Minimum value	Maximum value
		Frenchman Springs Member, Wanapum Basalt			
Scandium	4	38.2	0.8	37.1	38.8
Chromium	4	29.8	2.0	27.1	31.5
Cobalt	4	38.6	1.6	37.2	40.8
Cesium	4	0.94	0.33	0.48	1.22
Barium*	3	453	55	390	490
Lanthanum	4	25.3	7.3	20.2	36.0
Cerium*	4	52.1	15.0	32.9	69.9
Neodymium	3	33.7	4.1	29.8	38.0
Samarium	4	5.00	2.69	1.00	6.66
Europium	4	1.95	0.18	1.77	2.20
Terbium	4	1.02	0.20	0.73	1.18
Ytterbium	4	3.02	0.89	1.75	3.79
Lutetium	4	0.60	0.30	0.30	1.00
Hafnium	4	4.29	0.10	4.18	4.42
Tantalum	4	0.76	0.07	0.71	0.87
Thorium	4	3.40	0.08	3.34	3.50
Uranium	0	NA	NA	NA	NA

Source: All data used to obtain statisical parameters for trace element concentrations are from BRMC Index Record No. B062297-99 and _____.

NOTE: All values are in p/m.

NA = Not applicable.

*Concentrations for these elements were determined by x-ray fluorescence and instrumental neutron activation analysis; concentrations for all other elements were determined only by instrumental neutron activation analysis.

Table 4.1-17. Petrographic modes for basalt flows in the upper buffer zone

Sample	Mean (%)	Standard deviation	Mean (%)	Standard deviation
	RRL06-2295.7[a]		RRL06-2392.6[a]	
Plagioclase	41.92	2.17	35.44	1.22
Pyroxene	22.54	0.77	16.26	0.77
Mesostasis	20.38	2.16	24.29	1.09
Iron-titanium oxides	5.20	0.59	3.83	0.48
Alteration Products	5.23	0.60	16.53	1.10
Other	1.68	0.29	2.58	0.41
Olivine	3.05	0.62	1.08	0.29
	RRL06-2196.0[a]		RRL06-2552.7[a]	
Plagioclase	34.80	0.92	37.83	2.03
Pyroxene	20.05	0.72	17.53	0.52
Mesostasis	26.54	0.73	26.49	2.13
Iron-titanium oxides	5.59	0.51	5.28	0.54
Alteration Products	8.23	1.12	6.35	0.80
Other	2.74	0.53	3.25	0.45
Olivine	2.05	0.63	3.28	0.23
	Average Priest Rapids Member (N = 12)[b]		Average Rosa Member (N = 10)[b]	
Plagioclase	41.00	4.32	40.83	5.95
Pyroxene	23.27	4.06	23.75	3.25
Glass	21.50	6.02	20.00	8.79
Opaques	9.81	2.71	9.85	2.60
Alteration Products	1.50	1.63	4.32	3.26
Olivine	3.25	1.58	1.69	1.52
	Average Frenchman Springs Member (N = 15)[b]			
Plagioclases	37.88	6.76		
Pyroxene	20.86	6.25		
Glass	20.00	7.02		
Opaques	9.95	2.53		
Alteration Products	3.87	2.42		
Olivine	1.38	1.23		

[a]Data from BRMC Index Record No. B052844-47.

[b]Statistical parameters derived from data in Taylor (1976, p. 109).

Table 4.1-18. General temperature ranges for formation and existence of secondary minerals

Minerals	Approximate temperature range (°C)	Source*
Common		
Smectite	4 - 200	1, 2
Illite	200 - 300	3, 9
Celadonite	25 - 400	8, 14
Clinoptilolite	4 - 120	4, 10
Mordenite	65 - 250	18, 5
Opal	<50	4
Cristobalite	25 - 175	15, 7
Quartz	25 - 573	15
Tridymite	25 - 117	15
Less common		
Phillipsite	4 - 250	11, 5
Chabazite	4 - 85	11, 5
Erionite	4 - 120	11, 16
Analcime	4 - 140	11, 5
Wairakite	<600	5, 17
Pyrite	4 - <300	12, 5
Calcite	20 - <300	13, 5

* 1. Perry (1975).
2. Kristmannsdottir (1976).
3. Hoffman and Hower (1979).
4. Aoyagi and Kazama (1980).
5. Kristmannsdottir (1975).
6. Elders et al. (1981).
7. Brown and Ellis (1970).
8. Andrews (1980).
9. McDowell and Elders (1980).
10. Nathan and Flexer (1977).
11. Surdam (1981).
12. Berner (1971).
13. Donner and Lynn (1977).
14. Wise and Eugster (1964).
15. Deer et al. (1963, p. 180).
16. Ulmer and Grandstaff (1984).
17. Helgeson et al. (1978).
18. Gottardi and Galli (1985).

Table 4.1-19. Estimates of methane concentrations in groundwater from the reference repository location area

Borehole	Stratigraphic zone	CH_4 concentration (mg/L)	CH_4 saturation (%) (in situ)
DC-16A	Frenchman Springs Member	225-358	21-34
	Vantage interbed	345-663	31-60
	Rocky Coulee Flow	102-487	9-43
RRL-2	Cohassett flow bottom	392-1,135 (9-17-82)[a]	32-93
		378-593 (10-24-83)[a]	31-48
	Umtanum flow top	610-801	47-62
	Umtanum fracture zone	468-1,222	36-93
	Very-high-magnesium flow top	512-860	39-65
RRL-6B	Umtanum flow top	277-742	21-57
RRL-14	Cohassett flow top	363-645	31-55
		127-804	11-68
	Cohassett flow bottom	409-566	33-46
	Umtanum flow top	390	30

Source: Data are from Early (1986).
[a]Sample collection date.

Table 4.1-20. Estimated temperatures and pressures for Frenchman Springs Member and Cohassett flow basalts at the reference repository location (borehole RRL-2)

Description	Frenchman Springs Member (including Vantage interbed)	Cohassett flow
Depth range[a]		
(m)	585.8-819.0	912.3-992.1 (969.6)[c]
(ft)	1,921-2,686	2,992-3,254 (3,180)[c]
Temperature (°C)[b]	37.8-46.8	50.4-53.5 (52.7)[c]
Hydrostatic pressure[b]		
(mPa)	5.6-7.8	8.6-9.4 (9.2)[c]
(lb/in^2)	812-1,131	1,247-1,363 (1,334)[c]

[a]Depth ranges are based on position of upper and lower contacts of the respective horizons in RRL-2. Depth value in parentheses is depth to estimated repository midline (Early et al., 1983, p. I-186).

[b]Temperature and pressure ranges reported are based upon the equations given in Figures 4.1-10 and 4.1-12, respectively.

[c]Values in parentheses are estimated mean temperature and pressure values at the repository midline depths for each horizon in RRL-2.

Table 4.1-21. Composition of synthetic reference groundwaters used for experimental studies

Constituents	Concentration (mg/L)					
	GR-1[a]	GR-1A[b]	GR-2[c]	GR-2A[c]	GR-3[d]	GR-4[e]
Na^+	30.7	107	225	246	358	334
K^+	9.0	11.2	2.5	2.5	3.4	13.8
Ca^{2+}	6.5	2.0	1.06	1.01	2.8	2.2
Mg^{2+}	1.0	0.4	0.07	0.0	0.032	0.0
Cl^-	14.4	50	131	152	312	405
CO_3^{2-}	0	0	59	28.8	12.9	17.2
HCO_3^-	81.5	215	75	36.6	42.9	73.4
F^-	0	1.3	29	37	33.4	19.9
SO_4^{2-}	11.1	2.4	72	108	173	4.0
SiO_2	25	30	108	82	76.2	96.1
pH	8.0	8.5	10.0	10.0	9.8	9.7
Ionic strength	0.002	0.005	0.014	0.012	0.018	0.015

[a]Simulated groundwater for the Saddle Mountains and upper Wanapum Basalts (Salter et al., 1981b).
[b]Simulated groundwater for the Mabton interbed (Saddle Mountains Basalt; Barney, 1984).
[c]Simulated groundwater for the Grande Ronde Basalt (GR-2: Salter et al., 1981b; GR-2A: Barney, 1981a).
[d]Simulated groundwater for the Grande Ronde Basalt (Jones, 1982, p. 4).
[e]Simulated groundwater for the Grande Ronde Basalt in the reference repository location (Dill et al., 1984).

Table 4.1-22. Preliminary list of key radionuclides for a nuclear waste repository in basalt (based on 1,000-yr-old commerical spent fuel)

Element	Isotope[a]	1,000-yr inventory[b] (Ci/MTHM)	EPA limit[c] (Ci/MTHM)	Inventory / EPA limit
Americium	^{241}Am	1,430	0.1	14,300
Plutonium	^{240}Pu	649	0.1	6,490
Uranium	^{234}U	4.08	0.1	40.8
Carbon	^{14}C	2.16	0.1	21.6
Neptunium	^{237}Np	1.74	0.1	17.4
Curium	^{245}Cm	1.74	0.1	17.4
Nickel	^{59}Ni	6.34	1	6.34
Zirconium	^{93}Zr	3.32	1	3.32
Thorium	^{230}Th	0.0331	0.01	3.31
Niobium	^{94}Nb	2.18	1	2.18
Technetium	^{99}Tc	21.0	10	2.10
Tin	^{126}Sn	1.46	1	1.46
Cesium	^{135}Cs	0.765	1	0.765
Selenium	^{79}Se	0.710	1	0.710
Iodine	^{129}I	0.0568	0.1	0.568
Palladium	^{107}Pd	0.244	1	0.244
Samarium	^{151}Sm	0.241	1	0.241

NOTE: (1) Information based on PWR reactor spent fuel with a burnup of 60,000 MWd/MTIHM.
(2) EPA = U.S. Environmental Protection Agency.

[a]When more than one isotope of an element met the screening criteria (e.g., ^{241}Am, ^{242}Am, ^{243}Am), the one with the highest inventory is shown.

[b]From Roddy et al. (1985).

[c]From EPA (1985, p. 38087).

Table 4.1-23. Oxidation states of radionuclides reduced by 0.01M hydrazine in groundwater solutions

Element	Starting species	Reduced oxidation state	References
Uranium	UO_2^{2+}	Uranium(IV)	Kalnins and Gibson (1959)
Neptunium	NpO_2^+	Neptunium(IV)	Keller (1971); Koltunov and Tikhonov (1973)
Plutonium	PuO_2^+	Plutonium(IV) or Plutonium(III)	Koltunov and Zhuravleva (1974)
Technetium	TcO_4^-	Technetium(IV)	Spitsyn et al. (1983)
Selenium	SeO_3^{2-}	Selenium(-II)	Benzing et al. (1957)

Table 4.1-24. A summary of radionuclide sorption measurements completed for geologic solids and groundwaters found in the Columbia River Basalt Group

Geologic solids	Synthetic groundwater[a]	Radionuclides	Equilibration time (d)	Redox conditions[b]	Temperature (°C)
Umtanum flow basalt entablature, crushed	GR-1 GR-2 GR-3	Selenium, strontium, technetium, iodine, cesium, radium, uranium, plutonium, neptunium, americium, thorium	1-90	Oxidizing, reducing	23, 60, 150, 300
Cohassett flow basalt entablature, crushed	GR-3	Selenium, strontium, technetium, radium, uranium, plutonium, neptunium	1-90	Oxidizing, reducing	60
Umtanum flow top, crushed	GR-3	Selenium, zirconium, technetium, lead, radium, thorium, uranium, neptunium, plutonium	1-56	Oxidizing, reducing	60
Mixed secondary minerals from the Pomona flow, blended	GR-1 GR-2	Selenium, strontium, technetium, iodine, cesium, radium, uranium, neptunium, plutonium	60	Oxidizing, reducing	23, 60
Mabton interbed, unconsolidated	GR-1A	Selenium, technetium, tin, radium, uranium, neptunium, plutonium, americium	14	Oxidizing, reducing	23, 60, 85
Rattlesnake Ridge interbed, unconsolidated	GR-2	Selenium, strontium, technetium, cesium, radium, uranium, neptunium, americium	14	Oxidizing, reducing	23, 60, 85

NOTE: Not all combinations of experimental conditions shown in this table have been used for experiments with each solid material.

[a]Compositions of these synthetic groundwaters are given in Subsection 4.1.2.10.

[b]Oxidizing conditions = air-saturated solutions; reducing conditions = 0.05 to 0.1M hydrazine solutions.

Table 4.1-25. Sources of solid materials used in sorption measurements

Description	Sample number[a]	Source	References to detailed characterization
Crushed basalt entablature	RUE-1	Umtanum flow outcrop at the Emerson Nipple stratigraphic section (see Chapter 3)	Salter et al. (1981b, pp. 6-10) Palmer et al. (1982, pp. 13-16)
Crushed basalt entablature	RSB-1	Cohassett flow outcrop at Sentinel Gap stratigraphic section (see Chapter 3)	Long et al. (1984, pp. I-68 to I-79)
Crushed basalt flow top	--	Umtanum flow top from borehole cores	In preparation
Secondary minerals (smectite clay)	--	Pomona flow from excavation of Near-Surface Test Facility	Salter et al. (1981a, pp. 4-8) Palmer et al. 1982, pp. 38-42)
Unconsolidated interbed material	RO47A	Mabton interbed from borehole cores	Barney (1983, p. 4) Palmer et al. (1982, pp. 17-30)
Unconsolidated interbed material	--	Rattlesnake Ridge interbed from outcrop at Sentinel Gap, Washington	Barney (1982, p. 14) Palmer et al. (1982, pp. 50-54)

[a]Dashes indicate that no sample number has been assigned to the material.

Table 4.1-26. Time required for radionuclide sorption reactions to reach 90% completion on fresh basalt and altered basalt flow-top surfaces from GR-3 groundwater at 60 °C

Radionuclide	Solid sorbant[a]	Eh[b]	Initial concentration (M)	Final pH	Time required to reach 90% completion (h)
Thorium	Fresh basalt	O	2.05 E-10	8.7	>576
	Flow top	O	1.03 E-10	8.9	<0.25
Plutonium	Fresh basalt	O	1.06 E-10	8.4	151
		R	3.73 E-12	10.3	250
	Flow top	O	3.94 E-12	9.0	0.5
		R	3.84 E-12	10.5	<0.25
Neptunium	Fresh basalt	O	4.37 E-11	8.3	>840
		R	4.07 E-11	10.1	28
	Flow top	O	5.79 E-11	9.0	2
		R	5.04 E-11	10.3	<0.25
Uranium	Fresh basalt	O	4.38 E-07	8.3	168
		R	4.50 E-07	10.3	67
	Flow top	O	4.83 E-07	9.2	89
		R	5.04 E-07	10.9	<0.030
Radium	Fresh basalt	O	9.89 E-09	9.1	132
	Flow top	O	4.44 E-09	9.1	<0.25
Technetium	Fresh basalt	R	3.43 E-12	9.2	132
	Flow top	R	5.77 E-12	10.5	2
Lead	Fresh basalt	O	1.25 E-09	8.3	455
		R	1.25 E-09	10.8	276
	Flow top	O	1.25 E-09	8.8	<0.5
		R	1.25 E-09	10.8	<0.5
Zirconium	Fresh basalt	O	4.60 E-12	8.89	>1,560
	Flow top	O	4.60 E-12	10.7	0.83

[a]The fresh basalt used in these measurements was 16- to 60-mesh crushed basalt of the Cohassett flow entablature, except for thorium and zirconium where 20- to 60-mesh crushed basalt of the Umtanum flow entablature was used. The flow-top material was from the Umtanum flow.

[b]R = reducing conditions (0.1M hydrazine); O = oxidizing conditions (air-saturated solutions).

Table 4.1-27. Extent of radionuclide desorption from fresh basalt and altered flow-top basalt into GR-3 groundwater at 60 °C

Radionuclide	Sorbant[a]	Redox conditions[b]	Time (h)	Percent desorbed
^{237}Pu	Flow top	O	336	<1
	Fresh basalt	O	336	<1
^{235}Np	Fresh basalt	O	312	27
	Flow top	O	5 to 600	1.3
^{233}U	Fresh basalt	O	168	19
	Flow top	O	624	<0.1
^{95m}Tc	Fresh basalt	R	1,392	2.5

[a]The fresh basalt used in these measurements was 16- to 60-mesh crushed basalt of the Cohassett flow. The flow top was from the Umtanum flow.

[b]R = reducing conditions (0.1M hydrazine); O = oxidizing conditions (air-saturated solutions).

Table 4.1-28. Freundlich constants and K_d ranges for sorption of selected radionuclides on crushed basalts of the Umtanum and Cohassett flows at 60 °C (molar basis) (sheet 1 of 2)

Radionuclide	Basalt flow	Groundwater[a]	Eh[b]	K	N	r^2[c]	Standard error of estimate	Applicable concentration range (M)	K_d range (mL/g)
Selenium	Umtanum	GR-2	R	0.0062	0.998	1.000	0.31	1.2 E-13 - 1.9 E-06	6 - 43
			O	0.0018	0.996	1.000	0.030	1.8 E-13 - 8.3 E-06	1 - 3
	Cohassett	GR-3	R	0.101	1.01	1.000	0.033	9.4 E-13 - 9.2 E-07	100 - 110
			O	0.022	1.03	1.000	0.034	5.2 E-12 - 3.8 E-06	9 - 16
Strontium	Umtanum	GR-2	O	0.17	0.97	0.998	0.22	5.5 E-14 - 6.3 E-06	150 - 180
	Cohassett	GR-3	O	NA	NA	NA	NA	NA	NA
Cesium	Umtanum	GR-2	O	0.0087	0.84	0.994	0.24	3.6 E-12 - 3.4 E-04	20 - 440
Technetium	Umtanum	GR-2	R	0.32	1.02	1.000	0.0094	2.1 E-15 - 2.4 E-13	140 - 160
	Cohassett	GR-3	R	(d)	(d)	(d)	(d)	3.8 E-13 - 3.5 E-12	66 - 120
Radium[e]	Umtanum	GR-2	O	717	1.34	1.000	0.035	5.0 E-11 - 8.6 E-09	200 - 1,300
	Cohassett	GR-3	O	(d)	(d)	(d)	(d)	5.0 E-11 - 1.8 E-09	940 - 2,000
Uranium	Umtanum	GR-2	R	0.06	0.99	0.998	0.057	3.6 E-08 - 1.5 E-05	54 - 67
			O	0.0034	0.92	0.999	0.019	4.6 E-08 - 5.5 E-06	8 - 12
	Cohassett	GR-3	R	0.00015	0.54	0.981	0.13	5.0 E-09 - 1.3 E-06	72 - 890
			O	0.0002	0.68	1.000	0.003	9.9 E-08 - 5.3 E-06	10 - 34
Neptunium	Umtanum	GR-2	R	179	1.15	0.999	0.072	3.8 E-15 - 2.0 E-13	1,000 - 2,000
			O	0.0074	0.94	1.000	0.056	8.4 E-14 - 5.6 E-07	17 - 46
	Cohassett	GR-3	R	(d)	(d)	(d)	(d)	1.0 E-13 - 2.0 E-13	400 - 2,000
			O	(d)	(d)	(d)	(d)	2.0 E-12 - 2.1 E-11	11 - 13
Plutonium	Umtanum	GR-2	R	NA	NA	NA	NA	NA	NA
			O	0.951	1.12	0.931	0.040	6.7 E-15 - 2.5 E-14	18 - 24
	Cohassett	GR-3	R	6.04	1.00	0.916	0.302	5.7 E-15 - 3.9 E-14	4,600 - 9,000
			O	37.2	1.13	0.992	0.047	9.4 E-13 - 7.3 E-12	1,100 - 1,400

Table 4.1-28. Freundlich constants and K_d ranges for sorption of selected radionuclides on crushed basalts of the Umtanum and Cohassett flows at 60 °C (molar basis) (sheet 2 of 2)

Radionuclide	Basalt flow	Groundwater[a]	Eh[b]	K	N	r^2[c]	Standard error of estimate	Applicable concentration range (M)	K_d range (mL/g)
Zirconium	Umtanum	GR-3	R	0.107	0.96	0.999	0.026	1.4 E-13 - 9.8 E-11	250 - 320
			O	0.094	1.01	1.000	0.004	5.5 E-13 - 2.8 E-10	74 - 79
Lead	Umtanum	GR-3	R	(f)	(f)	(f)	(f)	2.7 E-10 - 5.2 E-09	2,800 - 5,900
			O	0.041	0.89	0.998	0.037	2.6 E-10 - 5.2 E-09	550 - 790

Note: (1) Data for cesium and strontium sorption on Umtanum basalt from Ames and McGarrah (1980); data for selenium, technetium, radium, uranium, neptunium, and plutonium sorption on Umtanum basalt from Ames et al. (1981); all other data is unpublished.

(2) NA = data are not available.

[a]Groundwater types are defined in table 6.4-3.

[b]R = reducing conditions (0.1M hydrazine); O = oxidizing conditions (air-saturated solutions).

[c]Coefficient of determination.

[d]Sorption reaction did not reach a steady state after 1,152 h for radium, 504 h for technetium, 168 h for neptunium (reducing), and 840 h for neptunium (oxidizing).

[e]Precipitation of radium is suspected for these measurements.

[f]Sorption data did not fit the Freundlich isotherm.

Table 4.1-29. Freundlich constants and K_d ranges for sorption of selected radionuclides on Umtanum flow-top material at 60 °C (molar basis) from GR-3 synthetic groundwater

Radionuclide	Eh[a]	K	N	r^{2b}	Standard error of estimate	Applicable concentration range (M)	K_d range (mL/g)
Selenium	O	0.0097	0.997	0.99	0.020	1.3 E-12 - 5.0 E-06	9 - 10
	R	(c)	(c)	(c)	(c)	5.2 E-14 - 2.8 E-07	350 - 490
Zirconium	O	0.865	1.01	0.99	0.0	6.6 E-15 - 3.8 E-11	650 - 660
	R	0.190	0.80	0.99	0.017	1.5 E-16 - 7.9 E-12	>10,000
Technetium	O	(d)	(d)	(d)	(d)	(d)	(d)
	R	4.8 E-06	0.67	0.84	0.15	7.5 E-14 - 1.1 E-12	40 - 330
Lead	O	(e)	(e)	(e)	(e)	1.0 E-12 - 7.9 E-12	4,100 - 6,000
	R					1.3 E-12 - 1.8 E-11	2,200 - 3,500
Radium	O	(e)	(e)	(e)	(e)	6.0 E-12 - 3.5 E-11	3,800 - >10,000
Thorium	O	1.79	0.986	0.99	0.18	1.1 E-14 - 4.0 E-11	3,400 - 4,300
Uranium	O	(c)	(c)	(c)	(c)	4.4 E-07 - 7.2 E-05	9.7 - 9.7
	R	0.0099	1.00	0.99	0.0076	5.0 E-07 - 9.9 E-05	9.7 - 9.7
Neptunium	O	(c)	(c)	(c)	(c)	2.8 E-13 - 2.3 E-12	226 - 480
	R	8,130	1.25	0.88	0.17	2.0 E-14 - 1.1 E-13	2,800 - 3,400
Plutonium	O	0.013	0.85	0.99	0.032	2.1 E-15 - 3.3 E-14	1,200 - 1,800
	R	(e)	(e)	(e)	(e)	1.9 E-14 - 6.0 E-14	190 - 630

Source: Unpublished data.

[a]R = reducing conditions (0.1M hydrazine); O = oxidizing conditions (air-saturated solutions).

[b]Coefficient of determination.

[c]Sorption reaction did not reach a steady state after 144 h for uranium, 1,344 h for neptunium, and 1,272 h for selenium.

[d]No sorption was observed.

[e]Because of the small concentration range studied, the Freundlich constants calculated for these measurements have large errors.

Table 4.1-30. Freundlich constants and K_d ranges for sorption of selected radionuclides on Pomona member basalt secondary minerals at 23 and 60 °C (molar basis)

Radionuclide	Groundwater[a]	Temperature (°C)	Eh[b]	K	N	r^{2c}	Standard error of estimate	Applicable concentration range (M)	K_d range (mL/g)
Strontium	GR-1	23	O	0.22	0.98	0.99	0.069	2.8 E-14 - 3.8 E-06	210 - 350
		60	O	0.85	1.03	0.99	0.22	3.5 E-14 - 2.3 E-06	270 - 940
	GR-2	23	O	0.15	0.98	0.99	0.059	3.0 E-14 - 4.4 E-06	210 - 330
		60	O	0.60	1.04	0.99	0.116	4.8 E-14 - 2.0 E-06	200 - 490
Technetium	GR-1	23	R	0.026	0.92	0.99	0.016	9.4 E-16 - 1.6 E-13	250 - 360
		60	R	0.00038	0.80	0.99	0.004	7.4 E-16 - 2.8 E-13	140 - 460
	GR-2	23	R	0.44	1.03	0.99	0.043	1.6 E-15 - 1.8 E-13	190 - 220
		60	R	1.19	1.05	0.99	0.034	1.6 E-15 - 1.6 E-13	200 - 250
Cesium	GR-1	23	O	0.026	0.77	0.99	0.246	7.2 E-14 - 4.5 E-05	210 - >10,000
		60	O	0.023	0.77	0.99	0.257	1.2 E-13 - 5.7 E-05	170 - >10,000
	GR-2	23	O	0.055	0.81	0.99	0.235	2.4 E-13 - 4.3 E-05	220 - 8,500
		60	O	0.034	0.80	0.99	0.375	4.0 E-13 - 6.2 E-05	150 - >10,000
Radium	GR-2	60	O	114	1.26	0.99	0.092	4.9 E-11 - 1.1 E-08	220 - 1,000
			R	2,340	1.39	0.99	0.056	5.5 E-11 - 7.3 E-09	240 - 1,500
Uranium	GR-1	23	O	0.0045	0.83	0.99	0.181	1.2 E-08 - 2.7 E-05	27 - 130
		60	O	0.057	0.84	0.99	0.117	6.8 E-10 - 2.7 E-06	360 - 1,500
	GR-2	23	O	0.0026	0.82	0.99	0.162	1.2 E-08 - 4.5 E-05	12 - 22
		60	O	0.55	0.97	0.99	0.124	8.5 E-10 - 9.5 E-08	770 - 1,200
Neptunium	GR-1	23	O	0.104	0.98	0.99	0.055	1.9 E-14 - 1.0 E-07	140 - 210
			R	5,280	1.29	0.99	0.126	9.8 E-15 - 3.6 E-13	380 - 1,200
		60	O	0.092	0.98	0.99	0.055	1.6 E-14 - 1.0 E-07	140 - 250
			R	36	1.13	0.99	0.008	8.0 E-15 - 4.8 E-13	480 - 810
	GR-2	23	O	0.050	0.91	0.99	0.161	2.9 E-15 - 3.6 E-08	160 - 1,700
			R	790	1.22	0.99	0.024	6.9 E-15 - 3.0 E-13	700 - 1,300
		60	O	0.12	0.97	0.99	0.069	1.8 E-14 - 7.7 E-08	180 - 310
			R	38.7	1.13	0.99	0.010	6.9 E-15 - 4.1 E-13	710 - 950
Plutonium	GR-2	23	O	5.7 E-11	0.33	0.99	0.011	1.4 E-17 - 6.3 E-16	1,070 - >10,000
		60	O	0.046	0.92	0.94	0.030	2.3 E-16 - 8.8 E-16	770 - 8,400

Source: Data from Ames et al. (1981).

[a]Groundwater types are defined in Table 6.4-3.

[b]R = reducing conditions (0.1M hydrazine); O = oxidizing conditions (air-saturated solutions).

[c]Coefficient of determination.

Table 4.1-31. Freundlich constants and K_d ranges for sorption of selected radionuclides on Mabton interbed material at 23 and 60 °C from GR-1A synthetic groundwater (molar basis)

Radionuclide	Temperature (°C)	Eh[a]	K	N	r^{2b}	Standard error of estimate	Applicable concentration range (M)	K_d range (mL/g)
Selenium	23	O	0.00081	0.85	0.996	0.031	9.5 E-09 - 1.5 E-05	2.7 - 11
		R	0.011	1.02	0.999	0.017	9.9 E-09 - 9.7 E-06	6.5 - 10
	60	O	0.0029	1.09	0.948	0.15	1.9 E-08 - 1.8 E-05	0.2 - 1.8
		R	0.059	1.08	0.999	0.0081	7.5 E-09 - 5.5 E-06	14 - 25
Technetium	23	O	0.00030	0.91	0.978	0.192	1.0 E-07 - 1.1 E-04	0.4 - 1.7
		R	0.44	1.09	0.978	0.219	3.9 E-09 - 1.9 E-06	69 - 210
	60	O	0.00094	1.01	0.982	0.145	1.2 E-07 - 1.0 E-04	0.3 - 9.6
		R	0.00011	0.58	0.974	0.146	5.1 E-09 - 1.7 E-05	11 - 150
Tin	23	O						
		R	(c)	(c)	(c)	(c)	(c)	(c)
	60	O						
		R						
Radium	23	O	183	1.18	0.971	0.150	1.2 E-12 - 2.2 E-10	620 - 3,800
		R	0.0556	0.91	0.994	0.072	1.2 E-11 - 2.3 E-09	320 - 690
	60	O	9.64	0.99	0.919	0.103	2.0 E-12 - 8.6 E-11	1,600 - >10,000
		R	0.084	0.98	0.990	0.105	6.8 E-12 - 5.9 E-09	90 - 210
Uranium	23	O	0.00040	0.74	0.999	0.020	2.4 E-09 - 4.9 E-06	10 - 74
		R	0.013	0.88	0.997	0.027	1.1 E-09 - 1.7 E-07	82 - 150
	60	O	0.25	0.96	0.992	0.120	2.9 E-10 - 2.4 E-07	410 - 670
		R	0.015	0.79	0.999	0.012	1.3 E-09 - 2.3 E-08	660 - 1,200
Neptunium	23	O	0.00028	0.69	0.994	0.143	9.9 E-09 - 2.7 E-05	10 - 75
		R	0.034	0.80	0.996	0.044	6.0 E-09 - 1.6 E-06	450 - 1,300
	60	O	0.00055	0.68	0.997	0.149	5.1 E-09 - 2.1 E-05	20 - 190
		R	0.0164	0.87	0.995	0.052	4.2 E-09 - 9.6 E-06	64 - 190
Plutonium	23	O	0.51	0.95	0.967		1.9 E-13 - 2.2 E-12	2,000 - 2,200
		R	(c)	(c)	(c)	(c)	(c)	(c)
	60	O	0.014	0.78	0.874		1.3 E-13 - 5.9 E-13	3,300 - 8,900
		R	(c)	(c)	(c)	(c)	(c)	(c)
Americium	23	O						
		R	(c)	(c)	(c)	(c)	(c)	(c)
	60	O						
		R						

Source: Data from Barney (1984).

[a]R = reducing conditions (0.05M hydrazine); O = oxidizing conditions (air-saturated solutions).

[b]Coefficient of determination.

[c]Steady-state concentrations of radionuclide tracers were below detection limits (about 6 E-08M for ^{119m}Sn, E-12M for ^{241}Am, and E-13M for ^{238}Pu), thus Freundlich constants could not be calculated.

Table 4.1-32. Freundlich constants and K_d ranges for sorption of selected radionuclides on sandstone of Rattlesnake Ridge interbed material at 23 and 60 °C from GR-2 groundwater (molar basis)

Radionuclide	Temperature (°C)	Eh[a]	K	N	r^2[b]	Standard error of estimate	Applicable concentration range (M)	K_d range (mL/g)
Selenium	23	R	0.010	1.03	0.98	0.185	3.3 E-08 - 1.8 E-05	4.6 - 13
	60	R	0.018	0.89	0.965	0.098	4.1 E-08 - 6.4 E-06	51 - 80
	85	R	0.70	1.06	0.99	0.089	2.9 E-09 - 1.3 E-06	170 - 320
Strontium	23	O	0.78	1.02	0.99	0.034	4.3 E-11 - 4.4 E-08	490 - 610
	60	O	1.17	1.03	0.99	0.049	3.6 E-11 - 3.9 E-08	600 - 730
	85	O	12.2	1.18	0.99	0.141	9.3 E-11 - 4.5 E-08	220 - 590
Technetium[c]	23	R	1,056	1.50	0.92	0.406	3.6 E-09 - 3.1 E-07	75 - 1,300
	60	R	4.9	1.3	0.99	0.061	1.3 E-08 - 3.4 E-06	25 - 120
	85	R	0.19	1.09	0.99	0.067	8.8 E-09 - 5.9 E-06	52 - 65
Cesium	23	O	0.0023	0.72	0.99	0.067	5.4 E-10 - 1.5 E-08	510 - 1,450
	60	O	0.0029	0.72	0.96	0.096	6.0 E-11 - 3.4 E-08	220 - 1,300
	85	O	0.0013	0.72	0.99	0.091	1.1 E-10 - 6.2 E-08	120 - 700
Radium	23	O	0.62	0.94	0.98	0.158	1.6 E-12 - 1.5 E-10	1,700 - 3,900
	60	O	0.13	0.91	0.991	0.028	3.6 E-12 - 5.8 E-10	860 - 1,500
	85	O	83.1	1.16	0.98	0.146	3.8 E-12 - 1.7 E-10	1,300 - 3,000
Uranium	23	R	0.013	0.94	0.99	0.028	4.5 E-10 - 6.3 E-07	32 - 50
	60	R	0.046	0.91	0.999	0.024	3.2 E-10 - 1.4 E-07	190 - 340
	85	R	0.0037	0.79	0.999	0.022	2.3 E-10 - 2.9 E-07	110 - 320
Plutonium	23	R	3.50	1.03	0.99	0.122	1.9 E-09 - 1.3 E-07	1,900 - 3,000
	60	R	(d)	(d)	(d)	(d)	2.5 E-07 - 3.9 E-07	3,100 - 4,500
	85	R	1,753	1.36	0.99	0.080	2.8 E-09 - 6.6 E-08	1,600 - 7,000
Americium	23	O	0.030	0.89	0.99	0.017	1.8 E-12 - 2.4 E-11	0 - 580
	60	O	2.89	1.03	0.99	0.205	8.2 E-13 - 4.0 E-12	1,400 - 2,600
	85	O	(d)	(d)	(d)	(d)	5.7 E-12 - 1.1 E-11	7,200 - 15,000

Source: Data from Barney (1982).

[a]R = reducing conditions (0.05M hydrazine); O = oxidizing conditions (air-saturated solutions).

[b]Coefficient of determination.

[c]Precipitations of technetium is suspected for the 23 and 60 °C isotherm measurements.

[d]Steady-state concentrations of radionuclide tracers were usually below detection limits (about 3 E-09M for ^{237}Np and E-12M for ^{241}Am), thus Freundlich constants could not be calculated.

Table 4.1-33. Freundlich constants for radionuclide sorption-desorption on Mabton interbed at 60 °C

Isotope	Eh*	S_o (mol/g)	N_s	N_d	N_s/N_d
Selenium	R	1.11 E-07	1.0	0.018	56
		2.76 E-08		0.027	37
Technetium	R	1.88 E-07	0.58	0.018	32
		3.50 E-07		0.003	193
Neptunium	O	3.13 E-07	0.68	0.45	1.5
		1.38 E-07		0.91	0.75
Neptunium	R	3.84 E-07	0.87	0.002	435
		1.81 E-07		0.002	435
Uranium	O	8.88 E-08	0.96	0.093	10
		2.11 E-08		0.074	13
Uranium	R	2.70 E-08	0.79	0.008	100
		8.58 E-09		0.003	263
Radium	R	7.65 E-12	0.98	0.016	61
		1.81 E-10		0.087	11

Source: Data from Barney (1984).
*R = reducing conditions (0.05M hydrazine); O = oxidizing conditions (air-saturated solution).

Table 4.1-34. Freundlich constants for sorption and desorption of cesium, strontium, and selenium (oxidizing conditions)

Radionuclide	Geologic material	N_s	N_d	N_s/N_d
Cesium	Umtanum flow basalt	0.83	0.31	2.7
Strontium	Umtanum flow basalt	1.39	0.08	17
Selenium	Secondary minerals	0.81	0.53	1.5

Table 4.1-35. Comparison of measured K_d ranges and values used for transport modeling

Element	Measured values (oxidizing conditions)			Measured values (reducing conditions)			Values used for modeling materials
	Umtanum flow basalt	Secondary minerals	Interbed materials	Umtanum flow basalt	Secondary	Interbed minerals	
Selenium	2-5	1-10	0.3-10	3-40	6-12	7-24	0.8
Strontium	40-450	200-1,000	220-700	--	--	--	30
Technetium	0-3	0-7	0.4-1.4	140-360	40-360	12-200	0
Cesium	18-1,100	150-14,000	115-4,300	100-540	1,100-5,000	--	100
Radium	50-1,300	220-1,000	250-1,000	80-1,900	240-1,500	110-580	20
Uranium	2-90	12-1,500	10-670	15-170	--	80-1,200	1
Neptunium	5-280	140-1,650	10-185	150-2,000	380-1,300	64-1,300	2
Plutonium	18-30	700-14,000	2,000-9,000			20,000-37,000	4
Americium	--	--	500-14,000	--	--	--	68
Iodine	0.05-1.8	0-2.3	--	--	--	--	0

NOTE: Values are in mL/g.

Table 4.1-36. Sorption of radionuclides on colloids and transfer of radionuclides from colloids to basalt in GR-3 groundwater at 60 °C

Radionuclide	Colloid	Eh[a]	Percent sorbed on colloid[b]	Percent of sorbed radionuclide transferred to basalt surfaces[b]
Uranium	Bentonite[c]	O	62	66
		R	73	85
Neptunium		O	47	64
		R	94	3
Technetium		O	1	0
		R	36	17
Selenium		O	4	100
		R	64	81
Uranium	Hydrated silica[d]	O	100	7
		R	98	0
Neptunium		O	99	14
		R	99	0
Technetium		O	0	0
		R	86	37
Selenium		O	0	0
		R	30	0
Radium		O	99	66
		R	99	84

[a]R = reducing conditions (0.1M hydrazine); O = oxidizing conditions (air-saturated solutions).

[b]After 26 d of equilibration.

[c]Particle size less than 2 μm (less than 0.000079 in.); 2.1 g colloid per liter.

[d]Mean particle size was 40Å; 50 g colloid per liter.

Table 4.1-37. Oxidation half reactions relating iron solid phases in Grande Ronde Basalt

No.	Oxidation half reaction
1.	$2Fe_3O_4 + H_2O = 3Fe_2O_3 + 2H^+ + 2e^-$ (magnetite) (hematite)
2.	$3FeS_2 + 28H_2O = Fe_3O_4 + 6SO_4^{2-} + 56H^+ + 44e^-$ (pyrite) (magnetite)
3.	$3FeSiO_3 + H_2O = Fe_3O_4 + 3SiO_2$ (amorphous) $+ 2H+ + 2e^-$ (iron-pyroxene) (magnetite)
4.	$2Fe(OH)_2 = Fe_2O_3 + H_2O + 2H+ + 2e^-$ (hematite)

Table 4.1-38. Oxidation half reactions relating species in solution in Grande Ronde Basalt groundwaters

No.	Oxidation half reaction	Log K	E°
1.	$HS^- + 4H_2O = SO_4^{2-} + 9H^+ + 8e^-$	-34.0	-0.25
2.	$Fe^{+2} = Fe^{+3} + e^-$	-13.01	-0.77
3.	$CH_4\ (g) + 2H_2O = CO_2\ (g) + 8H^+ + 8e^-$	-22.9	-0.17
4.	$CH_4\ (g) + 3H_2O = HCO_3^- + 9H^+ + 8e^-$	-27.3	-0.20
5.	$CH_4\ (g) + H_2O = CO\ (g) + 6H^+ + 6e^-$	-26.43	-0.26

Table 4.1-39. Eh calculations based on sulfide/sulfate equilibria

Date	Borehole	Eh (V)
11/16/82	DC-16A	-0.41
11/19/82	DC-16C	-0.38
2/18/83	DC-14	-0.37
2/22/83	DC-14	-0.38
3/01/83	DC-14	-0.38
3/04/83	DC-14	-0.38
3/15/83	DC-14	-0.40
4/11/84	DC-6	-0.40

Source: Dill et al., 1986, pp. 19.

Table 4.1-40. Eh calculations based on concentrations of iron(II), iron(III), and sulfur(-II)

Date	Borehole/zone (ft)	Fe^{2+}(µg/L)	Total iron(µg/L)		Total sulfide (µg/L)	Eh(mV)
			ICP[a]	AA[b]		
4/10/84	DC-14/ Grande Ronde 8 (3,260-3,335)	trace	10[c]	--	300	-70
4/11/84	DC-6/ Grande Ronde Composite (2,262-4,333)	trace	40[c]	--	80	-170
4/12/84	McGee/ Frenchman Springs (983-1,942)	100	100	--	<10	-65
4/12/84	McGee/Priest Rapids-Roza (691-928)	130	120	--	<10	+10
4/17/84	Enyeart/ Priest Rapids (935-1,092)	80	90	80	<10	+40

[a]ICP = iron concentration from inductively coupled plasma spectrometer analysis.
[b]AA = iron concentration from atomic absorption spectrophotometer analysis.
[c]Obtained from previous analyses.

Table 4.1-41. Significant geochemical variables of groundwater for radionuclide sorption at 23 °C

Radionuclide	Significant geochemical variables of groundwater
^{137}Cs	K^+, Na^+
^{85}Sr	Na^+, Ca^{2+}
^{226}Ra	Na^+, K^+
^{237}Np*	CO_3^{2-}, HCO_3^-
^{241}Am	CO_3^{2-}, HCO_3^-, Na^+

*Carbonate and bicarbonate decreased sorption of both neptunium(V) and neptunium(IV).

Table 4.2-1 The diffusion constant for tritium and chloride in packing material as a function of temperature

Temperature (°C)	Clay density (Mg/m^3)	Diffusion constant (10^{-10} m^2/s)	
		Tritium	Chloride
25	1.0	2.5	1.5
55	1.0	5.4	2.1
90	1.0	12	3.1
120	1.0	20	4.0
150	1.0	32	5.1

Source: Calculated using the empirical equations derived experimentally in Relyea et al. (1986, pp. 321-322).

Table 4.3-1. Comparison of minerals produced in basalt-groundwater experiments with minerals observed in Hanford Site basalts and in Iceland geothermal fields (sheet 1 of 2)

Experimental	Hanford	Iceland (<150 °C)	Iceland (>150 °C)
		Silica	
quartz	quartz		quartz
cristobalite	cristobalite	cristobalite	
tridymite	tridymite		
		Phyllosilicates	
smectite	smectite	smectite	smectite
illite		illite-smectite	chlorite-smectite
chlorite			chlorite
		Iron oxides	
iron oxyhydroxide	iron oxyhydroxide		
		hematite	magnetite
		Zeolites	
mordenite	mordenite	mordenite	mordenite
heulandite	phillipsite	heulandite	heulandite
wairakite	eronite	zeophyllite	wairakite
ferrierite	chabazite	chabazite	
clinoptilolite	clinoptilolite		
analcime		analcime	analcime
		gmelinite	
		gismondine	gismondine
		laumontite	laumontite
		scolecite	
		thomsonite	
		stilbite	stilbite

Table 4.3-1. Comparison of minerals produced in basalt-groundwater experiments with minerals observed in Hanford Site basalts and in Iceland geothermal fields (sheet 2 of 2)

Experimental	Hanford	Iceland (<150 °C)	Iceland (>150 °C)
		Others	
		pyrite	pyrrhotite
	celadonite	celadonite	
scapolite			
K-feldspar			albite
	gypsum	anhydrite	anhydrite
	calcite	calcite	calcite
	apatite	ankerite	ankerite
		sphene	prehrite
		truscottite	amphibole
		gyrolite	epidote

Note: It is emphasized that the list of minerals from Iceland is a compilation from many areas and must be related to the experimental work carefully until more detailed investigations have indicated specific areas more directly analogous. For example, the iron oxide assemblage observed in Icelandic geothermal fields differs from that observed in experiments or at the Hanford Site. The difference may arise as a function of temperature, oxygen fugacity and (or) water content in the various systems, and awaits the further investigation that establishes the best Icelandic analog (see Section 8.3.4.2.3).

Table 4.3-2. Mass balance for SCN^- and (K^+ and Na^+) from borehole DC-7/8 KSCN tracer test

Species	Mass injected, g (equivalent weights)	Mass recovered, g (equivalent weights)	Percent recovery
KSCN[a]	350 (3.60)	NA[b]	NA[b]
SCN^-	209 (3.60)	125.5 (2.16)	60
K^+	140.7 (3.60)	15.2 (0.39)	11
Na^+	0 (0)	49.2 (2.14)	NA[b]
$\Sigma(K^+ + Na^+)$	140.7 (3.60)	64.4 (2.53)	70

Source: Leonhart et al. (1984).

NOTE: Results show that mass balance between primary anions and cations involved is within 15%.

[a]KSCN = Potassium thiocyanate.

[b]NA = Not applicable.